FUNCTIONAL CHARACTERIZATION OF BOVINE HERPESVIRUS MAJOR TEGUMENT PROTEIN VP8

A Thesis Submitted to
The College of Graduate and Postdoctoral Studies
In Partial Fulfillment of the Requirements
For the Degree of Doctor of Philosophy in the
Department of Vaccinology and Immunotherapeutics,
University of Saskatchewan, Saskatoon,
Saskatchewan, Canada

By
SHARMIN AFROZ

PERMISSION TO USE

In presenting this thesis/dissertation in partial fulfillment of the requirements for a Postgraduate degree from the University of Saskatchewan, I agree that the Libraries of this University may make it freely available for inspection. I further agree that permission for copying of this thesis/dissertation in any manner, in whole or in part, for scholarly purposes may be granted by the professor or professors who supervised my thesis/dissertation work or, in their absence, by the Head of the Department or the Dean of the College in which my thesis work was done. It is understood that any copying or publication or use of this thesis/dissertation or parts thereof for financial gain shall not be allowed without my written permission. It is also understood that due recognition shall be given to me and to the University of Saskatchewan in any scholarly use which may be made of any material in my thesis.

Requests for permission to copy or to make other uses of materials in this thesis in whole or part should be addressed to:

Director
School of Public Health
104 Clinics Place
University of Saskatchewan
Saskatoon, Saskatchewan S7N 2Z4
Canada

OR

Dean
College of Graduate and Postdoctoral Studies
Room 116, Thorvaldson Building
110 Science Place
University of Saskatchewan
Saskatoon, SK, S7N 5C9
Canada

ABSTRACT

Bovine herpesvirus (BoHV-1) is an important bovine pathogen. The *ul47* gene-encoded VP8 is the most abundant protein of the BoHV-1 virion. VP8 is indispensable for BoHV-1 infection in cattle and a U_L47-deleted virus exhibits drastic reduction in replication in tissue culture. The reason for the inability of U_L47-deleted virus to replicate in cattle is unknown. Interferons (IFNs) secreted in response to viral infection trigger translocation of signal transducer and activator of transcription (STAT1) to the nucleus for induction of IFN-stimulated genes. We observed that VP8 interacts with STAT1 through two regions, amino acids 259-482 and 632-741. IFN-β production was significantly reduced in BoHV-1- but not in BoHV-1ΔU_L47-infected cells. VP8 did not alter STAT1 phosphorylation or degrade STAT1, but inhibited nuclear translocation of STAT1 to reduce IFN-β production. Thus, VP8 plays a vital role in inhibition of IFN-β signaling via interaction and sequestration of STAT1 in the cytoplasm.

VP8 also interacted with Ataxia telangiectasia mutated (ATM) and Nijmegen breakage syndrome-1 (NBS1), which are critical components in the DNA damage response. Association of VP8 with ATM and NBS1 did not affect ATM, but inhibited NBS1 activation. Consequently, phosphorylation of structural maintenance of chromosome-1 (SMC1), the downstream regulator of the ATM/NBS1 pathway, was abolished. BoHV-1 but not BoHV-1ΔU_L47 infection inhibited NBS1 and SMC1 phosphorylation. In addition, VP8 induced apoptosis through caspase-3 activation. Hence, VP8 blocks the ATM/NBS1/SMC1 pathway resulting in induction of apoptosis, which reveals a role of VP8 in the modulation of the DNA damage response.

We identified heat shock protein-60 (HSP60) as a mitochondrial interacting partner of VP8. VP8 co-localized with HSP60 in the mitochondria. Association of VP8 with mitochondria reduced mitochondrial membrane potential (MMP) and adenosine triphosphate (ATP) production. Mitochondrial functions were impaired in BoHV-1- but not in BoHV-1ΔU_L47-infected cells. Thus, VP8 might contribute to the deregulation of mitochondrial functions.

These results demonstrate that VP8 plays a crucial role during BoHV-1 infection by down-regulating IFN-β signaling, inhibiting the DDR pathway and deregulating mitochondrial functions. These functional characteristics of VP8 provide a (partial) explanation for the defective replication of BoHV-1ΔU_L47 in cell culture and its lack of virulence in cattle.

ACKNOWLEDGEMENTS

I would like to express my sincere gratitude to my supervisor Dr. Sylvia van Drunen Littel-van den Hurk for providing me with the opportunity to study in her lab. I am deeply grateful to her for her invaluable guidelines, support, and encouragement. I would like to express my sincere appreciation to my co-supervisor Dr. Michel Fodje for his constant support and motivation. The guidance and support from Dr. Sylvia van Drunen Littel-van den Hurk and Dr. Michel Fodje have been integral in the completion of this work.

I owe an immense debt of gratitude to my graduate committee members; Dr. Joyce Wilson, (Microbiology and Immunology), Dr. Yan Zhou (VIDO-Intervac), Dr. Yu Luo (Department of Biochemistry) for their valuable suggestions during my research. I would also like to thank my graduate chair and the Director of the Vaccinology and Immunotherapeutics program, Dr. Suresh Tikoo, for his continuous support.

I would like to thank past/present lab members of Dr. van Drunen Littel-van den Hurk's lab, especially Dr. Ravendra Garg, Ms. Laura Latimer, Ms. Marlene Snider, Dr. Kuan Zhang, Indranil Sarkar, Elisa Martinez and Amanda Wilson for their assistance during this project. I extend my sincere thanks to Dr. Robert Brownlie for his intellectual input.

I would like to express my gratitude to the Canadian Institutes of Health Research Training Grant in Health Research Using Synchrotron Techniques (CIHR-THRUST) and the Saskatchewan innovation and opportunity scholarship for sponsoring me. The research in our lab was funded by the Natural Sciences and Engineering Research Council (NSERC), and a Canadian Institutes of Health Research, Research Partnership Program (CIHR-RPP), which is gratefully acknowledged.

Finally, I would like to express my special thanks to my mom, Feroza Khatun and my husband, Dr. Kausar Alam for their continuous support, co-operation and patience during this work.

DEDICATION

This thesis is dedicated to my source of inspiration, my lovely mom,

Feroza Khatun,

Without her continuous love and support, I would have not been able to accomplish this work.

TABLE OF CONTENTS

LIST OF FIGURES

LIST OF TABLES

LIST OF ABBREVIATIONS

ActD	-	Actinomycin D
Alpha-TIF	-	Alpha-transducing factor
Apaf-1	-	Apoptotic protease activating factor-1
ATP	-	Adenosine triphosphate
ATM	-	Ataxia telangiectasia mutated
ATR	-	ATM- and RAD-related
ATRIP	-	ATR interacting protein
α-TIF	-	α-transducing factor
Bak	-	Bcl-2 homologous antagonist killer
Bax	-	Bcl-2-associated X protein
Bid	-	BH3-interacting domain death agonist
BoHV-1	-	Bovine herpesvirus-1
BRCA1	-	Breast cancer-1
CBP	-	Cyclic AMP response element-binding protein
cGAS	-	Cyclic GMP-AMP synthase
cGMP	-	Cyclic GMP-AMP
CHK2	-	Check point kinase 2
CHX	-	Cyclohexamide
CK2	-	Cellular kinase-2
CMV	-	Cytomegalovirus
CPD	-	Cyclobutane pyrimidine dimer
CRM1	-	Chromosome region maintenance
CTMP7	-	Carboxy-terminal modulator protein-7
DAPI	-	4′,6-diamino-2-phenylindole
DDB1	-	DNA damage binding protein
DDR	-	DNA damage response
DNA-PK	-	DNA-protein kinase
DSBs	-	Double-strand breaks
DUB	-	Deubiquitinase
dsRNA	-	Double-stranded RNA

EBTr	-	Embryonic bovine tracheal
EBV	-	Epstein-Barr Virus
E. coli	-	*Escherichia coli*
EYFP	-	Enhanced yellow fluorescent protein
EHV-1	-	Equine herpesvirus -1
EIF2A	-	Eukaryotic translation initiation factor
FACS	-	Flow cytometry cell sorting
FADD	-	Fas-associated death domain
GHV3	-	Gallid herpesvirus 3
GTP	-	Guanosine triphosphate
H2A	-	Histone-2A
HCF-1	-	Host cell factor-1
HCL	-	Hydrochloric acid
HCMV	-	Human cytomegalovirus
HEK	-	Human embryonic kidney
HVEM	-	Herpes virus entry mediator
HR	-	Homologous recombination
HSP60	-	Heat shock protein
HSV-1	-	Herpes Simplex Virus-1
ICP	-	Infected cell polypetide
IFN	-	Interferon
IRF-IFN	-	Interferon Regulatory Factor-IFN
IRF3	-	Interferon Regulatory Factor 3
IE	-	Immediate-early
IFI16	-	Interferon Gamma inducible protein 16
ISGs	-	IFN-stimulated genes
ISRE	-	Interferon-sensitive response element
ILTV	-	Infectious laryngotracheitis virus
IκBα	-	Inhibitory kappa B alpha
IKK	-	Inhibitor of Kappa B kinase
IPTG	-	Isopropyl β-D-1-thiogalactopyranoside

JAK	-	Janus kinase
KCl	-	Potassium chloride
KSHV	-	Kaposi's sarcoma-associated herpesvirus
K-63	-	Lysine-63
LAT	-	Latency associated transcript
LMP-1	-	Latent membrane protein-1
LR	-	Latency related
LR-RNA	-	Latency related RNA
MALDI-TOF	-	matrix-assisted laser desorption/ionization time-of-flight
MAVS	-	Mitochondrial antiviral-signaling protein
MDA5	-	Melanoma Differentiation-Associated protein 5
MDBK	-	Madin-Darby bovine kidney
MDV-1	-	Marek's diseases virus-1
MHV-68	-	murine gammaherpesvirus-68
MMP	-	Mitochondrial membrane potential
MOI	-	Multiplicity of infection
MPT	-	Mitochondrial permeability transition
MRN	-	MRE11-RAD50-NBS1
MTCs	-	Multi-subunit tethering complexes
MyD88	-	Myeloid differentiation response 88
NaCl	-	Sodium chloride
NBS1	-	Nibrin-1
NES	-	Nuclear export signal
NF-κβ	-	Nuclear factor-κβ
NHEJ	-	Nonhomologous End Joining
NLS	-	Nuclear localization signal
OAS	-	2-5-oligoadenylate synthase
ORF	-	Open reading frame
PACT	-	Protein kinase R activated protein
PABP	-	Polyadenylate-binding protein
PAMPs	-	Pathogen Associated Molecular Patterns

PBMC - Peripheral blood mononuclear cells
PBS - Phosphate buffer saline
PDCD4 - Programmed cell death protein 4
PDU - Procedure defined unit
PK - Protein kinase
PKR - Protein kinase R
PMSF - Phenylmethylsulfonyl fluoride
PML - Promyelocytic Leukemia
PRV - pseudorabies virus
PRRs - Pattern-recognition receptors
RIG I - Retinoic acid-inducible gene-I
RING - Really interesting new gene
RNF8 - Ring finger protein-8
RL - *Renilla Luciferase*
RLR - RIG-I-like receptor
RNR - Ribonucleotide reductase
RPA - Replication protein A
RT - Room Temperature
SD - Standard deviation
SDS-PAGE - Sodium Dodecyl Sulphate-Polyacrylamide gel electrophoresis
Sev - Sendai virus
SMC1 - Structural maintenance of chromosome-1
SOCS - Suppressor of cytokine signaling
SP - Sulphopropyl
SSB - DNA single-strand break
ssDNA - single-stranded DNA
SV5 - Simian virus 5
STAT1 - Signal transducer and activator of transcription-1
STING - Stimulation of IFN genes
SHV1 - Suid herpesvirus
TBK1 - TANK-binding kinase-1

TEV	-	Tobaco Etch Virus
TGN	-	Trans-Golgi network
TLRs	-	Toll-like receptors
TNF	-	Tumor necrosis factor
ToBP1	-	DNA topoisomerase 2 binding protein 1
TRADD	-	TNFR1-associated death domain
TRAF3	-	TNF receptor-associated factor 3
TRAF6	-	TNF-receptor-associated factor 6
TUNEL	-	Terminal deoxynucleotidyl transferase dUTP nick end labeling
Tyk2	-	Tyrosine kinase-2
Ub	-	Ubiquitin
UL	-	Unique long region
UL36USP	-	UL36-ubiquitin-specific protease
US3-PK	-	US3-Protein Kinase
USP7	-	Ubiquitin-specific-processing protease-7
US	-	Unique short region
UV	-	Ultraviolet light
vBcl2	-	viral Bcl2
vhs	-	virion host shut-off
VZV	-	Varicella-zoster virus
PRV	-	Pseudorabies virus
53BP1	-	P53-binding protein-1
9-1-1	-	RAD9-RAD1-HUS1

CHAPTER 1

LITERATURE REVIEW

1.1 Introduction.

1.1.1 Classification of BoHV-1.

Bovine herpesvirus-1 (BoHV-1) is an important bovine pathogen. BoHV-1 belongs to the family *herpesviridae,* the subfamily *alphaherpesvirinae*, and the genus *varicellovirus.* To date, all isolated BoHV-1 strains are differentiated into the following subtypes: 1.1, 1.2a, 1.2b and 1.3 (1). The BoHV-1 subtype 1.1 is associated with the clinical manifestation of respiratory diseases, whereas the subtype 1.2a is predominantly responsible for respiratory and genital infections (2). Subtype 1.1 strains are more pathogenic than subtype 1.2b strains (3). The subtype 1.3 strains are frequently associated with the respiratory infections (2, 4). Although different BoHV-1 subtypes are involved in a similar range of infections, a definitive identification of the strains depends on viral DNA analysis (5, 6). The most common strain is subtype BoHV-1.1 that tends to cause a variety of clinical manifestations in cattle.

1.1.2 Clinical Manifestations and Economic Importance.

BoHV-1 is a causative agent of severe contagious diseases in cattle. It is responsible for multiple clinical symptoms ranging from immune suppression, respiratory tract infections genital disorders, and vulvovaginitis to abortions in cattle (7). The most severe form of the disease is infectious bovine rhinotracheitis (IBR) (7, 8). BoHV-1 transmission is facilitated through either direct contact with the infected animal or exposure of mucosal surfaces to virus. In some cases, airborne transmission also occurs in susceptible animals (9). Other transmission routes include mating and artificial insemination within and from infected cattle, respectively (2). Therefore, genital disorders and abortions are more prevalent in breeding cattle. Primary infection with BoHV-1 starts with the association of virus at mucosal surfaces followed by a 1-6 day incubation period (10). Following incubation, infected animals develop clinical symptoms of respiratory disorders including nasal discharge, high fever, salivation and coughing (11). Occasionally, abortion is coupled with acute respiratory infection, although it can be triggered by BoHV-1 reactivation within 100 days of primary infection. BoHV-1 subtype 2a and 2b sometimes cause genital infections with increased urination symptoms (10).

Primary infection of BoHV-1 is frequently associated with secondary infections that extend the severity of disease. BoHV-1 infection results in immune suppression in the infected cattle. The impaired immune system together with BoHV-1 infection provides an environment suitable for infection with secondary pathogens including bovine viral diarrhea virus (BVDV), bovine parainfluenza virus-3 (BPIV-3), bovine respiratory virus (BRSV) and bacterial causative agents, such as *Mannheimia haemolytica, Mycoplasma bovis, and Pasteurella multocida* (12), leading to bovine respiratory diseases complex (BRDC) or shipping fever (7). BRDC symptoms include anorexia, excessive salivation, high fever, and nasal discharge. BoHV-1-induced BRDC is facilitated by down-regulation of major histocompatibility complex (MHC) class I (13, 14) and induction of apoptosis of infected cells (15).

The severity of BoHV-1 infection and secondary infections results in significant losses to the cattle industry (16, 17). Infection with BoHV-1 introduces IBR, BRDC, and other genital disorders, causes a significant reduction in animal productivity including weight loss and a decrease in milk production (7, 18). A recent report indicated a significant decrease in average daily milk production in BoHV-1-infected animals compared to non-infected animals (19). Due to BoHV-1-associated genital disorders, the abortion rate is increased in BoHV-1-positive animals (20). Genital disorders can result in infertility. During early pregnancy, BoHV-1 infection may also cause early embryonic death. Experimentally, BoHV-1-associated abortion has been observed anytime during gestation. However, in field conditions, BoHV-1-associated abortions were detected in the second half of gestation (21, 22). In Western Turkey, more than 50% of abortions in cattle is caused by BoHV-1 infection (23). A recent study from India reported that BoHV-1 was responsible for causing 21.4% abortion in the state of Punjab. In addition, in North-Africa the majority of the abortions, 42%, were attributed to BoHV-1 infection (24). Moreover, BoHV-1 infection is associated with other economic issues including reduced show value due to bilateral conjunctivitis, restlessness and restriction in international livestock trading (18).

1.1.3 Host Range of BoHV-1.

The host range of BoHV-1 is limited. Although herpes simplex virus-1 (HSV-1) and BoHV-1 belong to the same alphaherpesvirus family, BoHV-1 is restricted to hosts cattle and buffalo (25). The host and viral factors determine the ranges of virus infection in the host.

Successful virus infection is closely associated with viral attachment and penetration into host cells followed by viral DNA replication and export of virus particles (26). BoHV-1 naturally infects cattle and buffalo. However, BoHV-1 also infects and causes diseases in goats and sheep (27). In addition, BoHV-1-specific antibodies have been detected in Asian elephants (*Elephus maximus*) with no clinical symptoms (6). In some cases, this virus has also been isolated from ferrets, antelope, and wildebeest without causing disease (28). BoHV-1 is not infectious to mice, rats, guinea pigs or chick embryos. However, immunocompromised mice lacking interferon receptors can be infected with BoHV-1 (29). Rabbits can be infected experimentally if BoHV-1 is introduced into the conjunctival sac of a rabbit's eye (30). There are no reports of BoHV-1 infection either in human or in human cell lines.

1.1.4 Pathogenesis of BoHV-1.

BoHV-1 starts a productive infection at the mucosal surfaces. It primarily infects epithelial cells in the upper respiratory airway and genital tract mucosa. Viral entry into the cell is mediated through interaction between viral glycoproteins and host cell receptors (31). The lytic replication cycle of virus initiates with the entrance of the virus followed by subsequent viral gene expression and leads to the production of new progeny viruses. The progeny viruses are released into the extracellular environment. Subsequently, the extracellular viruses are spread throughout the infected host either by local dissemination or by systemic spread (viremia) (1). Viral spread through viremia or blood circulation gains access to distant organs or tissues causing clinical symptoms including abortion (32). Besides primary infection at the mucosal surfaces, BoHV-1 neuroinvasion occurs by cell-to-cell spread (11). The virus also establishes a latent infection in the sensory neurons of the peripheral nervous system. Reactivation from latency occurs when the latently infected animal is under stress or during transport from one place to another (33). Stress increases corticosteroid levels that trigger latency reactivation. Once reactivated, the BoHV-1 lytic replication cycle starts, which leads to production of infectious virus particles. Following reactivation infected cell protein 0 (ICP0) promoter activation triggers lytic gene expression (34).

1.2. Structural composition of BoHV-1.

The BoHV-1 virion is composed of four different components. The double-stranded DNA genome is enclosed within a capsid; the nucleocapsid is surrounded by a thick layer containing inner and outer tegument proteins, and an outer lipid envelope with glycoproteins. A schematic diagram of the BoHV-1 structure is presented in Figure 1.1.

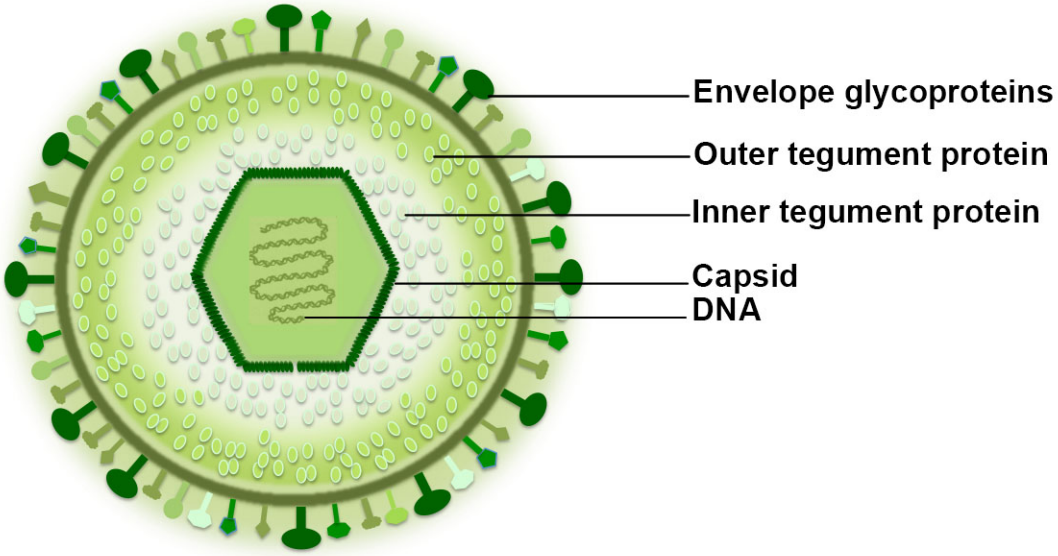

Figure. 1.1 A schematic diagram of BoHV-1 virion structure demonstrating enveloped glycoproteins, tegument proteins and nucleocapsid including DNA.

The BoHV-1 virion consists of four different compartments, the lipid envelope containing glycoproteins, tegument proteins, capsid, and double-stranded DNA.

1.2.1 BoHV-1 Genome.

BoHV-1 is an enveloped double-stranded DNA virus with approximately 135 kilobase pair (kbp) genome (35). Based on the presence of inverted or directly repeated sequences, the herpesviruses genomes are categorized as A-F genomes. The BoHV-1 genome belongs to the class D genome. Class D herpesviruses include varicella-zoster virus (VZV), pseudorabies virus (PRV) and equine herpesvirus 1 (EHV-1). The BoHV-1 genome consists of two unique sequences, a unique long (U_L) and a unique short (U_S) sequence. The L segment is fixed in a single orientation or prototype (P) orientation, whereas the S segment is flanked by large inverted repeats (36). During packaging of the virus, the long linear double-stranded DNA or concatemer is cleaved into individual genomes. During packaging the concatemer DNA is cleaved, and the orientation of the L segment is altered to form inverted L genome. The DNA is then packaged into the virion. Thus, the concatemeric DNA contains a large number of L segments, while the virion DNA consists of a low level of inverted L segments (36). The BoHV-1 genome is composed of 73 open reading frames (ORF) (37). Among them, 33 ORFs are essential and 36 are identified as non-essential. Based on *in vitro* replication characteristics the importance of the remaining two dual copy ORFs is yet to be determined (38).

1.2.2 Envelope glycoproteins of BoHV-1.

The envelope of BoHV-1 contains 11 glycoproteins. These glycoproteins are involved in several steps of virus infection. Glycoproteins are responsible for initial attachment of the virus to the host cell, subsequent penetration, and virus spread between cells (39, 40). Thus, glycoproteins determine the viral tropism for tissues and organs. The identified BoHV-1 glycoproteins are gB (U_L27), gD (U_S6), gC (U_L44), gD (U_S6), gE (U_S28), gG (U_S4), gH (U_L22), gI (U_S7), gK (U_L53), gL (U_L1), gM (U_L10) and gN (U_L49.5)(7). According to a recent study the BoHV-1 virion contains nine glycoproteins, gB, gC, gD, gE, gG, gH, gI, gM, and gL, whereas the other two, gN and gK, were found in the infected cells but were not present in the virion (41). However, the absence of gN and gK in the BoHV-1 virion has been shown in one study only, so further confirmation is needed. The functions of these glycoproteins will be discussed below.

The three major glycoproteins of BoHV-1 are associated with various functions. The major glycoproteins of BoHV-1 are gB, gC, and gD, which can contribute to the virus attachment (39) and can induce immune protection (42). gB is a major component of the virion envelope and

one of the essential proteins of BoHV-1 (39). gB plays a crucial role in viral entry including attachment and penetration of the virus and subsequent virus spread. During viral entry, gB and gC initially bind to the cell surface heparan sulfate (43). Following the initial binding, gD and gB bind strongly to cell surface receptors, non-heparan sulfate (HS) and HS component, respectively (44). gB and gD are responsible for membrane fusion during viral entry (44, 45). gC is not essential for viral entry into the host cells, although deletion of gC attenuates the virus (39). Moreover, intramuscular immunization of gB, gC, and gD generates a high level of neutralizing antibodies, which protects cattle from the disease (42). This demonstrates that these proteins have antigenic properties (46). Thus, these glycoproteins are involved in multiple functions including virus attachment, entry, and spread.

Glycoproteins gE and gI are conserved in all alphaherpesviruses. gE and gI are not essential for virus growth in tissue culture (47). gE and gI are known to form a functional complex that is required for cell-to-cell spread as gE and gI deletion mutant viruses generate smaller plaques (48). Although gE and gI form complexes, a single deletion of either gene demonstrated some distinct characteristics. Incorporation of gE into the virion is not dependent on gI expression, but gE is essential for the integration of both gE and gI into the BoHV-1 virion (48). In a gE-negative virus, the gI is produced and released into the extracellular medium without being incorporated into the virion. A gE deletion mutant contributes to viral attenuation (49). Moreover, gE is relatively immunogenic and suitable as an antigenic marker (50). A gE-negative strain also elicits protective immunity and allows serological differentiation, indicating the potential use of a gE-deleted virus as a vaccine (50, 51).

The glycoprotein gG of BoHV-1 is secreted into the medium, interacts with chemokines and inhibits chemokine activity by blocking their interaction with their receptors (52). A gG-deletion mutant is less virulent indicating that the gG gene has immune evasion properties (53). gG facilitates junctional adherence among BoHV-1-infected cells and thus mediates cell-to-cell spread (40). Furthermore, BoHV-1 gG is an anti-apoptotic viral factor and contributes to the establishment of infection (54).

BoHV-1 gH is necessary for virus entry into the target cells (55). For proper antigenicity, processing, and transport, gH forms a complex with another glycoprotein, gL (56). Moreover, the gH-gL complex induces a neutralizing antibody response and mediates anchoring of gL to the plasma membrane (56). This complex contributes to cell penetration but not

attachment (57). BoHV-1 gK is another essential glycoprotein with a molecular mass of 36 kDa. gK is comprised of four transmembrane domains with an N-terminal cleavable signal (56). gK interacts with U_L20 and is essential for virus production and spread (58).

Glycoprotein gM is encoded by the *U_L10* gene and is associated with the virion and plasma membrane. gM plays a role in membrane penetration as well as cell-to-cell fusion. Deletion of gM in most herpesviruses suggests that it is dispensable for viral replication *in vivo* or *in* vitro (59-61). During BoHV-1 infection gM forms a complex with gN that is necessary for gM processing (62). In addition, PrV (pseudorabies virus) gM is involved in secondary envelopment (63) (64).

1.2.3 Role of *alphaherpesvirus* tegument proteins.

1.2.3.1 Role of tegument proteins in virion dissociation.

The space between the capsid and envelope of an extracellular virion is termed the tegument and contains several proteins that are called tegument proteins. The tegument of *Alphaherpesvirinae* consists of ~ 23 proteins (65). A growing range of functions is attributed to these tegument proteins throughout the course of a viral infection. Immediately after entering into the host cells, the virus releases its outer tegument proteins into the cytoplasm of the infected cell while some inner tegument proteins remain attached to the capsid (66). Virion tegument protein-mediated functions include but are not limited to: virus entry (67), transporting virion components to the nucleus, regulation of host or viral gene expression, immediate early gene transactivation (68), initiation of viral replication, and immune evasion (69).

During viral entry, attachment is not dependent on the tegument proteins but on the interaction of viral glycoproteins with host cell receptors. HSV-1 viral entry is often accomplished by the pH-independent endocytic pathway (70) or pH-dependent pathway (71). Immediately after entry, tegument dissociation depends on an energy consumption reaction such as phosphorylation that involves adenosine triphosphate (ATP), enzymes and ions (Mg+) (72). Since inactivation of virion-associated kinase activity by heat treatment completely blocks virion dissociation, phosphorylation is suggested as a mechanism of virion tegument proteins dissociation (72). Thus, different tegument proteins become the substrates of cellular kinases to facilitate tegument protein dissociation (72). For instance, cellular kinase-2 (CK2)-mediated phosphorylation of VP22 (viral protein) triggers the dissociation of VP22 from the HSV-1 virion.

Some viral kinases, such as US3 (73) and U_L13 (74) are incorporated into the virion to phosphorylate themselves or others to promote tegument dissociation (72).

Tegument protein dissociation from the incoming virion is correlated to the sequence of tegument protein incorporation during viral packaging. For instance, proteins that are incorporated into the tegument earlier during the infection cycle dissociate from the virion later than those incorporated later (75). Following entry, most of the tegument proteins leave the nucleocapsid, while a few remain associated with the capsid (66, 76). Inner tegument proteins such as US3, U_L36 and U_L37 are associated with the nucleocapsid during its transport to the nucleus (77), whereas outer tegument proteins U_L41, U_L11, U_L48, U_L47 and U_L49 are lost in the cytoplasm immediately after entry (66). A BoHV-1 virion demonstrating the inner and outer tegument proteins is illustrated in Figure. 1.1.

Table 1.1 Functions of HSV-1 tegument proteins.

Tegument protein	Functions	References
Roles in Dissociation		
U_S3	Phosphorylates tegument proteins to be disassembled	(72)
U_L13	Triggers viral tegument dissociation by phosphorylating other tegument proteins	(72)
U_L49	Promotes dissociation of other tegument proteins	(72)
Role in transporting capsid		
U_S11	Promotes anterograde transport of capsid	(78)
ICP0	Delivers viral capsid to the nuclear periphery through ubiquitin ligase activity	(79)
U_L14	Targets capsid to the nucleus	(80)
U_L35	Interacts with dynein to transport capsid to the nucleus	(81)
U_L36	Promotes nuclear translocation of incoming capsid, co-ordinates with U_L37 for maximal viral DNA delivery, promotes retrograde capsid transport toward the soma of neurons, and discharges viral DNA from capsid	(82-84)
U_L37	Translocates incoming virus capsid to the nucleus, and promotes maximum delivery of viral DNA	(85)
Roles in gene expression		
ICP0	Counteracts antiviral responses, leads transition from α to β gene transcription	(86-88)
ICP4	Functions as both transcriptional activator and repressor	(89, 90)
ICP34.5	Activates cellular translation initiation factor 2	(91, 92)

U_L14	Promotes nuclear localization of U_L48 to indirectly regulate IE or α gene transcription	(80)
U_L37	Influences transcriptional activation of IE genes	(93, 94)
U_L41	Degrades mRNA to promote viral mRNA turnover	(69, 95)
U_L46	Enhances U_L48-mediated gene transcription	(96)
U_L47	Facilitates U_L48-mediated transcriptional activity	(96)
U_L48	Initiates immediate early gene transcription	(97, 98)
U_L49	Virion incorporated U_L49 RNA influences gene expression	(99)
Roles in assembly and egress		
U_S2	Involves in trafficking of virion to apical surface	(100)
U_S3	Phosphorylates U_L31 and U_L34 for maximal egress efficiency and phosphorylates gB at outer nuclear membrane	(101-103)
U_L11	Forms tripartite complex with U_L16 and U_L48, establishes connection between tegument and membrane	(104-106)
U_L16	Interacts with U_L21 and U_L11 to promote tegumentation of capsid, and secondary development and cell to cell spread	(104, 105)
U_L21	Interacts with U_L16 and U_L11, facilitates additional tegumentation, promotes virus egress	(106)
U_L31	Forms complex with U_L34 to facilitate nuclear egress of nucleocapsid	(107-109)
U_L34	Interacts with U_L31 to promote nuclear egress of nucleocapsid	(109, 110)
U_L36	Facilitates capsid maturation, contributes to the tegumentation of capsid, promotes incorporation of U_L48 into the capsid	(106, 111, 112)
U_L37	Promotes virus maturation, facilitates tegumentation of	(106, 113)

	capsid	
U_L48	Forms complex with U_L41, U_L46, U_L47, and U_L49, links envelope and capsid during virion formation	(114-116)
U_L49	Facilitates complete virion formation	(117-119)

1.2.3.2 The role of tegument proteins in transporting capsid to the nucleus.

Tegument proteins facilitate transport of capsid to the nucleus. Following the dissociation of outer tegument proteins, the capsid is transported to the nucleus through microtubule-dependent interaction of inner tegument proteins with a cytoplasmic dynein/dynactin complex (81, 120). HSV-1 U_L35 has been found to interact with dynein suggesting that it might contribute to the transport of the nucleocapsid to the nucleus (81). Moreover, the two inner tegument proteins, U_L36 and U_L37 tightly control the movement of capsid toward the nucleus. Although no interaction of U_L36 or U_L37 with dynein has been observed as yet, they are likely to bind dynein and to play a role in navigating the incoming nucleocapsid toward the nucleus (82, 121).

U_L36 is essential for delivering viral DNA into the nucleus (122). The importance of U_L36 has been demonstrated by the fact that a U_L36-deletion mutant capsid migrated to the nuclear pore, but did not deliver its DNA into the nucleus (83). The N-terminus of U_L36 might play a role in releasing viral DNA to the nucleus (122, 123). To inject viral DNA from the nucleocapsid into the nucleus, U_L36 interacts with the nuclear pore complex (83, 84). Once U_L36 binds to the nuclear pore complex, it triggers the cleavage of the N-terminus of U_L36. The cleavage of U_L36 is crucial for discharging viral DNA from the nucleocapsid (122, 124). U_L25 also interacts with U_L36 and facilitates release of viral DNA into the nucleus (116, 125). Although U_L37 is not essential for capsid trafficking to the nucleus (85), incoming capsid transport is delayed in the absence of U_L37 (121). In addition, U_L37 is a strong interacting partner of U_L36. Structural analysis of U_L37 revealed that its N-terminus shares structural similarity with the components of cellular multi-subunit tethering complexes (MTCs), which control vesicular trafficking to the destination organelles by tethering transport vesicles (126). Thus, U_L36 and U_L37 contribute to navigate the nucleocapsid to the nucleus.

ICP0, an immediate early protein and an inner tegument protein of HSV-1, possesses ubiquitin ligase activity and interacts with the proteasome. ICP0 is tightly associated with the capsid through a really interesting new gene (RING) finger domain (127). Thus, virion ICP0 delivers the viral capsid to the nuclear periphery by proteasome-dependent degradation of virion or host proteins (79).

Following lytic infection of HSV-1, the amplified virus enters neurons to establish latent infection (128). Inner tegument proteins, U_L36 and U_L37, interact with the host transport

machinery, for instance the dynein-dynactin complex, to facilitate retrograde transport of the capsid toward the soma (cell body) or nucleus of a neuron (129). Following reactivation the lytic replication cycle leads to the formation of new virus particles (130)(131). Newly assembled virus particles then migrate through anterograde transport to infect epithelial cells (130).

1.2.3.3 Effect of tegument proteins on gene expression.

1.2.3.3.1 Herpes Simplex Virus (HSV-1) gene expression.

Once inside the nucleus, the viral genome is transcribed in a tightly regulated manner. Three groups of viral polypeptides denoted as immediate-early (IE), early (E), and late (L) are synthesized in a coordinated and sequential fashion during infection (132). The sequential expression of these genes is correlated because IE proteins are required for the expression of E proteins and subsequently, the E proteins functions are necessary for genome replication and late protein synthesis (132, 133). IE genes are first synthesized. IE gene expression occur in the absence of *de novo* protein synthesis (reviewed in (134)). To date, five IE genes have been identified, ICP4, ICP0, ICP22, ICP24, and ICP47. Although IE gene expression is not dependent on viral protein synthesis, its transactivation is dependent on VP16 (135). ICP0 and ICP27 play critical regulatory roles in gene regulation throughout the infection. These four IE proteins, ICP0, ICP4, ICP22 and ICP27, also function as transcriptional and translational regulators of early and late proteins. In spite of being a positive regulator of IE and late protein transcription, ICP4 also functions as a negative regulator for ICP0 (reviewed in (134)). After initial stages of virus infection, ICP4 halts ICP0 expression to block the inhibitory function of ICP0. ICP0 and ICP4 co-ordinately trigger the expression of E genes (134). These E proteins are required for DNA replication. The identified E gene products include scavenger enzymes including viral thymidine kinase and ribonucleotide reductase, and some enzymes, for instances viral DNA polymerase and DNA helicase, which are directly involved in DNA replication (reviewed in (134)). Finally, following DNA replication, the L genes are synthesized, and early gene expression wanes (reviewed in (134, 136)). The L genes encode mainly structural proteins to produce a complete virion including tegument proteins. Following protein synthesis, pro-capsids are formed and viral DNA is incorporated into the capsid. The capsid is assembled in the nucleus followed by the association of tegument proteins with the capsid (137). The virion then leaves the nucleus by primary envelopment in the perinuclear space and de-envelopment (138). Tegument protein

incorporation also occurs in the cytoplasm. The virion then acquires its final envelope through budding into post-Golgi compartment derived membranes, the process known as secondary envelopment (139). Enveloped virus -containing vesicles then migrate towards the cellular plasma membrane to fuse and release the infectious virion into the extracellular environment (140).

1.2.3.3.2 Role of tegument proteins on gene expression.

HSV-1 U_L48 (also denoted as VP16 or α-transducing factor (α-TIF)) is an outer tegument protein and is conserved in the *Alphaherpesvirinae* subfamily (106). HSV-1 U_L48 is crucial for lytic viral infection (68, 141). Immediately after viral entry, U_L48 dissociates from the viral capsid and forms an U_L48-induced transcription complex with host cell factor-1 (HCF-1) and octamer binding protein-1 (Oct-1). This complex formation is required for initiation of immediate early gene transcription (97, 98). The complex then binds to the IE promoters to trigger transcription of immediate early proteins, including ICP0, ICP4, ICP22, and ICP27, which in turn leads to the transcription of the first viral α, and β genes (142). Moreover, the expression of ICP0 and ICP4 is directly dependent on U_L48 (106). During reactivation from latency in the neuron, U_L48 also initiates immediate early gene transcription (143). Tegument protein U_L46 and U_L47 enhance U_L48-mediated transcriptional activity (96). Another tegument protein, U_L14, induces nuclear localization of U_L48 to regulate immediate early gene transcription indirectly (80). Importantly, the U_L14 homolog of the murine gammaherpesvirus-68 (MHV-68) ORF34 is essential for viral late gene expression (144).

HSV-1 ICP0 acts directly in the resistance of HSV-1 to interferon (IFN). This observation was supported by the fact that in IFN α/β knock-out mice a ICP0-deletion mutant replicated like wild type HSV-1 (86). This protein also plays a role in leading the transition from α to β viral gene expression (145). The shift from α to β viral gene expression depends on the RING finger domain of ICP0 (88). ICP0 forms a transcriptional complex with various viral gene promoters to facilitate transcriptional activation or repression (90, 146). Another tegument protein, ICP4, functions as both a transcriptional transactivator and repressor (89). In addition, ICP4-mediated transcription activation is regulated through binding with DNA and DNA-dependent oligomerization (147). The transition from β to γ genes transcription depends on DNA replication. ICP4 has been demonstrated to be necessary for the activation of γ genes (134).

HSV-1 tegument protein, U_L37 activates the NF-κβ signaling pathway by interacting with TNF-receptor-associated factor 6 (TRAF6) (93, 94). The NF-κβ activity influences the transcriptional activation of IE genes such as ICP0 (94). U_L37 also binds to the HSV-1 DNA binding protein, infected cell protein (ICP8), indicating another possible mechanism of regulation of IE gene transcription (148). Other HSV-1 tegument proteins, such as U_L47, U_L49, and U_S11 bind to the viral and cellular RNA before packaging into the virion (99). In newly infected cells, the virion-incorporated RNA influences gene expression and facilitates a condition suitable for initial infection (99). The U_L41 tegument protein, also called virion host shut-off (vhs) protein, suppresses viral and host cell protein synthesis by degrading mRNA's during early infection (69, 95). ICP34.5, another HSV-1 tegument protein, dephosphorylates cellular translation initiation factor 2 to preclude protein kinase R (PKR)-activated host protein shut-off functions (91, 92).

Some other tegument proteins such as HSV-1 thymidine kinase, U_L23 and a dUTPase enzyme U_L50 contribute to viral DNA replication through the nucleotide metabolism in neuronal cells; for instance, it prevents misincorporation of bases by the viral polymerase (149, 150). In addition, ICP34.5 has been found to be necessary for regulating viral DNA replication by interacting with proliferating cell nuclear antigens (151, 152).

1.2.3.4 Role of tegument proteins during viral assembly and egress.

Following completion of DNA replication, the virion assembly and egress from the nucleus to the cytoplasm are described by the widely accepted envelopment-de-envelopment-re-envelopment pathway (153). An overall pathway of herpesvirus assembly and egress describing the envelopment - de-envelopment - re-envelopment pathway is illustrated in Figure 1.2. During primary envelopment, from nucleus the capsid buds into the perinulcear region to obtain an envelope from the inner nuclear membrane. The fusion of the primary-enveloped membrane with the outer nuclear membrane is called de-envelopment. Finally, the re-envelopment includes the gaining of the final glycoprotein containing envelope before egress (105). The nuclear egress of the nucleocapsid is accomplished by the U_L31 and U_L34 protein complex. U_L31-U_L34 forms a complex through the interaction of multiple regions on the surface of each protein (107-109, 154) Protein complex formation is required for efficient budding of the nucleocapsid from the inner nuclear membrane (155). Formation of this protein complex causes the membrane to curve inwards to form a budding vesicle that encompasses the viral nucleocapsid (156). Thus, the

connection between the nuclear membrane and viral capsid is established through an interaction of the C-terminal region of U_L31. The N-terminal region of U_L31 facilitates the activation of nuclear egress (107). Another tegument protein, US3, regulates the primary envelopment at the inner nuclear membrane by phosphorylation of inner nuclear membrane proteins lamin A/C and emerin. Phosphorylation of lamin A/C results in increased permeability of the nuclear membrane (157-160). In addition, US3 phosphorylates U_L31 and U_L34 and this phosphorylation is required to evenly distribute U_L31 and U_L34 around the nuclear rim of HSV-1 infected cells (101, 102). HSV-1 VP13/14 also associates with U_L31-U_L34 complex to promote nuclear egress (161).

The tegument protein US3 is also involved in the de-envelopment of primary enveloped virions at the outer nuclear membrane. In HSV and PrV US3-deletion mutants the enveloped primary virions were accumulated at the nuclear membrane invaginations suggesting the importance of the function of US3 in de-envelopment at the outer nuclear membrane (101, 102, 162). Moreover, gB and gH also have a role in de-envelopement at the outer nuclear membrane (119). A gB and gH deletion mutant revealed the accumulation of primary virions in the perinuclear region, a similar phenotype to the US3-deletion mutant (163). The fusion of gB with the outer nuclear membrane is enhanced by US3-mediated phosphorylation of gB (103).

The re-envelopment or secondary envelopment is accomplished via incorporation of inner and outer tegument proteins onto the primary virion. The inner tegument proteins, U_L36 and U_L37 are vital for capsid maturation (106) and have been found to be associated with the intranuclear capsid (164, 165). Final tegumentation of the capsid was blocked in U_L36- and U_L37-deletion mutants resulting in accumulation of unenveloped capsids in the cytoplasm (106, 111, 113). U_L36 contains a capsid-binding domain that is crucial for direct interaction with capsid-associated protein U_L25 (166). During secondary envelopment, the molecular interaction of some outer tegument proteins such as U_L16 (tegument)-U_L11 (membrane), U_L48 (tegument)-gH (membrane), and U_L49 (tegument)-gE (membrane) makes the connection between viral capsid, tegument, and membrane (104, 105). U_L16 also interacts with capsid-binding tegument proteins, U_L21 and membrane-associated U_L11, for maximal incorporation of U_L16 into the mature virion. Thus additional anchoring of teguments to the membrane is achieved by the tripartite complex U_L11-U_L16-U_L21. U_L48 also interacts with outer tegument proteins such as U_L41, U_L46, U_L47, and U_L49 to link envelope and capsid during virion formation (114-116). Some tegument proteins also interact with different glycoproteins to facilitate the formation of a

complete virion. For example, the cytoplasmic tail of U_L49 interacts with HSV-1 gD and gE (117-119).

Navigation of the de-enveloped nucleocapsid to the secondary envelopment or re-envelopment site is facilitated by interaction of some tegument proteins and microtubule-dependent molecular motor proteins. For instance, HSV-1 tegument protein US11 interacts with both kinesin-1 and PAT, a kinesin-related protein (78, 167). U_L21, another HSV-1 tegument protein, associates with microtubules possibly to transport capsids to the trans-Golgi network (TGN)-derived vesicles, where the interaction of U_L21, U_L16 and U_L11 establishes a connection between capsid and membrane to facilitate the budding process (168, 169). HSV-1 U_L36 is also involved in transporting enveloped virions (170). Several other HSV-1 tegument proteins, such as U_L21 and U_L49, have been found to interact with microtubules (168, 171). However, the functions of U_L21 and U_L49 interactions remain to be determined. Another tegument protein of HSV-1, U_L37, binds with a cytoskeleton cross-linker dystonin, which is involved in microtubule-based transport (172). U_L37 and dystonin interaction might function as a linker between the capsids and molecular motor and thus, contributes to capsid transport (172). The virion nucleocapsid buds into a TGN-derived vesicle, and acquires an envelope together with an outer vesicular membrane (173). The virus-containing vesicles then migrate to the plasma membrane, and fuse with the plasma membrane to release mature virion (174). In neuronal cells, the glycoprotein gK is essential for viral egress (175).

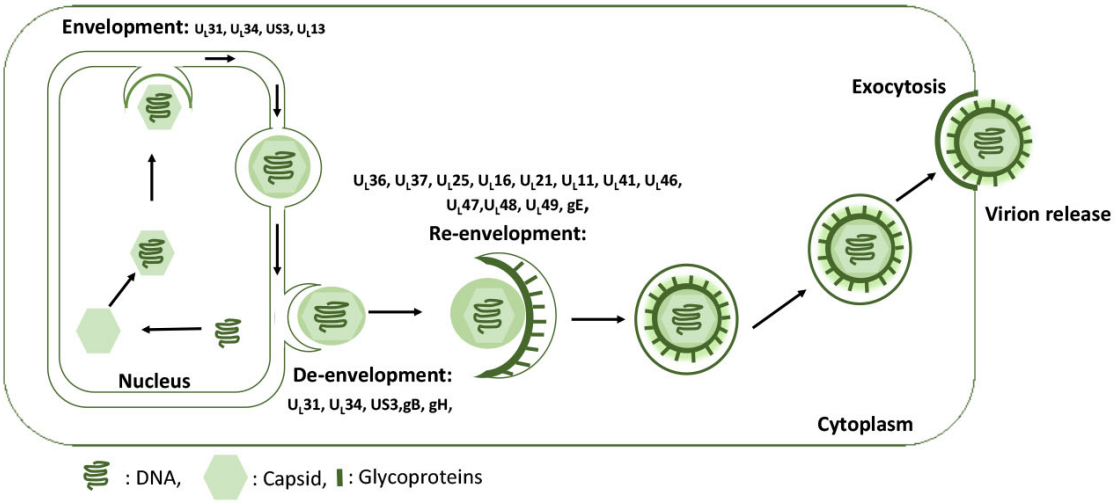

Figure. 1.2 An overall pathway of herpesvirus assembly and egress.

During herpesvirus assembly and egress the envelopment - de-envelopment -re-envelopment pathway is illustrated here.

1.2.3.5 VP8, the major tegument protein of BoHV-1.

The *ul47* gene product, VP8, is the most abundant tegument protein in BoHV-1 virions, and is conserved among different alphaherpesviruses (176-178). VP13/14, the *ul47* gene product of HSV-1, and pUL47 of pseudorabies virus (PRV) are homologues of VP8 (176, 177). In VP8-deleted BoHV-1, incorporation of tegument and other viral proteins was disrupted, resulting in dramatic changes in the morphology of the mature virion (179).

VP8 has been found to shuttle between cytoplasm and nucleus. VP8 is observed in the nucleus early during BoHV-1 infection (180, 181). This nucleocytoplasmic shuttling is attributed to the fact that VP8 contains two nuclear localization signals (NLS) at its N-terminus. NLS1 (^{11}RPRR^{15}) of VP8 is crucial for nuclear localization (182). However, the optimal nuclear localization of the entire VP8 protein requires a 9 amino acid peptide (180). NLS2 (R^{48}PRVRRPRP^{54}) is required for the proper function of NLS1 (180). Later during infection, nuclear VP8 is exported into the cytoplasm (180, 183). Nuclear export of VP8 is facilitated by a nuclear export signal (NES) containing largely hydrophobic and leucine-rich sequences. NES1, located within residues 600-609 (^{600}GVGLIAQRL^{609}), is found to be important (182). However, NES1 possesses weak nuclear export activity suggesting the presence of another possible NES within VP8. The second NES2 is located from amino acid 95 to 123 of VP8. Interestingly, NES2 is more efficient in transporting a fusion protein into the cytoplasm. Nevertheless, in the absence of NES1 and NES2, VP8 is still transported to the cytoplasm indicating another possible mechanism of nuclear export of this tegument protein (182).

VP8 is a multifunctional protein and is involved in interactions with multiple proteins throughout BoHV-1 infection. It interacts with cellular kinase CK2 and viral kinase US3 (184). Recently, it has been demonstrated that phosphorylated VP8 is involved in redistributing promyelocytic leukemia (PML) (185) and also facilitates optimal viral DNA encapsidation and virion incorporation (186). VP8 also associates with DNA damage-binding protein 1 (DDB1) possibly to modulate the DNA damage response (187). Moreover, VP8 associates with mRNA's of some glycoproteins, such as gB, gC and gD (188). In the context of BoHV-1 infection, a RNA-binding activity of VP8 has also been reported (188, 189).

1.2.3.6. Homologs of *ul47* gene product.

The HSV-1 *ul47*-encoded protein denoted as VP13/14 is homologous to BoHV-1 VP8. VP13/14 is involved in the regulation of alpha-transducing factor (alpha-TIF or VP16)-mediated transactivation of immediate early genes. Importantly, immediate early protein, ICP8 coordinates expression of VP13/14 (190). HSV-1 VP13/14 is posttranslationally modified by glycosylation and phosphorylation. Phosphorylated VP13/14 was observed in the virus-infected cells but not in the purified virion (178). In HSV-1-infected cells, VP13/14 is predominantly localized to the nucleus. Nuclear localization of VP13/14 is governed by the N-terminally localized NLS (191). Nuclear translocation is also associated with the US3-mediated phosphorylation of VP13/14 (192). Later during HSV-1 infection, two NES's drive the cytoplasmic localization of VP13/14. The NES functions through the chromosomal region maintenance (CRM1)-dependent or -independent pathway to navigate VP13/14 into the cytoplasm (183, 191). Moreover, nuclear egress of HSV-1 is facilitated through the interaction of VP13/14 with the transmembrane U_L31-U_L34 protein complex (161).. However, whether BoHV-1 VP8 forms a complex with U_L31-U_L34 to facilitate nuclear egress is not known.

VP13/14 possesses RNA binding activity and associates with polyadenylated RNA (189). VP13/14 expressed in *Escherichia coli* (*E. coli*) bound to RNA, while BoHV-1 VP8 did not (189). Thus, RNA binding activity of VP13/14 is independent of posttranslational modifications, whereas BoHV-1 VP8's RNA binding activity is dependent upon this modification (188, 189). VP13/14 associates with ICP27 to maintain the stability of mRNA without affecting the efficacy of reporter RNA translation (193, 194).

Another BoHV-1 VP8 homologous protein is encoded by the *ul47* gene of Marek's diseases virus-1 (MDV-1), a chicken herpesvirus. Although MDV-1 U_L47 is not essential for virus growth, a *ul47*-deleted MDV-1 mutant virus exhibited impaired growth properties (195). The *ul47* gene-encoded protein from another avian alphaherpesvirus, infectious laryngotracheitis virus (ILTV), is also not essential for *in vitro* replication, but required for virulence (196). Moreover, a PRV *ul47*-deletion mutant demonstrated impaired virion morphogenesis and a reduction in virus titer suggesting a role in virion assembly (177). In all cases, the *ul47* gene product was required for virulence. However, the detailed virulence mechanism of BoHV-1 VP8 or other homologous proteins is unknown.

1.3. Innate antiviral responses to Herpes Simplex Virus (HSV-1) infection.

Virus infections are detrimental to host cells. Host cells trigger innate cellular defenses in response to virus infection. Innate immune responses restrict viral replication, rendering the cells less permissive to virus infection. Largely pre-existing pattern recognition receptors (PRRs) such as Toll-like receptors (TLRs) of cells recognize viral components or pathogen-associated molecular pattern (PAMPs) (197). Recognition of PAMPs by PRRs triggers activation of intracellular signaling pathways to induce cellular cytokine, chemokine and interferon (IFN) production (197). Soon after virus infection, the recognition of PAMPS triggers the IFN signaling pathway.

1.3.1. Interferons and classification of interferons.

Interferons are cytokines secreted by the host cells in response to virus infection. IFNs are multifunctional cytokines that function as major components of innate immunity. The IFN response is one of the barriers that a virus has to overcome to establish infection. IFN possesses a unique ability to trigger the expression of IFN-stimulated genes (ISGs) and develop an antiviral state in neighbouring virus-infected cells.

IFNs can be categorized into two major groups based on their primary structure: type I and type II. Type I IFNs are secreted directly in response to virus infection and includes IFN-α, IFN- β, IFN-ε, IFN-κ and IFN-ω (198). IFN-γ belongs to the type II IFNs (199). The best-characterized IFNs are IFN-α and IFN-β synthesized by most cells in response to virus infection, while IFN-γ is secreted by activated T-lymphocytes and natural killer cells (199). All type I IFNs generally bind to the same cell surface receptor denoted as a type-I IFN receptor, whereas type II IFN binds to the type II IFN receptor (199). In vertebrates, type I interferon is crucial for controlling virus infection. Researchers reported that type I IFN receptor knockout mice are more susceptible to virus infection despite the presence of a normal adaptive immune system (200). On the other hand, type II IFN is involved in immune regulation. In spite of structural dissimilarities between these two types of IFN, the signaling cascades that activate these IFNs are occasionally overlapping. However, in many cases, the non-redundancy of these two systems elicits an efficient immune response against specific virus infections.

Another novel recently identified IFN, IFN-λ, denoted as type III IFN, consists of IFN-λ1, IFN-λ2, and IFN-λ3. Type III IFNs are structurally similar to the type I IFN, while the

receptor is different. Type III IFNs are induced by virus infection or double-stranded RNA (dsRNA) rendering cells less permissive to virus infection.

1.3.2. Modulation of IFN response by herpes simplex virus-1 (HSV-1) proteins.

Immediately after virus infection, viral constituents are recognized by surface, or intracellular receptors denoted as PRRs. PRRs are activated following recognition of PAMPs. PRR activation leads to the expression of genes with pro-inflammatory activities such as cytokines and type I IFN (reviewed in (201)). Cytosolic PRRs include an essential family of receptors such as Toll-like receptors (TLRs) or DNA or RNA sensors. TLRs bind to microbial elements leading to the activation of intracellular signaling cascades that promote an antiviral cellular response. Nevertheless, to evade host antiviral responses, HSV-1 has multiple viral evasion mechanisms to attenuate the host anti-viral response and to expedite virus infection (202). Therefore, inhibition of the innate antiviral immune response is crucial for the establishment of HSV-1 infection. Here we will discuss some of the HSV-1 proteins that function in modulating the type I IFN response.

1.3.2.1 Immediate early protein-0 (ICP0).

Inhibition of downstream IFN signaling is controlled by viral evasion mechanisms. All herpesviruses target Interferon Regulatory Factor-IFN, (IRF-IFN) pathways at different levels (165). The immediate early protein, ICP0, is involved in subverting type I IFN signaling pathways. During virus infection TLRs recognize PAMPS and recruit the downstream adaptor proteins such as myeloid differentiation primary response protein (MyD88), MyD88 adaptor-like protein (Mal) and Toll/interleukin 1 receptor domain-containing adaptor-inducing IFN-β (TRIF) leading to the activation of Interferon Regulatory Factors (IRFs) including IRF-3, IRF-7, and NF-κB (202, 203). This causes IRF3 hyperphosphorylation and translocation to the nucleus to activate the IFN-β promoter for initiation of the IFN response and IFN-β production (204). ICP0 is a multifaceted protein and possesses E3 ubiquitin ligase activity. During HSV-1 infection ICP0 blocks nuclear accumulation of IRF3 and thus, inhibits IFN production (205). Mechanistically, cytoplasmic localization of ICP0 is involved in degradation of IRF3 as well as in sequestration of IRF3 and CBP/300 (205-207). Cytoplasm-localized ICP0 is thought to be associated with the inhibition of IRF3 phosphorylation, dimerization and nuclear translocation. Another possible

mechanism of prohibiting IRF3-mediated IFN signaling includes either prevention or reversing the phosphorylation of IRF3, which is indispensable for nuclear translocation and dimerization of IRF3 (205, 206).

MyD88 consists of two domains, a death domain and a Toll-like receptor domain that functions as an adaptor molecule and is necessary for TLR-mediated inflammatory responses (208). ICP0 exerts its ubiquitin ligase activity, and its expression leads to a reduction in the level of TLR-adaptor proteins, MyD88 and Mal. Thus, it blocks the TLR-2 mediated IFN-signaling pathway (209). In addition, ICP0 inhibits TLR-activated nuclear factor (NF-κβ). To prevent TLR-mediated NF-κβ activation, ICP0 delocalizes USP7 from the nucleus to the cytoplasm. Once in the cytoplasm, USP7 interacts with TNF receptor-associated factor (TRAF6) and IKK-γ to dissociate their polyubiquitin chains, impeding activation by TLRs and their degradation. TRAF6 and IKK-γ are required for nuclear translocation of NF-κβ and subsequent activation of NF-κβ target genes (209). Another study demonstrated that ICP0 also binds with NF-κβ subunits p65 and p50 to prohibit nuclear accumulation of p65 and to degrade p50 by using E3 ubiquitin ligase activity in the ubiquitin-proteasome pathway (210).

Another possible mechanism by which host cells exert or initiate antiviral responses is through nuclear sensors. IFN-inducible protein-16 (IFI16) is a nuclear and cytoplasmic sensor, and a DNA binding protein. Although this protein is predominantly nuclear, unlike other DNA sensors, it shuttles between the cytoplasm and the nucleus (211, 212). During HSV-1 infection, IFI16 recognizes viral DNA in the nucleus, which leads to IFI16 acetylation and subsequently, IRF-3 phosphorylation to induce IFN-β signaling (213). An IFI16-mediated type I IFN response has been demonstrated in response to DNA virus infection (214, 215). One study revealed that during HSV-1 infection, IF116 is degraded by proteasome-mediated degradation, and this degradation is dependent on the E3 ubiquitin ligase activity of ICP0. Another report suggested that the degradation of IFI16 is not solely dependent on ICP0 as an ICP0-null mutant is able to degrade IFI16 (216). The discrepancy between the former and latter study has been explained by the fact that different cell types and different infection conditions were utilized.

1.3.2.2. ICP27.

Recent evidence indicates that ICP27 functions as a major modulator in down-regulation of IFN signaling during HSV-1 infection. ICP27 functions in multiple pathways to alter type I

IFN production. The NF-κB pathway triggers expression of genes involved in immune responses. In response to virus infection inhibitory kappa B (IκB) is phosphorylated and degraded by ubiquitination. NF-κB is released from IκB and translocates to the nucleus where it triggers transcription of the target genes (217). An ICP27-deletion mutant of HSV-1 produces a higher level of IFN-α/β in both HeLa cells and macrophages (136). Mechanistic studies revealed that ICP27 inhibits NF-κB and IRF3 activation to suppress IFN and cytokine induction during HSV-1 infection (136). Other research demonstrates that ICP27 binds inhibitory kappa B alpha (IκBα) to block its phosphorylation and ubiquitination and thus, ICP0 stabilizes IκBα (218). As a consequence, IFN production is reduced.

The Janus kinase (JAK)-signal transducer and activator of transcription (STAT) signaling pathway is activated by binding of ligands, such as IFN to their receptors (219). Activated JAK phosphorylates its substrates including STAT1 and STAT2. Phosphorylated STAT1 and STAT2 heterodimerize and translocate to the nucleus. Once in the nucleus, STATs bind to the IFN-response element to trigger IFN production (219). HSV-1 infection interferes with JAK-STAT signaling pathway. The potential mechanisms of inhibition of the JAK-STAT signaling pathway by HSV-1 ICP27 include blocking of STAT1 phosphorylation as well as inhibition of STAT1 translocation into the nucleus (220). Thus, ICP27 plays a pivotal role in immune response escape at early stages during HSV-1 infection.

1.3.2.3 ICP34.5.

TANK-binding kinase-1 (TBK1) functions as a critical player in both TLR-dependent and independent signaling pathways. Recognition of microbial components causes TBK1-mediated phosphorylation of IRF3 leading to cytokine expression. ICP34.5, a gamma protein of HSV-1, interacts with TBK1 and sequesters TBK1 to inhibit phosphorylation of IRF3 and its accumulation into the nucleus and thus, blocks induction of IFN-stimulated gene promoters (221, 222). As a result, ICP34.5 inhibits IFN production.

Double stranded-RNA dependent protein kinase (PKR) is activated by virus infection. Upon activation, PKR phosphorylates its downstream target, eukaryotic translation initiation factor-2α (eIF2α). The inhibition of eIF2α leads to blocking of viral and cellular mRNA translation, which prevents virus production (223). However, during HSV-1 infection, although PKR is activated, ICP34.5 interacts with and redirects phosphatase 1 alpha, which

dephosphorylates eIF2α to enable protein synthesis (92, 224).

1.3.2.4 US3.

Toll-like receptor 3- mediated type I IFN production is well characterized. It can induce the expression of type I IFN by detection of double-stranded RNA. Impaired TLR-3 signaling results in higher HSV-1 replications. Similarly, in TLR3-deficient cells, HSV-1 infection produces much less IFN (225, 226). The tegument protein US3 of HSV-1 can reduce TLR3 expression and inhibit the TLR3-mediated IFN response. This finding was also supported by the fact that US3-deletion mutants exhibit stronger IRF3 activation and thus exerts a stronger type I IFN response (227). US3 also suppresses the TLR2 signaling pathway by inhibiting polyubiquitination of TRAF6. This inhibition was dependent on the kinase activity of US3 (228).

Activation of most of the PRRs including TLRs leads to the activation of the NF-κβ signaling pathway. This activation facilitates cytokine expression including type I IFN production (229). p65/RelA is a subunit of NF-κβ and functions as a crucial transcription factor in the innate immune response. Some DNA and RNA viruses antagonize innate immune responses by modulating the p65-mediated signaling pathway. Likewise, HSV-1 US3 hyperphosphorylates p65, inhibiting its nuclear translocation and thus abrogates NF-κβ activation to decrease IFN production (230).

IRF3 dimerization is associated with the activation of anti-viral responses particularly the production of type I IFN. US3, the serine/threonine kinase of HSV-1, can significantly down-regulate type I IFN production. This inhibition is facilitated by US3-mediated hyperphosphorylation of IRF3 and inhibition of its dimerization and nuclear accumulation (231).

1.3.2.5 US11.

RIG-I (retinoic acid-inducible gene)-like receptors (RLRs) include RIG-I and melanoma- differentiated-associated protein-5 (MDA5). These receptors are critical for initiating antiviral responses. RIG-I detects RNA containing 5'-triphosphate groups, while MDA5 recognizes double-stranded RNA (dsRNA) and stimulates adaptor proteins to activate IRF3 and NF-κB (232, 233). This activation triggers expression of type I IFN. HSV-1 infection down-regulates RLR signaling by interfering with multiple protein functions in this pathway. US11, one of the tegument proteins of HSV-1, is an RNA binding protein (234). US11 uses its carboxy-

terminal binding domain to interact with RIG-I and MDA5. The association of US11 with RIG-I and MDA5 abrogates the formation of MDA5/ mitochondrial antiviral signaling protein (MAVS) and RIG-I/MAVS complexes and consequently inhibits IFN-β production (235).

US11 also functions to suppress type I interferon production through interacting with the double-stranded RNA binding protein, protein kinase R activated protein (PACT). RIG-I interacts with PACT and gets activated to be functional (236). US11 interacts with PACT and thus, blocks the association of PACT with RIG-I to inhibit type I IFN production (237).

1.3.2.6 U_L41.

The *U_L41* gene product, vhs, is known as a crucial determinant of HSV-1 virulence (69). vhs is an mRNA-specific RNase that is involved in triggering rapid shutoff of host mRNA degradation and host cell protein synthesis (reviewed in (238)). vhs, a multifunctional protein, is involved in various immunomodulatory mechanisms including the regulation of IFN-α/β production during HSV-1 infection (239, 240). The interference of vhs with IFN production is demonstrated by the fact that vhs deficiency in HSV-1 increases susceptibility to IFN-α/β (241). Vhs inhibits phosphorylation of STAT1 and thereby, suppresses the JAK/STAT signaling pathway. This suppression of JAK/STAT1 signaling results in impaired expression of IRF7 and subsequently reduces IFN-α production. IRF7-mediated functions are crucial for the establishment of effective antiviral responses against HSV-1 infection (242). Vhs also up-regulates the suppressor of cytokine signaling (SOCS) expression that leads to the inhibition of IFN production. Thus, for the establishment of HSV-1 infection, vhs down-regulates the IFN signaling pathway.

1.3.2.7 U_L36.

TNF receptor-associated factor 3 (TRAF3) plays a critical role in the RLR signaling pathway by linking an upstream adaptor protein, MAVS, to TBK1 (243, 244). With the activation of TRAF3, lysine-63 (K-63) is polyubiquitinated. This is essential for the induction of the MAVS signaling pathway. MAVS recruits TBK1 to phosphorylate IRF3 for initiation of IFN production. UL36, the largest tegument protein of HSV-1, is conserved among the herpesviridae family and is indispensable for virus replication. The N-terminus of U_L36 contains a deubiquitinase (DUB) motif denoted as U_L36 ubiquitin-specific protease (U_L36USP) (123, 245). U_L36USP blocks IRF3

dimerization-mediated promoter activation and IFN-β transcription that are induced by Sendai virus (Sev) infection. In parallel, the DUB activity of U_L36USP is responsible for deubiquitination of TRAF3 and for prevention of the recruitment of downstream adaptor molecule TBK1. Hence it blocks IFN production (246).

1.3.3 Modulation of IFN responses by HSV-1 through DNA sensors.

Cytosolic DNA is detected by DNA sensors and triggers immune responses by inducing inflammatory gene expression. Thus, the DNA sensor can stimulate induction of antiviral responses, including IFN production, independent of RIG-I and TLRs (247). To date, a number of DNA sensors have been identified with potential roles in antiviral signaling pathways. Stimulation of IFN genes (STING) is predominantly expressed in T cells, epithelial cells, and endothelial cells, as well as in macrophages and dendritic cells, and is a crucial component for induction of type I IFN signaling by the detection of cytosolic DNA (248). STING functions by recruiting TBK1 and IRF3 for IRF3 phosphorylation and subsequent production of type I IFN. STING knockout mice showed increased susceptibility to HSV-1 infection, indicating the significance of STING in host restriction of HSV-1 infection (249). Researchers reported that viral proteins ICP0 or US3 are involved in altering the function and stability of STING in a cell type-dependent manner (250). However, HSV-1-facilitated immune evasion strategies of STING-mediated responses are still being elucidated.

Another recently identified DNA sensor denoted as cyclic GMP-AMP synthase (cGAS) belongs to the nucleotidyltransferase family and shares enzymatic and structural features with dsRNA-sensing 2-5-oligoadenylate synthase (OAS) (251). cGAS, a major component of the cGAS-STING pathway, undergoes significant conformational changes with the detection of dsDNA. Upon DNA binding, it catalyzes GTP and ATP to form an endogenous second messenger, cyclic GMP-AMP (cGMP). cGMP then binds to STING, inducing its activation by causing dramatic conformational changes to STING. Activated STING triggers phosphorylation of IRF3 via TBK1 to promote nuclear translocation IRF3. Subsequently, this cascade triggers transcription of type I IFN (252). HSV-1 infection interferes with the cGAS-mediated IFN signaling pathway. This interference is supported by evidence that significantly increased susceptibility was observed against HSV-1 infection in cGAS knockout mice compared to wild-type mice (215). The cGAS-mediated signaling pathway is dependent on STING. As a result, any

viral protein interfering with STING or its downstream component affects the cGAS pathway. Until now, only one HSV-1 protein, the *U_L41* gene product vhs, has been found to abrogate the cGAS-STING pathway (253). During HSV-1 infection, vhs reduces accumulation of cGAS to block viral DNA recognition by host cells as well as degrades cGAS via its RNAase activity to evade cGAS-STING mediated antiviral responses (253). In addition, recent research revealed that due to recognition of HSV-1 and Kaposi's sarcoma-associated herpesvirus (KSHV) genome by histone-2B-IFI16 (H2B-IFI16), the complex IFI16-breast cancer-1-H2B (IFI16-BRCA1-H2B) interacts with cGAS and STING to induce IFN-β production (254).

1.4 Modulation of DNA damage response by herpesviruses.

1.4.1 DNA damage response.

Damaged DNA includes any breaks in the DNA strand, missing base pairs in the DNA, or chemical-induced rearrangements of the bases (255). Throughout the lifespan of a cell, the cellular genomic integrity is threatened by intrinsic or extrinsic stresses, such as replication errors, uncontrolled recombination, microbial infections, endogenously metabolized by-products, reactive oxygen species, and exposure to ultraviolet (UV) light or environmental mutagens (256). The most common DNA damages are DNA single-strand breaks (SSBs) and DNA double-strand breaks (DSBs) (reviewed in (257)). These DNA damages pose a severe threat to genomic DNA as they can lead to chromosomal aberration, abnormal amplification, and rearrangements finally leading to genomic instability.

To survive these detrimental situations, as well as to avoid the fundamental threat of genomic erosions, eukaryotic cells evolved a sophisticated and well-coordinated network denoted as DNA damage response (DDR) (258). The complex signaling network of DDR consists of recognition of DNA damage and transmission of signals to the regulators. The transmitted signals control the cell fate either by arresting the cell cycle, by triggering the DNA-repair pathway or by terminating cells by inducing apoptosis. The DDR pathway is orchestrated with two major kinases, ataxia-telangiectasia mutated (ATM) and ATM- and RAD-related (ATR) kinase. These kinases are the central regulator of DDR pathways and are activated in response to DNA damage (258). Over the past few decades, researchers revealed that virus infection and host cell DDR pathways are strongly inter-connected, and that the DDR pathway plays a pivotal role in the establishment of virus infection. As such, virus infection is associated with the activation or

repression of specific components of DDR pathways in a temporally coordinated manner to favor viral infection (259). In the following sections, the regulation of ATM- and ATR-mediated DDR pathways by different herpesviruses will be discussed. A schematic diagram demonstrating the modulation of DDR pathway by different herpesviruses, such as HSV-1, EBV, HCMV, and KSHV is presented in Figure 1.3.

1.4.2. Regulation of DDR pathways by different herpesviruses.

To date different herpesviruses are known to modulate the DDR pathways. The DDR signaling pathway contains a major kinase cascade, which mediates phosphorylation of downstream targets to facilitate major cellular events, such as DNA repair or apoptosis. ATM is one of the kinases and plays a vital role upstream of the DDR pathway. ATM is expressed in most of the tissues and loss of ATM activity results in autosomal recessive disorder ataxia-telangiectasia (260). ATM kinase functions as a master regulator of the DDR pathway. In response to DSBs or oxidative stress, the ATM-mediated DDR pathway coordinates cell-cycle checkpoint activation, DNA repair, and eventually decides the cell fate by inducing cell cycle arrest or apoptosis (reviewed in (261)). In resting cells, ATM is predominantly nuclear and exists in its inactive form as a homodimer. Upon DNA damage, ATM undergoes autophosphorylation at residue S1981. This autophosphorylation triggers the dissociation of ATM from its inactive homodimer form to generate an active monomer that facilitates phosphorylation of its various downstream targets (reviewed in (262)). A mutation in the S1981A of ATM fails to form active monomer and subsequently, loses the ability to activate ATM, highlighting the importance of ATM phosphorylation in ATM activation (263). Conversion of inactive ATM dimer to active ATM monomer has also been observed through the MRN (MRE11-RAD50-NBS1) complex (264). MRN complex unwinds the DNA ends, which are essential for ATM monomerization (265). Following DNA damage, one of the earliest events is the phosphorylation of a variant of histone, H2AX, by ATM kinase. This phosphorylated form of H2AX is known as **γ**H2AX (266). **γ**H2AX acts as a docking site for multiple DDR proteins. As a downstream regulator, the MRN complex also gets phosphorylated to carry out numerous functions including DNA recombination and DNA double-strand break repair. In the ATM/NBS1 pathway, upon DNA damage some proteins including NBS1 and breast cancer-1 (BRCA1) migrate to the DSB sites independent of the ATM activation. ATM is activated followed by recognition of DNA damage. Upon

activation, ATM phosphorylates multiple nucleoplasmic substrates including p53 and NBS1. Consequently, NBS1 phosphorylates SMC1 as a downstream target. Phosphorylation of SMC1 is critical for decreasing chromosomal aberrations and increasing cellular survival (267). Activated ATM also activates p53 to link the DNA damage response to cell cycle checkpoint pathways (268). p53 phosphorylation by ATM stabilizes p53. In addition, following DNA damage, ATM phosphorylates cellular checkpoint kinases CK1 and CK2, which subsequently phosphorylates p53, contributing further stabilization of p53 (269). Finally, p53 activation stimulates cell cycle checkpoint activation or induces apoptosis (270). In ATM-deficient cells, the level of DNA damage increases due to lack of DNA damage detection. Hence, the damaged DNA is sustained in the absence of DDR. Depending on the level of DNA damage, multiple pathways are activated. For instance, minor DNA damage activates sensor proteins to be recruited at the damaged site for DNA repair. However, if the damage is too extensive to repair, the DDR pathway gets activated to trigger some signal specialized transducer proteins (258). These effector proteins induce temporary cell cycle arrest or halt the cell cycle or trigger apoptotic pathways (258).

1.4.2.1 Modulation of DDR by HSV-1.

A contribution of the DDR pathway to HSV-1 DNA replication has been demonstrated. During HSV-1 infection several cellular factors including MRE11, RAD50, and NBS1 have been associated with homologous recombination (HR) (271). With sensing of DSB, HR is facilitated through MRN complex formation and ATM signaling. Following DNA damage, ubiquitination of histone-2A (H2A) by ring finger protein-8 (RNF8) and ring finger protein-168 (RNF168) facilitates recruitment of other downstream effectors such as p53-binding protein-1 (53BP1), RAD51 recombinase (RAD51), and breast cancer-1 (BRCA1) (reviewed in (272)). These effectors mediate homologous recombination to repair DSBs. HSV-1 manipulates the HR pathway during productive infection. Although HSV-1 requires HR cellular machinery components for efficient virus production, chromosomal integration assays reveal that it suppresses HR during infection (273). Besides, HSV-1 infection triggers ATM activation, which is demonstrated by the phosphorylation of ATM, NBS1, and checkpoint kinase-2 (CHK2) (271, 274). Similarly, an ATM- or MRN-deficient cell lines the virus production was reduced (271, 274, 275). However, the immediate early protein ICP0 of HSV-1 degrades RNF8 and RNF168

through ubiquitinase activity and thereby, inhibits the recruitment of BRCA1 and 53BP1 to the damaged foci (276). Thus, in spite of ATM activation during HSV-1 infection, HR is inhibited (273). Consequently, HSV-1 infection is suggested to block the HR to favor virus replication (271, 277).

ATR, another checkpoint kinase is also activated with the ATM substrates, and thus, ATR activation is related to ATM activation (278). ATR and ATR-interacting protein (ATRIP) are recruited to stretches of single-stranded DNA (ssDNA). The ATR signaling is initiated through ATR activation through recruitment of 9-1-1 (RAD9-RAD1-HUS1), which in turn recruits an ATR-activator, DNA topoisomerase 2 binding protein-1 (TopBP1). Subsequently, TopBP1 phosphorylates checkpoint kinase-1 (CHK1) to activate ATR-CHK1 signaling pathway (reviewed in (279)). Although ATM activation is observed during HSV-1 infection, it abrogates the ATR-CHK1 signaling pathway (280). A mechanistic study revealed that HSV-ICP8 and three proteins of the helicase/primase complex bind to the substrates of cellular replication protein A (RPA) and ATR. Binding of viral proteins to these substrates blocks recruitment of 9-1-1 complexes and therefore, prevents engagement of ToBP1. Subsequently, the ATR signaling is inhibited (281). The purpose of blocking the ATR pathway is not clear. However, since ATR signaling prevents DSB formation, it is anticipated that the DSB formation might be beneficial for HSV-1 replication (282). In spite of suppression of ATR signaling, HSV-1 infection has been found to recruit ATR pathway proteins to the virus replication compartment, which are vital for virus production. Thus, ATR-signaling proteins might function in favor of virus genome replication by inhibiting cellular DNA replication (279).

DNA-protein kinase (DNA-PK) signaling pathway responds to DSBs. Following detection of DSBs activated DNA-PK phosphorylates some effector protein to repair DSBs through nonhomologous end joining (NHEJ) (283). It is anticipated that during HSV-1 infection the presence of nicks and gaps in the HSV-1 genome will trigger the DNA-PK signaling pathway. However, during HSV-1 infection the DNA-PK signaling pathway is attenuated through an ICP0-mediated function (279, 284).

1.4.2.2 Regulation of DDR by Epstein-Barr Virus (EBV).

Epstein-Barr Virus **(**EBV) infection is known to modulate DDR pathways. EBV is a ubiquitous human herpes virus. EBV infection causes mononucleosis and sometimes cancers,

such as Burkitt's lymphoma and Hodgkin's lymphoma. Thus, EBV is classified as human tumor virus (285). EBV contains a 170 kilobase double-stranded DNA. It infects both B-lymphocytes and epithelial cells. In EBV-infected cells, the episome exists in the host cell nuclei as an extrachromosomal DNA enclosed with the histones (286). With the entrance of virus into the cells, the lytic DNA replication starts with the synthesis of viral DNA replication proteins. The EBV genome is replicated through a rolling circle mechanism generating long linear DNA concatemers like other herpesviruese, which are cleaved into individual genomes before packaging into viral capsid (287).

Like other herpesviruses, EBV is also involved in modulation of the DDR pathway. EBV infection is correlated to the deregulation of the ATM signaling pathway in Hodgkin's lymphoma. Down-regulation of ATM expression has been found to be associated with the EBV latent membrane protein-1 (LMP-1). In addition, suppression of DNA repair was observed in a LMP-1 expressing cell line through down-regulation of the ATM signaling pathway (288). Moreover, EBV-positive nasopharyngeal (NPC) cells had reduced levels of ATM transcripts and proteins (289). Similarly, upon exposure to γ radiation, EBV-infected cells demonstrated a defective DNA damage response. However, in one report, LMP1 has also been found to up-regulate ATM signaling through activation of the NF-κB pathway (290). This discrepancy could be due to the action of different levels of LMP1 or ATM expression in different cell lines (291). Importantly, a high level of LMP1 expression leads to the induction of apoptosis (292).

Another EBV protein, EBV Nuclear antigen 3C (EBNA3C), disrupts the G2/M cell cycle checkpoints. EBNA3C-expressing cells are unable to arrest cells in the G2/M checkpoints. Besides, being a crucial effector of the ATM/ATR pathway, CHK2 interacts with EBNA3C, and this interaction is involved in inhibition of cell cycle arrest (293). Importantly, ATM or CHK2 inhibition significantly increases the B-cells transformation efficiency. Thus, EBNA3C-mediated attenuation of DDR in EBV-infected cells promotes primary B-cell hyperproliferation (294). Overall, EBV infection down-regulates ATM expression to attenuate the ATM-mediated DDR pathway and subsequently, impedes the downstream effector functions. This disruption of the ATM-mediated pathway may contribute to the genomic instability and tumorigenesis, as well (291). In addition, EBV immediate-early lytic protein, BZLF1, also mislocalizes the DDR proteins followed by EBV infection (295). However, during lytic reactivation, EBV replication is triggered by ATM activation. It has been reported that the induction of BZLF1 is dependent on

ATM activation (296). Likewise, ATM knockdown in epithelial cells infected with EBV resulted in reduced virus production (296). Thus, EBV infection modulates the DDR pathway in both latency establishment and lytic reactivation. These findings indicate that the host cells closely monitor the viral DNA replication and in parallel, EBV exhibits different strategies to establish infection.

The involvement of the DNA-PK signaling pathway during EBV infection is less studied compared to the ATM- and ATR-signaling pathways. However, according to recent research during EBV infection DNA-PK signaling is impaired, and this attenuation was associated with the function of viral oncoprotein, LMP1 (297).

1.4.2.3 Regulation of DDR by human cytomegalovirus (HCMV).

Like other DNA viruses, HCMV infection also elicits DDR responses. The β herpesvirus, human cytomegalovirus (HCMV), is responsible for causing diseases in immunocompromised and immunosuppressed patients, including pneumonitis and retinitis (298). HCMV is an enveloped DNA virus with ~235 kilobase pair double-stranded DNA genome (299). Like HSV-1, HCMV DNA replication and gene expression are also coordinated in a tightly controlled manner, including immediate early (IE), early (E) and late (L) protein expression (300). The IE proteins coordinate expression of E and L proteins to initiate DNA replication. Some of these proteins are directly involved in viral DNA replication while others are associated with the modulation of cellular factors (301). The ATM or ATR signaling pathway is linked to the induction of cell cycle arrest or apoptosis. HCMV infection alters the cell cycle checkpoints to suppress cellular DNA synthesis, while favoring viral DNA replication. HCMV infection is known to both activate and inhibit the ATM-mediated DDR pathway. Induction of DDR by HCMV infection includes activation of ATM and its downstream targets such as H2AX, NBS1, CHK1, and CHK2. HCMV proteins IE1, IE2, pp71 and U_L97 can induce DSBs and subsequently, activate ATM, H2AX, and P53. Thus, they contribute to HCMV replication (reviewed in (302)). U_L35 is also involved in activation of DDR by inducing phosphorylation of H2AX and formation of 53BP1 foci to arrest the cell cycle. Thus, the ATM-mediated DDR pathway contributes to HCMV DNA replication.

However, although the ATM-mediated DDR pathway is activated during lytic infection, it has been reported that the downstream signaling components were blocked by HCMV infection

(303). For example, CHK2 activation was inhibited by HCMV infection. Following DNA damage, the DDR proteins migrate to the nucleus to coordinate the DNA repair proteins. However, later during HCMV infection, it alters the localization of ATM and CHK2 from the nucleus to the cytoplasm to interfere with their normal function. Thus, it is proposed that HCMV infection induces ATM-mediated checkpoint activation in response to DSBs, whereas the virus responds by mislocalization of checkpoint proteins to inhibit the signaling pathway (303). Luo et al, 2007 also reported the disruption of both ATM- and ATR-mediated signaling pathways by HCMV infection. At the initial stage of infection, phosphorylation of NBS1 was observed through ATM activation (304). However, the relocalization of NBS1 to the site of DNA damage was inhibited by HCMV infection (304). A relocalization of DDR proteins, such as P53, pATM, NBS1, RAD50, ATRIP, CHK1 and CHK2 to the replication compartment by HCMV infection was also reported (reviewed in (302). Thus, although HCMV infection activates the ATM-mediated DDR, it manipulates the localization of DDR protein to subvert the full activation of the ATM signaling pathway (304). EBV infection is also involved in disrupting the ATR signaling pathway. Disruption of ATR-CHK1 signaling is mediated through impaired activation of STAT3, which facilitates ATR-mediated phosphorylation of STAT3 (305).

1.4.2.4 Modulation of DDR by Kaposi's sarcoma-associated herpesvirus (KSHV).

The DDR pathway is also modulated by KSHV. KSHV (also known as human herpesvirus-8) belongs to the family of gamma-herpesviruses. It contains a large double-stranded DNA. KSHV is etiologically associated with Kaposi sarcoma (KS), a form of malignancy in human skin (306, 307). Like other members of the herpesvirus family, the KSHV lifecycle also consists of both latent and lytic phases. This virus is also involved in the regulation of the DDR pathway to ensure evasion of host cell antiviral defenses. KSHV encodes several homologs of host genes to modulate the host cell response. Such genes include viral interferon regulatory factor (vIRF1), viral interleukin-1 (vIL1), and viral Bcl2 (vBcl2) (reviewed in (308). Lytic replication of KSHV-1 results in sustained DDR in infected cells. The elevated level of γH2AX evidences the induction of DDR (309). This activation of DDR is induced before initiation of viral DNA replication. Researchers speculate that induction of DSBs can be the result of the action of viral mRNA export factor, ORF57 (310). Even though KSHV infection induces DDR activation, it suppresses ATM activation. Shin et al, 2006 demonstrated that the C-terminal

domain of vIRF1 interacts with ATM and reduced its phosphorylation (311). This, consequently, inhibits activation of the downstream proteins of the ATM pathway, such as P53, H2AX, and CHK2 (311). However, vIRF1 expression increases expression of the cell cycle regulatory protein CdC25, which is consistent with suppression of the ATM-mediated signaling pathway. vIRF1 also inhibits activation of p53, another downstream component of the ATM signaling pathway. vIRF1 interacts with p53, and this interaction is associated with suppression of acetylation and transcriptional activation of p53 (308, 312). Thus, KSHV infection alters downstream signaling of the DDR pathway.

1.5 Purpose of reshaping the DNA damage response by DNA viruses.

With a limited coding capacity of the viral DNA genome, it exploits the cellular machineries to facilitate their genome replication and to generate progeny viruses. Consequently, in favor of completing their life cycles DNA viruses hijack and manipulate cellular repair and replication processes (reviewed in (257)). Upon release of virus genomes into the infected cells nuclear sensors recognize them (313). In response, host cell defensive complexes are accumulated at the site where incoming viral genomes are localized. For instance, the HSV-1 genome containing nicks and single-strand gaps is delivered into the nucleus and thus, attract DNA repair factors (314).The initial purpose of this attraction is to inhibit virus replication by the host cells. Instead, viruses manipulate the DDR signaling to promote replication. Early DDR markers including γ-H2AX and MDC1 (mediator of DNA damage checkpoint protein-1) are localized to the incoming HSV-1 genome (276). However, the viral E3 ubiquitin ligase, ICP0 antagonizes this host defense by degrading RNF8 and RNF168 to prevent recruitment of downstream repair protein, 53BP1 (276). Thus, the selective disarming indicates that the exploitation of upstream DDR factors may facilitate recombination-mediated replication, whereas elimination of the downstream proteins prevents processing and silencing of the viral genome by host cells (reviewed in (257)). Thus, the activation of upstream signaling favors virus replication, but the execution of downstream signaling to cell cycle checkpoint or apoptosis often negatively affects virus replication (261). Therefore, viruses developed strategies to block downstream signaling. Thus, viruses activate or inactivate the components with the most profound consequences to facilitate their replication (261).

Although many DNA viruses activate the DDR pathways, whether it is beneficial or detrimental to the virus is still largely unknown. Depending on the type of the infection, such as latent or lytic infection, or on the structure of replicating DNA the role of the DDR varies (261). A common theme often reported is that during lytic replication by DNA viruses there is a requirement for DDR activation, signaling through PIKK (phosphatidylinositol 3-kinase like protein kinase) and specific subsets of DNA repair factors (reviewed in (261)). Additionally, to assure the cell survival during replication the downstream signalling leading to apoptosis or senescence is prevented by the viral proteins (reviewed in (261)). On the other hand, during latency the viral DNA persists without generating any progeny virus in specific cells, such as neuronal cells. It has been suggested that DDR might facilitate the establishment of latency and is exploited during reactivation (315). Prevention of ubiquitinylation of histone or recruitment of downstream repair factors by ICP0 contributes to virus genome silencing (276) leading to the establishment of latency. Thus, viruses harness the DDR machinery to optimize the signaling to be latent.

Oncogenic viruses, on the other hand, optimize the DDR signaling and utilize cell cycle regulatory proteins, such as Chk2 or p53 leading to cell proliferation (261). The expected outcome of attenuation of the DDR by oncogenic viruses is viral genome replication. However, it may result in unexpected consequences for the infected cells promoting uncontrolled cell proliferation and ultimately, tumorigenesis. Attenuation of the DDR by oncogenic viruses can be achieved by directly antagonizing the downstream components of the DDR pathway, such as checkpoint kinase p53 (reviewed in (261)). Herpesviruses, such as EBV and KSHV infection also impair DDR leading to cell proliferation. EBV and KSHV infection regulate S-phase entry to promote cell proliferation (294, 316). Hence, oncogenic herpesviruses alter the DDR signaling to bypass growth-suppressive effect and consequently, stimulate cell proliferation causing tumorigenesis (261).

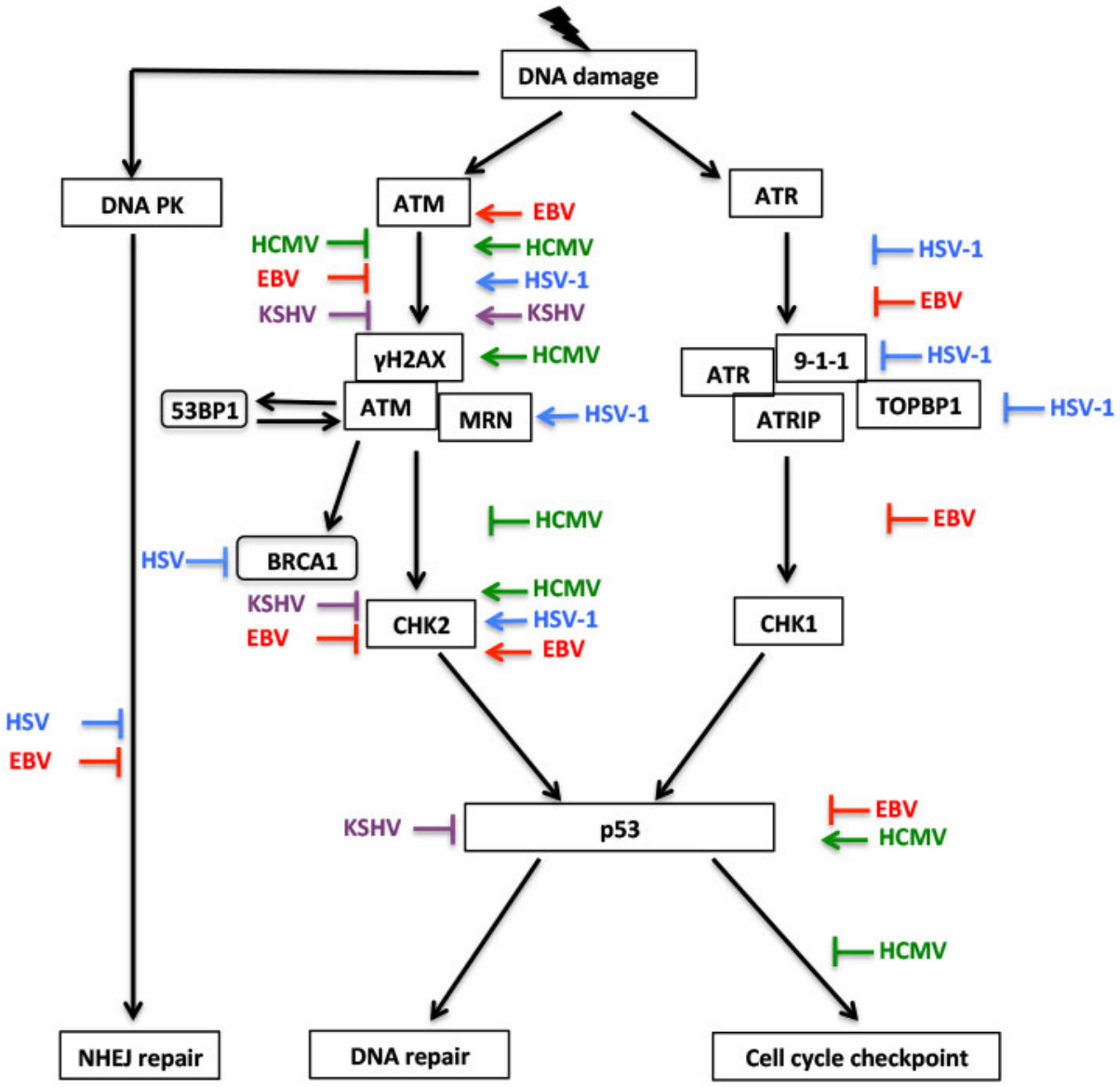

Figure. 1.3 Modulation of the DDR pathways by different herpesviruses.

Exposure of cells to DNA damage triggers activation of the major DDR pathways, the ATM, ATR, and DNA-PK pathways. Following DNA damage, ATM is activated by phosphorylation. ATM activation is associated with MRN complex recruitment. Activated ATM transmits DNA damage signals by activating histone 2AX (γH2AX). Activated ATM then transduces the signal to the downstream proteins by activating CHK2, 53BP1, and BRCA1. Activated CHK2 leads to the activation of P53. In the ATR pathway, exposure to damaged DNA triggers ATR kinase activation. Activated ATR interacts with ATRIP to recruit 9-1-1 complex (RAD9-HUS1-RAD1). RAD9, a subunit of 9-1-1 complex, binds to TOPBP1 to stimulate ATR kinase activity. Subsequently, activated ATR promotes activation of CHK1. Activated CHK1 mediates P53 activation. P53 activation by both the ATM and ATR pathways facilitates multiple functions, such as DNA repair and cell cycle checkpoint activation. A growing body of evidence demonstrated that different herpesviruses modulate the DDR pathways by activating or blocking

DDR pathway proteins. HSV-1 triggers ATM activation, phosphorylation of NBS1 (a component of MRN complex), and CHK2 activation, while blocking the ATM pathway by inhibiting recruitment of BRCA1. In addition, HSV-1 also abrogates DNA-PK to inhibit non-homologous end joining (NHEJ) repair. The ATR-CHK1 kinase pathway is also blocked by HSV-1 infection through preventing recruitment of the 9-1-1 complex and TOPBP1. Additionally, the DNA-PK signaling pathway is attenuated by HSV-1 infection. Similarly, EBV is also involved in both activation and prevention of ATM pathway. EBV induces phosphorylation of ATM, H2AX, and CHK2. Conversely, EBV-encoded oncoprotein, LMP-1 down-regulates the ATM signaling pathway. Moreover, EBV EBNA3C inhibits cell cycle arrest by interacting with CHK2. In addition, the ATR-CHK1 pathway, as well as P53 signaling is also inhibited by EBV infection. Moreover, EBV infection also blocks the DNA-PK signaling pathway. HCMV infection induces the DDR pathway by activating ATM, H2AX, CHK2, and p53, while also inhibiting the ATM-mediated pathway by altering the localization of ATM and CHK2. ATM-mediated checkpoint activation is also inhibited by HCMV infection. Although KSHV infection induces ATM activation by increased phosphorylation of H2AX, it abrogates ATM/p53 signaling. Consequently, CHK2 activation is prevented by KSHV infection.

1.6 Modulation of apoptosis by HSV-1 and BoHV-1.

1.6.1 Apoptosis.

Apoptosis, a prevalent form of cell death and a natural process, occurs in multicellular organisms for the development and maintenance of homeostasis. The apoptotic cells exhibit morphological and biochemical changes including DNA fragmentation, apoptotic body formation, plasma membrane blebbing, chromatin condensation and shrinkage of cells (317). These apoptotic morphological features are the results of the action of proteolytic enzymes triggered by the apoptotic stimuli. Apoptosis is also a necessary component of the responses to cellular injury (318). Induction of apoptotic pathways may occur by exposure of cells to endogenously synthesized (tumor necrosis factor & reactive oxygen species, (ROS)) or external (retinoic acid & ricin) components (319). Some cells undergo apoptosis in response to the infection with microbial pathogens, such as virus infection. Thus, virus infection triggers induction of apoptosis (320). Therefore, it is not surprising that viruses adopt multiple mechanisms to modulate apoptotic responses. These evolutionary mechanisms confer survival advantages to either the host cell or to the virus.

1.6.2 Apoptosis mechanism.

The mechanism of apoptosis involves highly complex and energy-dependent sequences of events consisting of three subsequent parts, initiation, execution and termination (321). The apoptotic signaling can be initiated by different factors including ROS, alkylating agents, chemotherapeutic agents and Fas ligands. The major mechanism of apoptosis involves the activation of two distinct pathways: i) extrinsic and ii) intrinsic or mitochondria-dependent pathways (321, 322).

The extrinsic pathway-mediated apoptotic signaling involves transmembrane receptor-associated interaction. These are classified as death receptors of the tumor necrosis factor (TNF) superfamily (323). These death receptor proteins contain “death domains” that are responsible for transmitting the death signal from the cell surface to intracellular networks. TNF-α/TNFR1 and first apoptosis signal ligand/receptor (FasL/FasR) are considered as death receptors and their corresponding ligands. The cascades of events involved in the extrinsic pathways are best characterized in TNF-α/TNFR1 and FasL/FasR systems (reviewed in (322). Binding of receptors with the corresponding homologous ligands triggers activation of death receptors. This results in

the recruitment of cellular adaptor proteins (322). For example, binding of Fas ligand to the Fas receptor causes engagement of the cytoplasmic adaptor protein (Fas-associated death domain) FADD. Similarly, anchoring of the TNF receptor to the TNF ligand triggers recruitment of the TNFR1-associated death domain (TRADD) (324, 325). Following recruitment, FADD interacts with procaspase-8, triggering activation of procaspase-8. With activation of procaspase-8, the execution phase of apoptosis is stimulated (326). The active procaspase-8 then facilitates the cleavage of its downstream executioners procaspase-3 to generate active caspase-3. Finally, the active caspase-3 proceeds to the induction of apoptosis by initiating fragmentation of DNA (327). The termination phase of apoptosis involves the inhibitory function of the cellular FLICE-inhibitory protein (cFLIP) that binds to the FADD or procaspase-8 to negatively regulate their activation (328).

In contrast, the intrinsic apoptotic-signaling pathway initiates apoptosis in response to intracellular signals. It involves an array of non-receptor-associated stimuli that directly act on intracellular targets and also includes mitochondria-dependent events (322). The intrinsic apoptotic pathway is also triggered by another set of stress stimuli within the cells such as DNA damage stress and ROS production (321). All of these intracellular stimulus events cause alterations in the inner mitochondrial membrane that results in an opening of mitochondrial permeability transition (MPT) pores. Consequently, the mitochondrial transmembrane potential is lost, resulting in induction of mitochondrial outer membrane permeabilization. This triggers the sequestration of pro-apoptotic protein such as cytochrome-C, from the intermembrane space into the cytoplasm (329). Subsequently, the released cytochrome-C forms a complex with apoptotic protease activating factor-1 (Apaf-1) and caspase-9 denoted as “apoptosome” (330, 331). The formation of apoptosome then leads to the activation of caspase-9 (332). The activated caspase-9 triggers activation of executioner caspases including caspase-3 (333). Finally, caspase-3 induces apoptosis by fragmentation of nucleosomal DNA. Apoptotic signaling through the intrinsic pathway is also tightly regulated by the anti-apoptotic Bcl-2 family member proteins such as Bcl-1 and Bcl-xL and by the pro-apoptotic Bcl-2 family proteins, for example, Bid (BH3-interacting domain death agonist), Bax (Bcl-2-associated X protein), and Bak (Bcl-2 homologous antagonist killer) (334). A schematic diagram representing the overall apoptosis mechanism and modulation of apoptosis by HSV-1 and BoHV-1 is shown in Figure 1.4.

1.6.3 Regulation of apoptosis by HSV-1.

To thwart viral infection, cells adopt innate anti-viral countermeasures that can delay virus replication and propagation. Apoptosis is one of the common anti-viral responses. In spite of inducing apoptosis, HSV-1 virus has strategies to promote HSV-1 infection and pathogenesis. For instance, HSV-1 encodes some anti-apoptotic virulence factors to counteract apoptotic responses. A HSV-1 regulatory protein immediate early protein, ICP24, blocks apoptotic cell death. ICP24 deletion mutant exhibits less apoptotic cell death as is evident based on reduced chromatin condensation, or DNA laddering compared to wild-type HSV-1 infection (335). Researchers demonstrated that HSV-1 gD prevents Fas-mediated apoptosis (336, 337). A mechanistic study indicated that HSV-1 entry is facilitated through binding of herpes virus entry mediator (HVEM), a gD receptor (338). Binding of HVEM to gD triggers NF-κB signaling cascades (339). NF-κB activation promotes anti-apoptotic functions of gD by reducing caspase-8 activity and increasing expression of anti-apoptotic proteins (340). Furthermore, HSV-1 US3 is also involved in blocking apoptosis by phosphorylation of pro-apoptotic protein Bad and Bid, thereby inhibiting their apoptotic function (341). US3 also interacts with programmed cell death protein 4 (PDCD4) to block the apoptotic pathway (342). In addition, two R1 proteins, ICP6 and ICP10, contain ribonucleotide reductase (RNR) subunits, which also function as apoptotic inhibitors (343). Both of these proteins are responsible for inhibition of TNF-α- and Fas-mediated apoptosis. The RNR domain prohibits caspase-8 activation by directly binding with caspase-8 (343). The serine-threonine protein kinase (PK) domain-mediated function is associated with the abrogation of apoptosis in neuronal cells (344, 345). The late protein of HSV-1 glycoprotein-J (gJ) is also involved in blocking caspase activation to interrupt Fas-mediated apoptosis (346). gJ abrogates activation of caspase-3, 6, 8 and 9 to halt the cellular apoptotic responses (346). Another late protein of HSV-1, U_L14, also functions as viral apoptotic inhibitor since UL14-deleted virus exhibits a reduced ability to suppress apoptosis (347). Furthermore, neuronal apoptotic cell death inhibition is associated with the function of HSV-1 latency-associated transcript (LAT). LAT expression abolishes both the intrinsic and extrinsic apoptotic pathway by interfering with caspase-8 and caspase-9 activation. Thus, the LAT expression contributes to the neuronal survival during latency (348, 349).

Despite multiple anti-apoptotic mechanisms of HSV-1, it encodes some immediate early proteins that induce apoptosis. HSV-1 ICP0 triggers induction of apoptosis. In the presence of

translational inhibitor, cyclohexamide (CHX), wild-type HSV-1 promotes apoptosis, while lack of ICP0 expression halts the induction of apoptosis. ICP0-medaited activation of the apoptotic pathway is associated with activation of caspase-3. Another immediate early protein of HSV-1, ICP27, stimulates the apoptotic cell death pathway by increasing intracellular reactive oxygen species (ROS) and Bax expression, as well (350). ICP27 also facilitates p38 mitogen-activated protein kinase signaling to stimulate apoptosis signaling pathway (351). However, ICP27 has also been demonstrated as an inhibitor of apoptosis (352). Thus, it is conceivable that HSV-1 infection causes apoptotic cell death. However, HSV-1 apoptosis inhibitor proteins such as, ICP24, gD, gJ, and U_L14, eliminate the apoptotic signals to favor virus infection.

1.6.4 Regulation of apoptosis by BoHV-1.

Viruses are ancient intracellular parasites that adopted various strategies to utilize the host cells to replicate and spread. Therefore, it is not surprising that BoHV-1 adopted multiple mechanisms to regulate apoptosis during productive infection. BoHV-1 infection in cattle or permissive bovine cell lines causes rapid cell death (15, 353). A growing body of evidence suggests that several proteins of BoHV-1 are involved in both induction and inhibition of apoptosis. BoHV-1 was found to induce apoptosis in peripheral blood mononuclear cells (PBMC) (354). In addition, BoHV-1 causes apoptotic cell death in large numbers of immune cells *in vitro* such as T-lymphocytes, B-lymphocytes, and monocytes/macrophages (355), lymphoid and epithelial cells.

Induction of apoptosis by BohV-1 is mediated by multiple mechanisms. Researchers reported that both live and inactivated BoHV-1 induces apoptosis in mitogen-stimulated PBMCs. Since triggering of apoptosis was observed with inactivated BoHV-1 virus particles, it was postulated that the mechanism of apoptosis induction might include the attachment or penetration or the effect of viral structural proteins, such as glycoproteins or tegument proteins (354, 356). gH of BoHV-1 is important for virus penetration but not for attachment. A gH-deleted mutant was able to induce apoptosis indicating that attachment but not penetration is required for apoptosis induction by BoHV-1 (356). Since a gD-deleted mutant was unable to trigger apoptosis, gD was concluded to be necessary for apoptotic cell death associated with virus attachment (357). In addition, BoHV-1 infection of Madin Darby Bovine Kidney (MDBK) cells leads to the activation of caspases and p53 resulting in apoptotic cell death (358). An immediate

early protein, ICP0 (bICP0) also functions as an apoptosis inducer (359, 360). bICP0 causes activation of caspase-3, a major hallmark of apoptosis, leading to apoptotic cell death (360). Furthermore, a tegument protein of BoHV-1, VP22, induces apoptosis through activation of caspase-3 and upregulation of Bax (361). Xu et al, 2012 also demonstrated the involvement of a mitochondria-dependent pathway in induction of apoptosis during BoHV-1 infection (362). They revealed that BoHV-1 infection activates both intrinsic and extrinsic pathways to activate caspase-8, cleavage of Bid and caspase-9. These events consequently trigger upregulation of Bax expression and caspase-3 activation, finally leading to apoptosis of BoHV-1-infected cells (362). A recent report also demonstrated that BoHV-1-induced oxidative stress promotes mitochondrial dysfunction by reducing ATP production and mitochondrial membrane potential (MMP) (363). Thus, ROS-mediated mitochondrial damage contributes to cell death. Moreover, the ORF8, located in the unique short (Us) segment of the BoHV-1 genome, plays a role in promoting apoptotic cell death. Cells infected with a BoHV-1 ORF8 deletion mutant exhibited significantly down-regulated apoptotic processes, suggesting the contribution of ORF8 in apoptosis induction. The importance of induction of apoptosis by ORF8 was demonstrated by the fact that loss of ORF8 markedly reduced the release of progeny viruses from the infected cells to the extracellular environment (364). Furthermore, increased expression of ORF8 leads to DNA laddering and chromatin condensation due to apoptotic cell death. Thus, BoHV-1 has developed various strategies to induce apoptosis in infected cells.

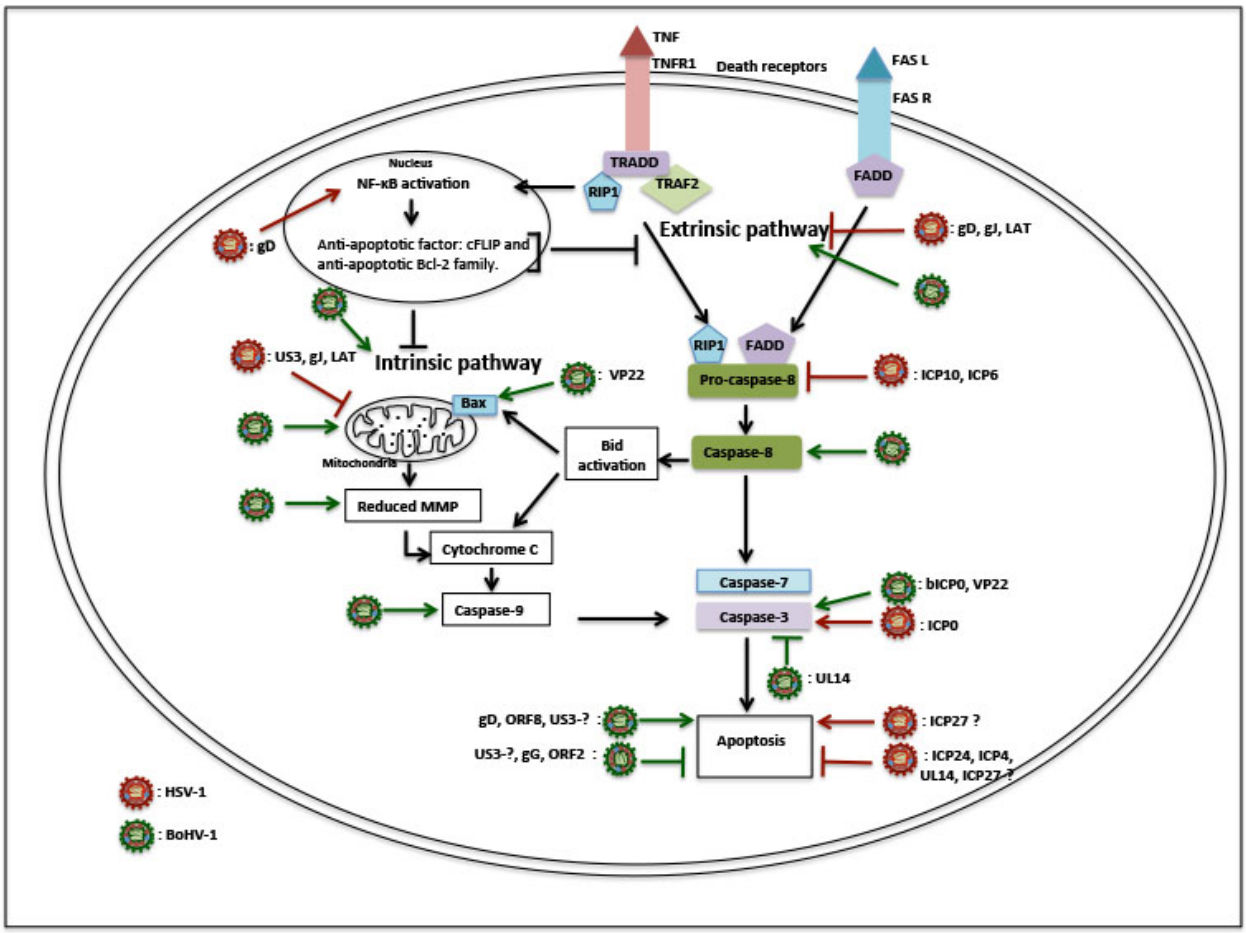

Figure. 1.4. Modulation of apoptosis by HSV-1 and BoHV-1.

Apoptosis is triggered through activation of the extrinsic or intrinsic pathway. Binding of death receptor, TNFR1 or Fas R, to its corresponding ligand, TNF and FasL, leads to the formation of a complex containing TRADD and FADD. TRADD-associated complex triggers NF-κB activation followed by expression of anti-apoptotic genes, for example anti-apoptotic Bcl2 family proteins and cFLIP. These anti-apoptotic factors block both the intrinsic and extrinsic pathways. In the extrinsic pathway, a secondary complex, consisting of FADD, pro-caspase-3 and RIP1, is formed, which triggers caspase-8 activation. Activated caspase-8 promotes caspase-3 and caspase-7 activation leading to apoptosis. In the intrinsic pathway, activation of BAX promotes reduction of mitochondrial membrane potential (MMP) leading to the release of cytochrome C. In parallel, caspase-8 also triggers Bid and Bax activation leading to cytochrome C release. Cytochrome C activates caspase-9 leading to caspase-3 and caspase-7 activation. These executioner caspases induce apoptosis. The anti-apoptotic and pro-apoptotic proteins encoded by HSV-1 modulate apoptotic signaling. HSV-1 gJ, LAT and gD inhibits both intrinsic and extrinsic pathways. gD promotes anti-apoptotic gene expression through NF-κB activation. US3 blocks the intrinsic pathway to inhibit apoptosis. ICP0 and ICP6 prohibit pro-caspase-8 activation. Other proteins, such as ICP24, ICP4, U_L14 and ICP27 prevent apoptosis. However, ICP27 also functions as an apoptotic inducer. In addition, ICP0 triggers caspase activation to induce apoptosis. BoHV-1 is also known to activate both the intrinsic and extrinsic pathways. In the extrinsic pathway, BoHV-1 activates pro-caspase-8. Several BoHV-1 proteins, such as bICP0,

VP22 trigger caspase-3 activation. gD, ORF8, and US3 also induce apoptosis. However, US3 has also been found to block apoptosis. BoHV-1 activates the intrinsic pathway through reduced MMP, Bax and Bid activation, cytochrome C release, and caspase-9 activation. Conversely, several anti-apoptotic proteins, such as gJ and ORF2, block BoHV-1-induced apoptosis.

BoHV-1 also evolved apoptosis evasion mechanisms to counteract the apoptotic stimuli. As such, like most of the DNA viruses, BoHV-1 also encodes proteins responsible for inhibition of apoptosis. In contrast to apoptosis inducers, a tegument protein U_L14 interferes with the apoptotic pathway (365). U_L14 expression in transfected cells can inhibit caspase-3 and caspase-9 activation and thereby increase cell survival in response to apoptotic stimuli (365). US3 of BoHV-1 is also involved in inhibition of apoptosis (366), although according to earlier reports US3 is not directly involved in blocking apoptosis (367). Furthermore, during latency, a latency related-RNA (LR-RNA) is abundantly expressed. The LR-RNA-encoded protein, ORF2, negatively regulates apoptotic responses to promote survival of latently infected neuronal cells (368). Likewise, another glycoprotein, gG, is capable of postponing the apoptotic process and thus, contributes to cell survival and efficient production of virus (54). Overall, BoHV-1 encodes a number of proteins throughout the infection cycle, either to induce or to abrogate the apoptotic processes. Therefore, it is conceivable that, although BoHV-1 infection induces apoptosis, some virus-encoded anti-apoptotic proteins inhibit the lethal effects of apoptosis. As a result, a delicate balance between anti-apoptotic and pro-apoptotic activity promotes productive virus infection.

Overall, since deletion of VP8 reduces BoHV-1 replication and egress, when grown in tissue culture, and prevents BoHV-1 replication in cattle (179), it was of interest to determine how VP8 contributes to BoHV-1 replication. Overcoming the cellular antiviral IFN response is a widely used strategy of viruses to promote infection. Hence, the first objective of this research was to determine the role of VP8 in regulation of IFN signaling during BoHV-1 infection. The DDR pathway also often functions as an antiviral response. Therefore, our second objective was to determine the effect of VP8 on the DDR pathway during BoHV-1 infection. Furthermore, HSP60 was identified as a new mitochondrial interacting partner of VP8. Hence, in our third objective we hypothesized that during BoHV-1 infection VP8 has an effect on mitochondrial functions. Overall, this research demonstrates various functions of VP8 during the life cycle of BoHV-1.

CHAPTER 2

HYPOTHESIS AND OBJECTIVES

2.1 Rationale and hypothesis.

The major tegument protein of BoHV-1, VP8, is indispensable for virus replication in cattle, and a VP8-deleted mutant virus demonstrates defective virus replication in cell culture (179). In addition, VP8 is abundantly incorporated into the mature BoHV-1 virion (41), suggesting the importance of VP8 during the lytic replication cycle. Upon fusion of viral envelope with the host cell membrane, VP8 is dissociated from the virion, and detected in the cytoplasmic compartment at 2 h post infection (187). This might reflect the significance of the function of VP8 at early stages of BoHV-1 infection. We hypothesize that VP8 contributes to the modulation of cellular antiviral responses against invading BoHV-1 during early infection, and thus, promotes BoHV-1 replication.

In the absence of VP8, the mutant virus exhibited drastic reduction in virus replication, suggesting a pro-viral role of VP8 during BoHV-1 infection. In addition, since a VP8-deleted mutant was avirulent *in vivo,* VP8 might be a potential candidate for modulating strong anti-viral responses. Therefore, we hypothesized that VP8 functions through alteration of anti-viral responses during BoHV-1 infection.

2.2 Objectives.

- Identify a role of VP8 in the establishment of BoHV-1 infection through inhibition of IFN-β signaling.
- Investigate the function of VP8 in the modulation of the DNA damage response pathway during BoHV-1 infection.
- Express and purify VP8, and investigate its role as mitochondrial interacting partner.

CHAPTER 3

VP8, THE MAJOR TEGUMENT PROTEIN OF BOVINE HERPESVIRUS-1, INTERACTS WITH CELLULAR STAT1 AND INHIBITS INTERFERON-β SIGNALING

Sharmin Afroz[1,2] , Robert Brownlie [1], Michel Fodje[3,] and Sylvia van Drunen Littel-van den Hurk[1,2,4]

[1] VIDO-InterVac, University of Saskatchewan, Saskatoon, SK, S7N 5E3, Canada; [2]Vaccinology & Immunotherapeutics, University of Saskatchewan, Saskatoon, SK, S7N 5E3, Canada. [3] Canadian Light Source, University of Saskatchewan, Saskatoon, SK, S7N 5E3, Canada. [4] Microbiology & Immunology, University of Saskatchewan, Saskatoon, SK, S7N 5E3, Canada.

Running title: BoHV-1 VP8 inhibits IFN-β signaling

Corresponding author*:
Dr. Sylvia van Drunen Littel-van den Hurk,
VIDO-InterVac
University of Saskatchewan,
120 Veterinary Road.
Saskatoon, SK, S7N 5E3, Canada.
Telephone: 1 + (306) 966-1559,
Fax: 1 + (306) 966-7478.

The information in this chapter was previously published:

Sharmin Afroz, Robert Brownlie, Michel Fodje and Sylvia van Drunen Littel-van den Hurk. VP8, the major tegument protein of bovine herpesvirus 1, interacts with cellular STAT1 and inhibits interferon beta signaling. Journal of Virology, 2016 Apr 29; 90(10):4889-4904. doi: 10.1128/JVI.00017-16.

3.1 Abstract

The *U_L47* gene product, VP8, is the most abundant tegument protein of bovine herpesvirus 1 (BoHV-1). Previously, we demonstrated that a *U_L47*-deleted BoHV-1 mutant (BoHV1-ΔU_L47) exhibits 100-fold-reduced replication *in vitro* and is avirulent *in vivo*. In this study, we demonstrated that VP8 expression or BoHV-1 infection inhibits interferon beta (IFN-β) signaling by using an IFN-α/β-responsive plasmid in a luciferase assay. As transducer and activator of transcription (STAT) is an essential component in the IFN-signaling pathways, the effect of VP8 on STAT1 was investigated. An interaction between VP8 and STAT1 was established by coimmunoprecipitation assays in both VP8-transfected and BoHV-1-infected cells. Two domains of VP8, amino acids 259 to 482 and 632 to 686, were found to be responsible for its interaction with STAT1. The expression of VP8 did not induce STAT1 ubiquitination or degradation. Moreover, VP8 did not reduce STAT1 tyrosine phosphorylation to down-regulate IFN-β signaling. However, the expression of VP8 or a version of VP8 (amino acids 219 to 741) that contains the STAT1-interacting domains but not the nuclear localization signal prevented nuclear accumulation of STAT1. Inhibition of nuclear accumulation of STAT1 also occurred during BoHV-1 infection, while nuclear translocation of STAT1 was observed in BoHV1-ΔU_L47-infected cells. During BoHV-1 infection, VP8 was detected in the cytoplasm at 2 h post infection without any *de novo* protein synthesis, at which time STAT1 was already retained in the cytoplasm. These results suggest that viral VP8 down-regulates IFN-β signaling early during infection, thus playing a role in overcoming the antiviral response of BoHV-1-infected cells.

3.2 Importance.

Since VP8 is the most abundant protein in BoHV-1 virions and thus may be released in large amounts into the host cell immediately upon infection, we proposed that it might have a function in the establishment of conditions suitable for viral replication. Indeed, while nonessential *in vitro*, it is critical for BoHV-1 replication *in vivo*. In this study, we determined that VP8 plays a role in down-regulation of the antiviral host response by inhibiting IFN-β signaling. VP8 interacted with and prevented nuclear accumulation of STAT1 at 2 h post infection in the absence of *de novo* viral protein synthesis. Two domains of VP8, amino acids 259 to 482 and 632 to 686, were found to be responsible for this interaction. These results provide a

new functional role for VP8 in BoHV-1 infection and a potential explanation for the lack of viral replication of the *U_L47* deletion mutant in cattle.

Key words: BoHV-1, VP8, IFN signaling, STAT1

3.3 Introduction.

Bovine herpesvirus-1 (BoHV-1) is responsible for several clinical manifestations, including rhinotracheitis, vulvovaginities and conjunctivitis, in cattle (26). BoHV-1 is composed of a double-stranded DNA surrounded by a nucleocapsid, a tegument and an envelope (369). Although the tegument is a major constituent in the BoHV-1 virion, it is the least studied. The tegument consists of at least 20 virus-encoded proteins (reviewed in (106)). Herpesvirus infection is mediated by the interaction of glycoproteins such as gB, gC and gD with cellular proteins (370). The majority of the tegument proteins is then released into the cytoplasm indicating that these proteins are the first to interact with the intracellular environment (66). Herpesvirus tegument proteins are involved in various functions including capsid transport, DNA replication, transcriptional and translational regulation, and viral assembly and egress (106). These functions suggest that tegument proteins contribute to the establishment of conditions suitable for viral replication.

The *ul47* gene product, VP8, is a 97 kD tegument protein and the most abundant protein in BoHV-1 virions (176). Although BoHV-1 VP8 is not essential for viral infection, a U_L47-deleted mutant (BoHV1-ΔU_L47) exhibits a smaller tegument structure and impaired growth in cell culture, and is avirulent in cattle (179). In addition, BoHV-1 VP8 plays a role in induction of humoral and cellular immunity (181). VP8 is monoubiquitinated and interacts with DNA damage binding protein-1 (DDB1) (187), which is a component of the Cul4A-DDB1 E3 ubiquitin ligase complex (371). Furthermore, VP8 remodeled the distribution of promyelocytic leukemia (PML) nuclear bodies (NBs) (185).

Viruses can establish an infection in the host cells by overcoming the antiviral defense mechanisms. The antiviral state is established by secretion of type I interferon (IFN), which is needed for the activation of other cellular genes. Interferons are categorized into type I (IFN-α, IFN-β, IFN-ω, IFN-κ and IFN-ε), type II (IFN-γ) and Type III (IFN-λ) depending on their primary structure [reviewed in (198, 372)]. IFN-α/β are synthesized by cells in response to viral

infections, whereas IFN-γ is secreted by activated T lymphocytes and natural killer cells in virus-infected cells. These types of IFN are involved in limiting the growth of target cells and in influencing cell apoptosis, thereby arresting viral spread. The activity of these IFNs is initiated by the binding of IFN-α/β and IFN-γ to their cell surface receptors (373). Some IFN-mediated cascades are regulated by the Janus tyrosine kinase/signal transducer and activator of transcription (JAK/STAT) pathway, whereas others are regulated by STATs to optimize transcription regulation of target genes (198). IFN-λs are induced by either interferon response factor (IRF3), IRF7 or NF-κB pathways (372). Recently, IFN-λ was identified as having antiviral properties against numerous viruses.

The activation of the JAK/STAT signaling pathway is initiated by binding of IFN-α/β to their receptors, which are composed of IFNAR1 and IFNAR2 subunits. Upon binding of IFN-α/β to its receptors, the IFNAR1 and IFNAR2 complex activates tyrosine kinase 2 (Tyk2) and Janus kinase 1 (JAK1) by transphosphorylation. Activated Tyk2 phosphorylates IFNAR1 on tyrosine 466, making a platform to bind STAT2. This facilitates phosphorylation of STAT2 by activated Tyk2, which in turn recruits STAT1. The newly recruited STAT1 is phosphorylated on tyrosine 701 residue by JAK1. Phosphorylated STAT1 and STAT2 form a heterodimer, which dissociates from the receptor and then translocates to the nucleus to bind with IRF9 and form a heterotrimeric complex, the IFN stimulated gene factor-3 (ISGF3) complex. The ISGF3 complex binds to the IFN response element for the induction of IFN-stimulated genes [reviewed in (373)].

Most viruses have developed specific mechanisms to circumvent the IFN response, either by reducing IFN production or by down-regulating the IFN signaling cascade (373). For example, rabies virus P protein (374), simian virus 5 (SV5) V protein (375), respiratory syncytial virus (376), human parainfluenza virus type-1 virus V protein (377) and mumps virus V protein (378) inhibit IFN-β signaling by proteasome-mediated degradation of STAT1 or STAT2, by reducing phosphorylation of STAT1 or STAT2, or by inhibiting nuclear translocation of STAT1. During BoHV-1 infection, inhibition of IFN signaling by infected cell protein bICP0 through degradation of IRF3 was observed (207). In the absence of IRF3 expression, bICP0 inhibits the ability of IRF7 to trans-activate the IFN-β promoter (379). Furthermore, bICP27 inhibits transcriptional activity of two bovine IFN-β gene promoters (IFN-β1 and IFN-β3) during transient transfection (380). However, no other protein of BoHV-1 has been reported to down-regulate IFN-β signaling.

Since BoHV-1 VP8 is essential for viral replication *in vivo*, we examined its effect on the IFN signaling pathway. We determined that VP8 down-regulates the IFN response, both in VP8-transfected and in BoHV-1-infected cells. VP8 interacted with STAT1, and this interaction required two distinct domains of VP8. Furthermore, VP8 acted as an IFN antagonist by preventing nuclear translocation of STAT1.

3.4 Materials and Methods.

3.4.1 Cell culture, virus infection and IFN treatment.

Madin-Darby bovine kidney (MDBK), embryonic bovine tracheal (EBTr), human embryonic kidney HEK293T, and Vero cells were grown in Eagle's minimum essential medium (MEM; Sigma-Aldrich Canada Ltd., Oakville, ON, Canada) supplemented with 10% heat-inactivated fetal bovine serum (FBS; Gibco, Life Technologies, Burlington, ON, Canada), 1% antibiotic-antimycotic (Life Technologies), and 10 mM HEPES buffer (Life Technologies). Cells were cultured with 5% CO_2 in a 37°C incubator. Wild-type BoHV-1 108, BoHV1-ΔU_L47, and BoHV1-UL47R were propagated in MDBK cells (8). MDBK cells were infected with BoHV-1 at a multiplicity of infection (MOI) of 0.5 unless indicated otherwise. Recombinant human IFN-β was purchased from PeproTech Inc. (Rocky Hill, NJ, USA), and bovine IFN-β was purchased from Kingfisher (Saint Paul, MN, USA).

3.4.2 Antibodies.

VP8-specific mouse monoclonal antibody was used as previously described (181). Rabbit antibodies specific for bICP0 and bICP4 were made in-house and used as described previously (179) (188). Rabbit polyclonal anti-STAT1 (catalog no. sc-345), anti-STAT1 p84/91 (catalog no. sc-346), anti-pSTAT1 (catalog no. sc-8394), anti-STAT2 (catalog no. sc-476), anti-ubiquitin (catalog no. sc-8071) and anti-fibrillarin (H-140) antibodies were obtained from Santa Cruz Biotechnology Inc. (Dallas, Texas, USA). Mouse monoclonal anti-FLAG (catalog no. F3165-0.2MG), anti-actin (catalog no. A2228) and anti-tubulin (catalog. no T6199) antibodies were purchased from Sigma-Aldrich. SV5 V5-specific rabbit antibody was purchased from Invitrogen, Life Technologies.

Table 3.1 Primer list for plasmid constructions using PCR (5' to 3'end)

Plasmid	Forward primer sequence	Reverse primer sequence
VP8	GAATCTAGAGCCACCATGGACTACAAAGACGATGAC	GGCAGTGAGCGCAACGCAATTAATG
VP8 121-741	GCGGTAGATCTGATTCAAGACTACTTGACGGCCCACCTG	GGCAGTGAGCGCAACGCAATTAATG
VP8 219-741	CGGTAGATCTGATTGAGCGGCTGTCGGAAGGG	GGCAGTGAGCGCAACGCAATTAATG
VP8 343-741	CGGTAGATCTGATTGGCGGCATGTACGTGGGCGCCCCTGAG	GGCAGTGAGCGCAACGCAATTAATG
VP8 538-741	GCGGTAGATCTGATTGCGGCGGCCTTCCGCGAAGTG	GGCAGTGAGCGCAACGCAATTAATG
VP8 632-741	CGGTAGATCTGATTGGCAGCCTGAACCTGCTGCTGAAC	GGCAGTGAGCGCAACGCAATTAATG
VP8 1-120	GAATCTAGAGCCACCATGGACTACAAAGACGATGAC	GAGCTCGAGTCAGCCGTGATTGGGGCCGCGGTTAG
VP8 1-258	GAATCTAGAGCCACCATGGACTACAAAGACGATGAC	GAGCTCGAGTCACTCCCCCGCAGCCGCAGCG
VP8 1-482	GAATCTAGAGCCACCATGGACTACAAAGACGATGAC	GAGCTCGAGTCAGGCCGACTGCAGCCCGGCGCCCGCGTAG
VP8 1-631	GAATCTAGAGCCACCATGGACTACAAAGACGATGAC	GAGCTCGAGTCACAGCCGCTGCGCGATCAGCCC
VP8 1-259	CGCGCCACCAGACATAATAGCTGAC	CAGCGGCACCTCTACCTGAGGCTG
VP8 1-371	CGCGCCACCAGACATAATAGCTGAC	CACGGATCCCCTACGCCTCAGTGGGCGGCA
VP8 259-371	CGCGCCACCAGACATAATAGCTGAC	CACGGATCCCCTACGCCTCAGTGGGCGGCAT
VP8 372-483	CGCGCCACCAGACATAATAGCTGAC	CACGGATCCCTAGTAGCGCTCATTTGCCGTGTAGCC
VP8 631-686	GTGACGGTGCGCGAGGGCACGCT	CACGGATCCCCTACCGCCGCTTGCCGGCCAG

3.4.3 Plasmids.

The *ul47* gene (GenBank accession no. AY530215.1) was cloned into pFLAG-CMV2 (Sigma-Aldrich) as described previously (184). The VP8 ORF was sub-cloned with a N-terminal FLAG tag into an expression vector (named pCMV4.1k) downstream from a human CMV promoter with intron A. The resulting plasmid was then used as a template in PCR to generate truncated versions of the FLAG-VP8 ORF, using the primers listed in Table 3.1. PCR fragments were cloned back into the pCMV4.1k expression vector to create the constructs described in the text. Correct ORFs of all constructs were verified by DNA sequencing. The pFLAG-CMV-2 plasmid was purchased from Sigma-Aldrich. The IFN-α/β responsive reporter plasmid, pISREluc, and pRL-TK have been described previously (375), and were kindly provided by Dr. Danielle Blondel, LVMS, CNRS, France. pISREluc contains the firefly luciferase gene fused with four tandem repeats of the IFN-inducible gene 9-27 ISRE. pRL-TK, which contains the herpes simplex virus thymidine kinase promoter region upstream of the *Renilla* luciferase gene, was used to normalize transfection. A Simian Virus 5 V expression plasmid, pSV5V, and pHis-Ub plasmids were kindly provided by Dr. Richard Randall, University of St. Andrews, School of Biology, St, Andrews, Fife, United Kingdom.

3.4.4 Luciferase assay.

Vero cells were used as IFN-deficient cells to demonstrate the effect of transient VP8 expression on IFN-treated and nontreated cells. Vero cells were seeded at a concentration of 7×10^4 cells per well in 24-well plates. The next day, the cells were transfected with pRL-TK and pISREluc together with pCMV4.1K (empty vector), pFLAG-EYFP, or pFLAG-VP8 by using Lipofectamine and Plus reagent (Invitrogen, Life Technologies). At 24 h posttransfection, cells were treated with 2,500 units/0.5 ml of human IFN-β or left untreated. While MDBK cells are routinely used for propagation of high-titer BoHV-1, they are very resistant to transfection. EBTr cells have a relatively good transfection efficiency and thus were used to determine the effects of VP8 on IFN during BoHV-1 infection. EBTr cells were transfected with pRL-TK and pISREluc plasmids, and 24 h later the cells were infected with BoHV-1 or BoHV-1-ΔU_L47. At 24 h post infection, the cells were treated with 400 ng/0.5 ml of bovine IFN-β or left untreated. Cells were harvested 6 h after IFN treatment in lysis buffer. Firefly and *Renilla* luciferase activity were assayed in the cell lysates according to the manufacturer's protocol (dual-luciferase reporter assay

system; Promega, Madison, WI, USA). The relative expression levels were determined by dividing the firefly luciferase values by the *Renilla* luciferase values. Actinomycin D (ActD; Sigma-Aldrich) was used to treat cells before the luciferase assay. EBTr cells were transfected with pRL-TK and pISREluc for 20 h. The transfected cells were treated with ActD at a concentration of 10 μg/ml for 1 h before mock infection or infection with BoHV-1 or BoHV1-U_L47R at an MOI of 4 or with BoHV-1-ΔU_L47 at an MOI of 10. ActD was maintained in the medium throughout the infection. One hour after addition of the virus ActD was removed, the medium was replaced with fresh medium, and cells were stimulated with bovine IFN-β for 1 h. Cell lysates were prepared and luciferase assays were performed as described above.

3.4.5 Preparation of cell lysates.

HEK293T and EBTr cells at 80 to 90% confluence were transfected with different plasmids by using Lipofectamine and Plus reagent (Invitrogen, Life Technologies). HEK293T cells were used for coimmunoprecipitation experiments. Cells were incubated with MEM for 48 h, washed with ice-cold PBS (pH 7.3), and lysed in lysis buffer (50 mM Tris, 150 mM NaCl, 1 mM EDTA, 1% Triton X-100, pH 7.4) supplemented with 10 μl/ml mammalian cell and tissue extract protease inhibitor cocktail (Sigma-Aldrich). Cells were gently rocked on a nutator for 3 to 4 min and then kept on ice for 30 min before centrifugation at 12,000 × *g* for 15 min at 4°C. The supernatant was collected in an Eppendorf tube and kept at −80°C for future use. EBTr cells were used for transfection and BoHV-1 infection. To prepare lysates, BoHV-1-infected cells were collected at 24 h post infection.

3.4.6 Immunoprecipitation and Western blotting.

Cell lysates prepared as described above were incubated with ant-VP8, anti-STAT1, or anti-ubiquitin antibody overnight at 4°C followed by incubation with protein G-Sepharose Fast Flow beads (GE HealthCare, Niskayuna, NY, USA) for 3 h at 4°C; alternatively, anti-FLAG M2 affinity gel (Sigma-Aldrich) was directly added to the cell lysates, and the mixtures were incubated at 4°C overnight. This was followed by three washes with buffer (50 mM Tris-HCl, 250 mM NaCl, 2% Triton X-100, pH 7.4). For Western blotting, 15 to 25 μg of the immune complexes or cell lysates was boiled for 5 min after addition of SDS-PAGE sample buffer. Proteins were separated on 10% or 8 to 16% SDS-PAGE gels and then transferred to

nitrocellulose membranes. The nitrocellulose membranes were blocked with 5% skim milk in phosphate-buffered saline-Tween-20 (PBST; 3.2 mM Na_2HPO_4, 0.5 mM KH_2PO_4, 1.3 mM KCl, 135 mM NaCl, 0.1% Tween 20, pH 7.4) for 2 h followed by incubation overnight at 4°C with anti-STAT1, anti-FLAG, anti-VP8, and/or anti-ubiquitin antibodies. The membranes were washed three times with PBST and incubated with IRDye680-conjugated anti-mouse IgG or IRDye-800CW-conjugated anti-rabbit IgG (LI-COR Bioscience, Lincoln, NE, USA). The proteins were detected with an Odyssey Infrared Imaging system (LI-COR Bioscience) followed by processing of images by Odyssey 3.0.16 application software (LI-COR Bioscience).

3.4.7 Cell fractionation.

Cytoplasmic and nuclear fractions were obtained as described previously (26). Cell fractionation was performed using Nuclei EZ Prep lysis buffer (Sigma). Briefly, cells were collected by trypsinization followed by lysis for 5 min on ice with the Nuclei EZ lysis buffer. The nuclei were collected by centrifugation at 500 × *g* for 5 min at 4°C. The incubation in lysis buffer and centrifugation were repeated five times to remove any loosely bound cytoskeletal components from the nuclei. The supernatants were pooled as cytoplasmic fraction and concentrated with an Amicon Ultra-15 Ultracel-10K filter unit (Millipore). For nuclear isolation, the nuclei were resuspended in 3 ml of 0.25 M sucrose, 10 mM $MgCl_2$, and 1 mM phenylmethylsulfonyl fluoride (PMSF), layered over a 3-ml cushion of 0.88 M sucrose, 0.5 mM $MgCl_2$, and 1 mM PMSF, and centrifuged at 2,800 × *g* for 10 min at 4°C. The nuclear pellet was resuspended in 200 μl of the Nuclei EZ storage buffer. The nuclei were counted with a hemocytometer, and equal numbers of nuclei were lysed by incubation with SDS at 100°C for 5 min. The purity of the nuclei was determined by Western blotting with fibrillarin- and tubulin-specific antibodies.

3.4.8 Immunofluorescence and confocal microscopy.

Vero cells were plated at a concentration of 2×10^5 cells per well in two-chamber Permanox slides (Lab-Tek, Naperville, IL, USA) and mock transfected or transfected with pFLAG-VP8 219-741 or pFLAG-VP8. At 24 h posttransfection, cells were fixed with 4% paraformaldehyde (Sigma-Aldrich) for 20 min at room temperature (RT) followed by permeabilization and blocking with 1% goat serum and 0.1% Triton X-100 in PBS. FLAG-

tagged proteins and STAT1 were detected by incubating cells with mouse monoclonal anti-FLAG (diluted 1:1,000) and rabbit anti-STAT1 (diluted 1:50) antibodies for 2 h at RT. MDBK cells were infected with BoHV-1 or BoHV1-U_L47R at an MOI of 4 or with BoHV1-ΔU_L47 at an MOI of 5 for 14 h and then fixed and stained as described above. For the time course experiment, MDBK cells were infected with BoHV-1 at an MOI of 4, and samples were fixed and blocked overnight. The next morning, cells were incubated with monoclonal anti-VP8 or anti-gB antibodies and rabbit anti-STAT1 antibodies for 2 h. Alexa Fluor 488 goat anti-mouse IgG and Alexa Fluor 633 goat anti-rabbit IgG (diluted 1:500; Invitrogen, Life Technologies) were used as secondary antibodies. Finally, mounting medium containing 4′,6-diamino-2-phenylindinole (DAPI) was added, and the slides were air dried for 24 h at RT. The cells were examined and images taken with a Leica SP5 confocal microscope (Leica Microsystems Inc., Concord, ON, Canada), using green laser excitation at 488 nm (Alexa 488), red laser excitation at 633 nm (Alexa 633), and 461 nm for DAPI. Final images were processed using the Image J browser.

3.5 Results.

3.5.1 VP8 inhibits IFN-β signaling.

While VP8 has been reported to be nonessential *in vitro*, it is critical for replication in cattle *in vivo*, which suggests that it might have a profound impact on the innate antiviral response. As type I IFN signaling constitutes one of the most powerful antiviral defense mechanisms, we examined whether VP8 plays a role in IFN down regulation by conducting luciferase reporter gene assays with Vero cells in the presence or absence of VP8 expression. Since Vero cells are IFN deficient, IFN-β responses were induced by addition of extracellular IFN-β. Vero cells were transfected with luciferase reporter plasmids pRL-TK and pISRE together with pCMV4.1K, pFLAG-EYFP, or pFLAG-VP8, and cells were stimulated with IFN-β at 24 h posttransfection or left untreated. IFN-β treatment of Vero cells resulted in induction of luciferase expression compared to untreated cells (Figure. 3.1A). When the cells were transfected with CMV4.1K or FLAG-EYFP, no inhibition of IFN-β signaling was observed. However, IFN signaling was reduced to 22% in VP8-expressing cells compared to cells transfected with pCMV4.1K or pFLAG-EYFP. This indicates transcriptional activation of the ISREs due to the formation of ISGF3 transcription complexes in the cells. Treatment of FLAG-VP8-transfected Vero cells with IFN-β demonstrated that the expression of VP8 inhibits IFN-β-responsive

transcription. The presence of VP8 in the cell lysates was confirmed by Western blotting with anti-VP8 antibody (Figure. 3.1B).

The IFN-β response was also investigated in the context of BoHV-1 infection. EBTr cells were transfected with luciferase reporter plasmids, and at 24 h posttransfection cells were mock infected or infected with BoHV-1 or BoHV1-ΔU_L47. IFN-β treatment of mock-infected cells resulted in significant production of luciferase, in contrast to what was observed for nontreated cells. However, BoHV-1 infection reduced the induction of luciferase expression by IFN-β to ~20% compared to mock infection (Figure. 3.1C) indicating inhibition of IFN signaling. Some luciferase activity was also observed in cells not treated with IFN-β, which can be attributed to the fact that EBTr cells are not IFN deficient. In BoHV1-ΔU_L47-infected cells, the luciferase activity was higher than that in BoHV-1-infected cells, further confirming the inhibitory effect of VP8 on the IFN response. These results suggest that VP8 functions as IFN-β antagonist during BoHV-1 infection.

Some residual down-regulation of the IFN response was observed in BoHV1-ΔU_L47-infected cells, which could be attributed to the presence of bICP0. To confirm the inhibition of IFN signaling by VP8 in the absence of any immediate early protein expression, ActD was used to inhibit transcription. EBTr cells were transfected with luciferase reporter plasmids, and at 20 h posttransfection cells were or were not pretreated with ActD before mock infection or infection with BoHV-1, BoHV1-ΔU_L47, or BoHV1-U_L47R. In BoHV-1- and BoHV-1-U_L47R-infected cells, the luciferase signal was reduced to ~20% without ActD treatment compared to mock-infected cells (Figure. 3.1D), while infection with BoHV1-ΔU_L47 reduced IFN signaling to ~70%. The expression of VP8 and two immediate early proteins, bICP0 and bICP4, is shown in Figure 3.1E. Since ActD is a transcription inhibitor, no expression of immediate early protein was observed in ActD-treated cells as expected. However, VP8 was detected at 2 h post infection in BoHV-1- and BoHV-1-U_L47R-infected cells regardless of ActD treatment (Figure. 3.1E & 3.1G), representing VP8 released from the virions. In the presence of ActD, IFN signaling was again inhibited by BoHV-1 or BoHV1-U_L47R infection to ~20%, while the mock and BoHV1-ΔU_L47 infection did not cause down-regulation of IFN signaling (Figure 3.1F) These experiments demonstrate that the residual inhibition of IFN signaling induced by BoHV1-ΔU_L47 was due to immediate early gene expression. Furthermore, inhibition IFN signaling was caused by VP8 released from the incoming virions in the absence of any immediate early protein expression.

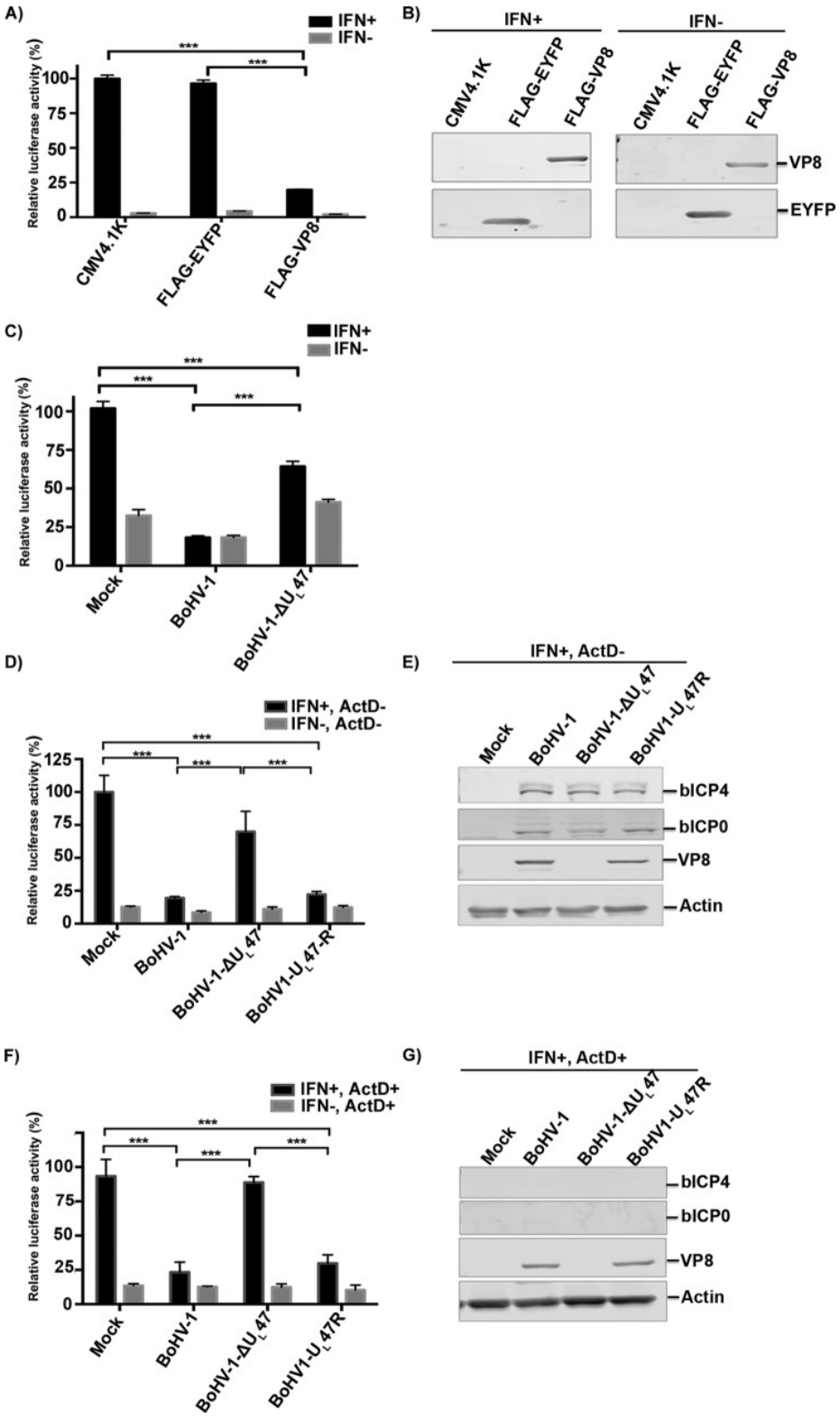

Figure. 3.1 Inhibition of IFN-β signaling by BoHV-1 VP8.

Vero cells were transfected with pISREluc and pRL-TK together with pCMV4.1K, pFLAG-EYFP, or pFLAG-VP8. (A) At 24 h posttransfection, cells were stimulated with 2,500 units of human IFN-β in 0.5 ml or left untreated. After 6 h of incubation, cell lysates were made and reporter gene activity was measured. (B) Expression of VP8 and EYFP was confirmed by Western blotting with monoclonal anti-FLAG antibody. (C) EBTr cells were transfected with pISREluc and pRL-TK. At 24 h posttransfection cells were mock infected or infected with BoHV-1 or BoHV1-ΔU_L47, and another 24 h later cells were treated with 400 ng of bovine IFN-β in 0.5 ml or left untreated. After 6 h of incubation, cell lysates were made and reporter gene activity was measured. (D to G) EBTr cells were transfected with pISREluc and pRL-TK, and at 20 h posttransfection cells were either left untreated (D and E) or were pretreated with ActD (F and G) before mock infection or infection with BoHV-1, BoHV1-ΔU_L47, or BoHV1-U_L47R. (D and F) At 1 h post infection, cells were stimulated with IFN-β for 1 h, and at 2 h post infection cell lysates were collected and reporter gene activity was measured. ActD was maintained in the medium throughout the infection. (E and G) Expression of VP8, bICP0, and bICP4 in untreated cells (E) but not in Act-treated cells (G) was confirmed by Western blotting with monoclonal anti-FLAG antibody and bICP0- and bICP4-specific rabbit antibodies, respectively. IFN-β-induced firefly luciferase reporter values were normalized to the expression of *Renilla* luciferase. The values are presented as percentages of IFN-stimulated controls and are expressed as means ± standard deviations (SD) for six samples. Statistical significance is indicated by asterisks (***, $P < 0.001$).

3.5.2 Identification of STAT1 as an interacting target of BoHV-1 VP8.

Since STATs play a critical role in IFN signaling, we determined whether VP8 might interact with STAT1 or STAT2. HEK293T cells were transiently transfected with pFLAG-EYFP or pFLAG-VP8. At 48 h posttransfection, cell lysates were prepared and incubated with anti-FLAG resin (Figure. 3.2A) and anti-STAT1 antibody followed by protein G-Sepharose (Figure. 3.2B). STAT1 was precipitated from pFLAG-VP8-transfected cells but not from pFLAG-EYFP- or mock-transfected cells (Figure. 3.2A). Anti-STAT1 antibody precipitated STAT1 from mock-, FLAG-EYFP-, and FLAG-VP8-transfected lysates (Figure. 3.2B), whereas it precipitated VP8 from the FLAG-VP8-, but not from mock- or FLAG-EYFP-transfected cell lysates (Figure. 3.2B). Expression of pFLAG-EYFP and pFLAG-VP8 in transfected cell lysates is confirmed in Figure. 3.2C. As further evidence of VP8 interaction with endogenous STAT1, MDBK cells were infected with BoHV-1 or BoHV1-ΔU_L47. At 24 h post infection cells were lysed, and proteins were precipitated with anti-bovine STAT1 antibody followed by Protein G Sepharose, and analyzed by Western blotting. As shown in Figure. 3.2D, VP8 was precipitated with cellular STAT1 in BoHV-1-infected cells, whereas no VP8 was pulled down from mock- or BoHV1-ΔU_L47-infected cell lysates. The expression of VP8 and STAT1 in BoHV-1-infected cells is shown in Figure. 3.2F. To pull down endogenous STAT1 with BoHV-1 VP8, mock, BoHV-1 or BoHV1-ΔU_L47-infected cell lysates were incubated with anti-VP8 antibody followed by Protein G Sepharose. STAT1 was precipitated with VP8-specific antibody in BoHV-1-infected cells but not in mock- or BoHV1-ΔU_L47-infected cells (Figure. 3.2E). To identify interactions between VP8 and STAT2, mock, FLAG-EYFP and FLAG-VP8 transfected lysates (Figure. 3.2G) were subjected to immunoprecipitation with anti-FLAG resin. Input lysates are presented in Figure. 3.2H. STAT2 was neither precipitated by FLAG-EYFP nor by FLAG-VP8. These results demonstrate that VP8 interacts with STAT1 in both transiently transfected and BoHV-1-infected cells. However, VP8 did not interact with STAT2.

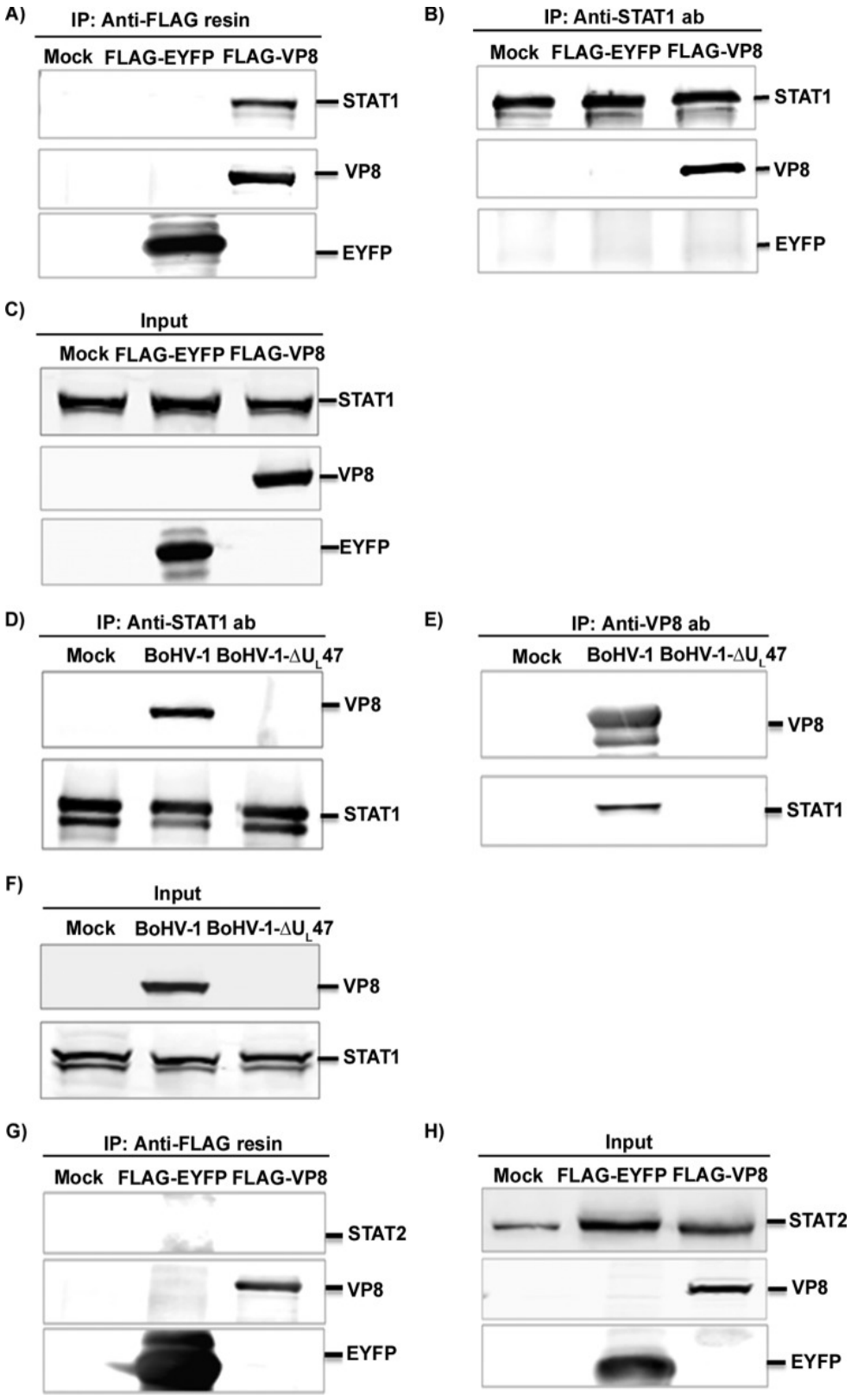

Figure. 3.2 BoHV-1 VP8 interacts with STAT1.

HEK293T cells were transfected with pFLAG-EYFP or pFLAG-VP8. (A and B) At 48 h posttransfection, cell lysates were generated and incubated with anti-FLAG resin (A) or anti-STAT1 antibody (B) followed by protein G-Sepharose. (C) Input lysates of mock-, pFLAG-EYFP-, and pFLAG-VP8-transfected cells that were used in the immunoprecipitation assays illustrated in panels A and B. (D to F) MDBK cells were mock infected or infected with BoHV-1 or BHV1-ΔU_L47. (D and E) At 24 h post infection, cell lysates were made and incubated with anti-STAT1 antibody (D) and anti-VP8 antibody (E), followed by protein G-Sepharose. (F) Expression of VP8 in BoHV-1-infected cells and STAT1 in mock-, BoHV-1-, or BoHV1-ΔU_L47-infected cells. (G and H) HEK293T cells were transfected with pFLAG-EYFP or pFLAG-VP8. (G) At 48 h posttransfection, cell lysates were collected and incubated with anti-FLAG resin. (H) Input lysates of mock-, pFLAG-EYFP-, and pFLAG-VP8-transfected cells that were used in the immunoprecipitation assay illustrated in panel G. VP8, EYFP, STAT1, and STAT2 were detected by Western blotting with monoclonal anti-VP8 and anti-FLAG antibodies and rabbit anti-STAT1 and anti-STAT2 antibodies, respectively.

3.5.3 Identification of interacting domains of VP8 with STAT1.

Since the central and C-terminal parts of VP8 are conserved between herpesviruses while the N-terminal part is not (Figure. 3.3), it was of interest to determine which domain of VP8 interacts with STAT1. Nine different plasmids containing N-terminally and C-terminally truncated, FLAG-tagged VP8-coding sequences were generated. First, plasmids encoding N-terminally truncated FLAG-tagged VP8 were used to investigate the role of the C-terminal domain of VP8 in the interaction with STAT1. Anti-STAT1 antibody precipitated all N-terminally truncated versions of VP8 (VP8 121-741, VP8 219-741, VP8 343-741, VP8 538-741 and VP8 632-741) as well as full-length VP8 (Figure. 3.4A) from transfected cells. As all of the N-terminally truncated VP8 versions contain amino acids 632-741, this suggests that a STAT1-binding domain is located within this region of VP8. To investigate the involvement of the N-terminal domain of VP8 in the interaction with STAT1, cell lysates with C-terminally truncated VP8 (VP8 1-120, VP8 1-258, VP8 1-482 and VP8 1-631) and full-length VP8 were analyzed by immunoprecipitation with anti-STAT1 antibody (Figure. 3.4C). This experiment demonstrated that VP8 was only precipitated by anti-STAT1 antibody when amino acids 259-482 were retained, and this occurred even though amino acids 632-741 were absent. Input cell lysates are presented in Figure. 3.4B and 3.4D. These results indicate that the conserved central and C-terminal parts of VP8 contain two domains, 259-483 and 632-741, that mediate its interaction with STAT1. To further define the interacting regions of VP8, four additional VP8 truncations consisting of amino acids 1-371, 372-483, 631-686 and 687-741, were generated. The latter four truncations also contained amino acids 1-258, a domain shown not to interact with STAT1, at the N-terminal region to facilitate expression. VP8 259-371, VP8 372-483 and VP8 631-686, but not VP8 687-741, were immunoprecipitated with anti-STAT1 antibody (Figure. 3.4E). Input lysates demonstrating expression of these truncated VP8 versions and STAT1 are shown in Figure. 3.4F. This result demonstrates that domains within the 259-482 and 632-686 regions of VP8 are required for its interaction with STAT1. A schematic presentation summarizing VP8-interacting domains with STAT1 is provided in Figure. 3.5.

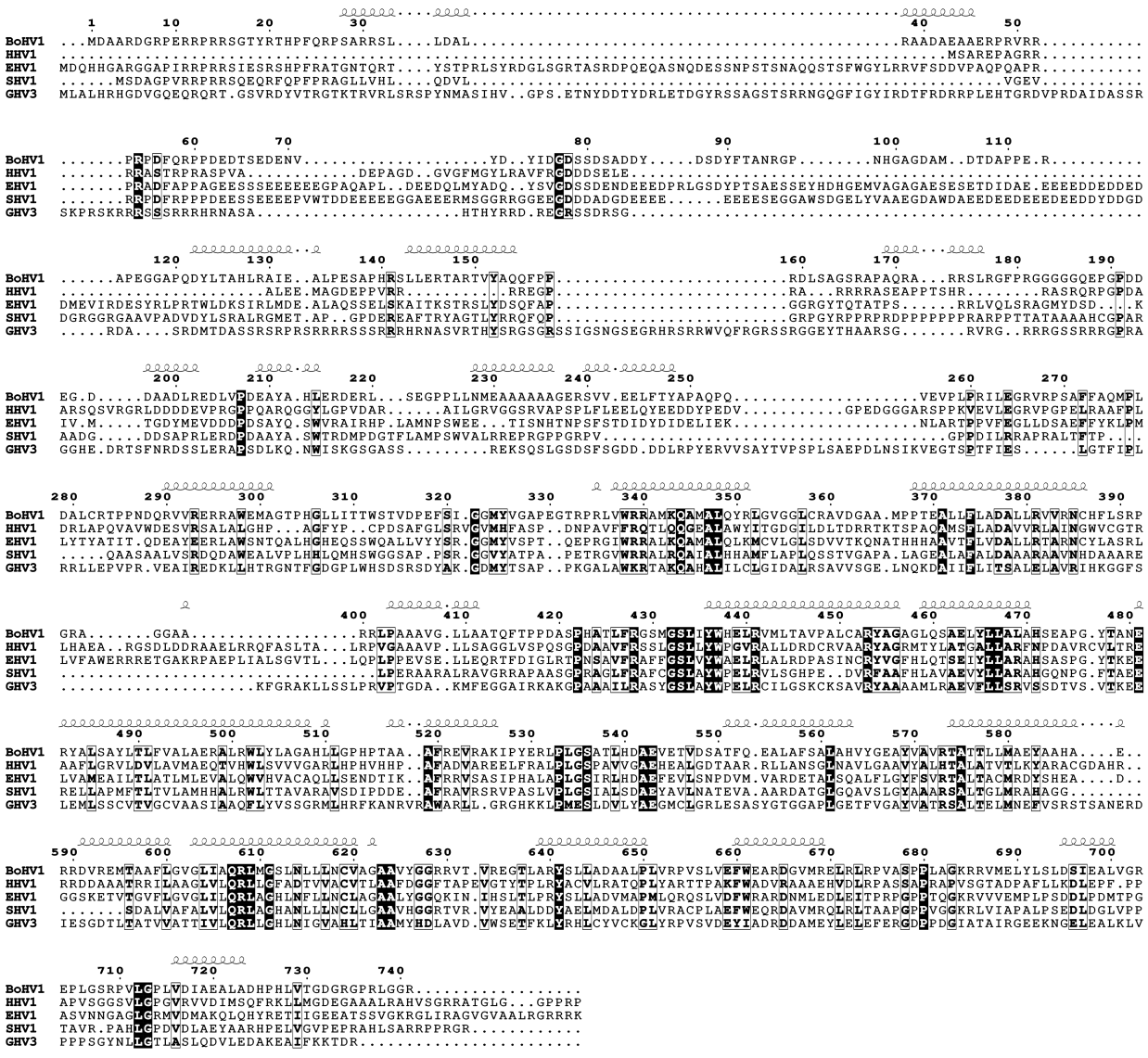

Figure. 3.3 Comparison of the amino acid sequences of BoHV-1 UL47 and its homologues.

The sequence labels are Bovine herpesvirus 1 (BoHV1), Human herpesvirus 1 (HHV1), Equine herpesvirus 1 (EHV1), Suid herpesvirus 1 (SHV1) and Gallid herpesvirus 3 (GHV3) UL47 protein. The consensus secondary structure prediction for the UL47 family is shown above the sequences. The prediction was carried out using PROFphd software (381, 382). Invariant residues are highlighted in bold letters with white boxes, and highly conserved residues in white bold text surrounded by black boxes. The alignment was generated using UniPro (citation) and the figure was generated using the ESPript server (382).

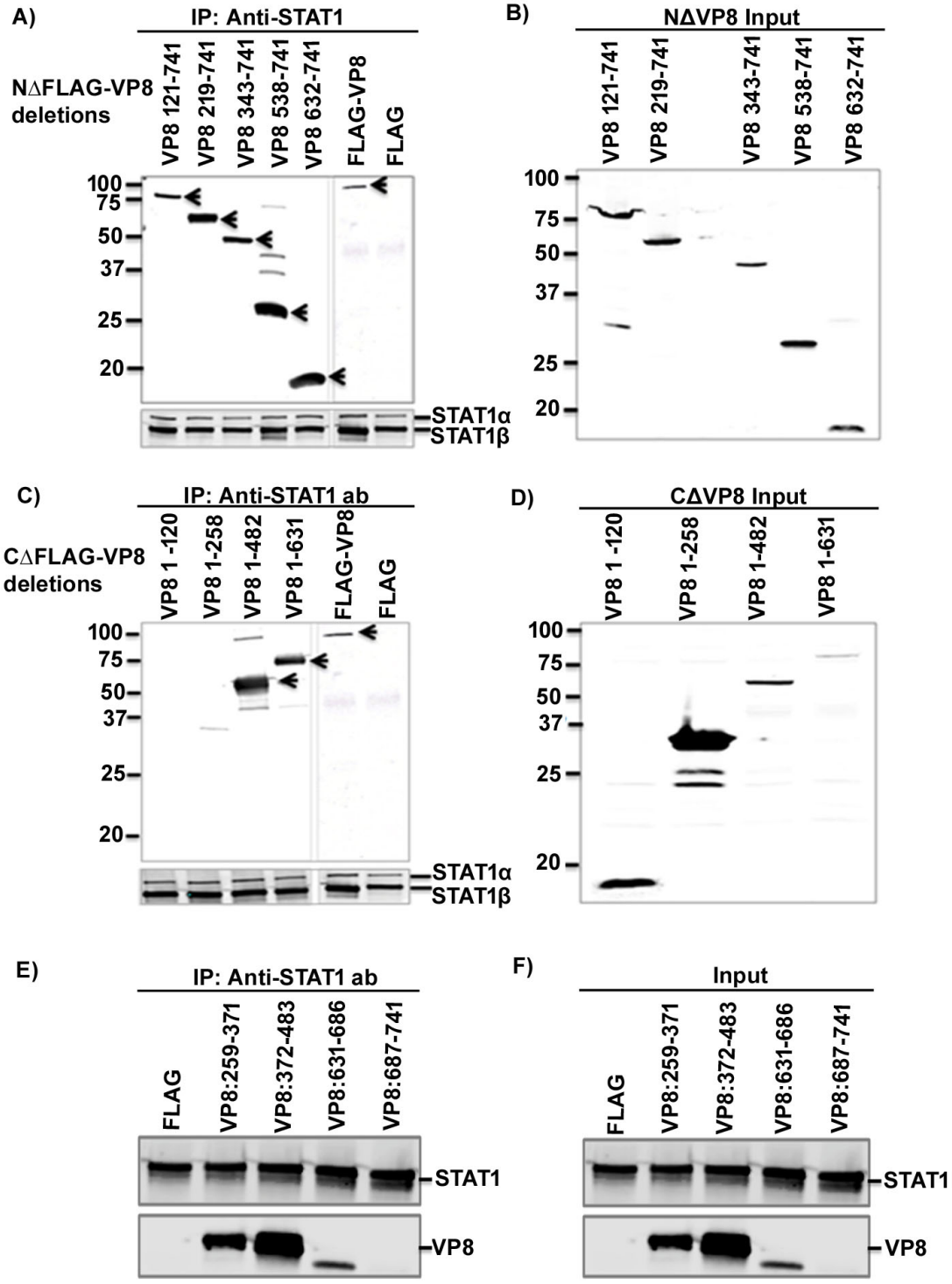

Figure. 3.4 Mapping of STAT1 interacting domains in BoHV-1 VP8.

HEK293T cells were transfected with plasmids containing FLAG, FLAG-VP8, or different N-terminally and C-terminally truncated FLAG-tagged VP8 versions as indicated. At 48 h posttransfection, cell lysates were made and incubated with anti-STAT1 antibodies (ab), followed by incubation with protein G-Sepharose. Immune complexes were separated by SDS-PAGE and

detected by Western blotting. Immunoprecipitation of N-terminally (A) and C-terminally (C) truncated FLAG-tagged VP8 with anti-STAT1 antibody. Input lysates of cells transfected with N-terminally (B) and C-terminally (D) truncated FLAG-tagged VP8. (E) Immunoprecipitation of VP8 259-371, 372-483, 631-686, and 687-741 with anti-STAT1 antibody. (F) Input lysates of cells transfected with VP8 259-371, 372-483, 631-686, or 687-741. Truncated and full-length VP8 and STAT1 were detected using antibodies specific for FLAG and STAT1, respectively. It should be noted that anti-STAT1 antibody detects both STAT1α and STAT1β. Molecular weight markers ($\times 10^{-3}$) are indicated in the left margins.

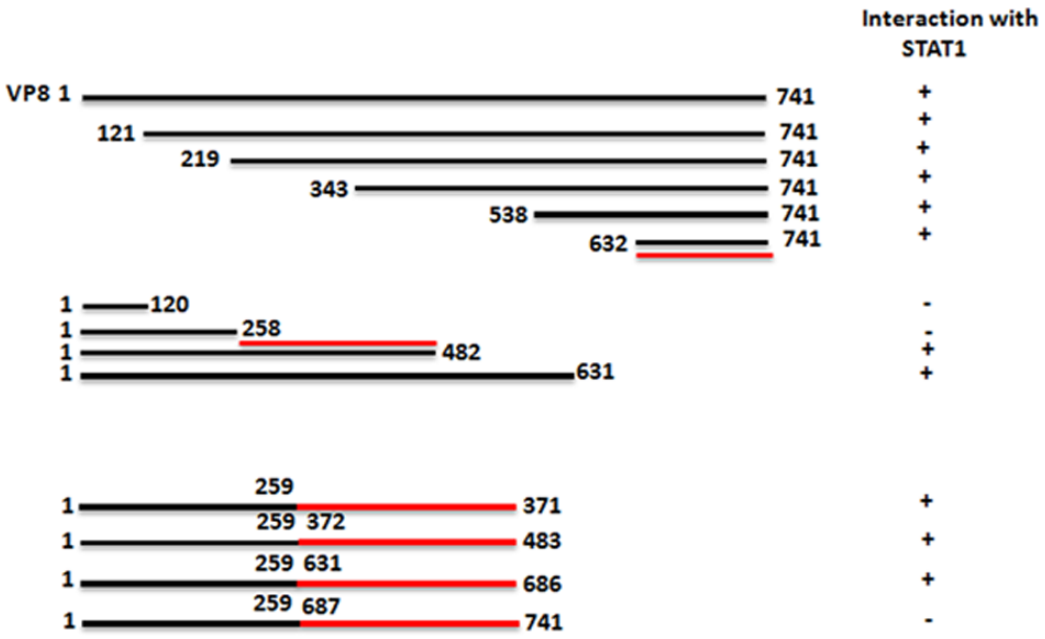

Figure. 3.5 Schematic representation of the interacting domains of VP8 with STAT1.

The solid lines represent the presence of VP8 amino acids and empty spaces represent the deleted portions of VP8. Interaction of VP8 with STAT1 is shown by the + sign and lack of interaction is indicated by the – sign. The first and last amino acids of each VP8 mutant are indicated. The red lines indicate STAT1-interacting domains of VP8.

3.5.4 Effects of VP8 on STAT1 ubiquitination and degradation.

STAT1 is a well-known transcriptional regulator. Some viral proteins, such as SV5 V protein, interact with STAT1 and mediate ubiquitination and subsequent degradation of STAT1 (375). Since BoHV-1 VP8 caused down-regulation of IFN-β signaling and interacted with STAT1, we investigated whether STAT1 is ubiquitinated and degraded in the presence of VP8 or SV5 protein V, which was used as positive control for detection of STAT1 ubiquitination. HEK 293T cells were co-transfected with pFLAG/pHis-Ub, pFLAG-VP8/pHis-Ub and pSV5V/pHis-Ub plasmids in the presence or in the absence of the proteasome inhibitor MG132. Since ubiquitin proteases cleave off ubiquitin from polyubiqutinated STAT1, His-Ub plasmid was used for transfection in each sample. To prevent cleavage of ubiquitin from ubiquitinated STAT1, the ubiquitin protease inhibitor guanidium hydrochloric acid was used at a final concentration of 6M in the lysis buffer. At 24 h post-transfection cell lysates were generated and incubated with His-60 nickel beads, and protein complexes were analyzed by Western blotting with anti-STAT1 antibody. Figure. 3.6A shows that ubiquitinated STAT1 was not pulled down in mock- and FLAG-VP8 transfected lysates, but was pulled down from SV5 V-transfected lysates. Input lysates are presented in Figure. 3.6B. In the absence of MG132 STAT1 was not detected (Figure. 3.6D), and thus not pulled down by His-Ub (Figure. 3.6C). VP8 was precipitated by anti-ubiquitin antibody (Figure. 3.6E), and anti-VP8 antibody pulled down ubiquitinated VP8 from FLAG-VP8 transfected lysates, but not from FLAG-transfected lysates (Figure. 3.6F), which confirms that VP8 is ubiquitinated as shown previously and validates the ubiquitin-specific antibody. This demonstrates that, although BoHV-1 VP8 interacts with STAT1, STAT1 is not ubiquitinated by the presence of VP8. This confirms that STAT1 is not degraded by the proteasome. Taken together these results suggest that BoHV-1 VP8 interacts with STAT1 without mediating ubiquitination or degradation of STAT1.

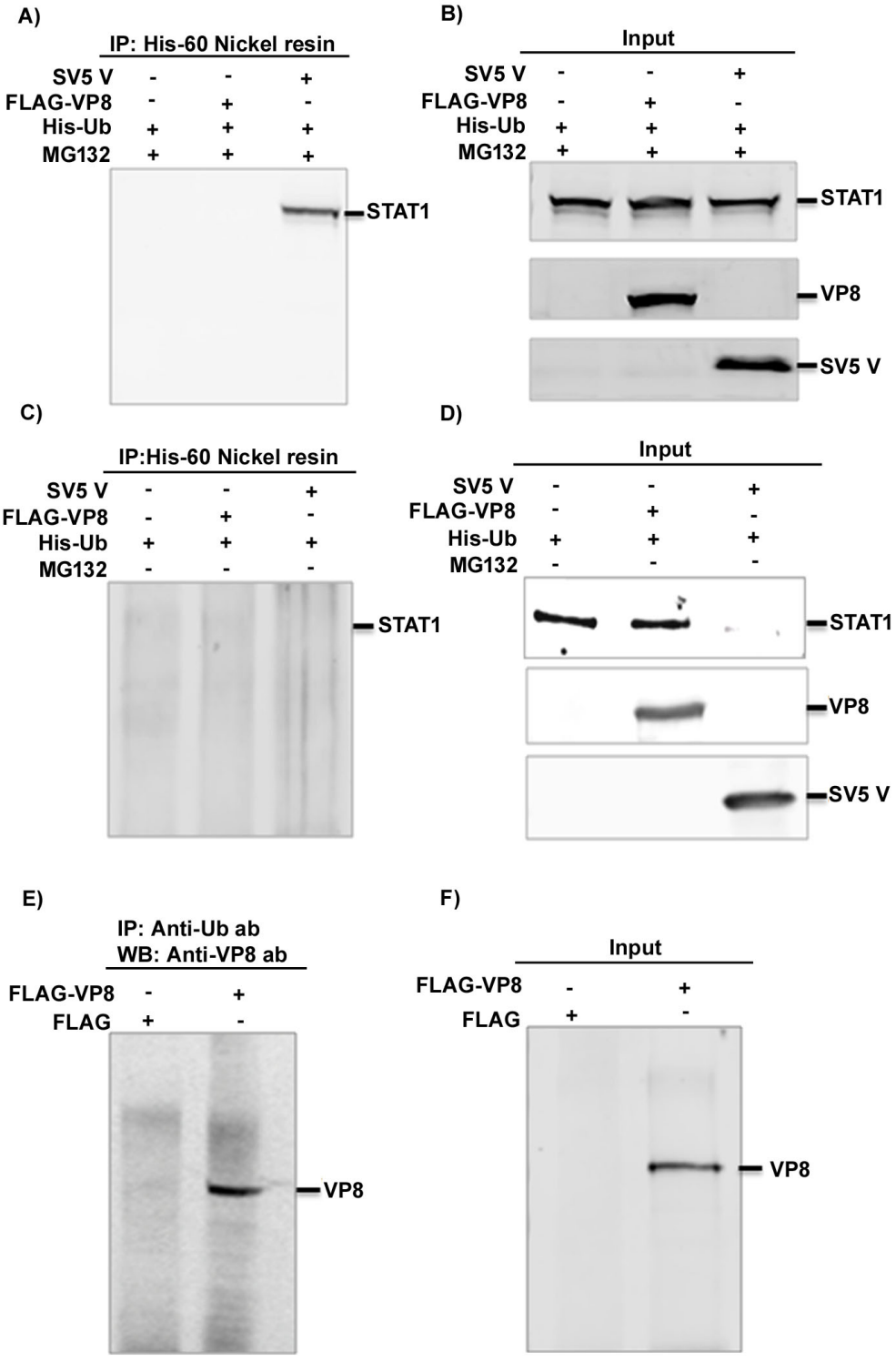

Figure. 3.6 Cellular STAT1 is not ubiquitinated by the presence of BoHV-1 VP8.

Cellular STAT1 is not ubiquitinated by the presence of BoHV-1 VP8. (A to D) HEK293T cells were transfected with pFLAG/pHis-Ub, pFLAG-VP8/pHis-Ub, and pSV5V/pHis-Ub in the presence or absence of 10 μM MG132. At 24 h posttransfection, cell lysates were generated and incubated with His-60 nickel resin in the presence (A) or absence (C) of MG132 followed by Western blotting with anti-STAT1 antibody. Input lysates of pFLAG/pHis-Ub-, pFLAG-VP8/pHis-Ub-, and pSV5V/pHis-Ub-transfected cells are shown in panels B and D. (E and F) HEK293T cells were transfected with pFLAG or pFLAG-VP8. At 24 h posttransfection, cell lysates were generated and incubated with antiubiquitin antibody (E) and anti-VP8 antibody (F), followed by protein G-Sepharose. Monoubiquitinated VP8 was detected by Western blotting with anti-FLAG antibody (E) or with anti-Ub antibody (F).

3.5.5 Effect of VP8 on STAT1 tyrosine phosphorylation.

IFN-α and -β signaling is stimulated by binding of IFN-α and -β to the cell surface receptors. Engagements of IFN receptors leads to phosphorylation of STAT1, STAT2 and several other cellular kinases (reviewed in (373)). To investigate whether VP8 impairs this stage in IFN-β signaling, IFN-β-induced STAT1 tyrosine phosphorylation was examined (Figure. 3.7). Vero cells were transfected with pFLAG-EYFP or pFLAG-VP8. At 24 h posttransfection cells were stimulated with human IFN-β for 4 h or left untreated. Cell lysates were separated by SDS-PAGE and transferred to nitrocellulose membrane, and STAT1 and STAT1 phosphorylated at tyrosine residue Y^{701} were detected using anti-STAT1 and anti-pSTAT1 antibodies, respectively. As a loading control actin was detected by anti-actin antibody. STAT1 started to be phosphorylated within 10 min of IFN-β treatment compared to non-treated cells in the presence of both FLAG-EYFP and FLAG-VP8. The total STAT1 and phosphorylated STAT1 amounts were similar in the presence and absence of VP8 in the cells, which indicates that the expression of VP8 does not reduce STAT1 phosphorylation.

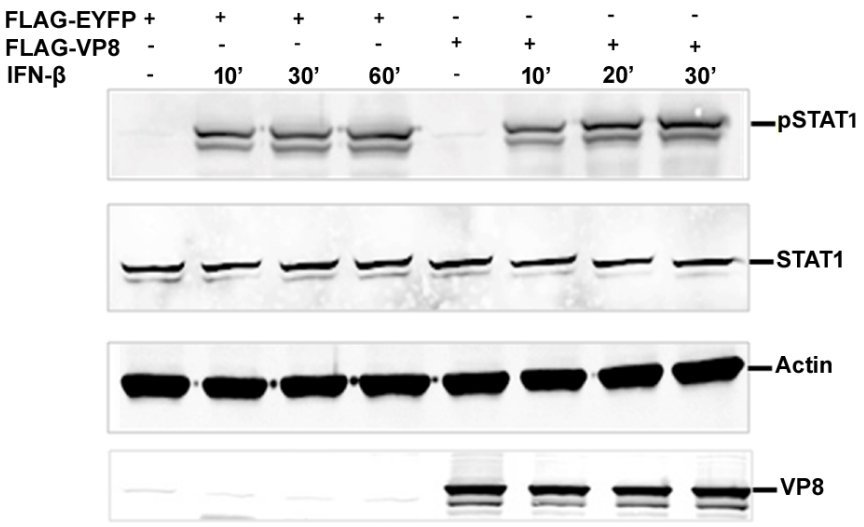

Figure. 3.7 VP8 does not affect STAT1 tyrosine phosphorylation.

Vero cells were transfected with pFLAG-EYFP or pFLAG-VP8. At 24 h posttransfection, cells were stimulated with IFN-β (2,500 units/0.5 ml) for 10, 30, and 60 min, and cell lysates were generated. Twenty-five micrograms of cellular protein were loaded and separated on a 10% gel for Western blot analysis. Phosphorylated STAT1, STAT1, and VP8 were detected by anti-pSTAT1, anti-STAT1, and anti-VP8 antibodies, respectively. As a protein loading control, actin was detected by anti-actin antibody.

3.5.6 VP8 inhibits IFN-β induced nuclear accumulation of STAT1.

In virus-infected cells nuclear translocation of STAT1 is stimulated by IFN-β. In the nucleus newly imported STAT1 together with STAT2 and IRF9 forms a multiprotein complex, ISGF3, which functions as transcriptional activator (reviewed in (373)). To further examine which step of IFN-β signaling is inhibited by VP8, we examined nuclear accumulation of STAT1 by immunofluorescence. Vero cells were transfected with pFLAG or with pFLAG-VP8 219-741, which expresses VP8 without nuclear localization signal (NLS) or with pFLAG-VP8. VP8 and STAT1 were detected with anti-FLAG and anti-STAT1 antibodies. As shown in Figure. 3.8A, IFN-β treatment of Vero cells redistributed STAT1 from the cytoplasm to the nucleus, whereas in non-treated cells STAT1 was cytoplasmic. Since the nuclear localization signal of VP8 was removed, VP8 219-741 was completely cytoplasmic and clearly prevented nuclear accumulation of STAT1 following IFN-β treatment (Figure. 3.8B). Without IFN-β treatment of VP8-expressing cells STAT1 was also cytoplasmic as expected. The translocation of STAT1 to the nucleus was also studied in the context of expression of full-length VP8, which is found mostly in the nucleus, while some if it is cytoplasmic. In most of the cells that expressed VP8, STAT1 remained cytoplasmic (Figure. 3.8C).

To examine the translocation of STAT1 in the context of infection, MDBK cells were mock-infected or infected with BoHV-1, BoHV1-ΔU_L47 or BoHV-1-U_L47R for 14 h. Cells were left untreated or were treated with IFN-β, and incubated with anti-VP8, anti-gB and bovine anti-STAT1 antibodies. As shown in Figure. 3.9A, IFN-β treatment of mock-infected cells resulted in transport of STAT1 into the nucleus, while without IFN-β treatment STAT1 was cytoplasmic. However, in BoHV-1 and BoHV-1-U_L47R-infected cells (Figure. 3.9B) IFN-β treatment did not result in nuclear accumulation of STAT1. To confirm the role of VP8 in inhibition of STAT1 nuclear translocation MDBK cells were -with BoHV1-ΔU_L47 (Figure. 3.9C). Infection with BoHV1-ΔU_L47 was confirmed by incubation with gB-specific monoclonal antibody. STAT1 was localized in the nucleus of BoHV1-ΔU_L47-infected cells, which confirms the role of VP8 in inhibition of STAT1 nuclear transport. These experiments demonstrated that nuclear accumulation of STAT1was inhibited by the presence of VP8.

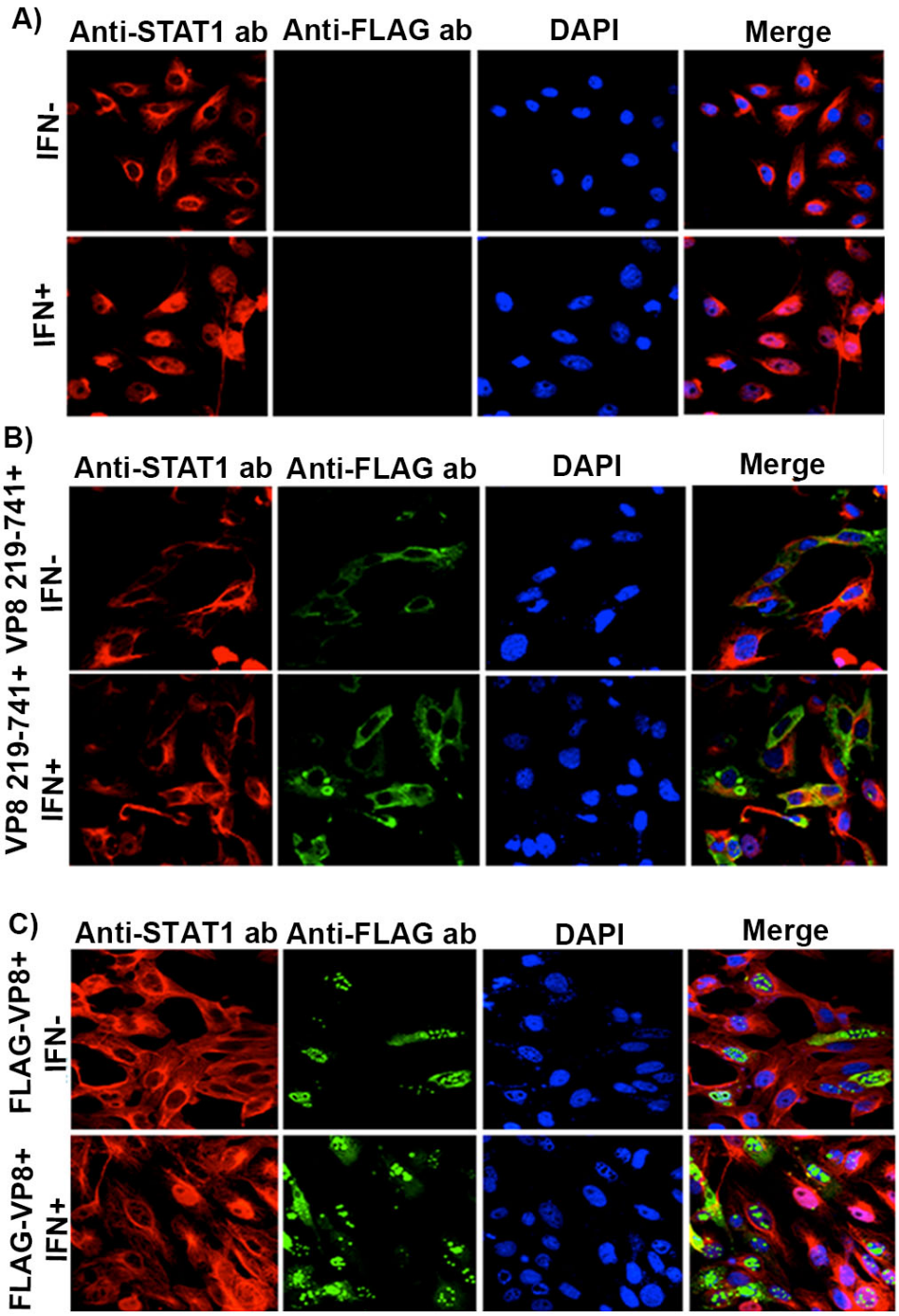

Figure. 3.8 VP8 prevents IFN-β-induced nuclear accumulation of STAT1.

Vero cells were transfected with A) pFLAG, B) pFLAG-VP8 219-741 or C) pFLAG-VP8. At 24 h post-transfection cells were stimulated with 2500 units of human IFN-β for 30 min or left untreated, followed by fixation with paraformaldehyde and permeabilization. Truncated and full-length VP8 were stained with monoclonal anti-FLAG antibody and Alexa-488-conjugated goat

anti-mouse IgG. STAT1 was detected with rabbit anti-STAT1 antibody and Alexa-633 conjugated anti-rabbit IgG. The nucleus was stained with Prolong gold DAPI. The cells were examined with a Leica SP5 confocal microscope.

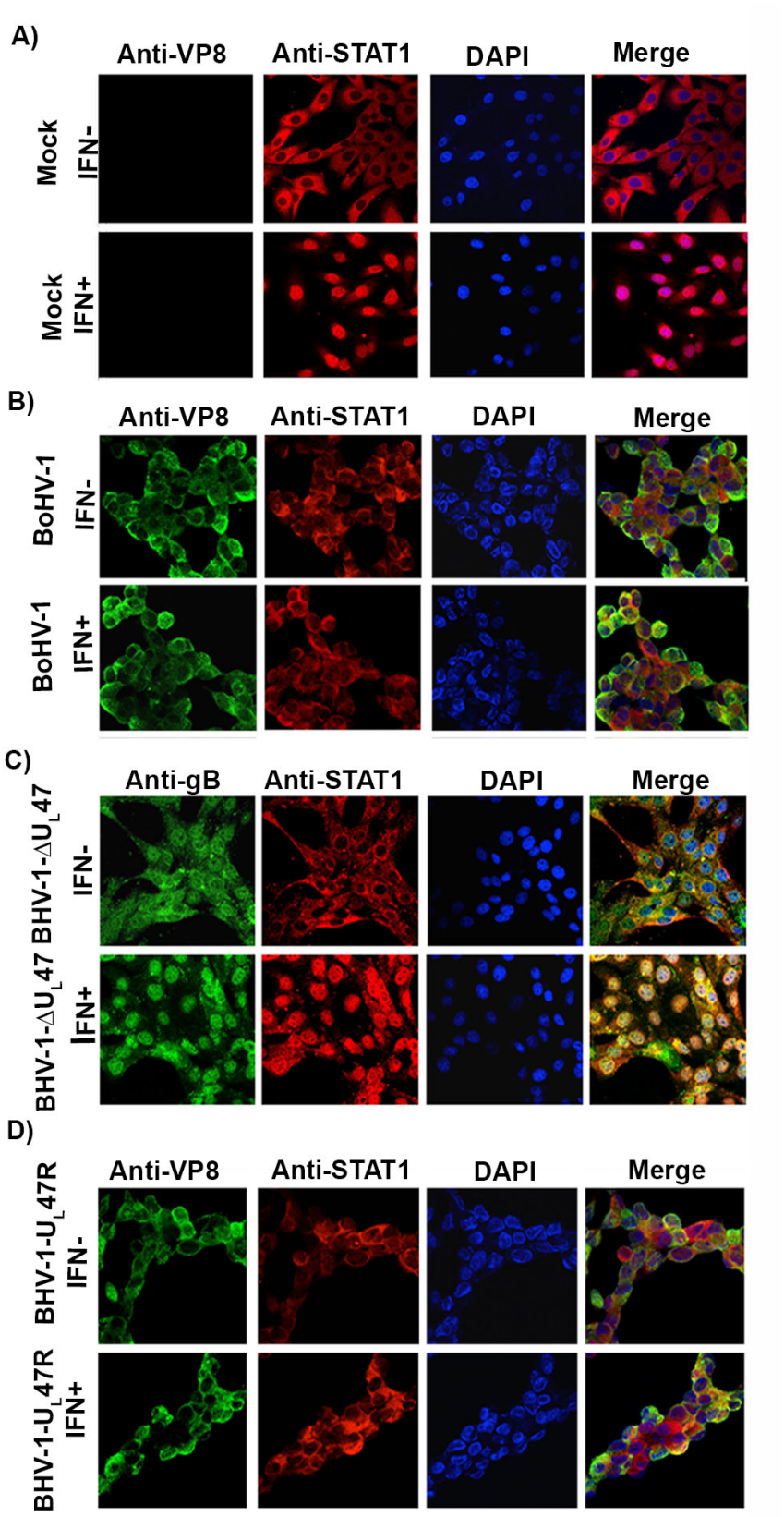

Figure. 3.9 BoHV-1 infection prevents IFN-β-induced nuclear accumulation of STAT1.

MDBK cells were A) mock-infected or B) infected with BoHV-1 at a MOI of 4 or C) with BoHV-1ΔU_L47 at a MOI of 5 and D) with BoHV-1-U_L47R at a MOI of 4. At 14 h post-infection cells were stimulated with bovine IFN-β for 30 min or left untreated. Cells were then fixed with paraformaldehyde, permeabilized and stained with monoclonal anti-VP8 or anti-gB antibodies and Alexa-488 conjugated goat anti-mouse IgG. STAT1 was detected with anti-STAT1 antibodies and Alexa-633 conjugated anti-rabbit IgG. DNA was labeled with Prolong gold DAPI. The cells were examined with a Leica SP5 confocal microscope.

3.5.7 Subcellular distribution of VP8 is correlated with the STAT1 translocation.

To determine how early after infection VP8 might be able to retain STAT1 in the cytoplasm, the subcellular localization of VP8 at early and late time points in the context of STAT1 retention was determined. MDBK cells were mock-infected or infected with BoHV-1 at a MOI of 4. At 2, 4, 6 or 14 h post-infection cells were stimulated with IFN-β or left untreated followed by VP8 and STAT1 detection (Figure. 3.10A & B). VP8 was detected as early as 2 h in the cytoplasm, while STAT1 was retained in the cytoplasm. As BoHV-1 infection progressed to 4 h, some VP8 was localized to the nucleus, but VP8 was also still present in the cytoplasm, as was STAT1. At 6 h post-infection most of the VP8 was detected in the nucleus, while STAT1 was still cytoplasmic. VP8 was again observed in the cytoplasm at 14 h post-infection. Throughout the entire period post-infection STAT1 was detected in the cytoplasm confirming that the retention of STAT1 was initiated with the incoming VP8 as early as 2 h.

To further confirm the subcellular distribution of VP8 at different stages of infection cytoplasmic and nuclear fractions were prepared from BoHV-1-infected MDBK cells at 2, 4, 6 and 14 h (Figure. 3.11) and then examined by Western blotting. The cytoplasmic (tubulin) and nuclear (fibrillarin) markers were used to validate the fractionation procedure. In agreement with the microscopy data VP8 was first detected in the cytoplasm at 2 h. At 4 h post-infection, VP8 gradually started to localize to the nucleus and at 6 h there was more VP8 in the nucleus than in the cytoplasm. However, at 14 h post infection most of the VP8 was present in the cytoplasm. According to these data incoming viral VP8 is present in the cytoplasm, and thus is capable of retaining STAT1 in the cytoplasm immediately after infection. Although VP8 then migrates from the cytoplasm to the nucleus, at late stages of infection it is again mostly in the cytoplasm. Since this large tegument protein is capable of STAT1 retention immediately after infection it explains the ability of VP8 to inhibit IFN signaling at the onset of BoHV-1 infection.

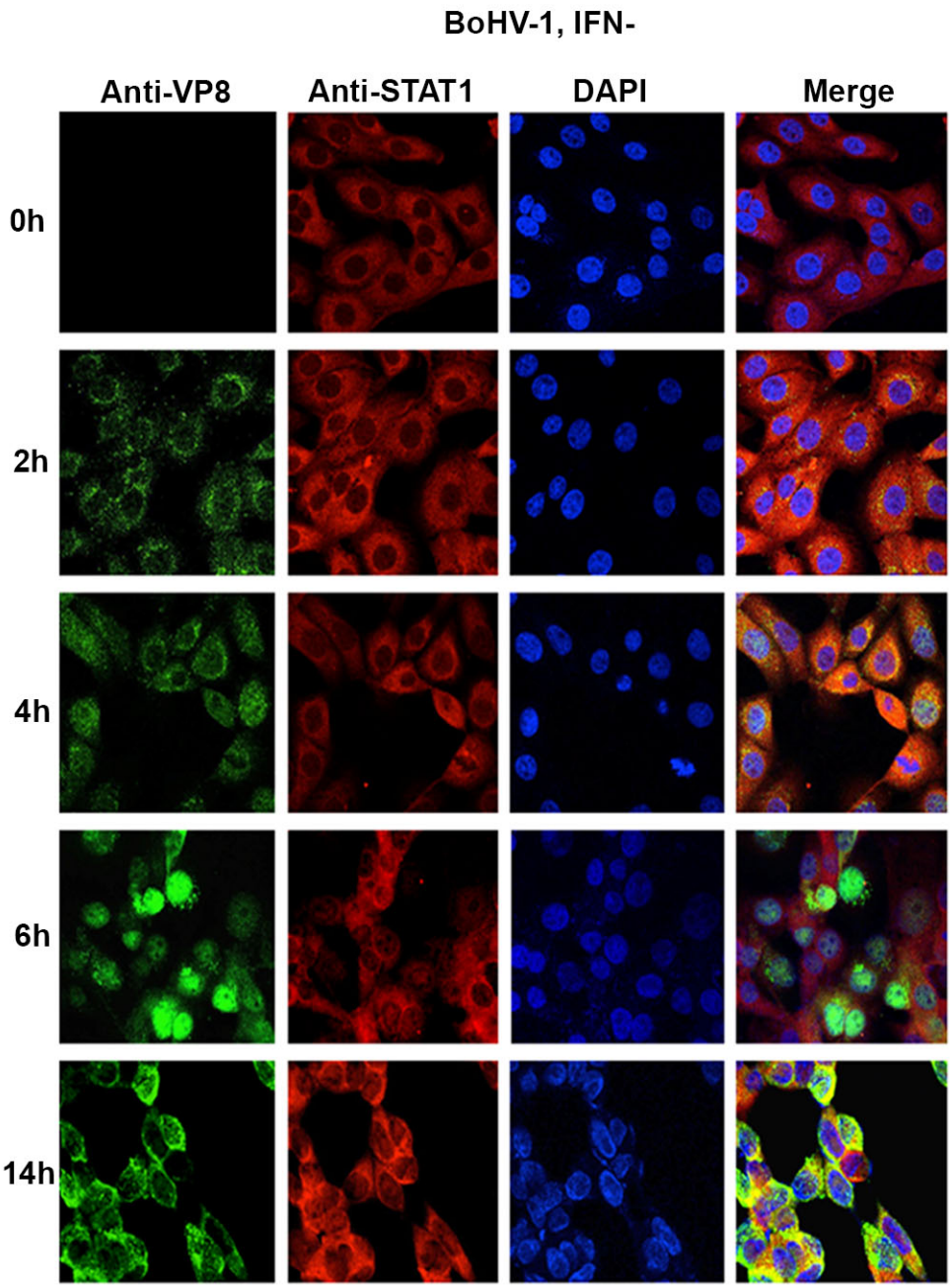

Figure. 3.10A Subcellular localization of BoHV-1 VP8 at different times post-infection.

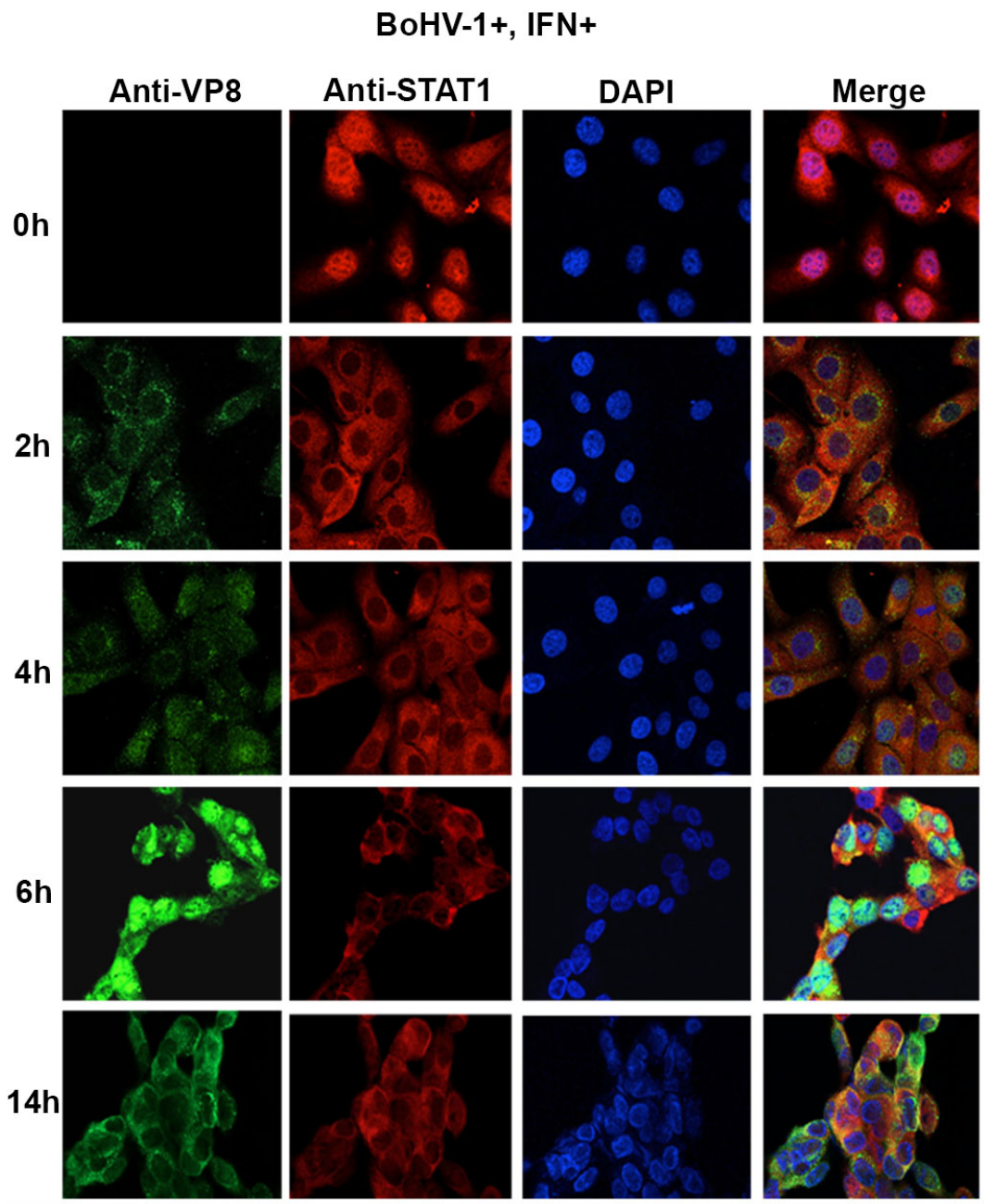

Figure. 3.10B Subcellular localization of BoHV-1 VP8 at different times post-infection.

MDBK cells were infected with BoHV-1 at an MOI of 4 for 2, 4, 6, and 14 h. The infected cells were left untreated (A) or stimulated with bovine IFN-β for 30 min (B). Cells were then fixed with paraformaldehyde, permeabilized, and incubated with monoclonal anti-VP8 and Alexa Fluor 488-conjugated goat anti-mouse IgG. STAT1 was detected with anti-STAT1 antibodies and Alexa Fluor 633-conjugated anti-rabbit IgG. DNA was labeled with Prolong gold DAPI. The cells were examined with a Leica SP5 confocal microscope.

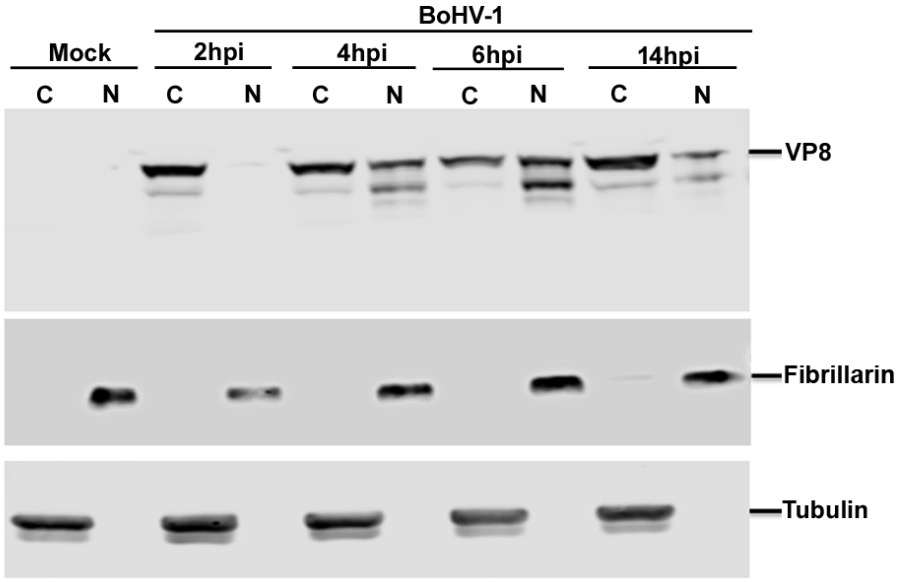

Figure. 3.11 Subcellular fractionation of BoHV-1 VP8 at different times during infection.

MDBK cells were mock infected or infected with BoHV-1 at an MOI of 4 for 2, 4, 6, and 14 h. The cells were collected by trypsinization at the indicated time points, followed by cytoplasmic and nuclear fractionation of proteins isolation as described in Materials and Methods. The resulting fractionations were analyzed by SDS-PAGE followed by detection of VP8 with anti-VP8 antibody. The fractionation procedure was validated by incubation with antibodies specific for the cytoplasmic and nuclear proteins tubulin and fibrillarin, respectively.

3.6 Discussion.

In response to viral infection, cells establish an antiviral state through type I IFN signaling; however, many viruses have evolved unique mechanisms to evade this response. With this study, we demonstrated that VP8 of BoHV-1 plays an important biological function by down-regulating IFN-induced responses. Transient expression of BoHV-1 VP8 inhibited IFN-β-induced transcriptional responses in transfected cells. Inhibition of IFN signaling was also observed in BoHV-1-infected cells, while BoHV1-ΔU_L47-infected cells showed partial recovery of IFN signaling compared to BoHV-1-infected cells. The presence of bICP0 and possibly bICP27 can also down-regulate the IFN responses(207, 379, 380), which might explain the incomplete recovery of IFN signaling in BoHV1-ΔU_L47-infected cells. To test this, ActD was added during BoHV-1 infection, which prevented immediate early gene expression. In ActD-treated cells, down-regulation of IFN signaling was observed in BoHV-1- or BoHV1-U_L47R-infected cells, but not in mock- or BoHV1-ΔU_L47-infected cells, which further confirmed the role of VP8 in down-regulation of IFN signaling.

Despite some homology between the BoHV-1 and human herpesvirus 1 (HHV-1) *U_L47* gene products, they differ in several respects. The HHV-1 *U_L47* gene product, VP13/14, interacts with polyadenylate-binding protein (PABP) and disrupts the association of PABP with PABP-interacting protein 2 (Paip2) jointly with its binding partner, ICP27 (193). Since Paip2 remains in the cytoplasm, Dobrikova et al. (193) mentioned that it was unclear whether the Paip2 dissociation is a primary event that happens in the cytoplasm after HHV-1 infection. Shu et al. demonstrated that the HHV-1 UL47 interacts with vhs-RNase and attenuates the degradation of all kinetic classes of viral mRNA and thereby regulates the expression of β and γ genes by controlling the expression of α gene products (194). Thus far, these functions have not been investigated for BoHV-1 VP8. Liu et al. presented data suggesting that HHV-1 VP13/VP14 forms a complex with UL31, UL34, and US3, which are critical for viral nuclear egress, and plays a regulatory role in HHV-1 primary envelopment (161). However, deletion of BoHV-1 UL47 did not result in impaired nuclear egress (179). HHV-1 *U_L47* (VP13/14) interacts with VP16 or alpha-transinducing factor (αTIF), and *U_L47*-deleted HHV-1 demonstrated impaired ability to induce immediate early promoter-regulated expression of a reporter gene (96, 383), but this effect was not observed for BoHV-1 VP8, as immediate early bICP4 mRNA transcripts were detected at similar levels in wild-type (WT), BoHV1-ΔU_L47, and BoHV1-U_L47R infected cells (179). In addition, when expressed

in *Escherichia coli* or insect cells, HHV-1 VP13/14, but not BoHV-1 VP8, bound directly to RNA (189). In contrast, VP8 expressed in mammalian cells interacts with bICP0, gB, gC, and gD mRNAs (188).

We identified cellular STAT1 as an interacting partner of BoHV-1 VP8 in both VP8-transfected and BoHV-1 infected cells. The domains of VP8 that interact with STAT1 were found to be located in two different regions, VP8 259-482 and 632-686. BLAST sequence analysis of BoHV-1 VP8 demonstrated high homology of amino acids 280 to 735 with U_L47-encoded proteins of human herpesvirus 1 and other herpesviruses and much less sequence similarity in the N-terminal region of amino acids 1 to 259 (Figure. 3.3) Furthermore, the predicted secondary structure for amino acids 280 to 735 was mostly alpha-helical, a feature that has previously been implicated in protein-protein interactions (188, 384). The crystal structure of STAT1 revealed that it has an alpha-helical coiled-coil domain starting at residue 130 and a DNA binding domain that is in the center of the STAT1 protein. The coiled-coil domain presents extensive possibilities for protein-protein interaction and, indeed, has been documented as interacting with other proteins (reviewed in reference (385)). For example, although the rabies virus P protein binding site on STAT1 could not be precisely determined, the P protein-interacting domain resides in the coiled-coil and DNA binding domain of STAT1 (374). This suggests that the BoHV-1 VP8 binding site on STAT1 may be present on the coiled-coil or DNA-binding domain.

Viruses have evolved different mechanisms to antagonize the IFN signaling pathway through STAT1 or STAT2 interaction with viral proteins. For example, several paramyxovirus family members such as human parainfluenza virus-2 and SV5 induce polyubiquitination and degradation of STAT1 to block IFN signaling through the P and V proteins, respectively (386). The C protein of Sendai virus down-regulates IFN signaling by inhibiting STAT1 phosphorylation and STAT1 degradation (387). The V protein of measles virus, also belonging to *Paramyxoviridae* family, blocks IFN signaling by reducing STAT1 and STAT2 phosphorylation (388). In contrast, mumps virus V protein antagonizes IFN-induced antiviral effects by both degradation of STAT1 and prevention of nuclear translocation of STAT1 (378). Similarly, the V protein of Nipah virus and Hendra virus, members of the *Henipa* virus genus, inhibit IFN-α/β and IFN-γ signaling by preventing both STAT1 phosphorylation and nuclear translocation (389, 390). The P protein of rabies virus, belonging to the *Rabdoviridae,* neither induces STAT1 degradation nor inhibits STAT1 phosphorylation, but prevents STAT1 nuclear accumulation (374). The viral protein pM27

of mouse CMV (MCMV) inhibits IFN signaling by inducing proteasomal degradation of STAT2 (123). These examples show that viral proteins antagonize the IFN-induced host antiviral effects through the JAK-STAT signaling pathway in different ways.

VP8 is the first BoHV-1 protein identified as interacting with STAT1, thus contributing to prevention of IFN signaling. Although the expression of BoHV-1 VP8 inhibited IFN signaling, VP8 induced neither ubiquitination nor degradation or phosphorylation of STAT1. However, translocation of STAT1 to the nucleus following IFN-β treatment was inhibited by full-length VP8 as well as a truncated form of VP8, which contains the domains for interaction with STAT1. After exposure to IFN, ligand-dependent tyrosine phosphorylation and STAT1 dimerization take place followed by the accumulation of STAT1s to the nucleus (391). The transport of the large protein complexes to the nucleus is facilitated by binding of importin-α with the NLS of STAT1 (392). Other residues in the coiled-coil domain are also responsible for nuclear import of some STAT proteins (263). A mutation in the STAT1 leucine residue at 407 (L407A) located in the DNA binding domain inhibited nuclear translocation of STAT1 (392). Similarly, McBridge et al. showed that STAT1 protein defective in DNA binding failed to accumulate in to the nucleus (392). Integrity of the DNA binding domain also determines nuclear retention of STAT1 (393). Since point mutations in the arginine and lysine-rich-residues in the DNA binding domain resulted in defective nuclear import of STAT1 (394), a lack of DNA binding is possibly associated with cytoplasmic retention of STAT1. Thus, an interaction between VP8 and the DNA-binding domain or coiled-coil domain of STAT1 could impede the nuclear transport machinery as well as the DNA binding function. The NLS of VP8, amino acids 51-54 (RRPR), regulates nuclear localization of VP8 (182). A truncated version of VP8 consisting of amino acids 219-741, which lacks the NLS but contains two VP8-STAT1 interacting domains, was completely cytoplasmic and also able to retain STAT1 in the cytoplasm.

Accumulation of STAT1 to the nucleus was not observed in BoHV1 and BoHV1-U_L47R-infected cells, while BoHV1-ΔU_L47 allowed translocation of STAT1 to the nucleus. BoHV1 VP8 is the most abundant tegument protein of the virion. Previously, the full-length VP8 was observed in the cytoplasm as early as 2 h and was visualized in the nucleus at 5 h post-infection (187). Thus, interaction of VP8 with STAT1 in the cytoplasm might interfere with the nuclear import of STAT1 early after initiation of infection. We demonstrated that VP8 is present in the cytoplasm at 2 h post-infection, at which time STAT1 was retained in the cytoplasm. Since VP8 is a late protein,

this suggests that viral VP8 released into the cytoplasm immediately after initiation of infection counteracts the establishment of an antiviral state by interacting with STAT1 to inhibit IFN signaling.

In summary, our data provide evidence that BoHV-1 VP8 inhibits IFN signaling early after initiation of infection in the absence of immediate early protein synthesis. Inhibition of IFN signaling appeared to occur through interference with nuclear translocation of STAT1 in both VP8-transfected and BoHV-1 infected cells. This is the first BoHV-1 protein shown to interact with cellular STAT1 to inhibit IFN-β signaling before the onset of virus replication. These results provide a new functional role for VP8 in BoHV-1 infection and a potential explanation for the lack of viral replication of the *U_L47* deletion mutant in cattle.

3.8 Acknowledgments.

We acknowledge Danielle Blondel (Laboratoire de Virologie Moléculaire et Structurale, LVMS, CNRS, France) for kindly providing plasmids pISREluc and pRL-TK and Richard Randall, University of St. Andrews, School of Biology, St. Andrews, Fife, United Kingdom, for kindly proving us with pSV5V and pHis-Ub plasmids. The confocal microscopy was performed in the College of Veterinary Medicine, University of Saskatchewan.

CHAPTER 4

LINKER BETWEEN CHAPTER 3 AND CHAPTER 5

In chapter 3, we demonstrated a function of incoming virion and cytoplasmic VP8 in the establishment of an anti-viral state to facilitate BoHV-1 replication. Upon virus infection, the cellular STAT1 must accumulate in the nucleus in order to trigger IFN-β production. We determined that BoHV-1 VP8 interacts with cellular STAT1 protein to prevent its translocation from the cytoplasm to the nucleus. The inhibition of STAT1 translocation was observed in BoHV-1- and BoHV-1U_L47R-infected but not in BoHV-1ΔU_L47-infected cells. Thus, the IFN-β production was significantly lower in BoHV-1-infected cells when compared to BoHV-1ΔU_L47-infected cells, suggesting that VP8 contributed to inhibition of IFN-β signaling and in turn, promoted BoHV-1 replication. This is in agreement with the previously demonstrated fact that U_L47-deleted virus has a 100-fold reduced titer in cell culture and is avirulent in cattle. Therefore, the interference with IFN-β signaling by VP8 may benefit BoHV-1 replication.

Due to the presence of NLS and NES, VP8 is a nuclear-cytoplasmic shuttling protein. In chapter 5 we investigated pro-viral function of nuclear VP8. Virus interaction with the host cells promotes DDR response. We determined that VP8 formed a complex with DDR proteins, and this interaction revealed function of nuclear VP8 in the modulation of the DDR pathway.

CHAPTER 5

THE MAJOR TEGUMENT PROTEIN OF BOVINE HERPESVIRUS-1, VP8, INTERACTS WITH DNA DAMAGE RESPONSE PROTEINS AND INDUCES APOPTOSIS

Sharmin Afroz[1,2], Ravendra Garg[1] , Michel Fodje[3] and Sylvia van Drunen Littel-van den Hurk[1,2,4]

[1] VIDO-InterVac, University of Saskatchewan, Saskatoon, SK, S7N 5E3, Canada; [2]Vaccinology & Immunotherapeutics, University of Saskatchewan, Saskatoon, SK, S7N 5E3, Canada. [3] Canadian Light Source, University of Saskatchewan, Saskatoon, SK, S7N 5E3, Canada. [4] Microbiology & Immunology, University of Saskatchewan, Saskatoon, SK, S7N 5E3, Canada.

Running title: BoHV-1 VP8 induces apoptosis

Corresponding author*:
Dr. Sylvia van Drunen Littel-van den Hurk
University of Saskatchewan
120 Veterinary Road
Saskatoon, SK, S7N 5E3, Canada
Telephone: 1 + (306) 966-1559
Fax: 1 + (306) 966-7478

The information in following chapter was previously published:

Sharmin Afroz, Ravendra Garg , Michel Fodje and Sylvia van Drunen Littel-van den Hurk. Thmajor tegument protein of bovine herpesvirus-1, VP8, interacts with DNA damage response proteins and induces apoptosis. Journal of Virology, 16 May 2018, doi:10.1128/JVI.00773-18.

5.1 Abstract.

VP8, the *ul47* gene product in bovine herpes virus-1 (BoHV-1), is a major tegument protein, essential for virus replication *in vivo*. The major DNA damage response protein, ataxia telangiectasia mutated (ATM), phosphorylates Nijmegen breakage syndrome (NBS1) and structural maintenance of chromosome-1 (SMC1) proteins during the DNA damage response. VP8 was found to interact with ATM and NBS1 during transfection and BoHV-1 infection. However, VP8 did not interfere with phosphorylation of ATM in transfected or BoHV-1-infected cells. In contrast, VP8 inhibited phosphorylation of both NBS1 and SMC1 in transfected cells, as well as in BoHV-1-infected cells, but not in cells infected with a VP8 deletion mutant (BoHV-1ΔU_L47). Inhibition of NBS1 and SMC1 phosphorylation was observed at 4 h post infection by nuclear VP8. Furthermore, ultraviolet light (UV)-induced cyclobutane pyrimidine dimer (CPD) repair was reduced in the presence of VP8, and VP8 in fact enhanced etoposide or UV-induced apoptosis. This suggests that VP8 blocks the ATM/NBS1/SMC1 pathway and inhibits DNA repair. VP8 induced apoptosis in VP8-transfected cells through caspase-3 activation. The fact that BoHV-1 is known to induce apoptosis through caspase-3 activation is in agreement with this observation. The role of VP8 was confirmed by the observation that BoHV-1 induced significantly more apoptosis than BoHV-1ΔU_L47. These data reveal a potential role of VP8 in the modulation of the DNA damage response pathway and induction of apoptosis during BoHV-1 infection.

5.2 Importance.

To our knowledge, the effect of BoHV-1 infection on the DNA damage response has not been characterized. Since BoHV-1ΔU_L47 was previously shown to be avirulent *in vivo*, VP8 is critical for the progression of viral infection. We demonstrated that VP8 interacts with DNA damage response proteins and disrupts the ATM-NBS1-SMC1 pathway by inhibiting phosphorylation of DNA repair proteins, NBS1 and SMC1. Furthermore, interference of VP8 with DNA repair was correlated to decreased cell viability and increased DNA damage-induced apoptosis. These data show that BoHV-1 VP8 developed a novel strategy to interrupt the ATM signaling pathway and to promote apoptosis. These results further enhance our understanding of the functions of VP8 during BoHV-1 infection and provide an additional explanation for the reduced virulence of BoHV-1ΔU_L47.

Key words: BoHV-1, VP8, DNA damage, DNA repair, apoptosis

5.3 Introduction.

Upon DNA damage, a variety of cellular responses are induced in eukaryotic cells. Damaged DNA poses a continuous threat to genomic stability, which results in the activation of a network of sensors, transducers, and activator proteins. These proteins conduct different physiological responses including the arrest of cell cycle progression and activation of DNA repair or if the damage is too severe, induction of apoptosis or cell death (395, 396) Immediately after exposure to genotoxic stress, the cellular regulatory mechanism is triggered. At the recognition of damaged DNA, highly conserved cellular checkpoint proteins are rapidly induced to prevent cellular replication and damaged DNA propagation before the repair is completed. The major DNA damage response-signaling network includes ataxia telangiectasia mutated protein (ATM) and ataxia telangiectasia and Rad3 related protein (ATR). ATM and ATR respond to a variety of abnormal DNA structures leading to the initiation of a signaling cascade (265). In undamaged cells, ATM exists as a catalytically inactive dimer. After recognition of damaged DNA, ATM undergoes auto- or transphosphorylation at Serine-1981 that leads to catalytically active ATM monomers (263). Consequently, ATM activates downstream proteins including the Nijmegen breakage syndrome (NBS1) and structural maintenance of chromosome-1 (SMC1) proteins to signal checkpoint control (265). ATM activation by double-strand breaks (DSBs) facilitates the recruitment of DNA repair protein NBS1 (397), which leads to checkpoint activation through phosphorylation of NBS1 and SMC1. SMC1 functions as a downstream effector of the ATM/NBS1 pathway to activate the S-phase checkpoint, which is deficient in ataxia telangiectasia (A-T) and NBS patients (398).

Immediately after infection, cellular antiviral responses are aimed at preventing viral replication and spread. Host cells are exposed to large amounts of exogenous materials or abnormal DNA structures such as DNA ends, or unusual structures during viral replication. Thus, viral replication is recognized as DNA damage stress by the infected cells and triggers DNA damage signal transduction as a part of host immune-surveillance (399).

Herpesviruses are enveloped double-stranded DNA viruses containing ~150 kbp genomes (400, 401). Upon infection, the viral genome is replicated, producing highly branched

replication intermediates. During herpes simplex virus-1 (HSV-1) infection DSBs are generated (402). Consequently, HSV-1 induces cellular DNA damage responses through activation of ATM and its downstream effector molecules (274). Similarly, other herpesviruses such as Kaposi's sarcoma-associated herpesvirus (KSHV) induce ATM activation in primary endothelial cells (309). Murine gamma herpesvirus-68 (gammaHV68) also induces ATM activation (403). Although gamma herpesvirus M2 protein activates ATM, downstream signaling of the ATM pathway was inhibited by M2 protein (404). Thus, herpesviruses modulate the DNA damage response to favor viral replication in different ways.

Bovine herpesvirus-1 (BoHV-1) is an important pathogen in cattle, responsible for a variety of clinical symptoms, in particular respiratory and genital infections. VP8, the *U_L47* gene product, is the most abundant tegument protein in BoHV-1. BoHV-1 VP8 contains a nuclear localization signal and a nuclear export signal and thereby shuttles between the nucleus and cytoplasm (182). A U_L47-deleted virus (BoHV-1ΔU_L47) replicates less efficiently in cell culture and is avirulent in cattle supporting the importance of VP8 in the establishment of BoHV-1 infection (179). Although the precise role of VP8 in viral infection remains mostly unknown, some functions of VP8 are being elucidated. VP8 interacts with a cellular DNA damage binding protein-1, DDB1 (187). The signal transducer and activator of transcription (STAT1) is also an interacting partner of VP8. However, while the interaction of the paramyxovirus family V protein with DDB1 and STAT1 targets STAT1 for degradation (405), VP8 does not degrade STAT1 or interfere with STAT1 phosphorylation, but prevents translocation of STAT1 to the nucleus, thus inhibits interferon-β (IFN-β) signaling (405). Human cytomegalovirus (HCMV) also contributes to DDR activation by interacting with DDB1 (406), and the gamma herpesvirus M2 protein regulates the DNA damage response (DDR) pathway through interaction with DDB1 and ATM (404).

Since VP8 interacts with DDB1 (187), it was of interest to investigate whether VP8 interacts with other DNA damage response proteins, and plays a role in the modulation of the DDR during BoHV-1 infection. The data shown here reveal that VP8 interacts with ATM and NBS1, and prevents phosphorylation of NBS1 and SMC1. Thus, VP8 disrupts the ATM/NBS1/SMC1 pathway and inhibits DNA repair. Furthermore, VP8 increased DNA damage-induced apoptosis.

5.4 Materials and Methods.

5.4.1 Cells, viruses, and plasmids.

HeLa, MDBK, and HEK 293T cells were grown in Eagle's minimum essential medium (MEM, Sigma-Aldrich Canada Ltd, Oakville, ON, Canada). The medium was supplemented with 10% heat-inactivated fetal bovine serum (FBS, Gibco, Life Technologies, Burlington, ON, Canada), 1% antibiotic-antimycotic (Life Technologies) and 10 mM HEPES buffer (Life Technologies). Cells were cultured with 5% CO_2 in a 37°C incubator. BoHV-1 108, BoHV-1ΔU_L47 and BoHV-1U_L47R were propagated in MDBK cells (179). MDBK cells were infected with BoHV-1 at different multiplicities of infection (MOI) as mentioned elsewhere. The plasmids pFLAG and pFLAG-VP8 were previously described by Labiuk et al, 2009 (184) and Afroz et al, 2016 (405), respectively. EYFP was amplified from pEYFP by using forward primer 5′-CACAAGCTTCCACCGGTCGCCACCAT-3′ and reverse primer 5′-AGACTCGAGCGTGGGAGGTTTTTTAAAGCAAG-3′. The pFLAG-VP8 and the amplified EYFP were digested with HindIII and XhoI followed by ligation to generate pFLAG-EYFP.

5.4.2 Antibodies and chemical reagents.

VP8-specific murine monoclonal and glycoprotein C-specific rabbit polyclonal antibodies were used as previously described (405). ATM-, pATM-, NBS1-, pNBS1-, SMC1, and pSMC1 -specific antibodies were purchased from Abcam (Toronto, ON, Canada). Murine monoclonal actin- and FLAG-specific antibodies were purchased from Sigma-Aldrich Canada Ltd. Mouse monoclonal CPD-specific antibody was obtained from Cosmobio, Tokyo. Japan. Rabbit caspase-3-specific antibody was obtained from New England Biolabs. Etoposide was purchased from Sigma-Aldrich Canada Ltd.

5.4.3 Preparation of cell lysates.

HEK 293T and HeLa cells were transfected at 60-80% confluency with different plasmids. Lipofectamine and Plus reagents (Invitrogen, Life Technologies) were used for transfection. At 24 h post transfection, HEK 293T cells were washed with ice-cold PBS (pH 7.4). Cells were treated with lysis buffer (50 mM Tris, 150 mM NaCl, 1 mM EDTA, 1% Triton X-100, pH 7.4) supplemented with mammalian cell and tissue extract protease inhibitor cocktail (Sigma-Aldrich) and gently rocked on a nutator for 5 min followed by incubation on ice for 30 min. The

samples were centrifuged at 12,000 × *g* for 15 min at 4°C. The supernatants were collected in 1.5 ml Eppendorf tubes and kept at −80°C for future use. MDBK cells were lysed as described above.

5.4.4 Immunoprecipitation and Western blotting.

For immunoprecipitation cell lysates were generated as described above. Cell lysates were added to anti-FLAG M2 affinity gel (Sigma-Aldrich) and the mixtures were incubated overnight at 4°C; alternatively, cell lysates were incubated at 4°C overnight with primary antibodies, followed by incubation for 3 h at 4°C with Protein G Sepharose Fast Flow beads (GE Health Care, Niskayuna, NY, USA). The immune complexes were washed with wash buffer (50 mM Tris-HCl, 250 mM NaCl, 2% Triton X-100, pH 7.4) and subsequently boiled in SDS-PAGE sample buffer for 5 min. The immune complexes were then separated on 10% or 8 % SDS-PAGE gels followed by transfer to nitrocellulose membranes. The nitrocellulose membranes were blocked with 5% skim milk or 5% bovine serum albumin (BSA) in PBS containing Tween-20 (PBST; 3.2 mM Na_2HPO_4, 0.5 mM KH_2PO_4, 1.3 mM KCl, 135 mM NaCl, 0.1% Tween 20, pH 7.4) for 2 h followed by incubation with primary antibodies overnight at 4°C. The membranes were washed three times with PBST followed by incubation with IRDye680-conjugated anti-mouse IgG or IRDye-800CW-conjugated anti-rabbit IgG (LI-COR Bioscience, Lincoln, NE, USA). An Odyssey CLx Infrared Imaging system (LI-COR Bioscience) was used for protein detection and the images were processed using the Odyssey 3.0.16 application software (LI-COR Bioscience).

5.4.5 Immunofluorescence.

HeLa cells were plated at a concentration of 2×10^5 cells per well in two-chamber Permanox slides (Lab-Tek, Naperville, IL, USA). Cells were mock-transfected or transfected with pFLAG-EYFP or pVP8-EYFP. At 24 h post transfection, cells were either left untreated or treated with etoposide for 30 min. Subsequently, cells were fixed with 4% paraformaldehyde (Sigma-Aldrich) for 20 min at room temperature (RT) and permeabilized, followed by blocking with 1% goat serum and 0.1% Triton X-100 in PBS. The cells were incubated with primary antibodies for 2 h at RT. MDBK cells were infected with BoHV-1 or BoHV1-U_L47R at a MOI of 4 or with BoHV1-ΔU_L47 at a MOI of 5 for 14 h. The cells were either left untreated or treated

with etoposide for 30 min, followed by fixation and antibody incubations as described above. For the time course experiment, MDBK cells were infected with BoHV-1 at a MOI of 4, and the cells were fixed at indicated time points and blocked overnight followed by incubation with primary antibodies. Subsequently, the cells were incubated with AlexaFluor 488 goat anti-mouse IgG or AlexaFluor 633 goat anti-rabbit IgG (Invitrogen, Life Technologies) for 1 h. Mounting medium containing 4′,6-diamino-2-phenylindole (DAPI) was used to identify the nucleus, and the slides were air-dried for 24 h at RT. The cells were examined by using laser excitation at 488 nm (Alexa 488), 633 nm (Alexa 633) and 461 nm (DAPI). Confocal images were taken with a Leica SP5 confocal microscope (Leica Microsystems Inc., Concord, ON, Canada). Image J software was used to process the images.

5.4.6 Cyclobutane Pyrimidine Dimer identification.

HeLa cells were mock-transfected or transfected with pEYFP or pVP8-EYFP. At 24 h post transfection cells were irradiated with 10 J/m^2 UV-C. Cells were treated according to the manufacturer's instructions. Briefly, cells were either fixed with 4% formalin immediately after UV irradiation at 0 h or incubated for 24 h before fixation. The cells were permeabilized with 0.5% Triton X-100 followed by blocking with 20% FBS. The cells were then incubated with murine monoclonal anti-CPD antibody (Cosmo Bio Co, Japan) for 1.5 h at 37°C. The cells were washed 5 times with PBS and were then incubated with Alexa-Fluor 633 goat anti-mouse IgG. The images were captured with a Leica SP5 confocal microscope (Leica Microsystems Inc.) and processed with Image J software. A biological image-processing program, Fiji (407), was used to quantify the relative fluorescent intensities. The mean intensity within defined areas was shown as procedure defined unit (PDU).

5.4.7 Apoptosis assay.

HeLa cells at 60-70% confluency were mock-transfected or transfected with pFLAG or pFLAG-VP8. At 24 h post transfection cells were left untreated, treated with etoposide or exposed to UV and incubated for another 12 h. Cells were then harvested by trypsinization and were fixed with 1% paraformaldehyde followed by addition of 70% ethanol, and stored at -20°C overnight. The cells were analyzed by using an APO-BrdU TUNEL assay Kit (Molecular Probes, Thermofisher Scientific) according to the manufacturer's instructions. Briefly, the cells were

washed with the washing buffer before incubation with terminal deoxynucleotidyl transferase and BrdUTP at 37°C for 2 h. Cells were washed three times followed by incubation with Alexa Fluor 488 dye-labeled anti-BrdU antibody. After subsequent washes, the cells were analyzed by flow cytometry on a flow cytometry cell sorting (FACS) Calibur (BD Biosciences, Franklin Lakes, NJ, USA). All data were analyzed with Kaluza Software (v1.2) (Beckman Coulter Inc., Pasadena, CA, USA). Similarly, MDBK cells were mock-infected or infected with BoHV-1 or BoHV-1ΔU_L47 at indicated MOI's and the TUNEL assay was performed as described above.

5.5 Results.

5.5.1 VP8 is an interacting partner of ATM and NBS1.

To identify a potential interaction between VP8 and ATM, human embryonic kidney (HEK) 293T cells were mock-transfected or transfected with pFLAG-EYFP or pFLAG-VP8. At 24 h post transfection cell lysates were incubated with anti-FLAG beads and immune complexes were detected by anti-FLAG and anti-ATM antibodies. As shown in Figure. 5.1A, anti-FLAG beads precipitated EYFP and VP8 from pFLAG-EYFP- and pFLAG-VP8-transfected cells, respectively. ATM was precipitated from VP8-transfected cells, but not from mock- or EYFP-transfected cells, suggesting that VP8 interacts with ATM. To investigate the interaction of VP8 with ATM during infection, Madin-Darby bovine kidney (MDBK) cells were mock-infected or infected with BoHV-1 or BoHV-1ΔU_L47. Incubation with VP8-specific antibody followed by Protein G Sepharose Fast Flow beads resulted in precipitation of VP8 and ATM from BoHV-1-infected cells, but not from BoHV-1ΔU_L47-infected cells (Figure. 5.1B). Conversely, VP8 was precipitated with ATM-specific antibody from BoHV-1-infected cells, but not from mock- and BoHV-1ΔU_L47-infected cells (Figure. 5.1C), indicating interaction of VP8 with ATM during BoHV-1 infection.

Since ATM forms a complex with NBS1 (397), we investigated whether VP8 also interacts with NBS1. HEK 293T cells were mock-transfected or transfected with pFLAG-EYFP or pFLAG-VP8. Cell lysates were incubated with anti-FLAG resin followed by detection of immune complexes by anti-FLAG and anti-NBS1 antibodies. As demonstrated in Figure. 5.1D, anti-FLAG beads precipitated EYFP and VP8 from pFLAG-EYFP- and pFLAG-VP8-transfected cells, respectively. NBS1 was precipitated by anti-FLAG beads from VP8-transfected cells, but not from mock- and pFLAG-EYFP-transfected cells, suggesting that VP8 interacts with NBS1.

To demonstrate the interaction of VP8 with NBS1 during infection, MDBK cells were mock-infected or infected with BoHV-1 or BoHV-1 ΔU_L47. Cell lysates from infected cells were incubated with an anti-VP8 antibody followed by Protein G Sepharose Fast Flow beads. VP8-specific antibody precipitated VP8, as well as NBS1, from BoHV-1-infected cells, but not from mock- or BoHV-1 ΔU_L47-infected cells (Figure. 5.1E). Furthermore, incubation of BoHV-1-infected cell lysates with anti-NBS1 antibody followed by Protein G Sepharose Fast Flow beads precipitated VP8 from BoHV-1-infected cells (Figure. 5.1F), confirming that NBS1 interacts with VP8 during BoHV-1 infection. To investigate an interaction of VP8 with ATM and NBS1 as a complex, mock-, BoHV-1- and BoHV-1 ΔU_L47-infected cell lysates were incubated with an anti-VP8 antibody followed by Protein G Sepharose Fast Flow beads. As shown in Figure. 5.1G, anti-VP8 antibody pulled down NBS1 as well as ATM from BoHV-1 infected cells, but not from mock- and BoHV-1 ΔU_L47-infected cells. This experiment demonstrates that VP8 forms a complex with both NBS1 and ATM.

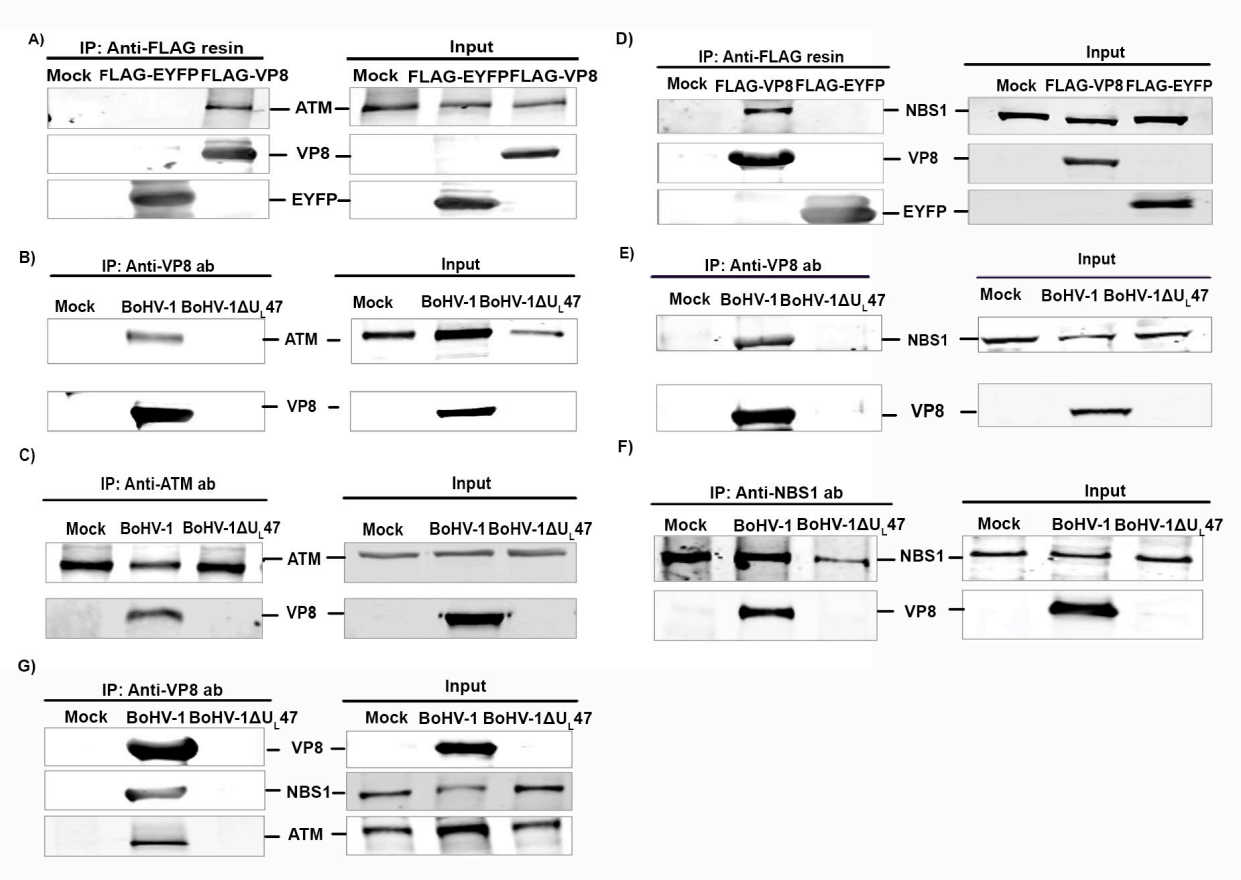

Figure. 5.1 VP8 is an interacting partner of ATM and NBS1.

A) HEK293T cells were mock-transfected or transfected with pFLAG-EYFP or pFLAG-VP8. Cell lysates were collected at 24 h post transfection and incubated with anti-FLAG resin. VP8 and ATM were detected by Western blotting with murine monoclonal anti-FLAG and rabbit anti-ATM antibodies, respectively. B) MDBK cells were mock-infected or infected with BoHV-1 or BoHV-1ΔU_L47 at a MOI of 2, and lysed after 24 h. Following incubation with anti-VP8 antibody and Protein G Sepharose Fast Flow beads, VP8, and ATM were detected by Western blotting with murine monoclonal anti-VP8 and rabbit anti-ATM antibodies, respectively. C) BoHV-1 cells were infected as described for Figure. 5.1B. Infected cells were lysed at 24 h post infection and incubated with rabbit anti-ATM antibody, followed by Protein G Sepharose Fast Flow beads. VP8 and ATM were detected by Western blotting with murine monoclonal anti-VP8 and rabbit anti-ATM antibodies, respectively. D) HEK293T cells were mock-transfected or transfected with pFLAG-EYFP or pFLAG-VP8. Cell lysates were collected at 24 h post transfection and incubated with anti-FLAG resin. VP8 and NSB1 were detected by Western blotting with murine monoclonal anti-FLAG and rabbit anti-NSB1 antibodies, respectively. E) MDBK cells were mock-infected or infected with BoHV-1 or BoHV-1ΔU_L47 at a MOI of 2, and lysed after 24 h. Following incubation with anti-VP8 antibody and Protein G Sepharose Fast Flow beads, VP8, and NSB1 were detected by Western blotting with murine monoclonal anti-VP8 and rabbit anti-NSB1 antibodies, respectively. F) BoHV-1 cells were infected as described for Figure. 5.1E. Infected cells were lysed at 24 h post infection and incubated with rabbit anti-NSB1 antibody, followed by

Protein G Sepharose Fast Flow beads. VP8 and NSB1 were detected by Western blotting with murine monoclonal anti-VP8 and rabbit anti-NSB1 antibodies, respectively. G) MDBK cells were mock-infected or infected with BoHV-1 or BoHV-1ΔU_L47 at a MOI of 2. At 24 h post infection cell lysates were collected and incubated with anti-VP8 antibody, followed by Protein G Sepharose Fast Flow beads. VP8, ATM, and NBS1 were detected by Western blotting with anti-VP8, anti-ATM and anti-NBS1 antibodies. IRDye680-conjugated anti-mouse IgG and IRDye-800CW-conjugated anti-rabbit IgG were used for detection. Input lysates are presented in the right panels.

5.5.2 VP8 interferes with the ATM/NBS1/SMC1 pathway by inhibiting phosphorylation of NBS1 and SMC1.

ATM, the checkpoint kinase, acts as a central signal transducer in response to ionizing radiation (IR) (408). Viral proteins such as hepatitis C virus NS3 protein interact with ATM and contribute to increased sensitivity of cells to DNA damage (409). Since VP8 interacted with ATM, we investigated whether VP8 influences ATM activation by interfering with its phosphorylation. Human malignant epithelial cells derived from Henrietta Lacks **(**HeLa) cells were mock-transfected or transfected with pEYFP or pVP8-EYFP. At 24 h post transfection cells were left untreated or treated with etoposide for 30 min and were then incubated with anti-phospho ATM (pATM) antibody. Etoposide is a topoisomerase II inhibitor enzyme that generates DNA double-strand breaks by inhibiting re-ligation of DNA strands (410) and activates ATM. As shown in Figure. 5.2A, in the absence of etoposide, pATM was not detected in mock-, pEYFP- and pVP8-EYFP-transfected cells. As expected, the addition of etoposide enhanced the level of pATM in mock- and pEYFP-transfected cells. Similarly, pATM was observed in the VP8-expressing cells in the presence of etoposide (Figure. 5.2B). These results suggest that VP8 expression does not interfere with ATM phosphorylation.

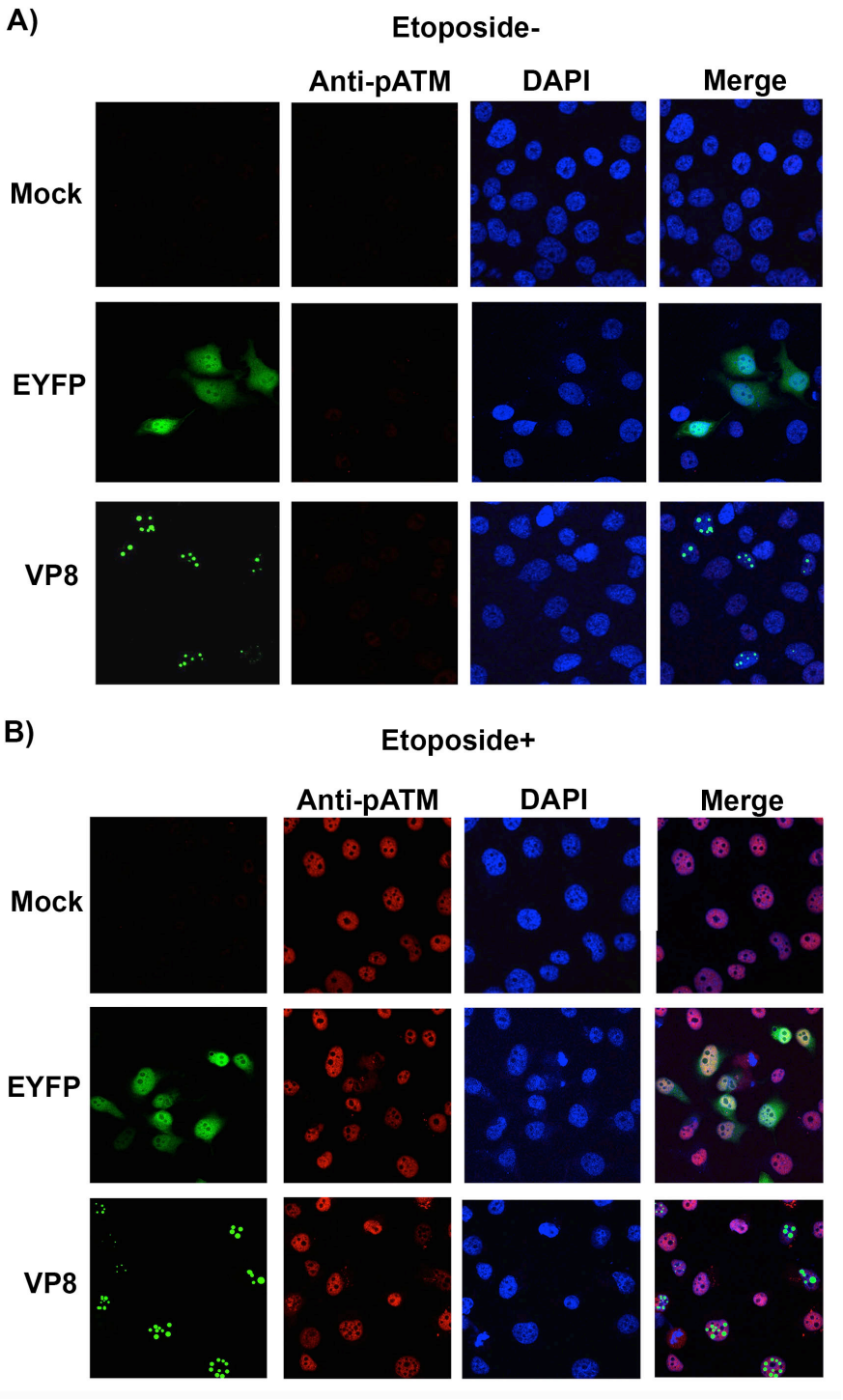

Figure. 5.2 BoHV-1 VP8 does not interfere with ATM phosphorylation.

HeLa cells were mock-transfected or transfected with pEYFP or pVP8-EYFP. At 24 h post transfection cells were A) left untreated or B) treated with etoposide. After 30 min of incubation cells were fixed with paraformaldehyde, permeabilized and incubated with rabbit anti-pATM antibody followed by incubation with Alexa-633-conjugated goat anti-rabbit IgG. Nuclei were

identified with Prolong gold DAPI mounting medium. The cells were examined with a Leica SP5 confocal microscope.

NBS1 is a key player of the MRE11-RAD50-NBS1 (MRN) complex and identified as a DNA repair protein after initial DNA damage (266). Disruption of the NBS1 function is lethal in mice (411). NBS1 plays a role in the DDR pathway by acting as a downstream target of ATM (397). Since VP8 interacted with ATM and NBS1 without influencing ATM phosphorylation, it was of interest to investigate whether VP8 interferes with phosphorylation of NBS1 as a downstream target. HeLa cells were mock-transfected or transfected with pEYFP or pVP8-EYFP, and were left untreated or treated with etoposide for 30 min at 24 h post transfection. Without etoposide treatment, phosphoNBS1 (pNBS1) was not detected in mock-, EYFP- and VP8-transfected cells (Figure. 5.3A). Although in etoposide-treated mock- and EYFP- transfected cells enhanced pNBS1 was detected, in VP8-expressing etoposide-treated cells no pNBS1 was observed (Figure. 5.3B), indicating that VP8 prevents phosphorylation of NBS1.

SMC1 acts downstream of the ATM/NBS1 pathway to activate S-phase checkpoint control and initiate DNA repair (398). Since phosphorylation of NBS1 is required for phosphorylation of SMC1 and subsequently for S-phase checkpoint activation (398), we investigated whether VP8 influences phosphorylation of SMC1. Cells were mock-transfected or transfected with pEYFP or pVP8-EYFP and treated with etoposide as described above. In the absence of etoposide, no phosphoSMC1 (pSMC1) was detected in mock-, EYFP- and VP8-transfected cells (Figure. 5.4A). However, after addition of etoposide SMC1 was phosphorylated in mock- and EYFP-transfected cells as expected, but not in VP8-expressing cells (Figure. 5.4B). These results indicate that VP8 inhibits SMC1 phosphorylation.

To further confirm the effects of VP8 on phosphorylation of NBS1 and SMC1, HeLa cells were mock-transfected or transfected with pEYFP or pVP8-EYFP. At 24 h post transfection cells were stimulated with etoposide as described above. EYFP-positive cells were sorted using a fluorescence-activated cell sorter (FACS). Equal amounts of cell lysate were examined by Western blotting for the presence of pNBS1 and pSMC1 (Figure. 5.5). While NBS1 and SMC1 were identified, pNBS1 and pSMC1 were not detected in the presence of VP8 after addition of etoposide, confirming the results shown by confocal microscopy. These experiments demonstrate that, although VP8 does not interfere with ATM phosphorylation, it inhibited phosphorylation of NBS1 and SMC1.

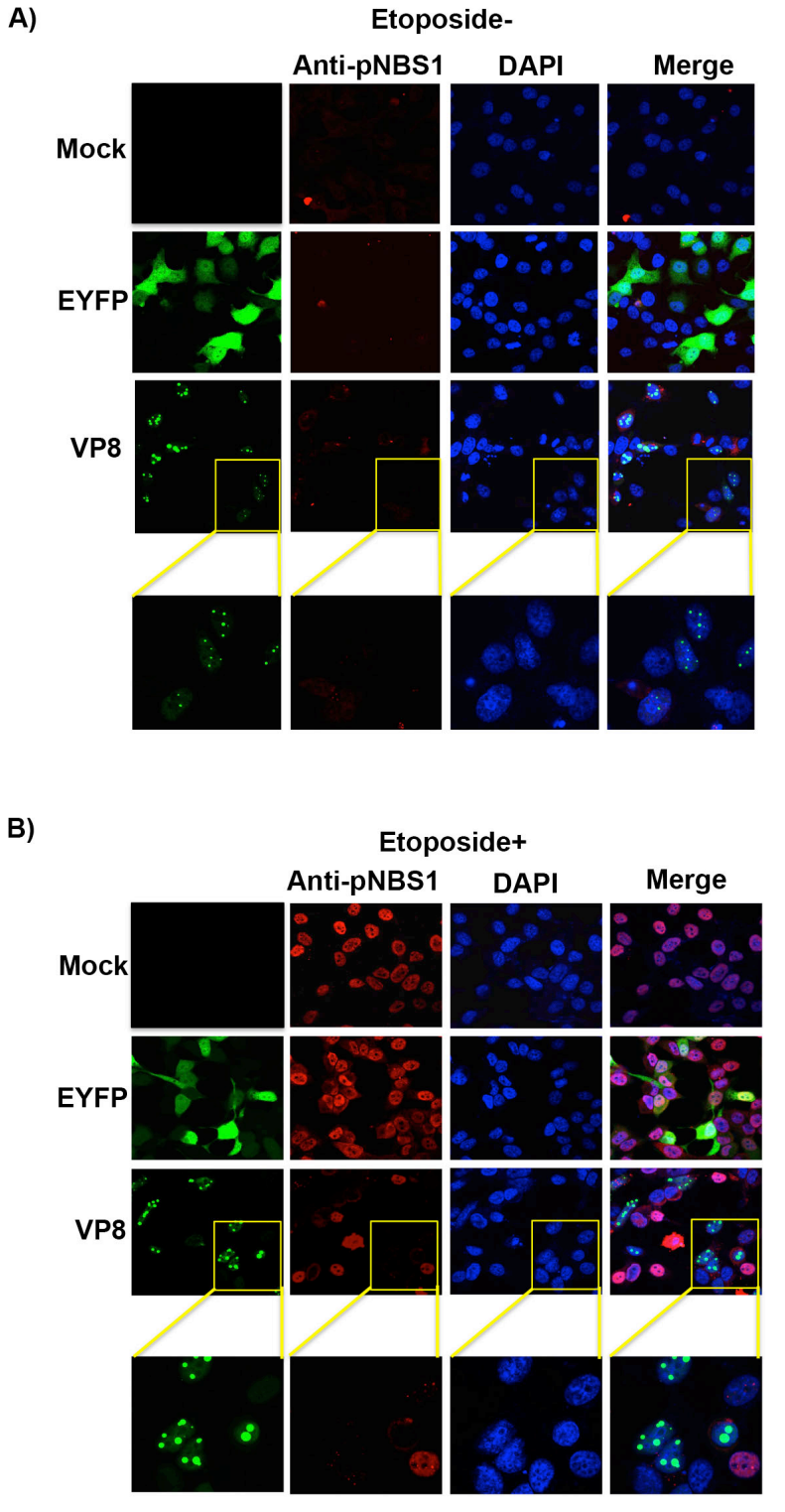

Figure. 5.3 VP8 inhibits NBS1 phosphorylation.

HeLa cells were mock-transfected or transfected with pEYFP or pVP8-EYFP. At 24 h post transfection cells were A) left untreated or B) treated with etoposide for 30 min. After fixation cells were incubated with rabbit anti-pNBS1 antibody followed by Alexa-633-conjugated goat

anti-rabbit IgG. Nuclei were identified with Prolong gold DAPI. The cells were analyzed with a Leica SP5 confocal microscope.

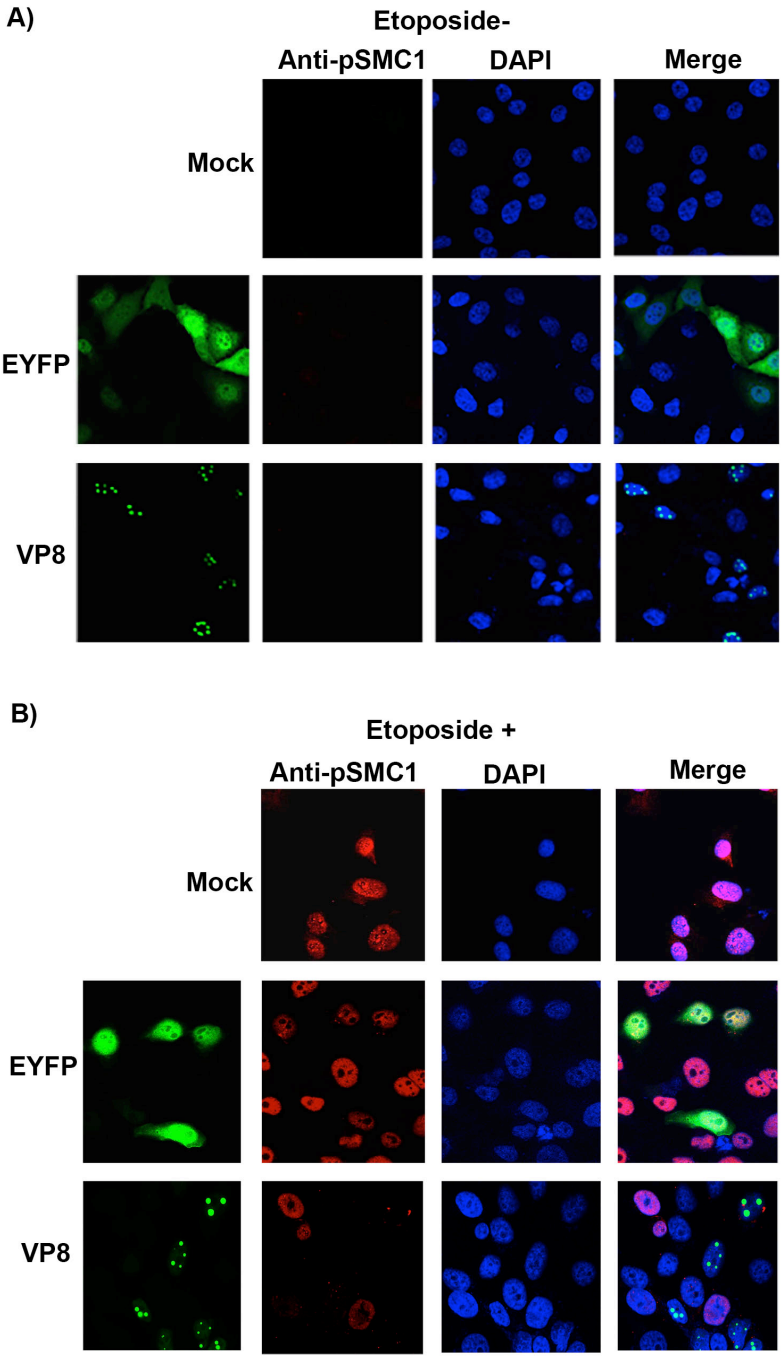

Figure. 5.4 VP8 impedes SMC1 phosphorylation.

HeLa cells were mock-transfected or transfected with pEYFP or pVP8-EYFP. At 24 h post transfection cells were A) left untreated or B) treated with etoposide for 30 min. After fixation cells were incubated with rabbit anti-pNBS1 antibody followed by Alexa-633-conjugated goat anti-rabbit IgG. Nuclei were identified with Prolong gold DAPI. The cells were analyzed with a Leica SP5 confocal microscope.

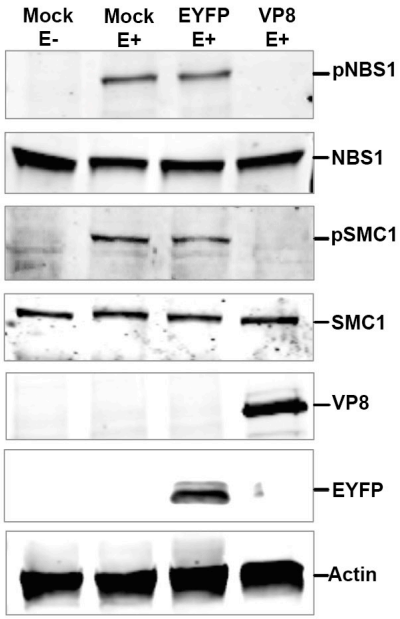

Figure. 5.5 Detection of phosphorylated NBS1 and SMC1 in VP8 transfected cells.

Hela cells were mock-transfected or transfected with pEYFP or pVP8-EYFP. At 24 h post transfection cells were either left untreated or treated with etoposide for 30 min. EYFP-positive cells were sorted by FACS and cell lysates were made in buffer containing protease and phosphatase inhibitors. Fifty micrograms of total protein of each sample were loaded. NBS1, pNBS1, SMC1, pSMC1, EYFP, VP8, and actin were detected by Western blotting with rabbit anti-NBS1, anti-pNBS1, anti-SMC1 and anti-pSMC1 antibodies and murine monoclonal anti-EYFP, anti-VP8 and anti-actin antibodies, respectively. IRDye-800CW-conjugated anti-rabbit IgG and IRDye680-conjugated anti-mouse IgG were used for detection.

5.5.3 VP8 does not affect ATM phosphorylation, but inhibits NBS1 and SMC1 phosphorylation during BoHV-1 infection.

Since VP8 did not interfere with ATM activation, but blocked phosphorylation of NBS1 and SMC1 in transfected cells, we examined the effect of BoHV-1 infection on ATM, NBS1 and SMC1 phosphorylation. MDBK cells were mock-infected or infected with BoHV-1, BoHV-1ΔU_L47 or BoHV-1U_L47R**.** At 14 h post infection cells were incubated with anti-pATM antibody. BoHV-1, BoHV-1ΔU_L47, and BoHV-1U_L47R induced similar levels of ATM phosphorylation (Figure. 5.6A and B). Since VP8 did not interfere with ATM phosphorylation, etoposide-treated BoHV-1-, BoHV-1ΔU_L47-, and BoHV-1U_L47R-infected cells were not examined.

To investigate NBS1 phosphorylation in infected cells, MDBK cells were mock-infected or infected with BoHV-1, BoHV-1ΔU_L47 or BoHV-1U_L47R**.** At 14 h post infection cells were left untreated or treated with etoposide for 30 min followed by incubation with a pNBS1-specific antibody. As shown in Figure. 5.7A, without etoposide treatment no pNBS1 was detected, while the addition of etoposide induced phosphorylation of NBS1 in mock-infected cells. However, in BoHV-1- and BoHV-1U_L47R-infected cells no pNSB1 was detected, even in the presence of etoposide (Figure. 5.7B and D), while in BoHV-1ΔU_L47-infected cells pNBS1 was observed regardless of etoposide treatment (Figure. 5.7C). The lack of pNBS1 in BoHV-1- and BoHV-1U_L47R-infected cells, but not in BoHV-1ΔU_L47-infected cells, was confirmed by Western blot analysis (Figure. 5.7E). The incoming virus particles of DNA viruses and subsequent DNA replication induce DNA damage responses to activate DNA repair proteins at early times post infection (412, 413). This explains why BoHV-1ΔU_L47 infection resulted in ATM activation and increased phosphorylation of NBS1.

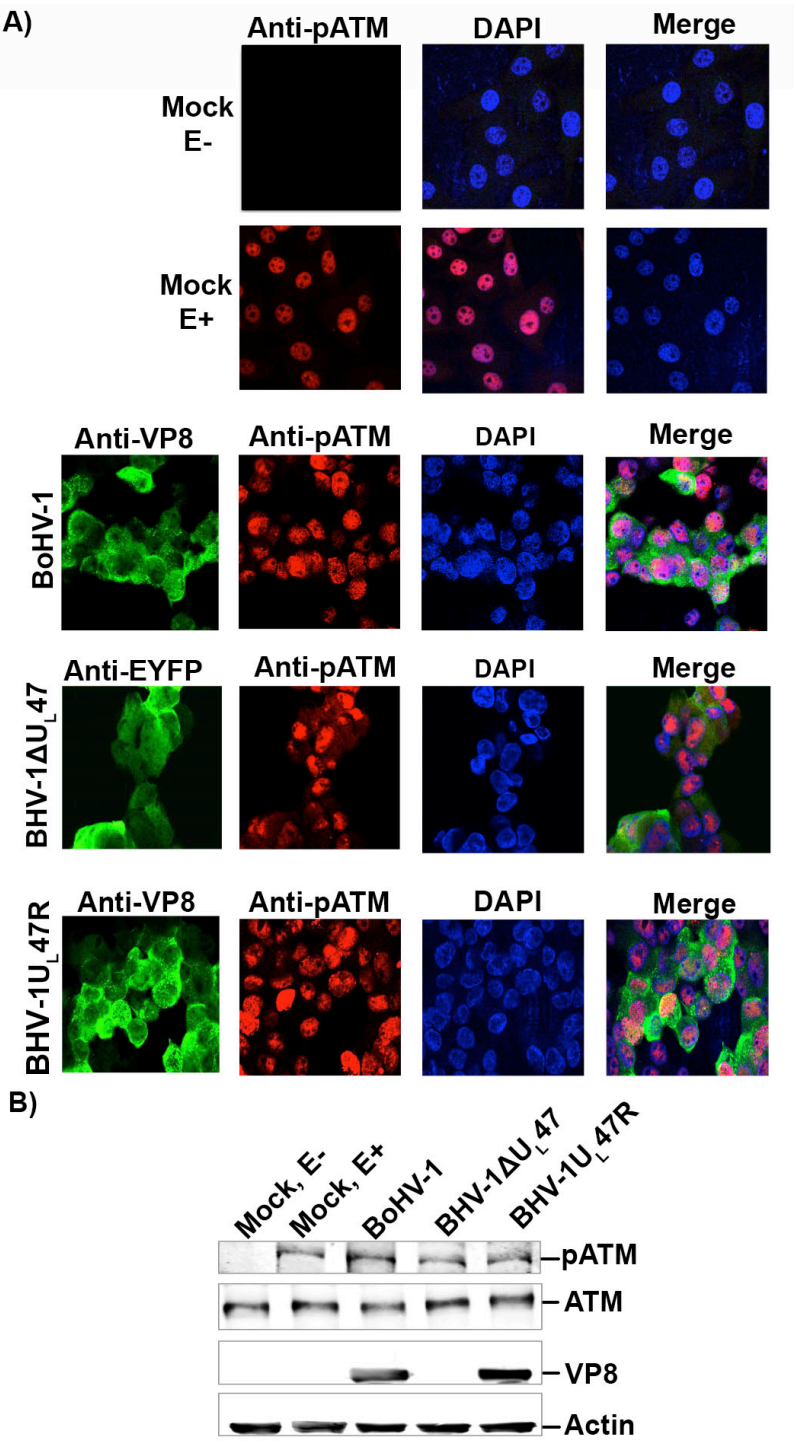

Figure. 5.6 VP8 does not interfere with ATM phosphorylation during BoHV-1 infection.

A) MDBK cells were mock-infected, infected with BoHV-1 at a MOI of 4, with BoHV-1ΔU_L47-EYFP at a MOI of 5, or with BoHV-1U_L47R at a MOI of 4. At 14 h post infection cells were fixed with paraformaldehyde, permeabilized and incubated with murine monoclonal anti-VP8- or anti-EYFP antibodies, and rabbit pATM-specific antibodies. Cells were incubated with Alexa-488-

conjugated goat anti-mouse IgG and Alexa-633-conjugated goat anti-rabbit IgG. Prolong gold DAPI was used to identify the nuclei. B) MDBK cells were mock-infected, infected with BoHV-1, with BoHV-1ΔU_L47 or with BoHV-1U_L47R as described in A). At 14 h post infection, mock-infected cells were either left untreated or treated with etoposide for 30 min. Cell lysates were collected and fifty micrograms of total protein of each sample were analyzed by Western blotting. ATM, pATM, VP8, and actin were detected with anti-ATM, anti-pATM, anti-VP8, and anti-actin antibodies, respectively.

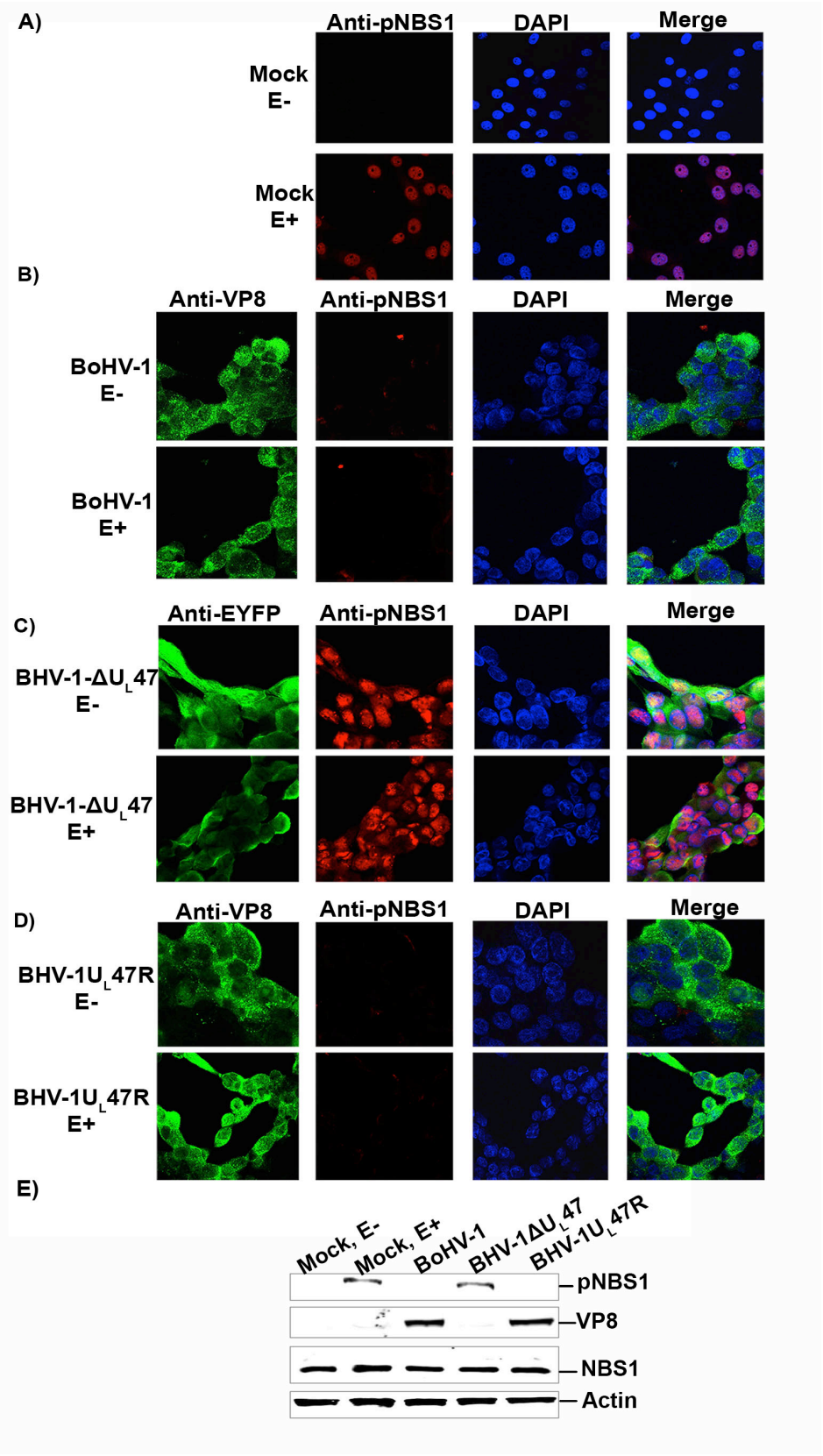

Figure. 5.7 Phosphorylation of NBS1 is inhibited by BoHV-1 but not by BoHV-1ΔU_L47.

MDBK cells were A) mock-infected or infected with B) BoHV-1 at a MOI of 4, C) BoHV-1ΔU_L47-EYFP at a MOI of 5, or D) BoHV-1U_L47R at a MOI of 4. At 14 h post infection cells were either left untreated or treated with etoposide for 30 min. Cells were then fixed with paraformaldehyde, permeabilized and incubated with murine monoclonal VP8- or EYFP specific antibodies, and rabbit pNBS1-specific antibodies. Alexa-488-conjugated goat anti-mouse IgG and Alexa-633-conjugated goat anti-rabbit IgG were used as secondary antibodies, respectively. Nuclei were identified with Prolong gold DAPI. The cells were examined with a Leica SP5 confocal microscope. "E" represents etoposide. E) MDBK cells were mock-infected or infected with BoHV-1, BoHV-1ΔU_L47 or BoHV-1U_L47R as described above. At 14 h post infection, mock-infected cells were either left untreated or treated with etoposide for 30 min. Cell lysates were collected and fifty micrograms of total protein of each sample were analyzed by Western blotting. NBS1, pNBS1, VP8, and actin were detected with anti-NBS1, anti-pNBS1, anti-VP8, and anti-actin antibodies, respectively.

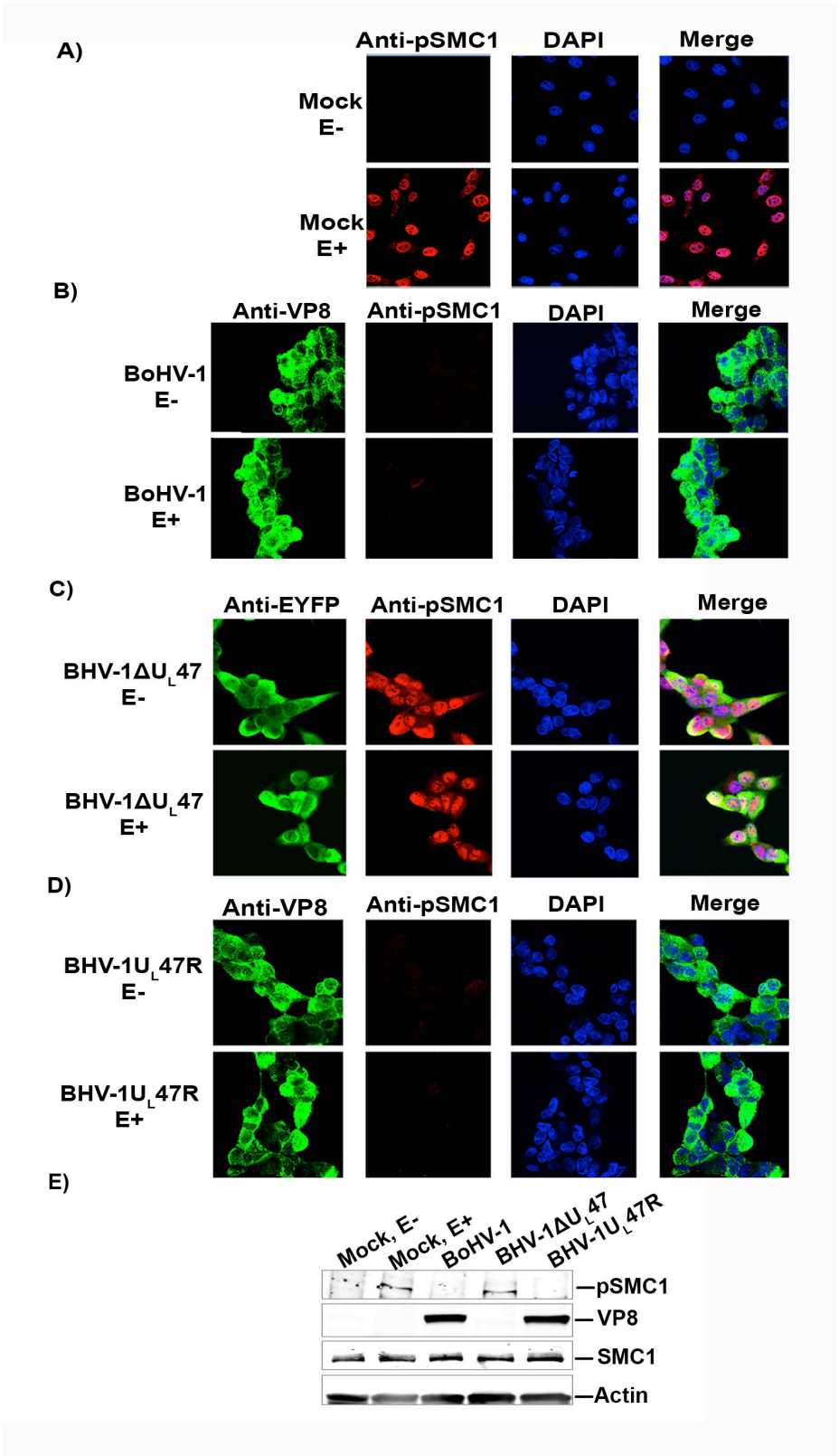

Figure. 5.8 BoHV-1 but not BoHV-1ΔU_L47 inhibits phosphorylation of SMC1.

MDBK cells were A) mock-infected or infected with B) BoHV-1 at a MOI of 4, C) BoHV-1ΔU_L47-EYFP at a MOI of 5, or D) BoHV-1U_L47R at a MOI of 4. At 14 h post infection cells were either left untreated or treated with etoposide for 30 min. The cells were fixed and incubated with murine monoclonal VP8- or EYFP- specific antibodies, and rabbit pSMC1-specific antibodies, followed by incubation with Alexa-488-conjugated goat anti-mouse IgG and Alexa-633-conjugated goat anti-rabbit IgG, respectively. Nuclei were identified with Prolong gold DAPI. The cells were examined with a Leica SP5 confocal microscope. "E" represents etoposide. E) MDBK cells were mock-infected or infected with BoHV-1, BoHV-1ΔU_L47 or BoHV-1U_L47R as described above. At 14 h post infection, mock-infected cells were left untreated or treated with etoposide for 30 min. Cell lysates were generated and fifty micrograms of total protein of each sample were analyzed by Western blotting. SMC1, pSMC1, VP8, and actin were detected with anti-SMC1, anti-pSMC1, anti-VP8, and anti-actin antibodies, respectively.

5.5.4 BoHV-1 infection inhibits phosphorylation of NBS1 and SMC1 early during infection.

Since NBS1 phosphorylation is essential for activation of S-phase checkpoint control by activating SMC1 (398), it was of interest to investigate at which time during BoHV-1 infection VP8 interferes with NBS1 and SMC1 phosphorylation. MDBK cells were either mock-infected or infected with BoHV-1. At 2 h post infection VP8 was cytoplasmic due to release of virion VP8 into the cytoplasm as previously shown (187, 405). The cytoplasmic VP8 did not inhibit phosphorylation of NBS1 or SMC1 (Figure. 5.9A, B). At 4 h post infection VP8 was nuclear and no pNBS1 was detected at this time point, or at 8 h post infection. Similarly, pSMC1 was observed at 2 h post infection, whereas at 4 h or 8 h post infection pSMC1 was not detected (Figure. 5.9B). A further analysis by Western blotting confirmed that NBS1 and SMC1 were phosphorylated at a low level at 2 h post infection, but were not phosphorylated at later time points (Figure. 5.9C). VP8 was detected as early as 2 h post infection and increased in concentration at later time points due to *de novo* synthesis, thus inhibiting NBS1 and SMC1 phosphorylation. Collectively, these results indicate that nuclear VP8 inhibits NBS1 and SMC1 phosphorylation from 4 h onwards during BoHV-1 infection.

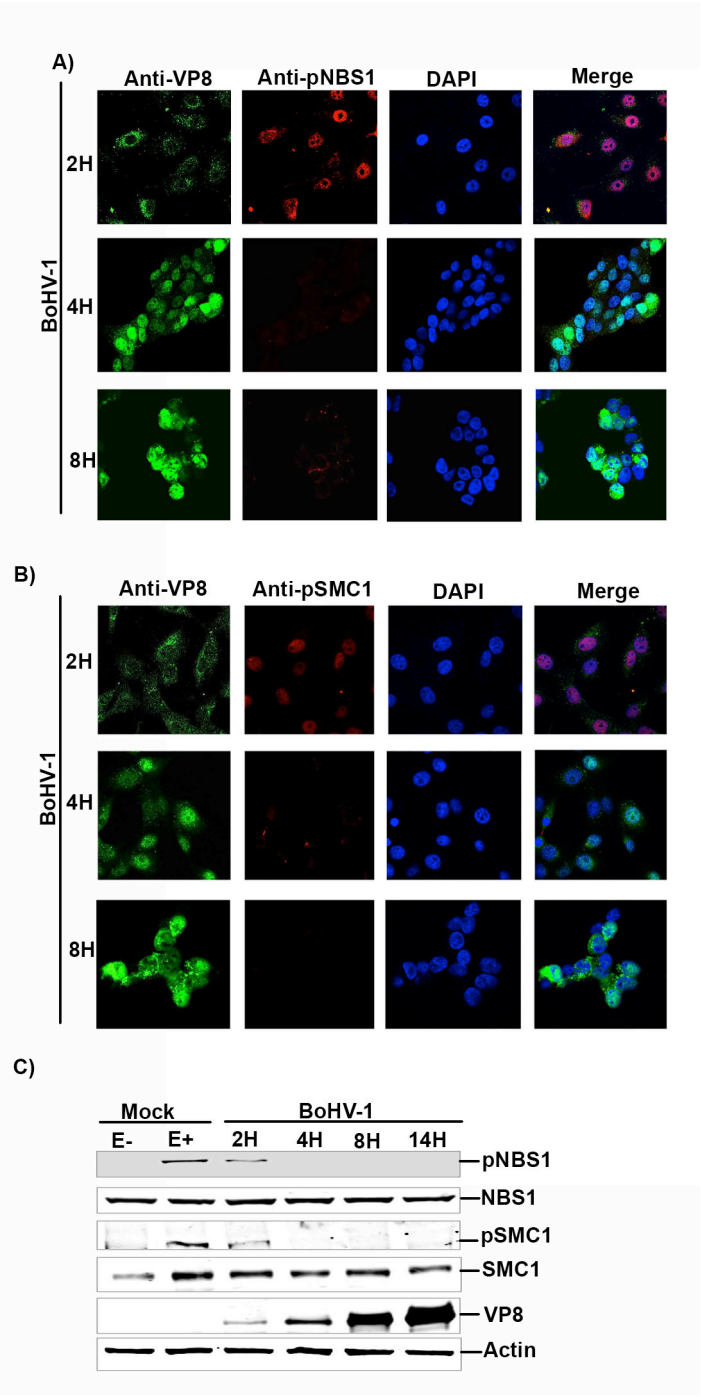

Figure. 5.9 Nuclear BoHV-1 VP8 inhibits phosphorylation of NBS1 and SMC1.

A) MDBK cells were infected with BoHV-1 at a MOI of 4. Cells were fixed and incubated at indicated time points with mouse monoclonal anti-VP8 and rabbit polyclonal anti-pNBS1 antibodies. B) MDBK cells were mock-infected or infected with BoHV-1 at a MOI of 4. Cells were fixed and incubated at indicated time points with mouse monoclonal anti-VP8 and rabbit polyclonal anti-pSMC1 antibodies. Alexa-488-conjugated goat anti-mouse IgG and Alexa-633-conjugated goat anti-rabbit IgG were used as secondary antibodies, respectively. Nuclei were identified with Prolong gold DAPI mounting medium. The cells were examined with a Leica SP5

confocal microscope. C) MDBK cells were mock-infected or infected with BoHV-1 at a MOI of 4. Mock cells were either left untreated or treated with etoposide for 30 min. BoHV-1 cell lysates were collected at 2, 4, 8, and 14 h post infection and fifty micrograms of total protein of each sample were analyzed by Western blotting. NBS1, pNBS1, SMC1, pSMC1, VP8, and actin were detected with anti-NBS1, anti-pNBS1, anti-SMC1, anti-pSMC1, anti-VP8, and anti-actin antibodies, respectively.

5.5.5 VP8 inhibits DNA repair.

Checkpoints constitute the central cellular surveillance that coordinates DNA repair. DNA repair is controlled throughout the cell cycle (414, 415). SMC1 phosphorylation contributes to S-phase checkpoint activation and repair of damaged DNA (416). Since VP8 inhibited NBS1 and SMC1 phosphorylation, which are both involved in DNA repair, we further examined the effect of VP8 on UV-induced cyclobutane pyrimidine dimer (CPD) repair. HeLa cells were mock-transfected or transfected with pEYFP or pVP8-EYFP. At 24 h post transfection cells were irradiated with UV. Cells were then either fixed immediately after UV treatment (0 h) or further incubated for 24 h. CPDs were identified with a monoclonal anti-CPD antibody. Increased CPD intensity was observed in mock-, EYFP- and VP8-expressing cells immediately after UV exposure. At 24 h post UV exposure the CPDs were repaired in mock- and EYFP-transfected cells, but not in VP8-expressing cells (Figure. 5.10A). To perform a quantitative analysis, the CPD intensity was measured in 50 cells for each sample (Figure. 5.10B) by using a biological image-processing program, Fiji (407). At 0 h a high level of UV-induced CPDs was observed in mock-, EYFP- and VP8-expressing cells. The UV-induced CPDs in mock- and EYFP cells were repaired after 24 h, while in VP8-expressing cells, the CPD intensity did not change, indicating impairment of DNA repair in the presence of VP8.

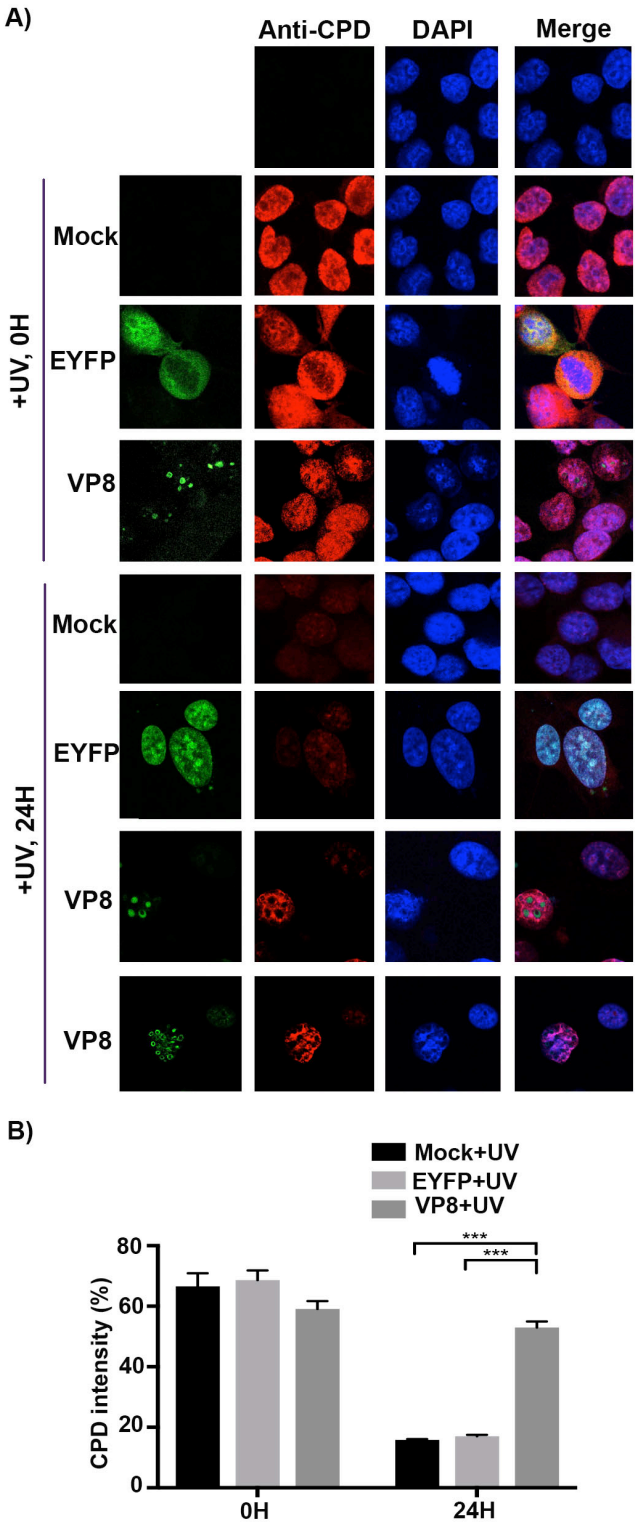

Figure. 5.10 VP8 inhibits DNA repair.

A) HeLa cells were mock-transfected or transfected with pEYFP or pVP8-EYFP for 24 h. Cells were UV irradiated at 10 J/m^2. Cells were fixed immediately after UV exposure or left to recover for 24 h, and then fixed with paraformaldehyde. Cells were permeabilized and stained with a monoclonal anti-CPD antibody followed by incubation with Alexa-633-conjugated goat anti-mouse IgG. B) CPD fluorescence intensity was measured in 50 cells in each sample using a biological image-processing program, Fiji (407). The values of PDU are presented as mean ± standard deviation (SD). Statistical significance is indicated by asterisks (***, $P < 0.001$).

5.5.6 VP8 induces apoptosis.

Successful virus infection involves efficient production and spread of its progeny. Viral proteins such as HIV-1 VPr protein induce apoptosis by inhibiting DNA repair (417). Recently it was shown that prevention of SMC1 phosphorylation leads to a defect in the S-phase checkpoint, and decreased cell survival after induction of DNA damage (416). Since VP8 inhibited phosphorylation of SMC1, we investigated whether VP8 mediates induction of apoptosis or increases DNA damage-induced apoptosis. HeLa cells were mock-transfected or transfected with pFLAG or pFLAG-VP8. To determine the extent of apoptosis, cells were left untreated, treated with etoposide or exposed to UV at 24 h post infection. After 12 h of etoposide induction or UV exposure cells were trypsinized and a TUNEL assay was performed. Compared to untreated mock- and pFLAG-transfected cells, the level of apoptosis was higher in untreated pFLAG-VP8-transfected cells (Figure. 5.11A). DNA damage induction by etoposide increased apoptosis in mock- and pFLAG-transfected cells to about 3% and 6%, respectively. However, in etoposide-treated VP8-transfected cells, apoptosis was increased to 26%, which demonstrates that VP8 enhances DNA-damage induced apoptosis. Furthermore, as we observed inhibition of DNA repair by VP8 following UV treatment (Figure. 5.10), we examined whether VP8 enhances UV-induced apoptosis. While UV-exposure of mock- and FLAG-transfected cells augmented apoptosis to 8% and 9% of cells, respectively, the percentage of apoptotic cells increased to ~55% in UV-treated VP8-transfected cells. This further confirms that DNA damage-induced apoptosis was increased in VP8-transfected cells.

It has been reported that caspase 3 is activated in response to unrepaired UV-induced DNA damage (418). To determine whether VP8 expression leads to cleavage of caspase-3, cells were mock-transfected or transfected with pFLAG-VP8 or pFLAG. An antibody that detects both the pro-caspase-3 and cleaved caspase-3 was used for detection. In VP8-expressing cells as well as in mock-transfected cells treated with etoposide cleaved caspase-3 was detected. However, cleaved caspase-3 was not detected in mock- and FLAG- transfected cells (Figure. 5.11B). This indicates that VP8 can activate caspase-3, and is in agreement with the fact that BoHV-1 infection activates caspase-3 to induce apoptosis (358, 362).

We also examined the role of VP8 in the induction of apoptosis in virus-infected cells. MDBK cells were mock-infected or infected with BoHV-1 or BoHV-1ΔU_L47. Cells were trypsinized, and a TUNEL assay was performed. As shown in Figure. 5.11C, in contrast to mock

infection, BoHV-1 infection caused apoptosis in 40% of the cells. However, the number of apoptotic cells was 8% in BoHV-1ΔU_L47-infected cells. Expression of VP8 in BoHV-1-infected cells was confirmed in Figure. 5.11D. To confirm infection with the BoHV-1ΔU_L47, expression of glycoprotein-C (gC) was demonstrated (Figure. 5.11D). The residual apoptosis in BoHV-1ΔU_L47-infected cells could be the result of the virus attachment process which was previously shown to induce apoptosis in BoHV-1-infected cells (356). Furthermore, gD was suggested to be involved in the induction of apoptosis (357), as well as the immediate early protein of BoHV-1, bICP0 (360). Since BoHV-1ΔU_L47 contains gD and bICP0, the residual apoptotic activity in BoHV-1ΔU_L47-infected cells is likely due to one or both of these proteins. Since a significant reduction (~32%) of apoptosis was observed in BoHV-1ΔU_L47-infected cells compared to wild type BoHV-1 infection, this demonstrates that VP8 contributes to induction of apoptosis.

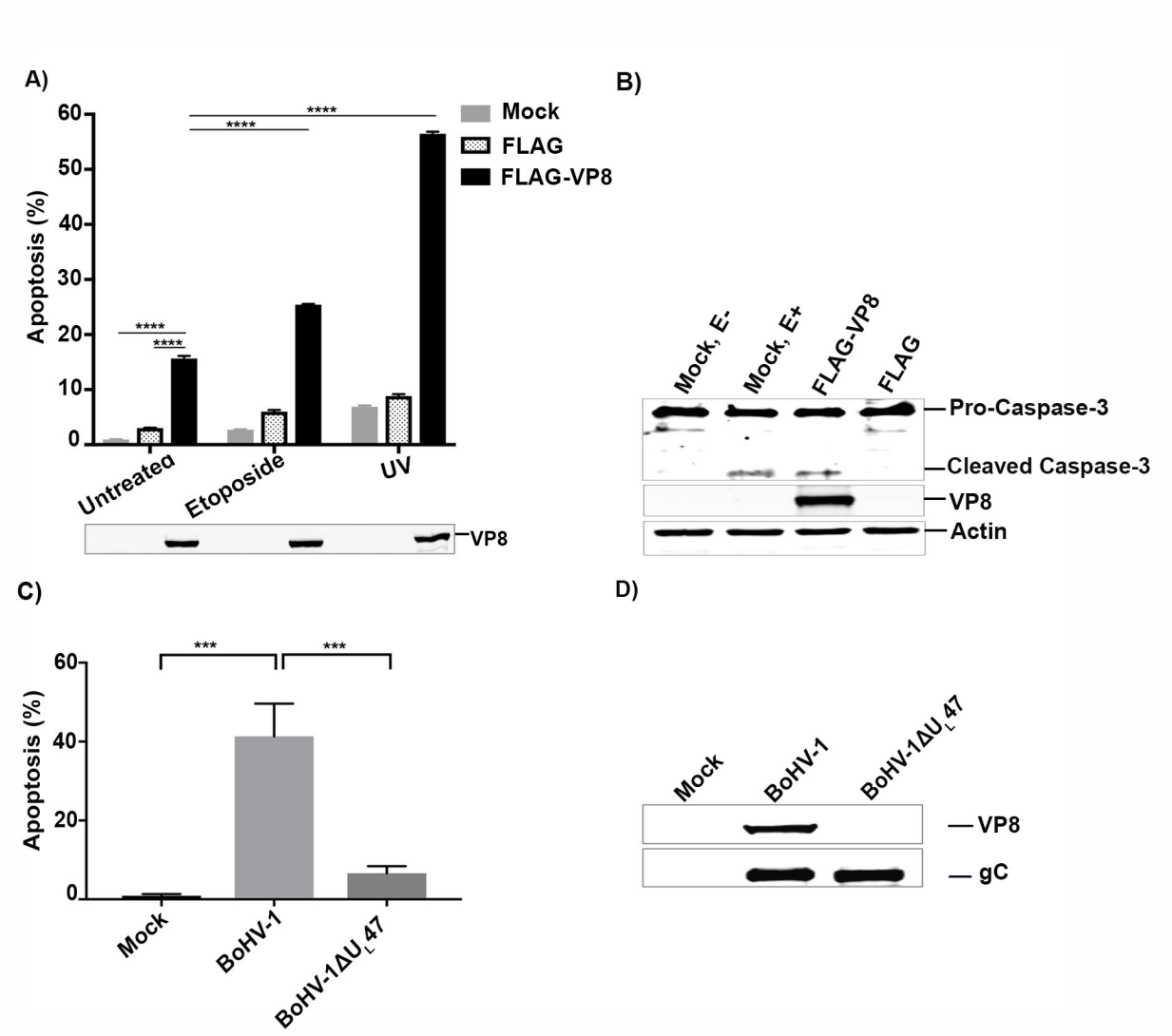

Figure. 5.11 VP8 induces apoptosis in transfected and BoHV-1 infected cells.

A) HeLa cells were mock-transfected or transfected with pFLAG or pFLAG-VP8. At 24 h post transfection cells were left untreated, treated with etoposide or irradiated with UV 50 J/m^2, and incubated for 12 h before trypsinization. Apoptosis was detected by TUNEL assay. The cells were analyzed by FACS. B) HeLa cells were mock-transfected or transfected with pFLAG or pFLAG-VP8. At 48 h post transfection, mock- infected cells were either left untreated or treated with etoposide. Cell lysates were collected and equal amount of proteins were analyzed by Western blotting. Caspase-3, cleaved caspase-3, VP8, and actin were detected with anti-caspase-3, anti-VP8, and anti-actin antibodies, respectively. C) MDBK cells were mock-infected or infected with BoHV-1 or BoHV-1ΔU_L47 at a MOI of 4. At 10 h post infection cells were trypsinized and apoptosis was measured by TUNEL assay. The cells were analyzed by FACS. D) Cell lysates were generated and VP8 and glycoprotein C (gC) were detected with murine monoclonal anti-VP8 and anti-rabbit polyclonal gC antibodies, followed by incubation with IRDye680-conjugated anti-mouse IgG and IRDye-800CW-conjugated anti-rabbit IgG, respectively.

5.6. Discussion.

During virus infection, host cells establish an intrinsic anti-viral defense, such as the IFN response and apoptosis. While some viruses counteract these responses by modulating the host immune responses, others manipulate the cellular machinery in favor of virus replication. In the present study, we demonstrated that VP8 interacts with ATM and NBS1. ATM is a central player in the DNA damage response and is activated immediately after DNA damage (265), by autophosphorylation at Serine-1981, which in turn leads to the phosphorylation of many downstream targets to coordinate DNA repair, cell cycle arrest and apoptosis (reviewed in (265)). Although VP8 interacted with ATM, VP8 did not interfere with ATM phosphorylation. However, although the ATM activation was not interrupted, VP8 inhibited NBS1 phosphorylation. VP8, ATM and NBS1 were detected as a complex indicating that VP8 interacts with both ATM and NBS1. Since interaction between NBS1 and ATM is required for NBS1 phosphorylation, VP8 might inhibit phosphorylation by blocking this interaction. Phosphorylation of SMC1 by ATM depends on NBS1 phosphorylation and is critical to activate the S-phase checkpoint (398). In fact, VP8 also inhibited SMC1 phosphorylation, which can prevent S-phase checkpoint activation (398, 416)**.** Overall, this shows that VP8 interacts with DNA damage response proteins and disrupts the ATM/NBS1/SMC1 pathway resulting in a defective DNA damage response.

BoHV-1, but not BoHV-1ΔU_L47, inactivated the ATM/NBS1 pathway by reducing phosphorylation of NBS1, further supporting this function of VP8. Inhibition of NBS1 phosphorylation was mediated by nuclear VP8 from 4 h onwards during infection. In contrast to BoHV-1, HSV-1 does not disrupt the ATM signaling pathway. Interestingly, Lou et al. revealed that in two closely related species such as white-cheeked gibbon (*Nomascus leucogenys*) and siamang (*Symphalangus syndactylus*), NBS1 functions differently during the establishment of HSV-1 infection (419), supporting the possibility of distinctive NBS1 role in the establishment of herpesvirus infections. Moreover, unlike HSV-1, HCMV disrupts both ATM and ATR pathways to subvert full activation of S-phase checkpoints (304) and Kaposi's Sarcoma-associated herpesvirus inhibits the ATM signal transduction pathway by compromising the ATM/P53 DNA damage response checkpoint (311).

Viruses have developed unique strategies to circumvent host-cell responses while others hijack cellular DNA damage response proteins for their propagation or replication. Similar to BoHV-1, homologous recombination repair is also inhibited during HSV-1 infection (279).

Furthermore, murine gamma herpesvirus 68 (γHV68) M2 protein interacts with the DNA repair complex, DDB1/ATM/COP9/cullin (404). Although γHV68 M2 protein induced ATM activation, the DNA damage response was abolished. Adenovirus E4 protein also reorganizes the MRN complex resulting in degradation (420). Adenovirus deregulates the host cell machinery in favor of viral genome processing, whereas HSV-1 activates and manipulates the DNA damage response. Thus, viral proteins use various distinct and overlapping mechanisms to accomplish viral propagation.

Non-repaired DNA induces apoptosis in DNA repair-deficient cells (421). Similarly, inhibition of DNA repair has been implicated in the induction of apoptosis by HIV VPr (417). Previously, BoHV-1 has been shown to induce apoptosis (356, 360, 364). Interestingly, VP8 appeared to contribute to induction of apoptosis outside the context of infection, as well as during BoHV-1 infection. We observed more apoptosis in BoHV-1-infected cells compared to BoHV-1ΔU_L47-infected cells. A low level of apoptosis was still observed in BoHV-1ΔU_L47-infected cells, which can be contributed to other BoHV-1 proteins, for instance gD (357), ORF8 (364), and/or bICP0 (360). Since according to previous reports, prevention of SMC1 phosphorylation leads to a defect in the S-phase checkpoint and decreased cell survival after induction of DNA damage (416)**,** prevention of SMC1 phosphorylation and abrogation of DNA repair by VP8 likely contributes to induction of apoptosis. Alternatively, VP8 may contribute to ATM activation, which can then phosphorylate p53 (thus leading to apoptosis). However, we observed activation of caspase 3 by VP8, and Dunkern et al, demonstrated that in repair-deficient cells UV-induced DNA damage triggered apoptosis independent of p53 and through caspase 3 activation (418). The fact that previously caspase-3-mediated apoptosis was observed in BoHV-1-infected cells (358) (362), further supports the contention that VP8 might function through caspase 3 activation to induce apoptosis.

While some viruses express anti-apoptotic proteins to favor virus pathogenesis, others also exhibit pro-apoptotic properties to manipulate the cellular machinery for efficient virus production. For example, influenza virus upregulates pro-apoptotic factors for viral replication (422, 423), and HIV-1 enhances pro-apoptotic gene expression for efficient virus production (424). Furthermore, HSV-1 immediate early protein ICP0 triggers apoptosis during HSV-1 infection to influence viral pathogenesis (425). Induction of apoptosis by VP8 might expedite the egress and progression of BoHV-1 infection. In BoHV-1ΔU_L47-infected cells, the release of

infectious virus particles into the culture medium was reduced more than 1,000 fold compared to BoHV-1-infected cells which suggested reduced egress of BoHV-1ΔU_L47 virions (179).

In summary, BoHV-1 developed a novel evasion mechanism, whereby VP8 targets DNA damage response proteins. Without interfering with ATM activation, VP8 abrogated downstream signaling and thus, impaired the DNA repair mechanism. As a consequence, VP8 increased DNA damage-induced apoptosis. VP8 is the first BoHV-1 tegument protein reported to interfere with the DNA damage response pathway. These results illustrate a potential role of VP8 in the modulation of DNA damage response during BoHV-1 infection.

5.7 Acknowledgments.

We acknowledge Yurij Popowych for his assistance in FACS cell sorting. This research was supported by grant 90887-2010 RGPIN from the Natural Sciences and Engineering Research Council of Canada. SA was partially supported by a Canadian Institutes of Health Research Training Grant in Health Research Using Synchrotron Techniques (CIHR-THRUST). This is VIDO manuscript number 822.

CHARPTER 6

LINKER BETWEEN CHAPTER 5 AND CHAPTER 7

In BoHV-1-infected cells, VP8 is observed in the cytoplasm early during infection. As infection progresses VP8 is localized to the nucleus, followed by translocation of VP8 into the cytoplasm later during infection. The results in chapter 5 demonstrated that the subcellular localization of VP8 is associated with its function. In the nucleus, interaction of VP8 with DDR proteins, ATM and NBS1, inhibited ATM-mediated DDR pathway resulting in induction of apoptosis.

The C-terminal domain of VP8 consists of mostly alpha-helices and is homologous to other herpesviruses *ul47* gene products. However, there is no structural information available for any of the herpesvirus *ul47* gene products. Therefore, we set out to determine the structure of VP8 by expressing it in different expression systems.

6.1 Expression and purification of VP8.

VP8 was first expressed in baculovirus by using the Bac-to-Bac baculovirus expression system (Invitrogen). Briefly, VP8 was cloned into pFast-Bac donor plasmid. The recombinant donor plasmid was transformed into competent DH10Bac *E. coli* cells. Recombinant bacmid DNA was transfected into the *Spodoptera frugiperda* (Sf9) insect cells. The recombinant baculovirus passage-1 stock was secreted in the media. Following amplification of the baculovirus stock, the virus titer was determined and was used for subsequent infection of Sf9 cells for large scale VP8 production.

Secondly, to express VP8 in the mammalian secretory system, tissue plasminogen activator (tPA) signal and His tag were introduced at the N-terminus and C-terminus of VP8, respectively. VP8 was cloned into the pEB5.2 vector. Following screening of positive clones, HEK 293T cells were transfected with the VP8 recombinant vector. Secretion of VP8 in the media was screened for several days by Western blotting.

For large scale VP8 production, VP8 was cloned into a lentivirus transfer vector, TRiP. VP8 was introduced with the N-terminals FLAG tag and C-terminal His tag. A VP8 positive clone was selected base on antibiotic selection. To generate the lentivirus, HEK 293T cells were transfected with the VP8 containing transfer vector, packaging vector psPAX2, and envelope vector pMD2. At 16 h post transfection medium was replaced with antibiotic containing medium.

The recombinant lentivirus was secreted into the medium. At 48 h post transfection supernatants were collected and screened for VP8 production. The supernatant was used for subsequent infection to express VP8.

Finally, the truncated VP8 was expressed in *E. coli* with the addition of sumoylation-Histidine (SUMO-His) tag at the N-terminus. VP8 was purified using affinity chromatography. To eliminate further contaminating proteins, truncated VP8 was subjected to size-exclusion chromatography. Sephadex-G-25 resin was used to pack the column followed by passing the purified VP8 through the column. The eluted protein was collected in multiple fractions. The collected fractions were analyzed by SDS-PAGE gel (Figure. 6.2A). Nonetheless, pure VP8 was not obtained through gel filtration chromatography.

Ion exchange chromatography was performed with the truncated VP8 to separate other non-specific contaminating proteins. Q-Sepharose anion resin was used to incubate the purified protein. Following incubation of protein with the beads and subsequent washes, the proteins were eluted with a salt gradient. For cation exchange chromatography, the purified VP8 was incubated with sulphopropyl (SP) Sepharose. After multiple washes the proteins were eluted with the different salt concentrations. However, the unknown protein was not separated from VP8 by using on exchange chromatography (Figure. 6.2B).

6.2 Results and Discussion.

In this study, we expressed VP8 in multiple expression systems. First, we chose to express VP8 in baculovirus expression system. However, the expression of VP8 was too low for large scale VP8 production. Secondly, VP8 recombinant lentivirus was generated. However, VP8 was not expressed in the lentivirus expression system. Thirdly, since VP8 was transiently expressed in mammalian cells, we cloned VP8 in the mammalian secretory system with addition of tPA signal peptide. Nonetheless, VP8 was not secreted in the mammalian secretory system. The effort to express full length VP8 in *E. Coli* was also unsuccessful (demonstrated by a previous researcher form our lab). Therefore, since the C-terminal domain of VP8 is enriched with alpha-helices (Figure. 6.1A), we attempted to express the C-terminal domain in *E. coli.* Addition of the SUMO tag, which is responsible for increasing solubility of any protein, to VP8 enhanced its expression in *E. Coli*. Nonetheless, VP8 formed a strong complex with another bacterial protein.

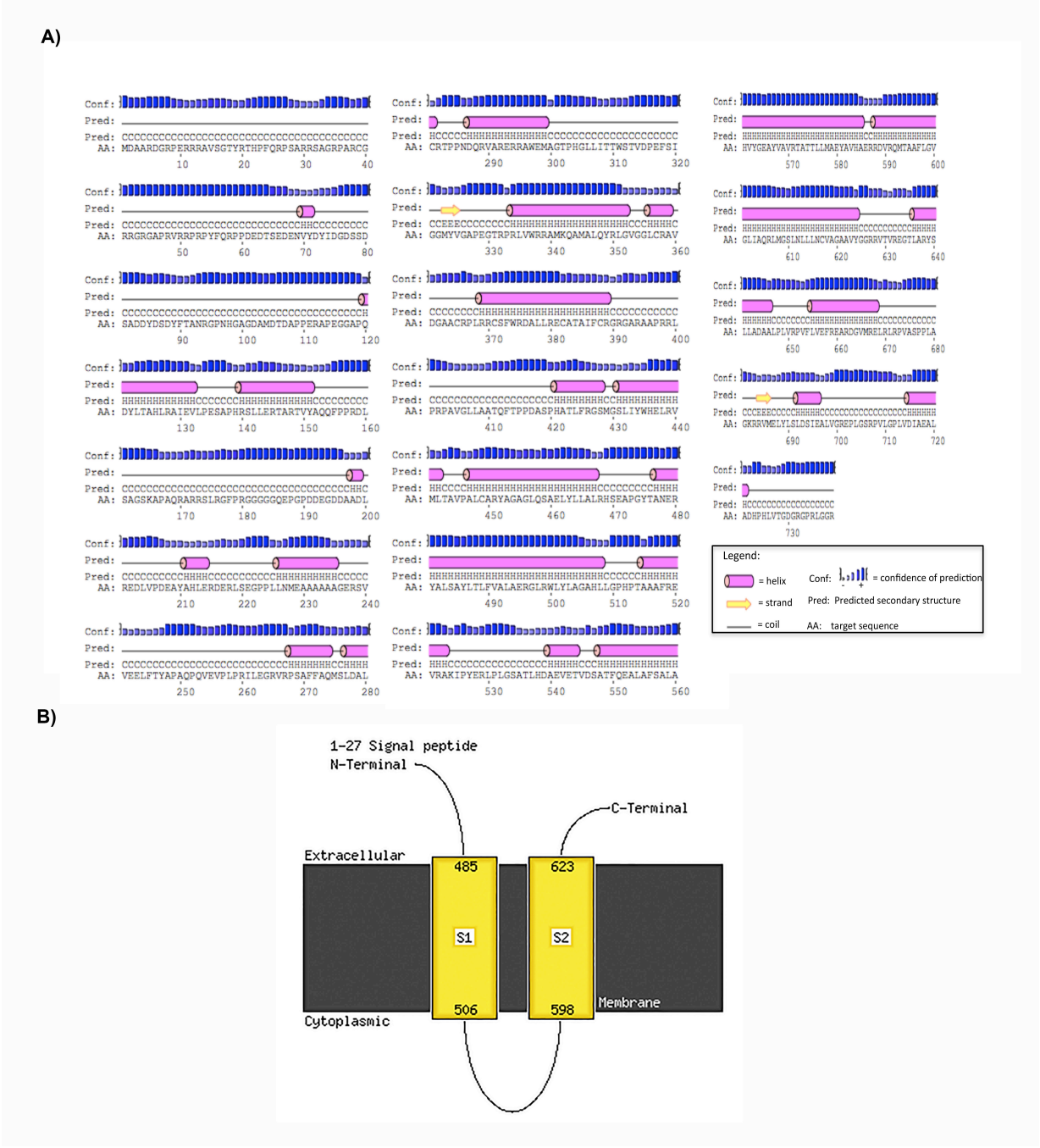

Figure. 6.1 Predicted secondary structure of VP8.

A) BoHV-1 VP8 amino acid sequences were analyzed with PSIPRED. Pink colour rods represent helical structures, Yellow arrows represent strand and the black lines indicate coil structures. Blue colour represents conf: confidence of prediction, pred: predicted secondary structure and AA: amino acids. B) The Phyre 2 analysis was used for the prediction of transmembrane helices in VP8 (426).

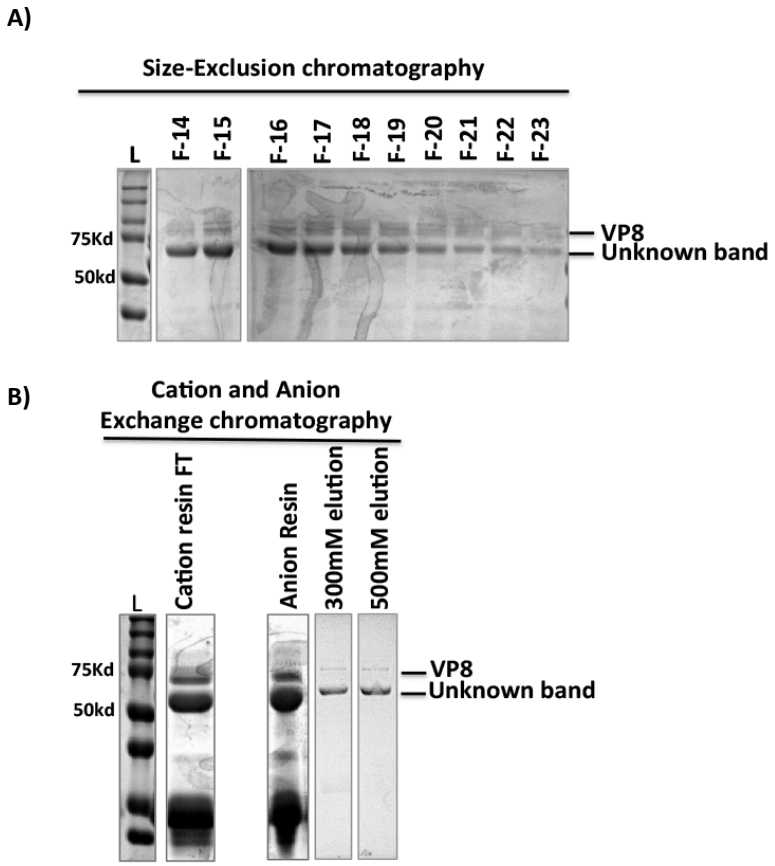

Figure. 6. 2 Expression and purification of VP8.

A) SUMO-His-VP8 219-741 was VP8 was expressed in *E. coli*. VP8 was purified by using a Nickel column. Size-exclusion chromatography was used for further purification of VP8. Fractions (F) were collected and analyzed by SDS-PAGE. F14-F23 are presented. B) VP8 was purified by using a cation resin (Left panel) and an anion resin (Right panel). The purified protein was analyzed by SDS-PAGE.

For structural analysis we proceeded further for crystallization screening of VP8 and the unknown bacterial protein complex. However, crystallization screening of VP8 and the unknown bacterial protein complex did not reveal any condition suitable for VP8 crystallization. Furthermore, concentrating VP8 at a concentration higher than 1 mg/ml was not possible as it precipitated at higher concentration. Recent predicted secondary structural analysis suggested that VP8 contains some transmembrane domains (Figure. 6.1B). This might explain the difficulties in expressing, purifying, and crystallizing VP8. Thus, in the future, modifying the crystallization screening approach might facilitate VP8 crystallization.

In the process of VP8 expression and purification, we identified a novel mitochondrial interacting partner of VP8. In the following chapter, we demonstrate another potential function of VP8 associated with the mitochondrial function.

CHAPTER 7

THE BOVINE HERPESVIRUS MAJOR TEGUMENT PROTEIN, VP8, INTERACTS WITH HOST HSP60 CONCOMITANT WITH DEREGULATION OF MITOCHONDRIAL FUNCTION

Sharmin Afroz[1,2], Robert Brownlie[2], Michel Fodje[3],, and Sylvia van Drunen Littel-van den Hurk[1,2,4]

[1] VIDO-InterVac, University of Saskatchewan, Saskatoon, SK, S7N 5E3, Canada; [2]Vaccinology & Immunotherapeutics, University of Saskatchewan, Saskatoon, SK, S7N 5E3, Canada. [3] Canadian Light Source, University of Saskatchewan, Saskatoon, SK, S7N 5E3, Canada. [4] Microbiology & Immunology, University of Saskatchewan, Saskatoon, SK, S7N 5E3, Canada.

Running title: BoHV-1 VP8 and mitochondrial protein interaction

Corresponding author*:
Dr. Sylvia van Drunen Littel-van den Hurk
VIDO-InterVac
University of Saskatchewan
120 Veterinary Road
Saskatoon, SK, S7N 5E3, Canada
Telephone: 1 + (306) 966-1559
Fax: 1 + (306) 966-7478

The information in the following chapter was submitted to Virus Research.

7.1 Abstract

The *ul47* gene product, VP8, is a major tegument protein of BoHV-1. While VP8 is not essential for virus replication in cell culture, a U_L47-deleted virus exhibits a smaller tegument structure and is avirulent in cattle. To elucidate the structure of VP8, we expressed an N-terminally truncated version of VP8 in *E. coli*. However, the recombinant VP8 consistently co-purified with a tightly associated bacterial protein; this protein was identified by mass spectrometry as GroEL, which has considerably homology with mammalian HSP60, thus suggesting a new role for VP8 in virus/host interaction. A physical interaction of HSP60 and VP8 in both VP8-transfected and BoHV-1-infected cells was demonstrated by immunoprecipitation. Analysis of different truncated VP8 constructs revealed that amino acids 259-482 and 632-741 are involved in binding to HSP60. Full-length VP8 and VP8 219-741 (containing both interacting domains, 259-482 and 632-741) co-localized with HSP60 and mitochondria. VP8 was localized in the mitochondria at 2-14 h post infection in BoHV-1-infected cells. The mitochondrial membrane potential (MMP) was reduced in both VP8-transfected and BoHV-1-infected cells and was further reduced by overexpression of HSP60 in the presence of VP8. In addition, VP8 expression also decreased the ATP concentration during transfection, as well as BoHV-1 infection. Thus, VP8 may play a role in the deregulation of mitochondrial function through interaction with HSP60. This is consistent with the fact that BoHV-1 infection is known to promote mitochondrial dysfunction.

7.2 Introduction.

Bovine herpesvirus (BoHV-1) is an alpha herpesvirus and a major pathogen in cattle (11, 427), causing several diseases, including conjunctivitis, infectious bovine rhinotracheitis (IBR), balanoposthitis and abortions in cattle. Thus, BoHV-1 contributes significantly to economic losses of the North American cattle industry (11). BoHV-1 is a double-stranded DNA virus with a ~140kb genome. It contains four different compartments; a DNA core enclosed within a capsid, a thick tegument layer and an outer envelope with glycoproteins (428). The tegument of the BoHV-1 virion is the most complex structure containing ~ 20 virus-encoded proteins. The functions of the proteins in the tegument are not well understood. Immediately after fusion of the glycoproteins to the host cell membrane, herpesviruses release their tegument proteins into the cytoplasm (66). Thus, the tegument proteins are the first proteins to get into

contact with the intracellular environment, possibly to promote virus infection. Besides the structural role of the tegument proteins, these proteins contribute to multiple regulatory functions including DNA replication, transcriptional regulation, capsid transport, and kinase activity (106). Hence, the tegument proteins play a significant role during the establishment of virus infection.

The *ul47* gene product, VP8, is the most abundant tegument protein (176). VP8 is not essential for viral replication *in vitro*. However, a *U_L47*-deleted BoHV-1 mutant has a smaller tegument structure and does not replicate in cattle (179). VP8 contains a nuclear localization signal (NLS) and a nuclear export signal (NES). These signals are responsible for shuttling of VP8 between the cytoplasm and nucleus (182). Early during infection the virion VP8 and the *de novo* synthesized VP8 can be detected in the cytoplasm. With the progression of infection VP8 localizes to the nucleus and later during infection VP8 is again observed in the cytoplasm (181, 187). VP8 has also been detected in the cisternae of the Golgi and found to interact with gB, gC, and gD mRNAs (181, 188).

Mitochondria play a pivotal role in supplying energy and regulating apoptotic cell death processes, which are crucial for cell mortality. Human herpes simplex virus-1 (HSV-1) infection has been associated with deregulation of mitochondrial function. During HSV infection mitochondrial protein synthesis is progressively reduced (429, 430). HSV-1 infection also induces mitochondrial membrane disruption (431). Murata et al, demonstrated that mitochondria migrate to the perinuclear region with the tegument proteins U_L41 and U_L46 during HSV-1 infection (432). Similarly, some tegument proteins accumulate in the perinuclear region of the cytoplasm (433, 434). The tegument protein U_L16 also contains a mitochondrial localization signal and interacts with mitochondria (435). Likewise, BoHV-1 infection induces mitochondrial dysfunction and is associated with the stimulation of apoptosis (358, 362). Moreover, BoHV-1 infection leads to mitochondrial dysfunction through induction of reactive oxygen species (363). Since some viral proteins targeted to mitochondria are also meant to subvert host defenses (reviewed in (436)), the de-regulation of mitochondrial functions by tegument proteins might be correlated to the establishment of virus infection.

Several functions of VP8 are mediated by interaction with other host or other viral proteins, indicating that VP8 is a multifunctional protein and is extensively involved in host-pathogen interactions. BoHV-1 VP8 interacts with cellular CK2 and viral US3 kinase (184). Furthermore, VP8 interacts with DNA damage-binding protein-1 (DDB1) (187), and with the

cellular signal transducer and activators of transcription (STAT1) to down-regulate interferon- β (IFN-β) signaling (405). Homologues of VP8 are present in different herpesviruses. The C-terminal domain of VP8 is enriched with alpha-helical structures and is conserved among some herpesviruses (405).

VP8 may exert more functions by interacting with additional viral or cellular proteins. The C-terminal domain of VP8 contains mostly α-helical structures (24), which mediate protein-protein interactions (437). While expressing and purifying an N-terminal truncated VP8 for structural analysis in *Escherichia coli*, we observed a strongly interacting protein that co-purified with VP8. By mass spectrometry this bacterial protein was identified as GroEL, which shows conserved homology with mammalian heat shock protein-60 (HSP60). HSP60 is a molecular chaperone located in the cytoplasm and mitochondria and implicated in correct folding and transport of proteins to the mitochondrial matrix. We demonstrated that VP8 interacts with HSP60 in both VP8-transfected and BoHV-1-infected cells. Furthermore, we determined that VP8 localized to mitochondria resulting in deregulation of mitochondrial functions.

7.3 Materials and Methods.

7.3.1 Cells, viruses and plasmids.

Madin-Darby bovine kidney (MDBK) and HeLa cells were maintained in Eagle's minimum essential medium (MEM, Sigma-Aldrich Canada Ltd, Oakville, ON, Canada) supplemented with 10% heat-inactivated fetal bovine serum (FBS, Gibco, Life Technologies, Burlington, ON, Canada), 10 mM HEPES buffer (Life Technologies) and 1% antibiotic-antimycotic (Life Technologies). A 37°C incubator with 5% CO_2 was used to culture the cells. BoHV-1, BoHV1-ΔU_L47 and BoHV-1U_L47R were generated previously, (179) and were propagated in MDBK cells. The plasmid pFLAG-VP8 which allows expression of VP8 with a N-terminal FLAG tag from a cytomegalovirus (CMV) promoter was described previously (Labiuk et al., 2009) The bacterial expression vector pET His6 Sumo TEV LIC was a gift from Scott Gradia (Addgene plasmid # 29659). A HSP60 expression plasmid was obtained from Sino Biologicals Inc., Wayne, PA, USA.

7.3.2 Antibodies and other reagents.

BoHV-1 VP8-specific mouse monoclonal antibody was raised and used as previously described (181). HSP60 rabbit polyclonal antibody was obtained from Cell Signaling Technology, Beverly, MA, USA. Murine monoclonal anti-FLAG antibody was purchased from Sigma-Aldrich Canada Ltd, (Oakville, ON, Canada). A mitochondria detection kit, MITO-ID Red detection kit, was obtained from Enzo Life Sciences, Inc. (Farmingdale, NY, USA). ATPlite 1step Luminescence Assay system was purchased from PerkinElmer (Waltham, MA, USA).

7.3.3 Cell lysates, immunoprecipitation, and Western blotting.

HeLa cells were seeded one day before transfection and grown to 60-70% confluency. The cells were transfected with different plasmids with Lipofectamine and Plus reagents (Invitrogen, Life Technologies). At 24 h post transfection ice-cold phosphate-buffered saline (PSB, pH 7.4) was used to wash the cells followed by incubation with lysis buffer (50 mM Tris, 150 mM NaCl, 1 mM EDTA, 1% Triton X-100, pH 7.4). The lysis buffer was supplemented with mammalian cell and tissue extract protease inhibitor cocktail (Sigma-Aldrich). The cell and lysis buffer mixture was incubated on ice for 30 min followed by centrifugation at 12,000 × *g* for 15 min at 4°C. The cell lysates were collected and stored at −80°C for future use. MDBK cells were infected with different viruses, and cell lysates were collected as described above.

For immunoprecipitation, the cell lysates were incubated with anti-FLAG resin overnight. Alternatively, the cell lysates were incubated with anti-HSP60 antibody overnight followed by incubation with G-Sepharose Fast Flow beads (GE HealthCare, Niskayuna, NY, USA). The protein complexes were washed, and the bound proteins were eluted by adding SDS-PAGE sample buffer followed by boiling. The protein samples were analyzed on 10% or 8-16% gradient gels. The proteins were transferred to a nitrocellulose membrane followed by incubation with blocking buffer (5% skim milk in PBS containing Tween-20). The membrane was incubated with an appropriate primary antibody followed by incubation with IRDye680-conjugated anti-mouse IgG or IRDye-800CW-conjugated anti-rabbit IgG (LI-COR Bioscience, Lincoln, NE, USA). The images were detected with an Odyssey Infrared Imaging system (LI-COR Bioscience).

7.3.4 Expression and purification of truncated VP8.

A truncated ORF of VP8 (amino acids 219 – 741) was PCR amplified using the primers GAGGGATCCGAGCGGCTGTCGGAAGGGCCCCCGCTCCTCAAC and CACCTCGAGCTACCGGCCGCCCAGGCGCGGGCCCCGCCCATC, and then cut with BamHI and XhoI and cloned into a modified version of pET His6 Sumo TEV LIC. This allowed for expression of truncated VP8 with an N terminal SUMO together with his tag. A N-terminal SUMO has been shown to enhance expression and solubility of proteins (438); previous attempts to express VP8 in *E. coli* without SUMO were unsuccessful (results not shown). A Tobaco Etch Virus (TEV) protease site between the SUMO-his and VP8 allows for removal of the N-terminal tag from the purified protein. Recombinant protein was expressed in transformed BL21 (DE3) cells by inducing mid-log phase cells with Isopropyl β-D-1-thiogalactopyranoside (IPTG) at a final concentration of 250 mM and further incubation at 37˚C for 5 h. The cells were harvested by centrifugation at 10,000 x g for 15 min. and resuspended in 20 mM imidazole, 200 mM sodium phosphate buffer, supplemented with a SIGMA*FAST* Protease Inhibitor Cocktail tablet. The cells were lysed with a cell disruptor (Constant system, LTD. USA) and purified with a GE Healthcare His-Trap column. The purified protein was digested with Ac-TEV protease to cleave SUMO-His from the truncated VP8 and was re-purified on the Nickel column. The pure truncated VP8 was concentrated with an Amicon concentrator tube. Proteins were analyzed by SDS-PAGE followed by Coomassie Brilliant Blue staining and destaining.

7.3.5 Mass spectrometry.

SUMO-His tagged truncated VP8 expressed in bacteria was purified using a Nickel column. The purified protein was analyzed by SDS-PAGE and stained with Coomassie Brilliant Blue in 10% acetic acid, 40% methanol. After destaining the gel, the proteins bands were excised and treated for in-gel trypsin digestion. The protein samples were then analyzed using matrix-assisted laser desorption/ionization time-of-flight mass spectrometry (MALDI-TOF-MS) in the Alberta Proteomics and Mass Spectrometry Facility, University of Alberta, Edmonton, Canada. Briefly, the excised protein bands were destained (100 mM ammonium bicarbonate/acetonitrile (50:50)); reduced (10 mm BME in 100 mm bicarbonate), alkylated (55 mM iodoacetamide in 100 mm bicarbonate) and dehydrated. The dehydrated samples were trypsinized with 6 ng/µl trypsin (Promega Sequencing grade) overnight at room temperature (RT). 97% water/2% acetonitrile/1%

formic acid was used for extraction of the tryptic peptides. The second extraction was performed using 50% of the first extraction buffer and 50% acetonitrile. Nanoflow HPLC (Easy-nLC II, Thermo Scientific) coupled to a LTQ XL-Orbitrap hybrid mass spectrometer (Thermo Scientific) was used to resolve the tryptic peptide fractions. The peptide mixtures were injected onto the column, and the mass spectrometer data were obtained. The data processing was performed with Proteome Discoverer 1.4 (Thermo Scientific) and UniProt (uniprot.org) bovine, *E. coli* and VP8 databases. The data was searched with SEQUEST (Thermo Scientific).

7.3.6 Immunofluoresence.

HeLa or MDBK cells were seeded in two-chamber Permanox slides (Lab-Tek, Naperville, IL, USA) in MEM supplemented with 5% FBS. Lipofectamine and Plus reagents were used for mock transfection or transfection with pFLAG-VP8. At 24 h post transfection cells were fixed with 4% paraformaldehyde followed by permeabilization with 0.1% Triton X-100. The cells were blocked with 1% goat serum in PBS. Subsequently, the cells were incubated with primary antibodies for 2 h at RT. MDBK cells were mock-infected or infected with BoHV-1. The infected cells were fixed, permeabilized and incubated with primary antibodies. Following subsequent washes, the cells were incubated with Alexa Fluor 488 goat anti-mouse IgG or Alexa Fluor 633 goat anti-rabbit IgG (diluted 1:500; Invitrogen, Life Technologies). The nuclei were incubated with 4′,6-diamino-2-phenylindole (DAPI) containing mounting medium. For detection of mitochondria, a MITO-ID red detection kit (Farmingdale, NY, USA) was used. The cells were treated with MITO-ID red dye according to the manufacturer's instruction. Green laser excitation at 488 nm (Alexa 488), red laser excitation at 633 nm (Alexa 633), and 461 nm for DAPI were used to analyze the confocal images. A Leica SP5 confocal microscope (Leica Microsystems Inc., Concord, ON, Canada) was used to obtain immunofluorescence images.

7.3.7 Measurement of cellular ATP levels.

The cellular ATP level was determined with an ATPLite 1step Luminescence assay system (PerkinElmer, Waltham, MA, USA). HeLa cells were cultured in 96-well plates and mock-transfected or transfected with pFLAG or pFLAG-VP8. At 48 h post transfection, the ATP level was measured according to the manufacturer's instruction. Briefly, the ATPLite substrate was added to the wells followed by incubation for 5 min at RT with shaking. Luciferase signals

emitting at 560 nm were detected with a VICTOR X light luminescence plate reader (PerkinElmer). ATP concentration was determined from the standard curve. MDBK cells were mock-infected or infected with BoHV-1, BoHV1-ΔU_L47 or BoHV1-U_L47R. At 24 h post-infection the ATP level was detected as described above.

7.3.8 Mitochondrial membrane potential detection.

A NIR mitochondrial membrane potential kit (Sigma-Aldrich) was used to detect mitochondrial membrane potential. HeLa cells were mock-transfected or transfected with pFLAG or pFLAG-VP8. At 48 h post-transfection cells were stained with the cationic membrane potential dye according to the manufacturer's instruction. MDBK cells were mock-infected or infected with BoHV-1, BoHV1-ΔU_L47 or BoHV1-U_L47R. At 24 h post infection the cells were trypsinized and processed to examine the mitochondrial membrane potential. Briefly, mitochondrial membrane potential dye, Near Infrared (NIR), was added to trypsinized cells followed by incubation for 15-30 min. After subsequent washes, the cells were resuspended in assay buffer and were analyzed by FACS. Fluorescence intensity was monitored with a flow cytometer equipped with a 635 nm red diode laser and a 661 nm filter.

7.3.9 RNA interference.

HeLa cells were seeded in 6-well plates one day before transfection. The cells were transfected with control and HSP60 siRNA (SMART-pool ON-TARGETplus HSP60 siRNA, Dharmacon, USA). At 24 h post transfection cells were transfected again with HSP60 siRNA together with the pFLAG-VP8. At 48 h post transfection of HSP60 siRNA and 24 h post transfection of pFLAG-VP8, the cell lysates were collected. The protein concentration was measured, and 50 μg of each protein sample were analyzed by Western blotting.

7.4 Results.

7.4.1 Identification of an *in vitro* interacting partner of BoHV-1 VP8.

BoHV-1 VP8 consists of 741 amino acids. Multiple sequence alignment and secondary structure prediction searches demonstrated that the C-terminal domain of VP8 is conserved between different herpesviruses and is rich in alpha-helical structures (405). SUMO-His-VP8 219-741 was purified by Nickel affinity chromatography (Figure 7.1A). As shown in Figure. 1A,

VP8 with an apparent molecular weight of 75 kDa co-purified with a 60 kDa bacterial protein. Some other minor contaminating proteins were also present with VP8 after the first round of purification. After cleavage of SUMO-His with Ac-TEV protease (Figure. 7.1A), we observed nearly complete digestion, which resulted in 52 kDa VP8 and 25 kDa SUMO-His (Figure. 7.1A). However, the bacterial protein of 60 kDa remained present even after an additional round of Nickel column affinity purification (Figure. 7.1A); Western blotting confirmed that the 60 kDa protein was not a truncated form of VP8 (Figure. 7.1B) as polyclonal VP8-specific antibody recognized the 52 kDa VP8, but not the 60 kDa protein. This suggested that VP8 specifically and strongly associated with a bacterial protein, which consistently co-purified with VP8.

The identity of the co-purified 60 kDa protein was determined by mass spectrometry of the protein bands excised from the gels before TEV digestion and after final purification (Figure. 7.1A); in both cases the mass spectrometry analysis showed high hit scores with *E. coli* GroEL (Figure. 7.1C). GroEL, a 60 kDa chaperonin protein, is required to maintain proper folding of many proteins. Alignment analysis (Figure. 7.1D) demonstrated considerable sequence similarity between bacterial GroEL and bovine and human HSP60. The bacterial GroEL lacks the N-terminal sequences that are responsible for targeting HSP60 to mitochondria in bovine and human cells. The fortuitous observation that recombinant VP8 strongly associated with bacterial GroEL led to the hypothesis that VP8 interacts with host HSP60 during viral infection contributing to virulence; the HSP60 may serve to stabilize VP8 or translocate the VP8 to the mitochondria leading to impairment of mitochondrial function.

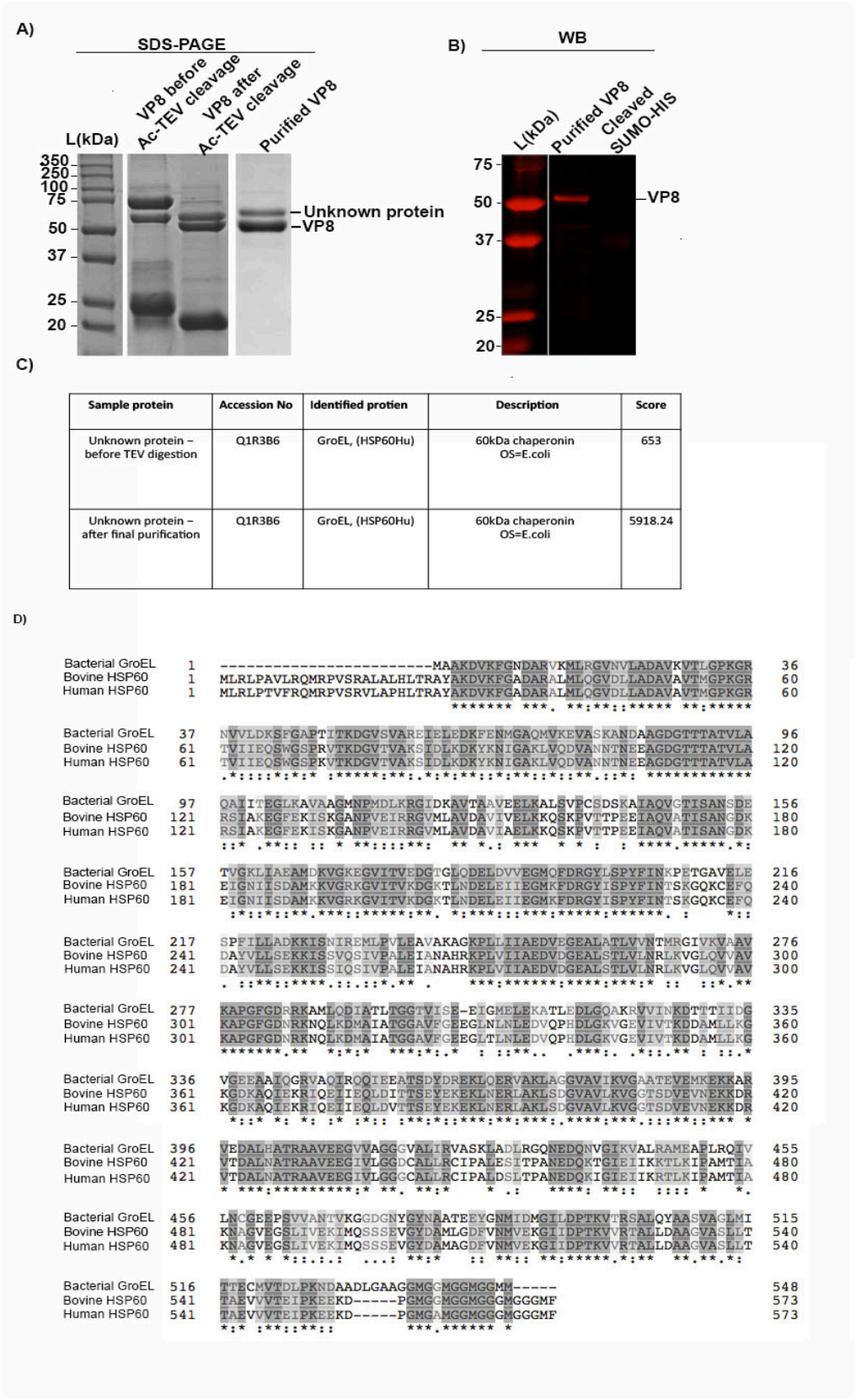

Sample protein	Accession No	Identified protien	Description	Score
Unknown protein – before TEV digestion	Q1R3B6	GroEL, (HSP60Hu)	60kDa chaperonin OS=E.coli	653
Unknown protein – after final purification	Q1R3B6	GroEL, (HSP60Hu)	60kDa chaperonin OS=E.coli	5918.24

Figure. 7.1. Identification of a bacterial protein co-purifying with recombinant VP8.

A) SUMO-His-VP8 219-741 was expressed in BL21 cells. Nickel column-purified VP8 was digested with Ac-TEV protease and was analyzed by SDS-PAGE followed by Commassie Brilliant Blue staining. B) Final purified VP8 and purified SUMO-His were analyzed by Western blotting. L represents protein molecular weight ladder in kDa. C) Purified VP8 was analyzed by SDS-PAGE followed by Coomassie Brilliant Blue staining. The upper 60kDa band (from Figure. 7.1A) was excised and analyzed by MALDI-TOF-MS. The identified peptides were used to search Uniprot data bases and the sum of the score of peptides is presented in the table. D) Sequence homology between bacterial GroEL and bovine and human HSP60 was analyzed by ClustalW. The gray boxes represent homologous sequences.

7.4.2 Interaction of BoHV-1 VP8 with HSP60 *in vivo*.

Interaction between cellular HSP60 and VP8 was determined by immunoprecipitation following transfection of HeLa cells with plasmid expressing FLAG-tagged VP8; cell lysates were collected at 24 h post transfection (Figure. 7.2A left panel). Anti-FLAG resin precipitated VP8 and EYFP from VP8- and EYFP-transfected cells, respectively, whereas HSP60 was precipitated with FLAG-VP8, but not with FLAG-EYFP. This shows that VP8 interacts with HSP60 in transfected cells. Similarly, mock-, pFLAG- and pFLAG-VP8-transfected cell lysates were analyzed by reverse immunoprecipitation with an anti-HSP60 antibody (Figure. 7.2B). HSP60-specific antibody precipitated HSP60 from mock-, FLAG- and FLAG-VP8-transfected cells. However, HSP60 precipitated only FLAG-VP8, and not FLAG-EYFP, confirming interaction of VP8 with HSP60.

To demonstrate interaction of VP8 with HSP60 in BoHV-1-infected cells, MDBK cells were mock-infected or infected with BoHV-1 or BoHV-1ΔU_L47. At 24 h post infection cell lysates were collected and incubated with a VP8-specific antibody (Figure. 7.2C). Anti-VP8 antibody precipitated VP8 from BoHV-1-infected cells, but not from mock- or BoHV-1ΔU_L47-infected cells. The precipitated VP8 pulled down HSP60 from BoHV-1-infected cells, but not from mock- or BoHV-1ΔU_L47-infected cells, thus demonstrating that VP8 interacts with HSP60 during BoHV-1 infection. This was validated by reverse precipitation of VP8; mock-, BoHV-1- and BoHV-1ΔU_L47-infected cell lysates were incubated with an anti-HSP60 antibody (Figure. 7.2D) followed by Protein G Sepharose. HSP60-specific antibody pulled down HSP60 from mock-, BoHV-1- and BoHV-1ΔU_L47-infected cell lysates, while VP8 was precipitated only from BoHV-1-infected cells. This confirms that HSP60 interacts with VP8 in BoHV-1-infected cells. Altogether, these experiments demonstrate interaction of VP8 with HSP60 in both VP8-transfected and BoHV-1-infected cells.

To determine the domain of VP8 interacting with HSP60, five different FLAG-tagged, N-terminally truncated VP8 versions (VP8 121-741, VP8 219-741, VP8 343-741, VP8 538-741, and VP8 632-741) were analyzed for precipitation of HSP60 (Figure. 7.2E). Anti-FLAG resin pulled down all N-terminally truncated VP8 versions and HSP60 indicating that a region between amino acids 632-741 of VP8 is sufficient for interaction with HSP60. In addition, cells were transfected with C-terminally truncated VP8 versions (VP8 1-120, VP8 1-258, VP8 1-482, VP8 1-631) and incubated with anti-FLAG resin. Only two C-terminally truncated VP8 versions (VP8

1-482 and VP8 1-631) precipitated HSP60. This experiment revealed that amino acids 259-482 of VP8 were sufficient to precipitate HSP60. Collectively, this suggests that regions within amino acids 259-482 and 632-741 of VP8 are involved in binding of VP8 to HSP60.

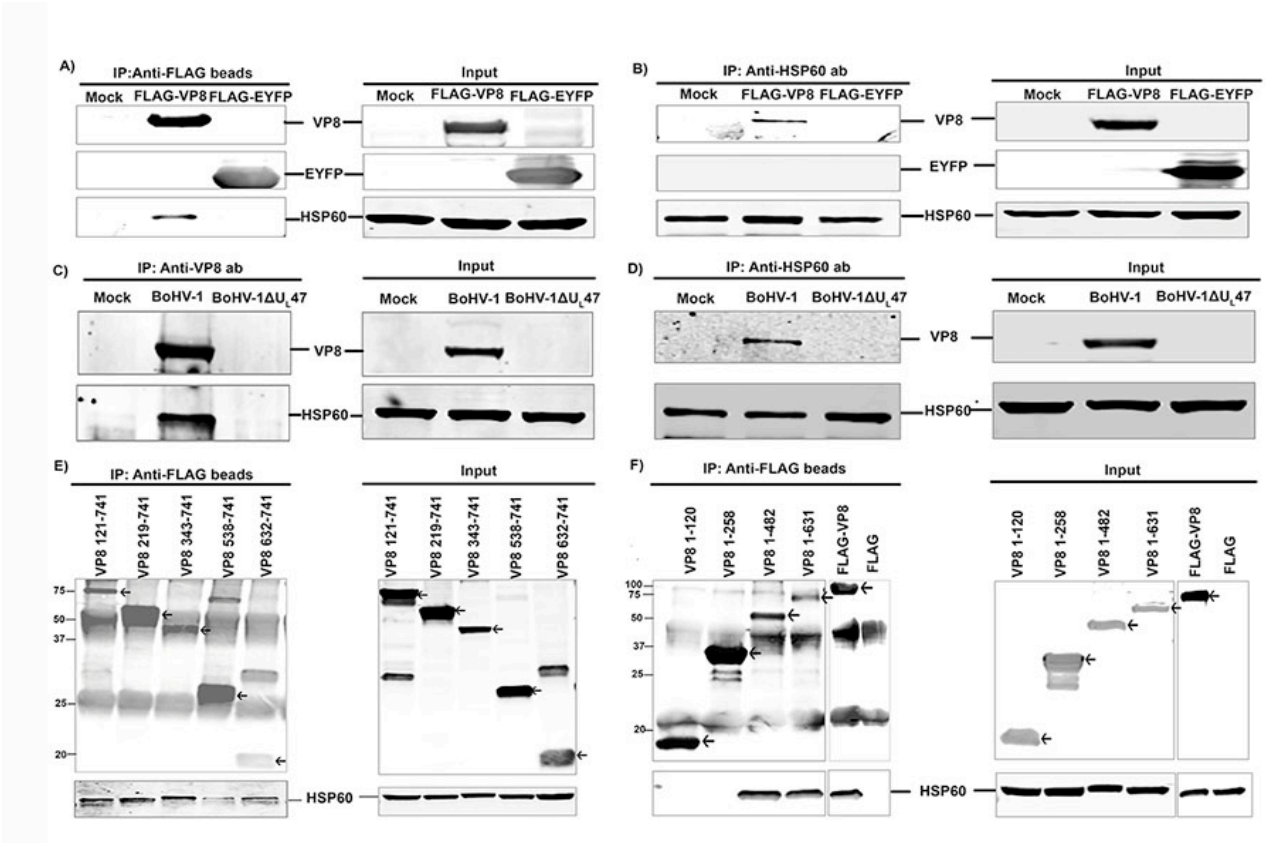

Figure. 7.2 Interaction of BoHV-1 VP8 with HSP60 in eukaryotic cells.

A) HeLa cells were mock-transfected or transfected with pFLAG-EYFP or pFLAG-VP8. Cell lysates were collected at 24 h post transfection and incubated with anti-FLAG beads. Precipitated proteins (left panel) and input lysates (right panel) were detected with anti-FLAG and anti-HSP60 antibodies. B) HeLa cells were mock-transfected or transfected with pFLAG-EYFP or pFLAG-VP8. Cell lysates were collected at 24 h post transfection and incubated with rabbit anti-HSP60 antibody, followed by with protein G Sepharose. The left panel represents precipitated proteins and the right panel represents input lysates. A) and B) precipitated proteins and input lysates were detected with anti-FLAG and anti-HSP60 antibodies. C) MDBK cells were mock-infected or infected with BoHV-1 or BoHV-1ΔU_L47 at an MOI of 3, and at 24 h post infection cell lysates were collected and incubated with mouse anti-VP8 antibody followed by protein G Sepharose. Precipitated proteins (left panel) and input lysates (right panel) were detected with anti-VP8 and anti-HSP60 antibodies. D) MDBK cells were mock-infected or infected with BoHV-1 or BoHV-1ΔU_L47 as described above. At 24 h post infection cell lysates were collected and incubated with anti-HSP60 antibody followed by protein G Sepharose. Precipitated proteins (left panel) and input lysates (right panel) were detected with anti-VP8 and anti-HSP60 antibodies. E) HeLa cells were mock-transfected or transfected with five N-terminally truncated VP8 versions. Cell lysates were collected at 24 h post transfection and incubated with anti-FLAG beads. Precipitated proteins were detected with anti-FLAG and anti-HSP60 antibodies. Left panel and right panels represent precipitated proteins and input lysates, respectively. F) HeLa cells were mock-transfected or transfected with pFLAG or pFLAG-VP8 or four different C-terminally truncated VP8 versions. Cell lysates were collected at 24 h post transfection and incubated with

anti-FLAG beads. Precipitated proteins were detected with anti-FLAG and anti-HSP60 antibodies. Left panel and right panels show precipitated proteins and input lysates, respectively.

7.4.3 HSP60 co-localizes with VP8 but does not alter VP8 expression.

Since VP8 interacts with HSP60 in mammalian cells, we investigated whether VP8 co-localized with HSP60. HeLa cells were mock-transfected or transfected with pFLAG-VP8 or pFLAG-VP8 219-741. At 24 h post transfection cells were incubated with anti-FLAG or anti-HSP60 antibodies. FLAG-VP8 219-741 contains the domains involved in binding to HSP60, but it lacks a nuclear localization signal. As demonstrated in Figure. 7.3A, VP8, as well as VP8 219-741 co-localized with HSP60. To demonstrate co-localization of HSP60 with VP8 in BoHV-1-infected cells, MDBK cells were mock-infected or infected with BoHV-1. At 14 h post infection the cells were incubated with anti-VP8 and anti-HSP60 antibodies. As indicated in Figure. 7.3B, some VP8 was also co-localized with HSP60 in BoHV-1-infected cells. These experiments demonstrate VP8 is partially co-localized with HSP60.

HSP60 is known to regulate the folding and maintain the stability of mitochondria-imported proteins (439). Since VP8 interacted and co-localized with HSP60, we investigated whether HSP60 was required for VP8 stability. HeLa cells were transfected with control or HSP60-specific siRNA, and 24 h later the cells were again transfected with HSP60-specific siRNA and with pFLAG-VP8. At 24 h after transfection with pFLAG-VP8 cell lysates were collected, and equal amounts of the cell lysates were analyzed by Western blotting. The HSP60 level was similar in mock- and control siRNA-transfected cells (Figure. 7.3C), but was substantially reduced in cells transfected with HSP60-specific siRNA. However, the level of VP8, as detected by Western blotting, was not notably altered by the silencing of HSP60 suggesting, that HSP60 does not play a major role in maintaining VP8 protein levels.

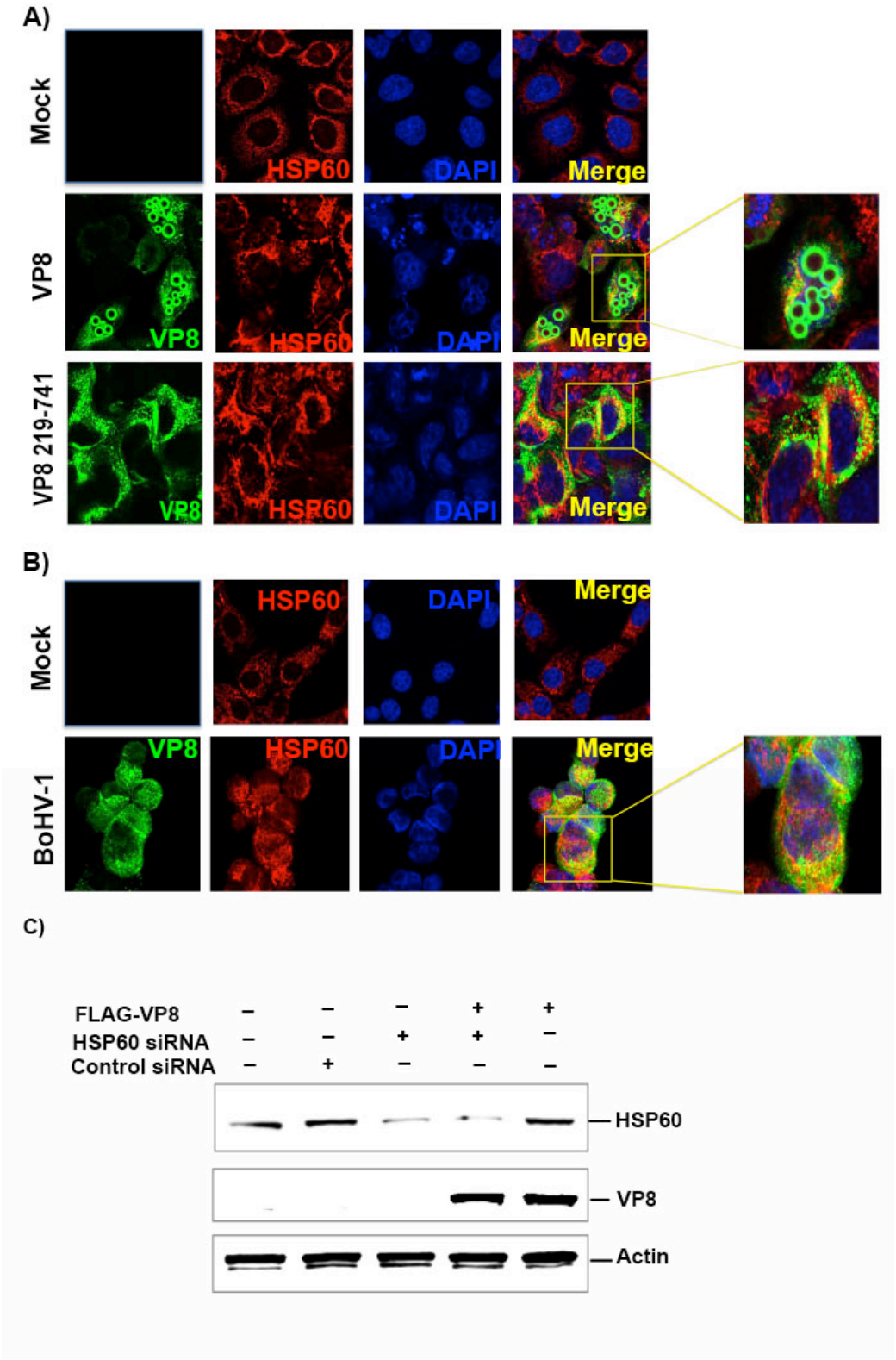

Figure. 7.3 HSP60 co-localizes with VP8, but does not alter VP8 expression.

A) HeLa cells were mock-transfected or transfected with pFALG-VP8 or pFLAG-VP8 219-741. At 24 h post transfection cells were incubated with mouse anti-FLAG and rabbit anti-HSP60 antibodies followed by incubation with Alexa Fluor 488-conjugated goat anti-mouse and 633-conjugated goat anti-rabbit IgG. Nuclei were identified with DAPI. Yellow boxes represent higher magnifications of the selected areas. B) MDBK cells were infected with BoHV-1 at a MOI of 3 for 14 h. The infected cells were incubated with monoclonal anti-VP8 and polyclonal anti-HSP60 antibodies followed by incubation with Alexa Fluor 488-conjugated goat anti-mouse and Alexa Fluor 633-conjugated goat anti-rabbit IgG. Nuclei were identified with DAPI. Yellow box represents higher magnifications of the selected area. C). HeLa cells were mock-transfected or transfected with control siRNA or with HSP60 siRNA for 24 h before transfecting again with control siRNA or with HSP60 siRNA together with FLAG-VP8 or with only FLAG-VP8. At 24 h post transfection cell lysates were collected, and 50 µg protein of each sample were analyzed by SDS-PAGE and Western blotting. HSP60, VP8 and actin were detected with anti-HSP60, anti-FLAG and anti-actin antibodies, respectively.

7.4.4 Localization of HSP60 and VP8 to mitochondria.

HSP60 is a mitochondrial protein and contains a mitochondrial localization signal (440). We confirmed the localization of HSP60 to the mitochondria by incubating HeLa cells with anti-HSP60 antibody and mito-tracker red dye (Figure. 7.4A). Since VP8 interacts with HSP60, and HSP60 localizes to mitochondria, we anticipated that VP8 might be localized with the mitochondria. HeLa cells were mock-transfected or transfected with pFLAG-VP8 or pFLAG-VP8-219-741. At 24 h post transfection the cells were incubated with anti-FLAG antibody and with mito-tracker red dye. The full-length VP8 and VP8 219-741 were both partially localized to mitochondria (Figure. 7.4B), which indicates that like HSP60, VP8 is targeted to the mitochondria and that the C-terminal domain of VP8, VP8 219-741, mediates the mitochondrial localization of VP8. To investigate localization of VP8 to the mitochondria during BoHV-1 infection, MDBK cells were mock-infected or infected with BoHV-1. At 14 h post infection cells were incubated with anti-VP8 antibody and mito-tracker red dye. As shown in Figure. 7.4C, VP8 partially localized to mitochondria in BoHV-1-infected cells. These experiments confirm partial localization of VP8 to mitochondria in both VP8-transfected and BoHV-1-infected cells.

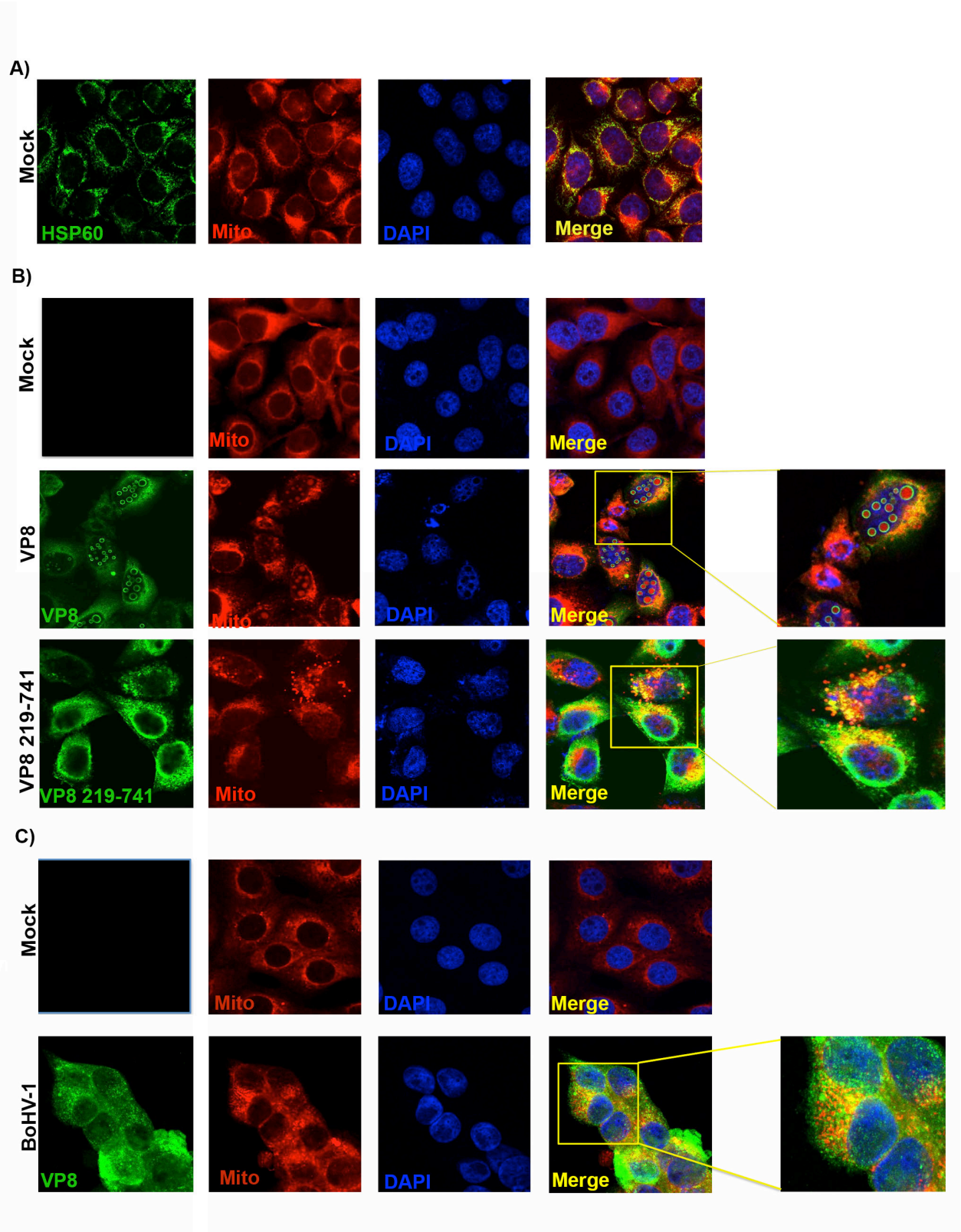

Figure. 7.4 Localization of HSP60 and VP8 to mitochondria.

A) HeLa cells were incubated with polyclonal anti-HSP60 antibody followed by Alexa Fluor 488-conjugated goat anti-mouse IgG. Mitochondria were identified with mitotracker red dye followed by nuclear staining with DAPI. B) HeLa cells were mock-transfected or transfected with pFLAG-VP8 or pFLAG-VP8 219-741. At 14 h post transfection cells were incubated with monoclonal anti-FLAG antibody followed by Alexa Fluor 488-conjugated goat anti-mouse IgG. Mito-tracker red dye was used to identify mitochondria. Nuclei were incubated with DAPI. C) MDBK cells were infected with BoHV-1 at a MOI of 3 for 14 h. The infected cells were incubated with a monoclonal anti-VP8 antibody followed by Alexa Fluor 488-conjugated goat anti-mouse IgG. Mitochondria were incubated with mito-tracker red dye. DAPI was used to identify the nucleus. Yellow boxes represent higher magnifications of selected areas.

7.4.5 Localization of VP8 to mitochondria at different time points during BoHV-1 infection.

Since VP8 localized to mitochondria in both VP8-transfected and BoHV-1-infected cells, it was of interest to investigate at which time point this occurs during infection. MDBK cells were mock-infected or infected with BoHV-1, and at different times post infection the cells were fixed and incubated with an anti-VP8 antibody and mito-tracker red dye. As shown in Figure. 7.5, VP8 was cytoplasmic at 2 h post infection, as previously demonstrated (187, 405), and some VP8 was localized to the mitochondria at this time. As the infection progressed, at 4 h post infection VP8 was observed in the nucleus, the peri-nuclear region, and the cytoplasm. Some of the peri-nuclear VP8 co-localized with the mitochondria. At 6 h post infection most of VP8 was nuclear, but some peri-nuclear VP8 located to the mitochondria. Later during infection, VP8 is exported to the cytoplasm. At 14 h post infection, VP8 was localized in the cytoplasm and some VP8 was observed in the mitochondria. This experiment illustrates that VP8 partially localized to mitochondria at different time points throughout BoHV-1 infection.

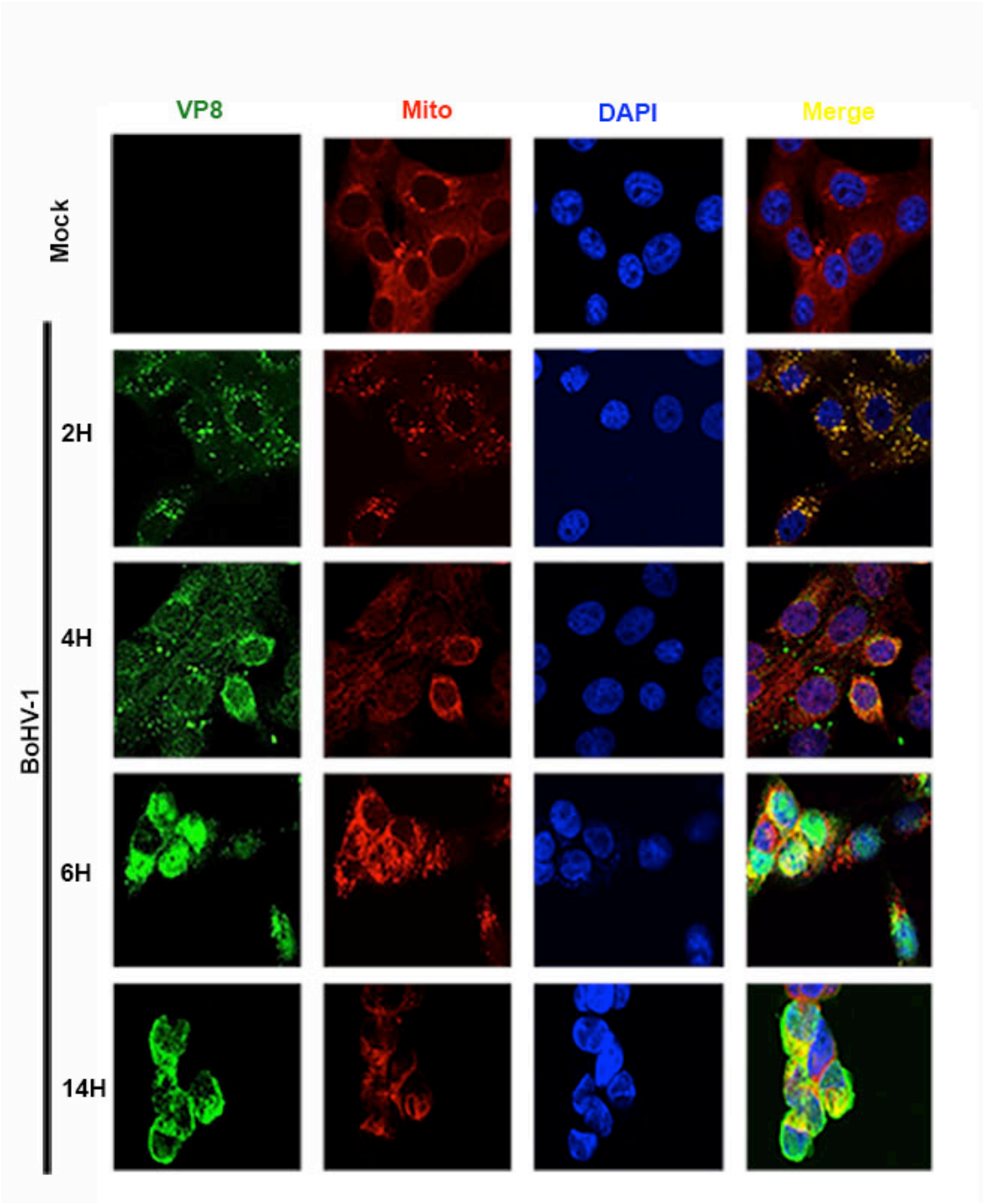

Figure. 7.5 Localization of VP8 to mitochondria during BoHV-1 infection at different time points.

MDBK cells were mock-infected or infected with BoHV-1 at a MOI of 3. Cells were fixed at 2, 4, 6 h and 14 h, and then incubated with a monoclonal anti-VP8 antibody followed by Alexa Flour 488-conjugated goat anti-mouse IgG. Mitochondria were identified with mito-tracker red dye. DAPI was used to identify the nucleus.

7.4.6 Effect of VP8 on mitochondrial function.

During HSV-1 and BoHV-1 infection mitochondrial dysfunction is caused by the reduction of mitochondrial membrane potential (363, 432). Since VP8 interacted with HSP60 and localized to the mitochondria, we examined whether VP8 causes mitochondrial dysfunction. To detect the mitochondrial membrane potential in VP8-transfected cells in the absence of any other viral protein, HeLa cells were mock-transfected or transfected with pFLAG, pFLAG-VP8 or pFLAG-VP8 219-741. At 48 h post transfection the MMP was determined with the NIR MMP dye and was analyzed by FACS (Figure. 7.6A). The MMP was reduced from approximately 98% in mock- or pFLAG- transfected cells to about 78% in pFLAG-VP8 or pFLAG-VP8 219-741-transfected cells.

To determine the involvement of VP8 and HSP60 in reduction of the MMP, we analyzed the cellular MMP in the presence of exogenous HSP60 and VP8. HeLa cells were mock-transfected or transfected with pFLAG, pFLAG-VP8, pFLAG-VP8 219-741 or pFLAG-VP8 1-219 (the domain that does not interact with HSP60) together with empty vector or HSP60 (Figure. 7.6B). At 48 h post transfection, cells were incubated with NIR MMP dye, and the MMP was determined by FACS. As demonstrated in Figure. 7.6B, transfection of cells with empty vector together with pFLAG-VP8 or pFLAG-VP8 219-741 significantly reduced the MMP (~ 68-71%) when compared to mock transfection or transfection with pFLAG together with empty vector (~ 95%). However, in the cells co-transfected with pFLAG-VP8 1-219 and empty vector the MMP was maintained at ~ 91%. In addition, when cells were co-transfected with pFLAG-VP8 or pFLAG-VP8 219-741 and HSP60, the MMP significantly declined (~ 49-53%) when compared to cells co-transfected with or pFLAG-VP8 1-219 and HSP60 (~ 88%). Introduction of HSP60 and pFLAG did not reduce the MMP. This experiment demonstrates that overexpression of VP8 and HSP60 contributes to the reduction of MMP, and that VP8 219-741 causes reduction of MMP at a similar level as VP8.

Since we observed loss of MMP in VP8-transfected cells, we determined the effect of VP8 on MMP in BoHV-1-infected cells. For this experiment, MDBK cells were mock-infected or infected with BoHV-1, BoHV-1ΔU_L47 or BoHV-1U_L47R. At 24 h post infection the cells were processed for MMP detection, and were evaluated by FACS. As indicated in Figure. 7.6C, in mock- and BoHV-1ΔU_L47-infected cells the MMP was maintained in approximately 90% of the cells, whereas the MMP was retained in approximately 70% of the BoHV-1 and BoHV-

1U_L47R-infected cells. Since the BoHV-1ΔU_L47 infection retained MMP in a higher percentage of cells compared to BoHV-1- and BoHV-1U_L47R-infection, VP8 can reduce the MMP during BoHV-1 infection.

VP8 was localized to mitochondria early post infection. To determine whether the localization of VP8 to mitochondria at these early time points reduces the MMP, we determined the MMP at 2 h and 4 h post infection (Figure. 7.6D). MDBK cells were mock-infected or infected with BoHV-1, BoHV-1ΔU_L47 or BoHV-1U_L47R. The cells were collected at 2 h and 4 h post infection and then incubated with NIR MMP dye. The cellular MMP was analyzed by FACS. As indicated in Figure. 7.6D, the MMP was maintained at these time points of the infection. This experiment demonstrates that the localization of VP8 to mitochondria at early infection does not cause reduction of MMP.

Mitochondria are associated with the energy metabolism by generation of ATP. Proper mitochondrial membrane potential maintains maximal ATP production. Many viruses modulate mitochondrial function for infection. HSV-1, as well as BoHV-1, reduce ATP production during productive infection (363, 432). Since we observed reduction of MMP in the presence of VP8, to further confirm mitochondrial dysfunction by VP8, we evaluated the total cellular ATP level in VP8-transfected cells HeLa cells were mock-transfected or transfected with pFLAG, pFLAG-VP8, or pFLAG-VP8 219-741. At 48 h post transfection the total ATP concentration was measured. As demonstrated in Figure. 7.7A, the total ATP concentration was significantly decreased in VP8- and VP8 (VP8 219-741)-transfected cells when compared to mock- and FLAG-transfected cells. Thus, this experiment suggests that the presence of VP8 reduced the total ATP level in transfected cells. To determine the effect of VP8 on the total ATP level during BoHV-1 infection, MDBK cells were mock-infected or infected with BoHV-1, BoHV-1ΔU_L47 or BoHV-1U_L47R. At 24 h post infection, the cellular ATP concentration was evaluated (Figure. 7.7B). The amount of total ATP was reduced significantly in cells that were infected with BoHV-1 or BoHV-1U_L47R. However, in BoHV-1ΔU_L47-infected cells the ATP concentration was not affected. Hence, VP8 contributes to the reduction of ATP levels during BoHV-1 infection.

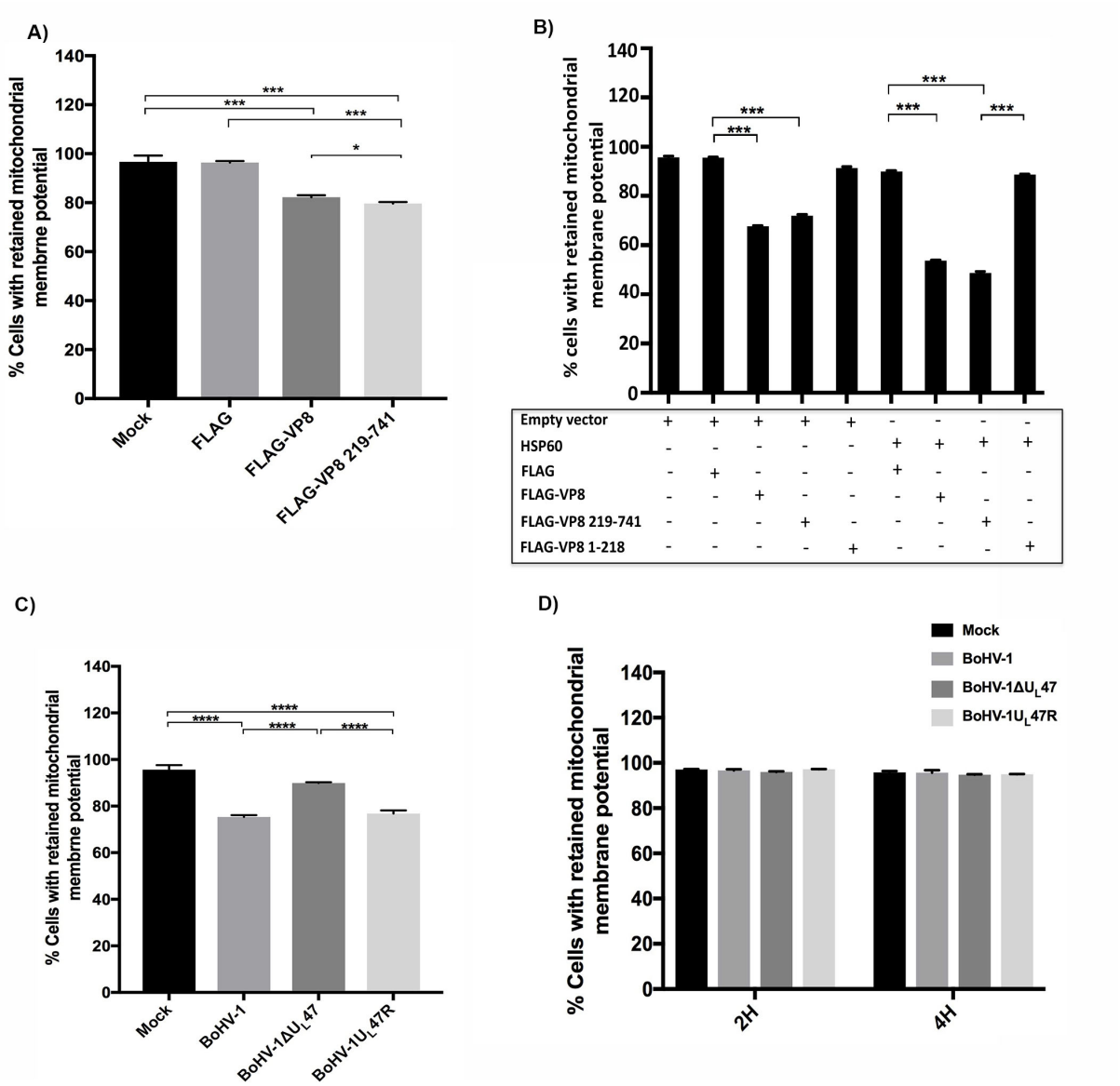

Figure. 7.6 Effect of VP8 on mitochondrial membrane potential.

A) HeLa cells were mock transfected or transfected with pFLAG, pFLAG-EYFP, pFLAG-VP8 or pFLAG-VP8 219-741. At 48 h post transfection cells were trypsinized and incubated with NIR MMP dye. The cells were analyzed by FACS. B) Hela cells were transfected with empty vector together with pFLAG, pFLAG-VP8, pFLAG-VP8 219-741, pFLAG-VP8 1-218, or pHSP60, or transfected with pHSP60 together with pFLAG-VP8, pFLAG-VP8 219-741 or pFLAG-VP8 1-218. At 48 h post transfection the cells were trypsinized and then incubated with NIR MMP dye. The cells were analyzed by FACS. C) MDBK cells were mock-infected or infected with BoHV-1, BoHV-1ΔU_L47 or BoHV-1U_L47R at a MOI of 3 for 24 h. The MMP was detected with the NIR dye and the cells were analyzed by FACS. D) MDBK cells were mock-infected or infected with BoHV-1 at a MOI of 3. At 2 h and 4 h post infection, the cells were trypsinized and then incubated with MMP dye. The cells were analyzed by FACS. Statistical significance is indicated by asterisks (****, $P < 0.0001$).

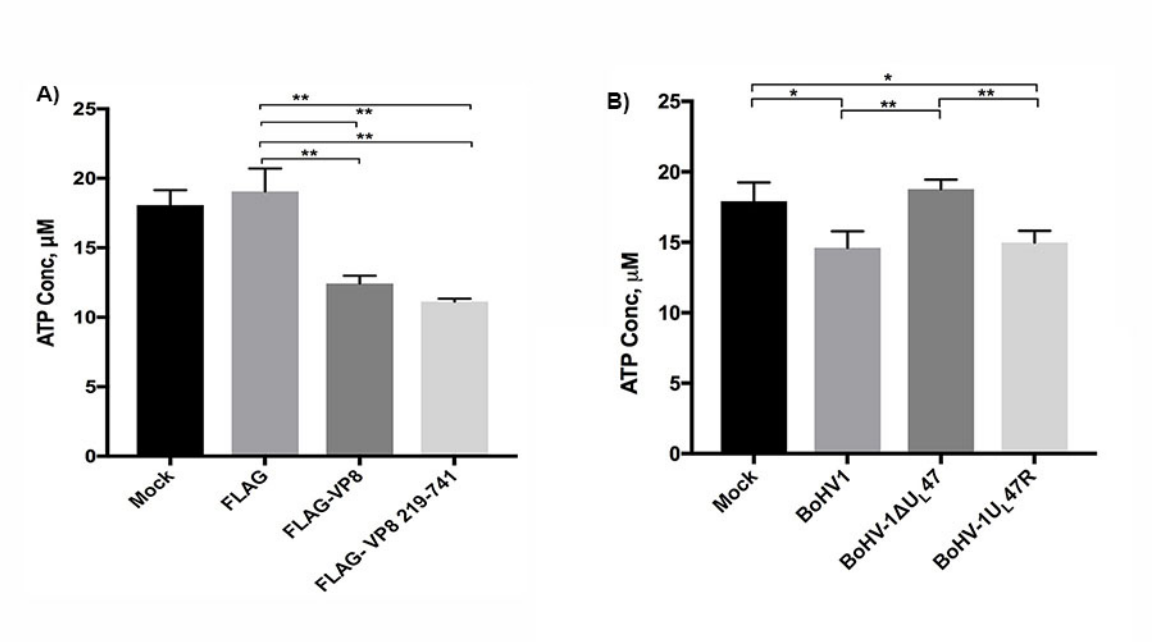

Figure. 7.7. Reduction of ATP production by BoHV-1 VP8.

A) HeLa cells were mock-transfected or transfected with pFLAG, pFLAG-EYFP, pFLAG-VP8 or pFLAG-VP8 219-741. The ATP concentration was determined at 48 h post transfection. B) MDBK cells were mock-infected or infected with BoHV-1, BoHV1-ΔU_L47 or BoHV1-U_L47R at an MOI of 3. ATP concentrations were determined 24 h post infection. Statistical significance is indicated by asterisks (*, $P < 0.05$; ***, $P < 0.01$).

7.5 Discussion.

To obtain purified protein for structural characterization purposes, we expressed VP8 in *E.coli*. Since the C-terminal domain of VP8 is enriched with alpha-helices (405), we expressed this C-terminal VP8 (amino acids 219-741) in *E. coli.* The addition of a SUMO tag, which often enhances production and solubility of recombinant proteins, permitted substantial expression of soluble VP8 in *E. coli*. However, the recombinant VP8 consistently co-purified with a strongly associated bacterial protein, which was identified by mass spectrometry as GroEL protein, which shows substantial homology with mammalian HSP60, a mitochondrial chaperone protein. VP8 was subsequently shown to interact with mammalian HSP60 in eukaryotic cells both after transfection with VP8-expressing plasmids and infection with BoHV-1, to further confirm mitochondrial dysfunction by VP8-1virus. Domains in the C-terminal region of VP8, amino acids 259-482 and 632-741, were identified to be involved in the binding of VP8 with HSP60. Like HSP60, VP8 localized to the mitochondria. The localization of VP8 to the mitochondria led to mitochondrial dysfunction as determined by the reduction of mitochondrial membrane potential and ATP levels.

MASCOT analysis of MALDI-TOF-MS revealed that bacterial GroEL was tightly associated with VP8 with a high score. GroEL is a homolog of mammalian HSP60. Among the three structural domains of GroEL or HSP60, apical, intermediate and equatorial, the equatorial domain contains the most α-helical structures and facilitates interactions with other proteins (441). BoHV-1 VP8 might bind to this equatorial domain of HSP60 in a similar manner as other substrates of HSP60. GroEL substrates usually contain two or more domains with α-helices or β-sheets (442). According to the predicted secondary structure, the VP8 C-terminal domain is enriched with α-helical structures (405). Interestingly, analysis of VP8 showed that sequences in its C-terminal domain, amino acids 259-482 and 632-741, were involved in interaction of VP8 and HSP60. Hence, the presence of α-helices at the C-terminus of VP8 might facilitate association of HSP60 and VP8. As HSP60 is a chaperone protein that promotes proper protein folding and stability (439), we speculated that HSP60 might promote VP8 stability. However, the knock down of HSP60 by using HSP60-specific siRNA, did not alter the VP8 levels suggesting that HSP60 does not play a major role in maintaining the level of VP8 expression, but may serve to guide VP8 to mitochondria or VP8 moves to the mitochondria to interact with HSP60 and thus disturb mitochondrial functions.

HSP60 is a predominantly mitochondrial protein. The 26 amino acids at the N-terminus of HSP60 drive this protein to the mitochondria (440). Mitochondria are vital organelles to regulate cellular functions. Targeting mitochondria is a widely known strategy that viruses use for their survival, replication, and escape from the cells. For instance, hepatitis C (HCV) proteins localize to mitochondria where their function is impaired through reduction in MMP and increase of reactive oxidative stress (ROS) during productive infection (443). Similarly, HIV Vpr is targeted to mitochondria and facilitates reduction of MMP (444). Other viral proteins, such as hepatitis B virus X (HBx) protein, interact with HSP60 as well as with mitochondria (445), cause mitochondrial aggregation and reduce mitochondrial membrane potential (446). HBx-mediated cell death through association with HSP60 was also observed (445). Moreover, hepatitis C virus (HCV) protein also associates with mitochondria to promote the reduction of MMP during productive infection (443).

During BoHV-1 infection, VP8 was detected in the mitochondria at 2 h and continued to be localized to the mitochondria till 14 h post infection. HSV-1 tegument proteins, U_L41 and U_L46, are associated with mitochondria, and the authors suggested that these tegument proteins migrate to the peri-nuclear region with mitochondria (432). In the present study, we demonstrated that VP8 reduces MMP and ATP concentration. This was mediated by the full-length VP8, or a C-terminal domain containing HSP60 binding sites. HSP60 maintains MMP, since down-regulation of HSP60 reduces cellular MMP (447). Thus, the interaction with HSP60 and VP8 in the mitochondria might facilitate down-regulation of the function of HSP60 in maintaining MMP and subsequently reduction of MMP. Proper maintenance of MMP is associated with a normal level of ATP production. Any changes in the MMP level reduces ATP production (448). In agreement with the fact that VP8 expression decreased cellular MMP, a reduction in the ATP production was also observed in presence of VP8. Additionally, we observed that during BoHV-1 infection, VP8 reduced MMP and ATP concentrations, whereas BoHV-1ΔU_L47 did not influence MMP and the ATP levels. These observations suggest a role of VP8 in perturbing mitochondrial function during infection by reducing mitochondrial membrane potential and ATP levels. In agreement with these results, BoHV-1 infection is known to induce mitochondrial dysfunction through reducing MMP, increasing oxidative stress and reducing ATP levels (363), which can be (partially) ascribed to VP8. As mentioned above, different viral proteins localize to

mitochondria to deregulate mitochondrial functions. Therefore, it is plausible that BoHV-1 VP8 targets mitochondria to interfere with mitochondrial functions.

In conclusion, we report a new role for the multifunctional VP8 of BoHV-1. VP8 interacts with HSP60, which may facilitate translocation of VP8 to mitochondria. In addition, or alternatively, the interaction of HSP60 with VP8 may prevent it from maintaining the MMP which results in reduce ATP production and mitochondrial dysfunction during BoHV-1 infection.

7.6 Acknowledgements.

We acknowledge Dr. Ravendra Garg for his technical assistance in FACS reading. We also acknowledge Scott Gradia for the pET His6 Sumo TEV LIC cloning vector (Addgene plasmid # 29659). The grant 90887-2010 RGPIN from the Natural Sciences and Engineering Research Council of Canada supported this research. SA was partially supported by a Canadian Institutes of Health Research Training Grant in Health Research Using Synchrotron Techniques (CIHR-THRUST). This is VIDO manuscript number 847.

CHAPTER 8

GENERAL CONCLUSIONS AND DISCUSSION

8.1 General conclusions.

- After fusion of the BoHV-1 envelope with the host cell membrane, VP8 from the tegument region of incoming virions are released into the host cytoplasm. At 2 h post infection, VP8 is observed in the cytoplasm. VP8 then interacts with cellular STAT1 in the cytoplasm using its two domains amino acids 259-482 and 632-741.

- The interaction of VP8 with STAT1 does not interfere with phosphorylation or degradation of STAT1. However, this interaction prevents nuclear accumulation of STAT1.

- Since VP8 inhibited IFN expression, the inhibition of STAT1 nuclear accumulation by VP8 is likely associated with the inhibition of STAT1-mediated transcription of interferon-inducible genes.

- With the progression of BoHV-1 infection, the DDR pathway gets activated. We demonstrated that VP8 interacts with the DDR pathway proteins, ATM and NBS1.

- The interaction of VP8 with ATM does not interfere with ATM phosphorylation. However, the interaction of VP8 with NBS1 inhibits NBS1 phosphorylation, and NBS1-depended SMC1 phosphorylation.

- As a result, DNA repair is inhibited in the presence of VP8. This inhibition prevents DNA repair, which eventually leads to the activation of apoptotic pathway. Thus, VP8 increases DNA damage-induced apoptosis through caspase-3 activation.

- During infection, some VP8 interacts with mitochondrial chaperonin protein HSP60 and localizes to mitochondria.

- The mitochondrial localization of VP8 induces mitochondrial dysfunction by reducing mitochondrial membrane potential or by decreasing ATP production.

8.2 General discussion.

Type I IFN response is one of the host defense mechanisms against virus infection. Virus infection triggers activation of transcription factors, IRFs, leading to transcriptional activation of IFN genes. However, IFN signaling is modulated by viruses to establish infection. During virus infection, the cellular antiviral state is established through type I IFN signaling. Nonetheless, viruses counteract these anti-viral responses through multiple mechanisms, such as modulation of IFN response or alteration of the DDR pathway. Here we observed that like other viruses, BoHV-1 infection down-regulates IFN-β signaling. Inhibition of IFN-β signaling is associated with the interaction of VP8 and STAT1.

In the first section, we demonstrated that during BoHV-1 infection, IFN-β signaling was significantly reduced in the presence of VP8. Conversely, in BoHV-1ΔU_L47 infected cells the luciferase signal indicating IFN production was increased. Even though incomplete recovery was observed in BoHV-1ΔU_L47-infected cells, the induction of IFN-β signaling was significantly higher in comparison to BoHV-1-infected cells. The residual luciferase activity in BoHV-1ΔU_L47-infected cells could be attributed to the presence of bICP0, which is involved in down-regulation of IFN-β signaling (207, 379). To preclude the involvement of bICP0 in the regulation of IFN-β signaling, the transcription inhibitor, ActD was used to treat the cells. As expected, treatment of cells with ActD mediated complete recovery of luciferase signaling in BoHV-1 Δ U_L47-infected cells, whereas inhibition of luciferase signaling was observed in BoHV-1- and BoHV-1U_L47R-infected cells. Hence, we speculate that in the absence of newly synthesized protein, incoming virion VP8 functions to down-regulate IFN-β signaling. A similar function of the HSV-1 U_L47 gene product, VP13/14, is not known. Although BoHV-1 VP8 is a homologue of HSV-1 VP13/14, there are some functional differences between these two protein functions. For instance, HSV-1 VP13/14 interacts with US3, U_L13 and U_L14, which are crucial for nuclear egress (161). In contrast, *U_L47*-deleted BoHV-1 was not defective in nuclear egress (179). Moreover, HSV-1 VP13/14 forms a complex with VP16 or alpha-transducing factor (α-tTIF), and VP13/14-deleted HSV-1 was unable to induce immediate early promoter-mediated reporter gene expression (96, 383). However, BoHV-1 VP8 is did not have such function, as mRNA transcript

of bICP4 was detected at a similar level in BoHV-1-, BoHV-1ΔU_L47- and BoHV-1U_L47R-infected cells (179).

Next we demonstrated the mechanism by which VP8 down-regulates IFN-β signaling. Binding of IFN-α/β to its corresponding receptors, IFNAR1 and IFNAR2 subunits activates the JAK/STAT signaling pathway. This binding initiates cascades of signaling responses to phosphorylate STAT1 and STAT2. A STAT1/2 homodimer then translocates to the nucleus to form a heterotrimeric complex. The heterotrimeric complex associates with the interferon response element to stimulate IFN production (373). With the entrance of BoHV-1 into host cells, the viral tegument proteins including VP8 and capsid are dissociated in the cytoplasm (66). This dissociation brings VP8 in contact with the host cytoplasmic proteins. We observed that VP8 interacted with cellular STAT1 in both VP8-transfected and BoHV-1-infected cells. VP8 interacted with STAT1 using two domains, amino acids 259-482 and 632-686. The predicted secondary structure of VP8 revealed that the VP8 C-terminal domain is enriched with alpha-helical structures. The alpha-helical structures of a protein are associated with protein-protein interactions (384). Hence, the domain of VP8 containing alpha-helices facilitates VP8 and STAT interaction. Association of VP8 with STAT1 did not interfere with ubiquitination or degradation of STAT1. However, the interaction of VP8 with STAT1 prevented nuclear translocation of STAT1 in BoHV-1- and BoHV-1U_L47R-infected cells, whereas STAT1 was localized to the nucleus in BoHV-1ΔU_L47-infected cells. Importantly, the inhibition of STAT1 translocation is mediated through the interacting domains of VP8, amino acids 259-482 and 632-.686. With regards to cytoplasmic retention of STAT1 by VP8, subcellular fractionation of BoHV-1-infected cells at different time points also supported that VP8 and STAT1 are localized in the cytoplasm.

Viruses adapt multiple strategies to antagonize type I IFN signaling through interactions with the cellular proteins, STAT1 or STAT2. For instance, simian virus 5 (SV5) targets STAT1 for ubiquitination and degradation to inhibit IFN signaling (386). Conversely, mumps virus V protein exhibits its antiviral activity through STAT1 degradation, as well as through prevention of STAT1 translocation into the nucleus (378). Consequently, mumps virus V protein impedes IFN-β signaling. Similarly, VP8 alters the translocation of STAT1 to interfere with the IFN-β signaling. However, the mechanism whereby VP8 retains STAT1 remains unclear. STAT1 contains a DNA binding domain and a coiled-coil domain. Previously, it was shown that the mutation or alteration in the integrity of the DNA binding domain or coiled-coil domain was

associated with the retention of STAT1 in the cytoplasm (393). Moreover, preventing binding of STAT1 NLS with importin-α disrupts STAT1 accumulation into the nucleus (392). Similarly, the rabies virus P protein binds with the coiled-coil or DNA-binding domain and subsequently, prohibits STAT1 translocation into the nucleus. Conceivably, binding of VP8 with STAT1 either interferes with the importin-α and STAT1 binding or with the coiled-coil or DNA binding domain function of STAT1. Thus, VP8 might alter the nuclear transport mechanism of STAT1 to interfere with STAT1 translocation. In macrophages and dendritic cells, activation of the JAK/STAT signaling pathway prevents HSV-1 replication. However, blocking this pathway supports HSV-1 replication (449). Thus, impeding IFN signaling promotes HSV-1 replication (449). Likewise, since BoHV-1ΔU_L47 is defective in replication in cell culture and unable to replicate in cattle (179), VP8 promotes BoHV-1 replication by preventing IFN signaling. VP8 was observed in the cytoplasm as early as 2 h post infection and prevented nuclear accumulation of STAT1. Thus, the prevention of nuclear import of STAT1 by VP8 at early infection counteracted the establishment of the antiviral state to promote BoHV-1 replication. This is in agreement with the fact that a VP8-deleted mutant is avirulent *in vivo* (179).

Another potential function of VP8 that we determined is the interference in the DDR pathway during BoHV-1 infection. VP8 interacted with DDR proteins, ATM and NBS1. ATM is the key player in the DDR pathway. Upon detection of the presence of DNA damage, ATM is activated by phosphorylation at serine-1981. The activated ATM, in turn, triggers phosphorylation of the DDR downstream targets, such as NBS1 or SMC1 to coordinate DNA repair, cell cycle arrest, or apoptosis (265). We observed that the interaction VP8 with ATM did not interfere with ATM phosphorylation. However, the interaction of VP8 with NBS1 blocked NBS1 phosphorylation. SMC1 is another downstream target of ATM, and also gets phosphorylated by ATM. However, the phosphorylation of SMC1 is dependent on NBS1 phosphorylation (398). As VP8 impeded NBS1 phosphorylation, the SMC1 phosphorylation was also inhibited by VP8. Since VP8 immunoprecipitates both ATM and NBS1 as a complex, VP8 might block ATM and NBS1 interaction to inhibit the phosphorylation of NBS1 and thereby, prevent SMC1 phosphorylation. Inhibition of NBS1 and SMC1 phosphorylation was observed in both BoHV-1- and BoHV-1U_L47R-infected cells but not in BoHV-1ΔU_L47-infected cells, clearly indicating the involvement of VP8 in the prohibition of NBS1 and SMC1 phosphorylation. At the beginning of infection, at 2 h post infection, NBS1 and SMC1 were phosphorylated. At this pint

VP8 was present in the cytoplasm. VP8 contains a NLS, with the progression of infection VP8 was localized to the nucleus. VP8 was observed in the nucleus at 4 h post infection. Researchers reported that with the incoming HSV-1 virus genome, the DDR pathway gets activated (271). Phosphorylation of NBS1 or SMC1 at early infection can be the result of incoming virus particles. However, at 4 h post infection when VP8 was localized to the nucleus, no phosphorylation of NBS1 or SMC1 was observed, indicating an involvement of nuclear VP8 in the inhibition of NBS1 and SMC1 phosphorylation. Some viruses evolved unique strategies to counteract host cell responses, while others hijack and manipulate DDR pathway for viral propagation and replication. HSV-1 infection activates the ATM pathway (274), which is different from BoHV-1 infection. However, the ATR pathway, another major DDR signaling component is inhibited by HSV-1 infection (281). Besides, murine gamma herpesvirus 68 (γHV68) M2 protein interacts with ATM. Although this interaction triggers ATM activation, it blocks ATM downstream signaling (403). Adenovirus also deregulates the DDR machinery by reorganizing the MRN complex to favor viral genome processing (420). Hence, different viral proteins manipulate distinct or overlapping mechanisms for the accomplishment of virus propagation.

SMC1 phosphorylation contributes to S-phase checkpoint activation to facilitate DNA repair (416). Since VP8 prevented SMC1 phosphorylation, UV-induced damaged DNA repair was inhibited by VP8. Similarly, homologous recombination-mediated DNA repair was abrogated during HSV-1 infection (273). Since reduced cell viability is associated with inhibition of SMC1 phosphorylation and DNA repair (416), VP8-induced apoptotic cell death was observed in VP8-expressing cells. Moreover, UV- or etoposide-induced DNA damage increased DNA damage-induced apoptosis in VP8-expressing cells. Consequently, the BoHV-1-infected cells were more apoptotic than BoHV-1ΔU_L47-infected cells. Researchers demonstrated that UV-induced DNA damage triggered the intrinsic apoptosis pathway through activation of caspase 3 in repair-deficient cells (418). Likewise, VP8 prevented DNA repair and triggered cleavage of procaspase 3 and activation of caspase 3 to induce apoptosis. Moreover, multiple researchers demonstrated that BoHV-1 induced apoptosis through caspase 3 activation (355, 359, 362), supporting the contention that VP8 triggers apoptosis through caspase 3 activation. These findings are in line with increased apoptosis in BoHV-1-infected cells, where cells are exposed to a large amount of replicating viral DNA or abnormal DNA structures. While different viruses

express some anti-apoptotic proteins to promote viral pathogenesis, some viruses encode pro-apoptotic proteins to manipulate the cellular machinery for efficient virus production. For instance, human immune deficiency virus (HIV) stimulates pro-apoptotic gene expression for maximal virus production (424), and influenza virus triggers pro-apoptotic factors for efficient virus replication. Moreover, HSV-1 ICP0 induces apoptosis during infection (422, 423). Furthermore, BoHV-1 is known to induce apoptosis through multiple protein functions (355, 359, 364). Because of the fact that BoHV-1ΔU_L47 infection demonstrated 1000-fold reduced extracellular infectious virus particles compared to BoHV-1 infection, VP8 might contribute to the release of virus particles through induction of apoptosis. The purpose of reshaping the DDR pathway by VP8 might be to block ATM signaling and thus, circumvent host surveillance. For instance, during HSV-1 infection the ATR pathway is impaired in order to facilitate recombination-dependent repair and to promote virus replication (280, 282). Eventually, the inhibition of DDR by VP8 triggers apoptosis possibly to expedite the release of infectious virions into the extracellular environment. Although BoHV-1 is released into the extracellular environment by exocytosis (450), in BoHV-1ΔU_L47 infected cells the extracellular virus titer was reduced to approximately 1000-fold (179). This suggests that the induction of apoptosis by VP8 might accelerate infectious virion release.

Since VP8 is involved in carrying out multiple functions during productive infection, and its homologous proteins are present in other herpesviruses, we attempted to crystalize VP8. However, the challenge resided with the large-scale full-length or truncated VP8 production in both prokaryotic and mammalian expression systems. The predicted secondary structure revealed that VP8 is a large protein with mostly alpha-helical structures at its C-terminal domain. The alpha-helical structures of a protein are predominantly involved in protein-protein interaction (437). With the notion that VP8 is involved in multiple functions via protein-protein interaction, we aimed to get the crystal structure of the C-terminal domain of VP8 (amino acid 219-741). Finally, modification of C-terminal VP8 with the SUMO-His tag facilitated prokaryotic expression. However, VP8 was complexed with the bacterial GroEL protein during bacterial expression that led us to identify another interacting partner of VP8, HSP60. With the aim of obtaining the structure of VP8 and GroEL as a complex, we proceeded for crystallization screening with the method suitable for soluble protein crystallization. Nevertheless, no suitable condition for VP8 crystallization was observed. There could be one plausible explanation of not

getting crystal structure of VP8. Recent predicted secondary structure analysis of VP8 showed that VP8 has some hydrophobic domains. This may explain the difficulties in expression and subsequent purification of VP8. Notably, a membrane protein crystallization approach instead of soluble protein crystallization might promote VP8 crystallization.

Subsequently, we determined that VP8 interacts with a mitochondrial protein, HSP60. In both VP8-transfected and BoHV-1-infected cells, VP8 interacted with HSP60 and localized to mitochondria. The amino acids 219-741 of the C-terminal domain of VP8 were required for interaction with HSP60, as well as mitochondrial localization. During BoHV-1 infection, VP8 was localized to mitochondria at 2 h post infection. The localization of VP8 to mitochondria at 2 h post infection can be attributed to two facts. First, some viral proteins localize to mitochondria at early stages of infection to be transported to the nucleus. The HSV-1 tegument protein UL41 also localizes to mitochondria and is transported to the perinuclear region (432). Likewise, early during BoHV-1 infection, VP8 likely migrates to the perinuclear region through localization to mitochondria. Second, HSP60 functions as a chaperone protein and is involved in protein folding (451). Given the role of HSP60 in protein folding, it is conceivable that the interaction of VP8 with mitochondrial HSP60 might regulate VP8 folding or expression. Nonetheless, the later explanation can be eliminated since knocking down of HSP60 does not alter VP8 expression pattern. With the progression of infection, VP8 is exported from the nucleus to the cytoplasm. At 2-6 h post infection, VP8 is translocated to the mitochondria. Zhang, 2017 (PhD thesis) indicated that around 6 h post infection VP8 was localized to a distinct compartment before accumulation in the Golgi apparatus (452). This may correlate with mitochondrial localization of VP8 at 6 h post infection. Upon investigation into the mitochondrial function in the presence of VP8, we observed that VP8 reduced MMP. Since proper maintenance of MMP is associated with proper mitochondrial function and ATP production (125), we observed that VP8 also reduced ATP production. Additionally, BoHV-1 infection significantly reduced MMP and ATP production, whereas BoHV-1ΔU_L47 infection did not influence the MMP or ATP production. BoHV-1 and HSV-1 are known to decrease mitochondrial membrane potential and to reduce ATP production, which is in line with our observations (363, 432). Hence, during BoHV-1 infection, mitochondria-localized VP8 contributed to the deregulation of mitochondrial function. Different viruses are known target mitochondria for their replication, survival, and escape from the cells. HCV proteins localized to mitochondria deregulate mitochondrial function by reducing MMP

and increasing ROS (443). Similarly, HIV Vpr localized to mitochondria and decreased MMP (444). Therefore, it is plausible that BoHV-1 VP8 targets mitochondria for deregulation of mitochondrial functions. Impaired mitochondrial functions such as reduced MMP, increased ROS production, and decreased ATP production are involved in induction of apoptosis (453). Since VP8 induces apoptosis, dysregulation of mitochondrial function by VP8 might promote induction of apoptosis during virus infection.

Overall, this research demonstrated that BoHV-1 VP8 is involved in multiple functions that were associated with the subcellular localization of VP8. After fusion of BoHV-1 glycoproteins with the host cell membrane receptors, VP8 from the tegument region of BoHV-1 is released into the host cytoplasm. The cytoplasmic VP8 then interacts with cellular STAT1 to retain it in the cytoplasm. This interaction of VP8 with STAT1 during early infection inhibits IFN-β signaling possibly to create an environment suitable for virus infection. As the infection progresses, VP8 translocates to the nucleus. In the nucleus, VP8 interacts with ATM and NBS1 to modulate the DDR pathway. The interaction of VP8 with ATM and NBS1 does not influence ATM activation but prohibits NBS1 and SMC1 phosphorylation, which eventually blocks DNA repair. This inhibition of DNA repair increases the accumulation of unrepaired DNA, which eventually led to the activation of the apoptotic pathway. Upon completion of the nuclear function, VP8 is exported out of the nucleus. During infection, VP8 is also localized to the mitochondria. Localization of VP8 to mitochondria is mediated through interaction with mitochondrial chaperone protein HSP60. The interaction of VP8 with mitochondrial HSP60 induces mitochondrial dysfunction by reducing MMP and by decreasing ATP production. Eventually, VP8 activates apoptotic pathway through caspase-3 activation to induce apoptosis. Finally, VP8 accumulates in the Golgi apparatus (shown in a separate study by Zhang et al Thesis, 2017), where packaging of VP8 into the virus particles takes place. With the final incorporation of VP8 into the virion, the virus leaves the host cell for subsequent infection. During subsequent infection, the incorporated VP8 will function as incoming VP8 to modulate the cellular environment.

In summary, we have demonstrated that VP8 functions to down-regulate IFN-β signaling, and to promote apoptosis in addition to its already identified essential roles in virus DNA encapsidation and virion incorporation. It is evident that VP8 is capable of carrying out multiple pro-viral functions. Continued functional characterization of VP8 may aid in

understanding its role in BoHV-1 pathogenesis. Additionally, structural characterization of VP8 may provide molecular detail into the function of VP8 or other homologous proteins, as well.

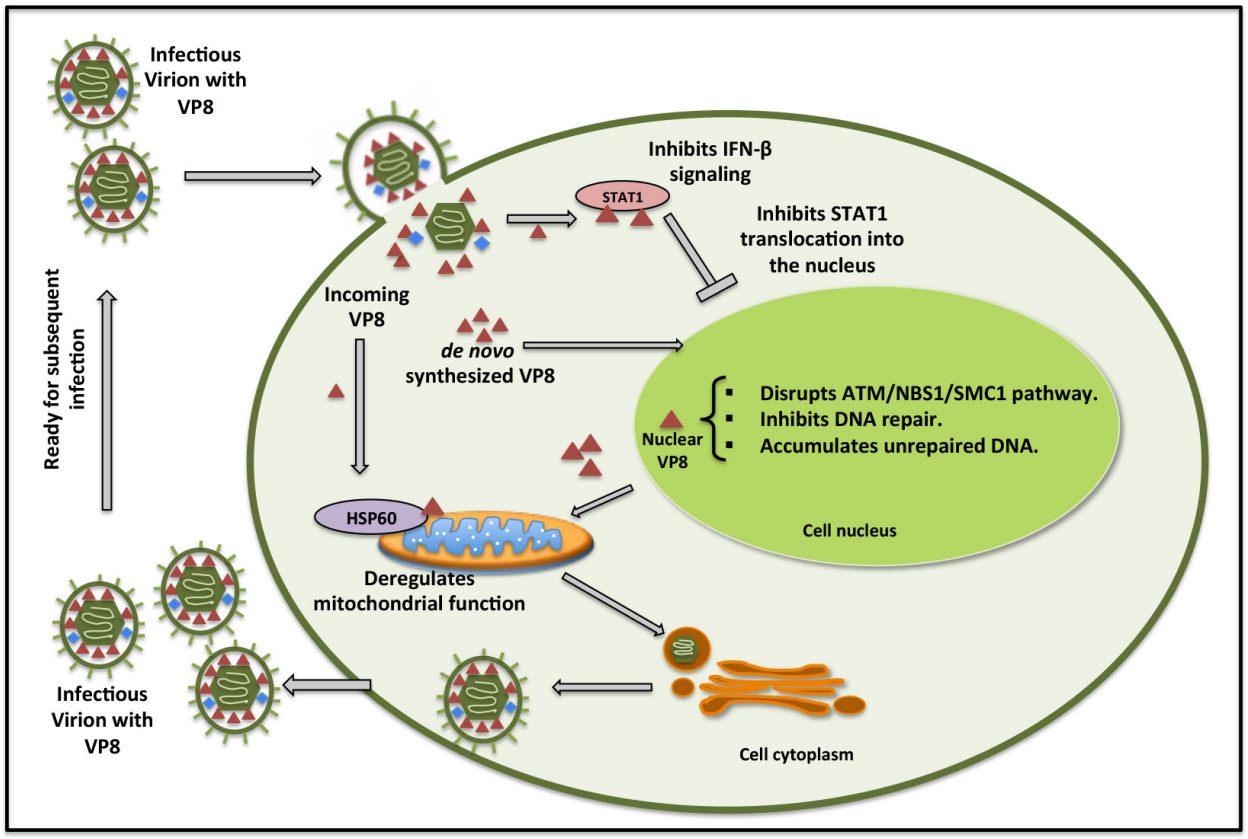

Figure. 8.1 Summary of VP8-assocatied functions during BoHV-1 infection

VP8-associated functions during BoHV-1 infection are outlined here. The cellular cytoplasm, nucleus, mitochondria, and Golgi apparatus are illustrated. Firstly, the BoHV-1 envelope is fused with the host cell plasma membrane. Following fusion, the capsid and tegument proteins including VP8 referred to as incoming VP8, are released into the host cell cytoplasm. Incoming VP8 in the cytoplasm binds to STAT1 to block IFN-β signaling. Some VP8 also localizes to mitochondria. During BoHV-1 infection *de novo* VP8 is synthesized and translocated to the nucleus. In the nucleus, VP8 has the potential to disrupt the ATM/NBS1/SMC1 pathway, inhibit DNA repair, leading to accumulation of unrepaired DNA. Subsequently, this triggers apoptosis. Later during infection, VP8 is exported to the cytoplasm. In the cytoplasm, VP8 is localized to the mitochondria to deregualte mitochondrial function. In addition, VP8 is accumulated in the Golgi apparatus to be incorporated into the progeny virus. Finally, the complete virions with abundantly incorporated VP8 are released into the extracellular environment. The infectious virions are ready for subsequent infection.

8.3 Future Directions.

In BoHV-1-infected cells, the fusion of the viral envelope with the host cell membrane releases the tegument proteins into the cytoplasm. Thus, at the pre-immediate-early stage of BoHV-1 infection VP8 is released into the cytoplasmic compartment. Following initiation of the infection, VP8 interacts with STAT1 to retain it in the cytoplasm to counteract IFN response. However, the mechanism of STAT1 retention by VP8 remains unknown. STAT1 contains coiled-coil and DNA-binding domains, which have been found to be necessary for the navigation of STAT1 into the nucleus (394, 454). Viral proteins, for instance, rabies virus P protein, binds to the coiled-coil and DNA-binding domains of STAT1 to inhibit its translocation into the nucleus (374). In the future, the introduction of mutations in the coiled-coil or DNA binding domain of STAT1 would help us to explore the possible mechanism of STAT1 retention in the cytoplasm by VP8. Besides, nuclear import of STAT1 is also associated with the NLS-dependent binding with importin-α. Any interference with the STAT1 NLS and importin-α binding prohibits nuclear accumulation of STAT1 (392). Hence, the interaction of VP8 with STAT1 can disrupt binding of STAT1 and importin-α to keep STAT1 in the cytoplasm. Future experiments can be planned to investigate the association of STAT1 with importin-α in the presence or in the absence of VP8.

VP8 is known to interact with cellular DDB1 and STAT1 (187). Thus, VP8 tends to interact with several proteins including DDR proteins, ATM and NBS1, to modulate the DDR pathway. DDB1 has been found to be associated with a complex with DDR protein, ATM and viral protein (404). However, during BoHV-1 infection, whether the interaction of VP8 with these multiple proteins is DDB1-dependent or -independent remains to be determined. Therefore, future research in DDB1-knockout bovine cell lines will resolve this issue. In this regard, the crisper/cas9 system can be used to knockout DDB1. The DDB1-knockout cell lines can be tested for VP8-associated interactions and functions during BoHV-1 infection. Besides, similar strategies can be used to knock out cellular STAT1. STAT1-knockout cell lines can be tested for VP8-mediated functions, such as VP8 and DDB1 or ATM interaction, or inhibition of NBS1 or SMC1 phosphorylation. Thus, these experiments will determine whether these VP8-associated functions are STAT1-dependent or -independent.

Previous and current research demonstrates that VP8 is involved in protein-protein interaction for its functions. The C-terminal domain of VP8 is enriched with alpha-helical structures, which promotes protein-protein interactions (405). Therefore, in this study, we

attempted to crystallize the C-terminal domain of VP8 using soluble protein crystallization. However, given the fact that there was no condition suitable for VP8 crystallization, we obtained information that can be implemented in future crystallization approaches. For example, recent predicted secondary structure analysis revealed that VP8 contains some transmembrane domains. This might explain the difficulties in expression and purification of VP8, as well as in obtaining highly concentrated VP8. Thus, future research can focus on crystallization of VP8 using membrane protein crystallization instead of soluble protein crystallization approach. Finally, the tertiary structure of VP8 will provide information towards synthesizing a potential inhibitor.

Following BoHV-1 challenge or immunization with purified VP8, T cell proliferation and antibody production were stimulated (181). Recent research also demonstrated that HSV-1 VP13/14, the homolog of BoHV-1 VP8, is a tegument antigen recognized by $CD8^{+}$T cells. Epitope mapping and subsequent immunological analysis indicated that the C-terminal domain of HSV-1 VP13/14 is immunogenic (455). However, the antigenic properties of various BoHV-1 VP8 domains remain to be determined. In this regard, the full-length and truncated VP8 versions can be tested for VP8 domain-specific immunogenic properties. Therefore, in future, the combination of structural analysis of truncated VP8, and the use of different truncated VP8 versions as vaccine candidates will provide information towards vaccine development against BoHV-1 infection.

REFERENCES

1. **Muylkens B, Thiry J, Kirten P, Schynts F, Thiry E.** 2007. Bovine herpesvirus 1 infection and infectious bovine rhinotracheitis. Vet Res **38:**181-209.
2. **van Oirschot JT.** 1995. Bovine herpesvirus 1 in semen of bulls and the risk of transmission: a brief review. Vet Q **17:**29-33.
3. **Edwards S, White H, Nixon P.** 1990. A study of the predominant genotypes of bovid herpesvirus 1 found in the U.K. Vet Microbiol **22:**213-223.
4. **D'Arce RC, Almeida RS, Silva TC, Franco AC, Spilki F, Roehe PM, Arns CW.** 2002. Restriction endonuclease and monoclonal antibody analysis of Brazilian isolates of bovine herpesviruses types 1 and 5. Vet Microbiol **88:**315-324.
5. **Engels M, Steck F, Wyler R.** 1981. Comparison of the genomes of infectious bovine rhinotracheitis and infectious pustular vulvovaginitis virus strains by restriction endonuclease analysis. Arch Virol **67:**169-174.
6. **Metzler AE, Matile H, Gassmann U, Engels M, Wyler R.** 1985. European isolates of bovine herpesvirus 1: a comparison of restriction endonuclease sites, polypeptides, and reactivity with monoclonal antibodies. Arch Virol **85:**57-69.
7. **Jones C, Chowdhury S.** 2010. Bovine herpesvirus type 1 (BHV-1) is an important cofactor in the bovine respiratory disease complex. Vet Clin North Am Food Anim Pract **26:**303-321.
8. **Misra V, Babiuk LA, Darcel CL.** 1983. Analysis of bovine herpes virus-type 1 isolates by restriction endonuclease fingerprinting. Arch Virol **76:**341-354.
9. **Wentink GH, van Oirschot JT, Verhoeff J.** 1993. Risk of infection with bovine herpes virus 1 (BHV1): a review. Vet Q **15:**30-33.
10. **Yates WD.** 1982. A review of infectious bovine rhinotracheitis, shipping fever pneumonia and viral-bacterial synergism in respiratory disease of cattle. Can J Comp Med **46:**225-263.
11. **Jones C, Chowdhury S.** 2007. A review of the biology of bovine herpesvirus type 1 (BHV-1), its role as a cofactor in the bovine respiratory disease complex and development of improved vaccines. Anim Health Res Rev **8:**187-205.
12. **Taylor JD, Fulton RW, Lehenbauer TW, Step DL, Confer AW.** 2010. The epidemiology of bovine respiratory disease: What is the evidence for predisposing factors? Can Vet J **51:**1095-1102.
13. **Nataraj C, Eidmann S, Hariharan MJ, Sur JH, Perry GA, Srikumaran S.** 1997. Bovine herpesvirus 1 downregulates the expression of bovine MHC class I molecules. Viral Immunol **10:**21-34.
14. **Hariharan MJ, Nataraj C, Srikumaran S.** 1993. Down regulation of murine MHC class I expression by bovine herpesvirus 1. Viral Immunol **6:**273-284.
15. **Winkler MT, Doster A, Jones C.** 1999. Bovine herpesvirus 1 can infect CD4(+) T lymphocytes and induce programmed cell death during acute infection of cattle. J Virol **73:**8657-8668.
16. **Graham DA.** 2013. Bovine herpes virus-1 (BoHV-1) in cattle-a review with emphasis on reproductive impacts and the emergence of infection in Ireland and the United Kingdom. Ir Vet J **66:**15.

17. **Mehmet F. Can1* VSA, and Cengiz Yalçın3.** 2016. Estimation of production and reproductive performance losses in
dairy cattle due to bovine herpesvirus 1 (BoHV-1) infection. Veterinarski Arhiv**:**499-513.
18. **Biswas S, Bandyopadhyay S, Dimri U, Patra PH.** 2013. Bovine herpesvirus-1 (BHV-1) - a re-emerging concern in livestock: a revisit to its biology, epidemiology, diagnosis, and prophylaxis. Vet Q **33:**68-81.
19. **Statham JM, Randall LV, Archer SC.** 2015. Reduction in daily milk yield associated with subclinical bovine herpesvirus 1 infection. Vet Rec **177:**339.
20. **Mahajan V, Banga HS, Deka D, Filia G, Gupta A.** 2013. Comparison of diagnostic tests for diagnosis of infectious bovine rhinotracheitis in natural cases of bovine abortion. J Comp Pathol **149:**391-401.
21. **Anderson ML.** 2007. Infectious causes of bovine abortion during mid- to late-gestation. Theriogenology **68:**474-486.
22. **Crandell RA.** 1986. Infectious bovine rhinotracheitis. JL Howard (Ed), Current veterinary therapy food animal practice (2nd ed), WB Saunders Co**:**pp. 470-472.
23. **Tuncer-Goktuna P, Alpay G, Oner EB, Yesilbag K.** 2016. The role of herpesviruses (BoHV-1 and BoHV-4) and pestiviruses (BVDV and BDV) in ruminant abortion cases in western Turkey. Trop Anim Health Prod **48:**1021-1027.
24. **Lucchese L, Benkirane A, Hakimi I, El Idrissi A, Natale A.** 2016. Seroprevalence study of the main causes of abortion in dairy cattle in Morocco. Vet Ital **52:**13-19.
25. **Brake F, Studdert MJ.** 1985. Molecular epidemiology and pathogenesis of ruminant herpesviruses including bovine, buffalo and caprine herpesviruses l and bovine encephalitis herpesvirus. Aust Vet J **62:**331-334.
26. **Nandi S, Kumar M, Manohar M, Chauhan RS.** 2009. Bovine herpes virus infections in cattle. Anim Health Res Rev **10:**85-98.
27. **Whetstone CA, Evermann JF.** 1988. Characterization of bovine herpesviruses isolated from six sheep and four goats by restriction endonuclease analysis and radioimmunoprecipitation. Am J Vet Res **49:**781-785.
28. **Porter DD, Larsen AE, Cox NA.** 1975. Isolation of infectious bovine rhinotracheitis virus from Mustelidae. J Clin Microbiol **1:**112-113.
29. **Abril C, Engels M, Liman A, Hilbe M, Albini S, Franchini M, Suter M, Ackermann M.** 2004. Both viral and host factors contribute to neurovirulence of bovine herpesviruses 1 and 5 in interferon receptor-deficient mice. J Virol **78:**3644-3653.
30. **Rock D, Lokensgard J, Lewis T, Kutish G.** 1992. Characterization of dexamethasone-induced reactivation of latent bovine herpesvirus 1. J Virol **66:**2484-2490.
31. **Ellis JA.** 2009. Update on viral pathogenesis in BRD. Anim Health Res Rev **10:**149-153.
32. **Miller JM, Whetstone CA, Bello LJ, Lawrence WC.** 1991. Determination of ability of a thymidine kinase-negative deletion mutant of bovine herpesvirus-1 to cause abortion in cattle. Am J Vet Res **52:**1038-1043.
33. **Jones C, da Silva LF, Sinani D.** 2011. Regulation of the latency-reactivation cycle by products encoded by the bovine herpesvirus 1 (BHV-1) latency-related gene. J Neurovirol **17:**535-545.
34. **Efstathiou. CMPaS.** 2007. Molecular basis of HSV latency and reactivation.

35. **Engels M, Loepfe E, Wild P, Schraner E, Wyler R.** 1987. The genome of caprine herpesvirus 1: genome structure and relatedness to bovine herpesvirus 1. J Gen Virol **68 (Pt 7):**2019-2023.
36. **Schynts F, McVoy MA, Meurens F, Detry B, Epstein AL, Thiry E.** 2003. The structures of bovine herpesvirus 1 virion and concatemeric DNA: implications for cleavage and packaging of herpesvirus genomes. Virology **314:**326-335.
37. **Engels M, Giuliani C, Wild P, Beck TM, Loepfe E, Wyler R.** 1986. The genome of bovine herpesvirus 1 (BHV-1) strains exhibiting a neuropathogenic potential compared to known BHV-1 strains by restriction site mapping and cross-hybridization. Virus Res **6:**57-73.
38. **Robinson KE, Meers J, Gravel JL, McCarthy FM, Mahony TJ.** 2008. The essential and non-essential genes of Bovine herpesvirus 1. J Gen Virol **89:**2851-2863.
39. **Liang XP, Babiuk LA, van Drunen Littel-van den Hurk S, Fitzpatrick DR, Zamb TJ.** 1991. Bovine herpesvirus 1 attachment to permissive cells is mediated by its major glycoproteins gI, gIII, and gIV. J Virol **65:**1124-1132.
40. **Nakamichi K, Matsumoto Y, Otsuka H.** 2002. Bovine herpesvirus 1 glycoprotein G is necessary for maintaining cell-to-cell junctional adherence among infected cells. Virology **294:**22-30.
41. **Barber KA, Daugherty HC, Ander SE, Jefferson VA, Shack LA, Pechan T, Nanduri B, Meyer F.** 2017. Protein Composition of the Bovine Herpesvirus 1.1 Virion. Vet Sci **4**.
42. **Babiuk LA, L'Italien J, van Drunen Littel-van den Hurk S, Zamb T, Lawman JP, Hughes G, Gifford GA.** 1987. Protection of cattle from bovine herpesvirus type I (BHV-1) infection by immunization with individual viral glycoproteins. Virology **159:**57-66.
43. **Li Y, Liang X, van Drunen Littel-van den Hurk S, Attah-Poku S, Babiuk LA.** 1996. Glycoprotein Bb, the N-terminal subunit of bovine herpesvirus 1 gB, can bind to heparan sulfate on the surfaces of Madin-Darby bovine kidney cells. J Virol **70:**2032-2037.
44. **Li Y, van Drunen Littel-van den Hurk S, Babiuk LA, Liang X.** 1995. Characterization of cell-binding properties of bovine herpesvirus 1 glycoproteins B, C, and D: identification of a dual cell-binding function of gB. J Virol **69:**4758-4768.
45. **Tikoo SK, Fitzpatrick DR, Babiuk LA, Zamb TJ.** 1990. Molecular cloning, sequencing, and expression of functional bovine herpesvirus 1 glycoprotein gIV in transfected bovine cells. J Virol **64:**5132-5142.
46. **van Drunen Littel-van den Hurk S, Gifford GA, Babiuk LA.** 1990. Epitope specificity of the protective immune response induced by individual bovine herpesvirus-1 glycoproteins. Vaccine **8:**358-368.
47. **Jacobs L.** 1994. Glycoprotein E of pseudorabies virus and homologous proteins in other alphaherpesvirinae. Arch Virol **137:**209-228.
48. **Yoshitake N, Xuan X, Otsuka H.** 1997. Identification and characterization of bovine herpesvirus-1 glycoproteins E and I. J Gen Virol **78 (Pt 6):**1399-1403.
49. **Kaashoek MJ, Rijsewijk FA, Ruuls RC, Keil GM, Thiry E, Pastoret PP, Van Oirschot JT.** 1998. Virulence, immunogenicity and reactivation of bovine herpesvirus 1 mutants with a deletion in the gC, gG, gI, gE, or in both the gI and gE gene. Vaccine **16:**802-809.

50. **Kaashoek MJ, Moerman A, Madic J, Weerdmeester K, Maris-Veldhuis M, Rijsewijk FA, van Oirschot JT.** 1995. An inactivated vaccine based on a glycoprotein E-negative strain of bovine herpesvirus 1 induces protective immunity and allows serological differentiation. Vaccine **13:**342-346.
51. **van Engelenburg FA, Kaashoek MJ, Rijsewijk FA, van den Burg L, Moerman A, Gielkens AL, van Oirschot JT.** 1994. A glycoprotein E deletion mutant of bovine herpesvirus 1 is avirulent in calves. J Gen Virol **75 (Pt 9):**2311-2318.
52. **Bryant NA, Davis-Poynter N, Vanderplasschen A, Alcami A.** 2003. Glycoprotein G isoforms from some alphaherpesviruses function as broad-spectrum chemokine binding proteins. EMBO J **22:**833-846.
53. **M.J. Kaashoek FAF, R.C. Ruuls,.** 802-809. Virulence, immunogenicity and reactivation of bovine herpesvirus 1 mutants with a deletion in the gC, gG, gI, gE, or in both the gI and gE gene. Vaccine**:**802-809.
54. **Nakamichi K, Kuroki D, Matsumoto Y, Otsuka H.** 2001. Bovine herpesvirus 1 glycoprotein G is required for prevention of apoptosis and efficient viral growth in rabbit kidney cells. Virology **279:**488-498.
55. **Meyer G, Hanon E, Georlette D, Pastoret PP, Thiry E.** 1998. Bovine herpesvirus type 1 glycoprotein H is essential for penetration and propagation in cell culture. J Gen Virol **79 (Pt 8):**1983-1987.
56. **Khattar SK, van Drunen Littel-van den Harke S, Attah-Poku SK, Babiuk LA, Tikoo SK.** 1996. Identification and characterization of a bovine herpesvirus-1 (BHV-1) glycoprotein gL which is required for proper antigenicity, processing, and transport of BHV-1 glycoprotein gH. Virology **219:**66-76.
57. **van Drunen Littel-van den Hurk S, Khattar S, Tikoo SK, Babiuk LA, Baranowski E, Plainchamp D, Thiry E.** 1996. Glycoprotein H (gII/gp108) and glycoprotein L form a functional complex which plays a role in penetration, but not in attachment, of bovine herpesvirus 1. J Gen Virol **77 (Pt 7):**1515-1520.
58. **Haque M, Stanfield B, Kousoulas KG.** 2016. Bovine herpesvirus type-1 glycoprotein K (gK) interacts with UL20 and is required for infectious virus production. Virology **499:**156-164.
59. **MacLean CA, Robertson LM, Jamieson FE.** 1993. Characterization of the UL10 gene product of herpes simplex virus type 1 and investigation of its role in vivo. J Gen Virol **74 (Pt 6):**975-983.
60. **Baines JD, Roizman B.** 1991. The open reading frames UL3, UL4, UL10, and UL16 are dispensable for the replication of herpes simplex virus 1 in cell culture. J Virol **65:**938-944.
61. **Dijkstra JM, Visser N, Mettenleiter TC, Klupp BG.** 1996. Identification and characterization of pseudorabies virus glycoprotein gM as a nonessential virion component. J Virol **70:**5684-5688.
62. **Lipinska AD, Koppers-Lalic D, Rychlowski M, Admiraal P, Rijsewijk FA, Bienkowska-Szewczyk K, Wiertz EJ.** 2006. Bovine herpesvirus 1 UL49.5 protein inhibits the transporter associated with antigen processing despite complex formation with glycoprotein M. J Virol **80:**5822-5832.
63. **Brack AR, Dijkstra JM, Granzow H, Klupp BG, Mettenleiter TC.** 1999. Inhibition of virion maturation by simultaneous deletion of glycoproteins E, I, and M of pseudorabies virus. J Virol **73:**5364-5372.

64. **Owen DJ, Crump CM, Graham SC.** 2015. Tegument Assembly and Secondary Envelopment of Alphaherpesviruses. Viruses **7:**5084-5114.
65. **Loret S, Guay G, Lippe R.** 2008. Comprehensive characterization of extracellular herpes simplex virus type 1 virions. J Virol **82:**8605-8618.
66. **Granzow H, Klupp BG, Mettenleiter TC.** 2005. Entry of pseudorabies virus: an immunogold-labeling study. J Virol **79:**3200-3205.
67. **Schipke J, Pohlmann A, Diestel R, Binz A, Rudolph K, Nagel CH, Bauerfeind R, Sodeik B.** 2012. The C terminus of the large tegument protein pUL36 contains multiple capsid binding sites that function differently during assembly and cell entry of herpes simplex virus. J Virol **86:**3682-3700.
68. **Campbell ME, Palfreyman JW, Preston CM.** 1984. Identification of herpes simplex virus DNA sequences which encode a trans-acting polypeptide responsible for stimulation of immediate early transcription. J Mol Biol **180:**1-19.
69. **Smiley JR.** 2004. Herpes simplex virus virion host shutoff protein: immune evasion mediated by a viral RNase? J Virol **78:**1063-1068.
70. **Milne RS, Nicola AV, Whitbeck JC, Eisenberg RJ, Cohen GH.** 2005. Glycoprotein D receptor-dependent, low-pH-independent endocytic entry of herpes simplex virus type 1. J Virol **79:**6655-6663.
71. **Nicola AV, Hou J, Major EO, Straus SE.** 2005. Herpes simplex virus type 1 enters human epidermal keratinocytes, but not neurons, via a pH-dependent endocytic pathway. J Virol **79:**7609-7616.
72. **Morrison EE, Wang YF, Meredith DM.** 1998. Phosphorylation of structural components promotes dissociation of the herpes simplex virus type 1 tegument. J Virol **72:**7108-7114.
73. **Kato A, Yamamoto M, Ohno T, Tanaka M, Sata T, Nishiyama Y, Kawaguchi Y.** 2006. Herpes simplex virus 1-encoded protein kinase UL13 phosphorylates viral Us3 protein kinase and regulates nuclear localization of viral envelopment factors UL34 and UL31. J Virol **80:**1476-1486.
74. **Cano-Monreal GL, Tavis JE, Morrison LA.** 2008. Substrate specificity of the herpes simplex virus type 2 UL13 protein kinase. Virology **374:**1-10.
75. **Aggarwal A, Miranda-Saksena M, Boadle RA, Kelly BJ, Diefenbach RJ, Alam W, Cunningham AL.** 2012. Ultrastructural visualization of individual tegument protein dissociation during entry of herpes simplex virus 1 into human and rat dorsal root ganglion neurons. J Virol **86:**6123-6137.
76. **Maurer UE, Sodeik B, Grunewald K.** 2008. Native 3D intermediates of membrane fusion in herpes simplex virus 1 entry. Proc Natl Acad Sci U S A **105:**10559-10564.
77. **Copeland AM, Newcomb WW, Brown JC.** 2009. Herpes simplex virus replication: roles of viral proteins and nucleoporins in capsid-nucleus attachment. J Virol **83:**1660-1668.
78. **Diefenbach RJ, Miranda-Saksena M, Diefenbach E, Holland DJ, Boadle RA, Armati PJ, Cunningham AL.** 2002. Herpes simplex virus tegument protein US11 interacts with conventional kinesin heavy chain. J Virol **76:**3282-3291.
79. **Delboy MG, Nicola AV.** 2011. A pre-immediate-early role for tegument ICP0 in the proteasome-dependent entry of herpes simplex virus. J Virol **85:**5910-5918.
80. **Yamauchi Y, Kiriyama K, Kubota N, Kimura H, Usukura J, Nishiyama Y.** 2008. The UL14 tegument protein of herpes simplex virus type 1 is required for efficient

nuclear transport of the alpha transinducing factor VP16 and viral capsids. J Virol **82:**1094-1106.

81. **Douglas MW, Diefenbach RJ, Homa FL, Miranda-Saksena M, Rixon FJ, Vittone V, Byth K, Cunningham AL.** 2004. Herpes simplex virus type 1 capsid protein VP26 interacts with dynein light chains RP3 and Tctex1 and plays a role in retrograde cellular transport. J Biol Chem **279:**28522-28530.
82. **Antinone SE, Shubeita GT, Coller KE, Lee JI, Haverlock-Moyns S, Gross SP, Smith GA.** 2006. The Herpesvirus capsid surface protein, VP26, and the majority of the tegument proteins are dispensable for capsid transport toward the nucleus. J Virol **80:**5494-5498.
83. **Batterson W, Furlong D, Roizman B.** 1983. Molecular genetics of herpes simplex virus. VIII. further characterization of a temperature-sensitive mutant defective in release of viral DNA and in other stages of the viral reproductive cycle. J Virol **45:**397-407.
84. **Ojala PM, Sodeik B, Ebersold MW, Kutay U, Helenius A.** 2000. Herpes simplex virus type 1 entry into host cells: reconstitution of capsid binding and uncoating at the nuclear pore complex in vitro. Mol Cell Biol **20:**4922-4931.
85. **Roberts AP, Abaitua F, O'Hare P, McNab D, Rixon FJ, Pasdeloup D.** 2009. Differing roles of inner tegument proteins pUL36 and pUL37 during entry of herpes simplex virus type 1. J Virol **83:**105-116.
86. **Harle P, Sainz B, Jr., Carr DJ, Halford WP.** 2002. The immediate-early protein, ICP0, is essential for the resistance of herpes simplex virus to interferon-alpha/beta. Virology **293:**295-304.
87. **Quinlan MP, Knipe DM.** 1985. Stimulation of expression of a herpes simplex virus DNA-binding protein by two viral functions. Mol Cell Biol **5:**957-963.
88. **Gu H, Roizman B.** 2007. Herpes simplex virus-infected cell protein 0 blocks the silencing of viral DNA by dissociating histone deacetylases from the CoREST-REST complex. Proc Natl Acad Sci U S A **104:**17134-17139.
89. **DeLuca NA, McCarthy AM, Schaffer PA.** 1985. Isolation and characterization of deletion mutants of herpes simplex virus type 1 in the gene encoding immediate-early regulatory protein ICP4. J Virol **56:**558-570.
90. **Sampath P, Deluca NA.** 2008. Binding of ICP4, TATA-binding protein, and RNA polymerase II to herpes simplex virus type 1 immediate-early, early, and late promoters in virus-infected cells. J Virol **82:**2339-2349.
91. **Mulvey M, Poppers J, Sternberg D, Mohr I.** 2003. Regulation of eIF2alpha phosphorylation by different functions that act during discrete phases in the herpes simplex virus type 1 life cycle. J Virol **77:**10917-10928.
92. **He B, Gross M, Roizman B.** 1997. The gamma(1)34.5 protein of herpes simplex virus 1 complexes with protein phosphatase 1alpha to dephosphorylate the alpha subunit of the eukaryotic translation initiation factor 2 and preclude the shutoff of protein synthesis by double-stranded RNA-activated protein kinase. Proc Natl Acad Sci U S A **94:**843-848.
93. **Liu X, Fitzgerald K, Kurt-Jones E, Finberg R, Knipe DM.** 2008. Herpesvirus tegument protein activates NF-kappaB signaling through the TRAF6 adaptor protein. Proc Natl Acad Sci U S A **105:**11335-11339.

94. **Amici C, Rossi A, Costanzo A, Ciafre S, Marinari B, Balsamo M, Levrero M, Santoro MG.** 2006. Herpes simplex virus disrupts NF-kappaB regulation by blocking its recruitment on the IkappaBalpha promoter and directing the factor on viral genes. J Biol Chem **281:**7110-7117.
95. **Taddeo B, Roizman B.** 2006. The virion host shutoff protein (UL41) of herpes simplex virus 1 is an endoribonuclease with a substrate specificity similar to that of RNase A. J Virol **80:**9341-9345.
96. **Zhang Y, Sirko DA, McKnight JL.** 1991. Role of herpes simplex virus type 1 UL46 and UL47 in alpha TIF-mediated transcriptional induction: characterization of three viral deletion mutants. J Virol **65:**829-841.
97. **Wysocka J, Herr W.** 2003. The herpes simplex virus VP16-induced complex: the makings of a regulatory switch. Trends Biochem Sci **28:**294-304.
98. **Stern S, Tanaka M, Herr W.** 1989. The Oct-1 homoeodomain directs formation of a multiprotein-DNA complex with the HSV transactivator VP16. Nature **341:**624-630.
99. **Sciortino MT, Taddeo B, Poon AP, Mastino A, Roizman B.** 2002. Of the three tegument proteins that package mRNA in herpes simplex virions, one (VP22) transports the mRNA to uninfected cells for expression prior to viral infection. Proc Natl Acad Sci U S A **99:**8318-8323.
100. **Kang MH, Roy BB, Finnen RL, Le Sage V, Johnston SM, Zhang H, Banfield BW.** 2013. The Us2 gene product of herpes simplex virus 2 is a membrane-associated ubiquitin-interacting protein. J Virol **87:**9590-9603.
101. **Reynolds AE, Wills EG, Roller RJ, Ryckman BJ, Baines JD.** 2002. Ultrastructural localization of the herpes simplex virus type 1 UL31, UL34, and US3 proteins suggests specific roles in primary envelopment and egress of nucleocapsids. J Virol **76:**8939-8952.
102. **Ryckman BJ, Roller RJ.** 2004. Herpes simplex virus type 1 primary envelopment: UL34 protein modification and the US3-UL34 catalytic relationship. J Virol **78:**399-412.
103. **Wisner TW, Wright CC, Kato A, Kawaguchi Y, Mou F, Baines JD, Roller RJ, Johnson DC.** 2009. Herpesvirus gB-induced fusion between the virion envelope and outer nuclear membrane during virus egress is regulated by the viral US3 kinase. J Virol **83:**3115-3126.
104. **Mettenleiter TC.** 2004. Budding events in herpesvirus morphogenesis. Virus Res **106:**167-180.
105. **Mettenleiter TC.** 2002. Herpesvirus assembly and egress. J Virol **76:**1537-1547.
106. **Kelly BJ, Fraefel C, Cunningham AL, Diefenbach RJ.** 2009. Functional roles of the tegument proteins of herpes simplex virus type 1. Virus Res **145:**173-186.
107. **Funk C, Ott M, Raschbichler V, Nagel CH, Binz A, Sodeik B, Bauerfeind R, Bailer SM.** 2015. The Herpes Simplex Virus Protein pUL31 Escorts Nucleocapsids to Sites of Nuclear Egress, a Process Coordinated by Its N-Terminal Domain. PLoS Pathog **11:**e1004957.
108. **Reynolds AE, Ryckman BJ, Baines JD, Zhou Y, Liang L, Roller RJ.** 2001. U(L)31 and U(L)34 proteins of herpes simplex virus type 1 form a complex that accumulates at the nuclear rim and is required for envelopment of nucleocapsids. J Virol **75:**8803-8817.

109. **Roller RJ, Zhou Y, Schnetzer R, Ferguson J, DeSalvo D.** 2000. Herpes simplex virus type 1 U(L)34 gene product is required for viral envelopment. J Virol **74:**117-129.
110. **Fuchs W, Klupp BG, Granzow H, Osterrieder N, Mettenleiter TC.** 2002. The interacting UL31 and UL34 gene products of pseudorabies virus are involved in egress from the host-cell nucleus and represent components of primary enveloped but not mature virions. J Virol **76:**364-378.
111. **Desai PJ.** 2000. A null mutation in the UL36 gene of herpes simplex virus type 1 results in accumulation of unenveloped DNA-filled capsids in the cytoplasm of infected cells. J Virol **74:**11608-11618.
112. **Ko DH, Cunningham AL, Diefenbach RJ.** 2010. The major determinant for addition of tegument protein pUL48 (VP16) to capsids in herpes simplex virus type 1 is the presence of the major tegument protein pUL36 (VP1/2). J Virol **84:**1397-1405.
113. **Desai P, Sexton GL, McCaffery JM, Person S.** 2001. A null mutation in the gene encoding the herpes simplex virus type 1 UL37 polypeptide abrogates virus maturation. J Virol **75:**10259-10271.
114. **Elliott G, Mouzakitis G, O'Hare P.** 1995. VP16 interacts via its activation domain with VP22, a tegument protein of herpes simplex virus, and is relocated to a novel macromolecular assembly in coexpressing cells. J Virol **69:**7932-7941.
115. **Smibert CA, Popova B, Xiao P, Capone JP, Smiley JR.** 1994. Herpes simplex virus VP16 forms a complex with the virion host shutoff protein vhs. J Virol **68:**2339-2346.
116. **Vittone V, Diefenbach E, Triffett D, Douglas MW, Cunningham AL, Diefenbach RJ.** 2005. Determination of interactions between tegument proteins of herpes simplex virus type 1. J Virol **79:**9566-9571.
117. **Stylianou J, Maringer K, Cook R, Bernard E, Elliott G.** 2009. Virion incorporation of the herpes simplex virus type 1 tegument protein VP22 occurs via glycoprotein E-specific recruitment to the late secretory pathway. J Virol **83:**5204-5218.
118. **Chi JH, Harley CA, Mukhopadhyay A, Wilson DW.** 2005. The cytoplasmic tail of herpes simplex virus envelope glycoprotein D binds to the tegument protein VP22 and to capsids. J Gen Virol **86:**253-261.
119. **Farnsworth A, Wisner TW, Johnson DC.** 2007. Cytoplasmic residues of herpes simplex virus glycoprotein gE required for secondary envelopment and binding of tegument proteins VP22 and UL11 to gE and gD. J Virol **81:**319-331.
120. **Dohner K, Radtke K, Schmidt S, Sodeik B.** 2006. Eclipse phase of herpes simplex virus type 1 infection: Efficient dynein-mediated capsid transport without the small capsid protein VP26. J Virol **80:**8211-8224.
121. **Krautwald M, Fuchs W, Klupp BG, Mettenleiter TC.** 2009. Translocation of incoming pseudorabies virus capsids to the cell nucleus is delayed in the absence of tegument protein pUL37. J Virol **83:**3389-3396.
122. **Jovasevic V, Liang L, Roizman B.** 2008. Proteolytic cleavage of VP1-2 is required for release of herpes simplex virus 1 DNA into the nucleus. J Virol **82:**3311-3319.
123. **Abaitua F, O'Hare P.** 2008. Identification of a highly conserved, functional nuclear localization signal within the N-terminal region of herpes simplex virus type 1 VP1-2 tegument protein. J Virol **82:**5234-5244.
124. **Delboy MG, Roller DG, Nicola AV.** 2008. Cellular proteasome activity facilitates herpes simplex virus entry at a postpenetration step. J Virol **82:**3381-3390.

125. **Huttemann M, Lee I, Pecinova A, Pecina P, Przyklenk K, Doan JW.** 2008. Regulation of oxidative phosphorylation, the mitochondrial membrane potential, and their role in human disease. J Bioenerg Biomembr **40:**445-456.
126. **Pitts JD, Klabis J, Richards AL, Smith GA, Heldwein EE.** 2014. Crystal structure of the herpesvirus inner tegument protein UL37 supports its essential role in control of viral trafficking. J Virol **88:**5462-5473.
127. **Delboy MG, Siekavizza-Robles CR, Nicola AV.** 2010. Herpes simplex virus tegument ICP0 is capsid associated, and its E3 ubiquitin ligase domain is important for incorporation into virions. J Virol **84:**1637-1640.
128. **Enquist LW, Husak PJ, Banfield BW, Smith GA.** 1998. Infection and spread of alphaherpesviruses in the nervous system. Adv Virus Res **51:**237-347.
129. **Dohner K, Wolfstein A, Prank U, Echeverri C, Dujardin D, Vallee R, Sodeik B.** 2002. Function of dynein and dynactin in herpes simplex virus capsid transport. Mol Biol Cell **13:**2795-2809.
130. **Nicoll MP, Proenca JT, Efstathiou S.** 2012. The molecular basis of herpes simplex virus latency. FEMS Microbiol Rev **36:**684-705.
131. **Lycke E, Hamark B, Johansson M, Krotochwil A, Lycke J, Svennerholm B.** 1988. Herpes simplex virus infection of the human sensory neuron. An electron microscopy study. Arch Virol **101:**87-104.
132. **Roizman BK, D.M.; R.J. .** 2007. Herpes simplex virus, in Feilds Virology, 5. **2:**2501.
133. **Honess RW, Roizman B.** 1974. Regulation of herpesvirus macromolecular synthesis. I. Cascade regulation of the synthesis of three groups of viral proteins. J Virol **14:**8-19.
134. **Weir JP.** 2001. Regulation of herpes simplex virus gene expression. Gene **271:**117-130.
135. **O'Hare P.** 1993. The virion transactivator of herpes simplex virus. Seminars in virology **4**.
136. **Melchjorsen J, Siren J, Julkunen I, Paludan SR, Matikainen S.** 2006. Induction of cytokine expression by herpes simplex virus in human monocyte-derived macrophages and dendritic cells is dependent on virus replication and is counteracted by ICP27 targeting NF-kappaB and IRF-3. J Gen Virol **87:**1099-1108.
137. **Homa FL, Brown JC.** 1997. Capsid assembly and DNA packaging in herpes simplex virus. Rev Med Virol **7:**107-122.
138. **Mettenleiter TC, Klupp BG, Granzow H.** 2006. Herpesvirus assembly: a tale of two membranes. Curr Opin Microbiol **9:**423-429.
139. **Johnson DC, Baines JD.** 2011. Herpesviruses remodel host membranes for virus egress. Nat Rev Microbiol **9:**382-394.
140. **Hogue IB, Scherer J, Enquist LW.** 2016. Exocytosis of Alphaherpesvirus Virions, Light Particles, and Glycoproteins Uses Constitutive Secretory Mechanisms. MBio **7**.
141. **Pellett PE, McKnight JL, Jenkins FJ, Roizman B.** 1985. Nucleotide sequence and predicted amino acid sequence of a protein encoded in a small herpes simplex virus DNA fragment capable of trans-inducing alpha genes. Proc Natl Acad Sci U S A **82:**5870-5874.
142. **Roizman B, Gu H, Mandel G.** 2005. The first 30 minutes in the life of a virus: unREST in the nucleus. Cell Cycle **4:**1019-1021.

143. **Thompson RL, Preston CM, Sawtell NM.** 2009. De novo synthesis of VP16 coordinates the exit from HSV latency in vivo. PLoS Pathog **5:**e1000352.
144. **Wu TT, Park T, Kim H, Tran T, Tong L, Martinez-Guzman D, Reyes N, Deng H, Sun R.** 2009. ORF30 and ORF34 are essential for expression of late genes in murine gammaherpesvirus 68. J Virol **83:**2265-2273.
145. **Poon AP, Liang Y, Roizman B.** 2003. Herpes simplex virus 1 gene expression is accelerated by inhibitors of histone deacetylases in rabbit skin cells infected with a mutant carrying a cDNA copy of the infected-cell protein no. 0. J Virol **77:**12671-12678.
146. **Grondin B, DeLuca N.** 2000. Herpes simplex virus type 1 ICP4 promotes transcription preinitiation complex formation by enhancing the binding of TFIID to DNA. J Virol **74:**11504-11510.
147. **Kuddus RH, DeLuca NA.** 2007. DNA-dependent oligomerization of herpes simplex virus type 1 regulatory protein ICP4. J Virol **81:**9230-9237.
148. **Shelton LS, Albright AG, Ruyechan WT, Jenkins FJ.** 1994. Retention of the herpes simplex virus type 1 (HSV-1) UL37 protein on single-stranded DNA columns requires the HSV-1 ICP8 protein. J Virol **68:**521-525.
149. **Field HJ, Wildy P.** 1978. The pathogenicity of thymidine kinase-deficient mutants of herpes simplex virus in mice. J Hyg (Lond) **81:**267-277.
150. **Pyles RB, Sawtell NM, Thompson RL.** 1992. Herpes simplex virus type 1 dUTPase mutants are attenuated for neurovirulence, neuroinvasiveness, and reactivation from latency. J Virol **66:**6706-6713.
151. **Harland J, Dunn P, Cameron E, Conner J, Brown SM.** 2003. The herpes simplex virus (HSV) protein ICP34.5 is a virion component that forms a DNA-binding complex with proliferating cell nuclear antigen and HSV replication proteins. J Neurovirol **9:**477-488.
152. **Brown SM, MacLean AR, McKie EA, Harland J.** 1997. The herpes simplex virus virulence factor ICP34.5 and the cellular protein MyD116 complex with proliferating cell nuclear antigen through the 63-amino-acid domain conserved in ICP34.5, MyD116, and GADD34. J Virol **71:**9442-9449.
153. **Skepper JN, Whiteley A, Browne H, Minson A.** 2001. Herpes simplex virus nucleocapsids mature to progeny virions by an envelopment --> deenvelopment --> reenvelopment pathway. J Virol **75:**5697-5702.
154. **Bigalke JM, Heldwein EE.** 2015. Structural basis of membrane budding by the nuclear egress complex of herpesviruses. EMBO J **34:**2921-2936.
155. **Klupp BG, Granzow H, Mettenleiter TC.** 2000. Primary envelopment of pseudorabies virus at the nuclear membrane requires the UL34 gene product. J Virol **74:**10063-10073.
156. **Bigalke JM, Heuser T, Nicastro D, Heldwein EE.** 2014. Membrane deformation and scission by the HSV-1 nuclear egress complex. Nat Commun **5:**4131.
157. **Mou F, Forest T, Baines JD.** 2007. US3 of herpes simplex virus type 1 encodes a promiscuous protein kinase that phosphorylates and alters localization of lamin A/C in infected cells. J Virol **81:**6459-6470.
158. **Leach N, Bjerke SL, Christensen DK, Bouchard JM, Mou F, Park R, Baines J, Haraguchi T, Roller RJ.** 2007. Emerin is hyperphosphorylated and redistributed in

herpes simplex virus type 1-infected cells in a manner dependent on both UL34 and US3. J Virol **81:**10792-10803.
159. **Morris JB, Hofemeister H, O'Hare P.** 2007. Herpes simplex virus infection induces phosphorylation and delocalization of emerin, a key inner nuclear membrane protein. J Virol **81:**4429-4437.
160. **Mou F, Wills EG, Park R, Baines JD.** 2008. Effects of lamin A/C, lamin B1, and viral US3 kinase activity on viral infectivity, virion egress, and the targeting of herpes simplex virus U(L)34-encoded protein to the inner nuclear membrane. J Virol **82:**8094-8104.
161. **Liu Z, Kato A, Shindo K, Noda T, Sagara H, Kawaoka Y, Arii J, Kawaguchi Y.** 2014. Herpes simplex virus 1 UL47 interacts with viral nuclear egress factors UL31, UL34, and Us3 and regulates viral nuclear egress. J Virol **88:**4657-4667.
162. **Klupp BG, Granzow H, Mettenleiter TC.** 2001. Effect of the pseudorabies virus US3 protein on nuclear membrane localization of the UL34 protein and virus egress from the nucleus. J Gen Virol **82:**2363-2371.
163. **Farnsworth A, Wisner TW, Webb M, Roller R, Cohen G, Eisenberg R, Johnson DC.** 2007. Herpes simplex virus glycoproteins gB and gH function in fusion between the virion envelope and the outer nuclear membrane. Proc Natl Acad Sci U S A **104:**10187-10192.
164. **Bucks MA, O'Regan KJ, Murphy MA, Wills JW, Courtney RJ.** 2007. Herpes simplex virus type 1 tegument proteins VP1/2 and UL37 are associated with intranuclear capsids. Virology **361:**316-324.
165. **Padula ME, Sydnor ML, Wilson DW.** 2009. Isolation and preliminary characterization of herpes simplex virus 1 primary enveloped virions from the perinuclear space. J Virol **83:**4757-4765.
166. **Coller KE, Lee JI, Ueda A, Smith GA.** 2007. The capsid and tegument of the alphaherpesviruses are linked by an interaction between the UL25 and VP1/2 proteins. J Virol **81:**11790-11797.
167. **Benboudjema L, Mulvey M, Gao Y, Pimplikar SW, Mohr I.** 2003. Association of the herpes simplex virus type 1 Us11 gene product with the cellular kinesin light-chain-related protein PAT1 results in the redistribution of both polypeptides. J Virol **77:**9192-9203.
168. **Takakuwa H, Goshima F, Koshizuka T, Murata T, Daikoku T, Nishiyama Y.** 2001. Herpes simplex virus encodes a virion-associated protein which promotes long cellular processes in over-expressing cells. Genes Cells **6:**955-966.
169. **Guo H, Shen S, Wang L, Deng H.** 2010. Role of tegument proteins in herpesvirus assembly and egress. Protein Cell **1:**987-998.
170. **Shanda SK, Wilson DW.** 2008. UL36p is required for efficient transport of membrane-associated herpes simplex virus type 1 along microtubules. J Virol **82:**7388-7394.
171. **Martin A, O'Hare P, McLauchlan J, Elliott G.** 2002. Herpes simplex virus tegument protein VP22 contains overlapping domains for cytoplasmic localization, microtubule interaction, and chromatin binding. J Virol **76:**4961-4970.
172. **Pasdeloup D, McElwee M, Beilstein F, Labetoulle M, Rixon FJ.** 2013. Herpesvirus tegument protein pUL37 interacts with dystonin/BPAG1 to promote capsid transport on microtubules during egress. J Virol **87:**2857-2867.

173. **Turcotte S, Letellier J, Lippe R.** 2005. Herpes simplex virus type 1 capsids transit by the trans-Golgi network, where viral glycoproteins accumulate independently of capsid egress. J Virol **79:**8847-8860.
174. **Mingo RM, Han J, Newcomb WW, Brown JC.** 2012. Replication of herpes simplex virus: egress of progeny virus at specialized cell membrane sites. J Virol **86:**7084-7097.
175. **David AT, Saied A, Charles A, Subramanian R, Chouljenko VN, Kousoulas KG.** 2012. A herpes simplex virus 1 (McKrae) mutant lacking the glycoprotein K gene is unable to infect via neuronal axons and egress from neuronal cell bodies. MBio **3:**e00144-00112.
176. **Carpenter DE, Misra V.** 1991. The most abundant protein in bovine herpes 1 virions is a homologue of herpes simplex virus type 1 UL47. J Gen Virol **72 (Pt 12):**3077-3084.
177. **Kopp M, Klupp BG, Granzow H, Fuchs W, Mettenleiter TC.** 2002. Identification and characterization of the pseudorabies virus tegument proteins UL46 and UL47: role for UL47 in virion morphogenesis in the cytoplasm. J Virol **76:**8820-8833.
178. **Meredith DM, Lindsay JA, Halliburton IW, Whittaker GR.** 1991. Post-translational modification of the tegument proteins (VP13 and VP14) of herpes simplex virus type 1 by glycosylation and phosphorylation. J Gen Virol **72 (Pt 11):**2771-2775.
179. **Lobanov VA, Maher-Sturgess SL, Snider MG, Lawman Z, Babiuk LA, van Drunen Littel-van den Hurk S.** 2010. A UL47 gene deletion mutant of bovine herpesvirus type 1 exhibits impaired growth in cell culture and lack of virulence in cattle. J Virol **84:**445-458.
180. **Verhagen J, Hutchinson I, Elliott G.** 2006. Nucleocytoplasmic shuttling of bovine herpesvirus 1 UL47 protein in infected cells. J Virol **80:**1059-1063.
181. **van Drunen Littel-van den Hurk S, Garzon S, van den Hurk JV, Babiuk LA, Tijssen P.** 1995. The role of the major tegument protein VP8 of bovine herpesvirus-1 in infection and immunity. Virology **206:**413-425.
182. **Zheng C, Brownlie R, Babiuk LA, van Drunen Littel-van den Hurk S.** 2004. Characterization of nuclear localization and export signals of the major tegument protein VP8 of bovine herpesvirus-1. Virology **324:**327-339.
183. **Williams P, Verhagen J, Elliott G.** 2008. Characterization of a CRM1-dependent nuclear export signal in the C terminus of herpes simplex virus type 1 tegument protein UL47. J Virol **82:**10946-10952.
184. **Labiuk SL, Babiuk LA, van Drunen Littel-van den Hurk S.** 2009. Major tegument protein VP8 of bovine herpesvirus 1 is phosphorylated by viral US3 and cellular CK2 protein kinases. J Gen Virol **90:**2829-2839.
185. **Zhang K, Afroz S, Brownlie R, Snider M, van Drunen Littel-van den Hurk S.** 2015. Regulation and function of phosphorylation on VP8, the major tegument protein of bovine herpesvirus 1. J Virol **89:**4598-4611.
186. **Zhang K, Brownlie R, Snider M, van Drunen Littel-van den Hurk S.** 2016. Phosphorylation of Bovine Herpesvirus 1 VP8 Plays a Role in Viral DNA Encapsidation and Is Essential for Its Cytoplasmic Localization and Optimal Virion Incorporation. J Virol **90:**4427-4440.
187. **Vasilenko NL, Snider M, Labiuk SL, Lobanov VA, Babiuk LA, van Drunen Littel-van den Hurk S.** 2012. Bovine herpesvirus-1 VP8 interacts with DNA damage

binding protein-1 (DDB1) and is monoubiquitinated during infection. Virus Res **167:**56-66.
188. **Islam A, Schulz S, Afroz S, Babiuk LA, van Drunen Littel-van den Hurk S.** 2015. Interaction of VP8 with mRNAs of bovine herpesvirus-1. Virus Res **197:**116-126.
189. **Donnelly M, Verhagen J, Elliott G.** 2007. RNA binding by the herpes simplex virus type 1 nucleocytoplasmic shuttling protein UL47 is mediated by an N-terminal arginine-rich domain that also functions as its nuclear localization signal. J Virol **81:**2283-2296.
190. **Chen YM, Knipe DM.** 1996. A dominant mutant form of the herpes simplex virus ICP8 protein decreases viral late gene transcription. Virology **221:**281-290.
191. **Donnelly M, Elliott G.** 2001. Nuclear localization and shuttling of herpes simplex virus tegument protein VP13/14. J Virol **75:**2566-2574.
192. **Kato A, Liu Z, Minowa A, Imai T, Tanaka M, Sugimoto K, Nishiyama Y, Arii J, Kawaguchi Y.** 2011. Herpes simplex virus 1 protein kinase Us3 and major tegument protein UL47 reciprocally regulate their subcellular localization in infected cells. J Virol **85:**9599-9613.
193. **Dobrikova E, Shveygert M, Walters R, Gromeier M.** 2010. Herpes simplex virus proteins ICP27 and UL47 associate with polyadenylate-binding protein and control its subcellular distribution. J Virol **84:**270-279.
194. **Shu M, Taddeo B, Zhang W, Roizman B.** 2013. Selective degradation of mRNAs by the HSV host shutoff RNase is regulated by the UL47 tegument protein. Proc Natl Acad Sci U S A **110:**E1669-1675.
195. **Dorange F, Tischer BK, Vautherot JF, Osterrieder N.** 2002. Characterization of Marek's disease virus serotype 1 (MDV-1) deletion mutants that lack UL46 to UL49 genes: MDV-1 UL49, encoding VP22, is indispensable for virus growth. J Virol **76:**1959-1970.
196. **Helferich D, Veits J, Teifke JP, Mettenleiter TC, Fuchs W.** 2007. The UL47 gene of avian infectious laryngotracheitis virus is not essential for in vitro replication but is relevant for virulence in chickens. J Gen Virol **88:**732-742.
197. **Akira S, Uematsu S, Takeuchi O.** 2006. Pathogen recognition and innate immunity. Cell **124:**783-801.
198. **Platanias LC.** 2005. Mechanisms of type-I- and type-II-interferon-mediated signalling. Nat Rev Immunol **5:**375-386.
199. **Katze MG, He Y, Gale M, Jr.** 2002. Viruses and interferon: a fight for supremacy. Nat Rev Immunol **2:**675-687.
200. **Muller U, Steinhoff U, Reis LF, Hemmi S, Pavlovic J, Zinkernagel RM, Aguet M.** 1994. Functional role of type I and type II interferons in antiviral defense. Science **264:**1918-1921.
201. **Paludan SR, Bowie AG, Horan KA, Fitzgerald KA.** 2011. Recognition of herpesviruses by the innate immune system. Nat Rev Immunol **11:**143-154.
202. **Su C, Zhan G, Zheng C.** 2016. Evasion of host antiviral innate immunity by HSV-1, an update. Virol J **13:**38.
203. **Collins SE, Noyce RS, Mossman KL.** 2004. Innate cellular response to virus particle entry requires IRF3 but not virus replication. J Virol **78:**1706-1717.
204. **Mossman KL, Ashkar AA.** 2005. Herpesviruses and the innate immune response. Viral Immunol **18:**267-281.

205. **Melroe GT, DeLuca NA, Knipe DM.** 2004. Herpes simplex virus 1 has multiple mechanisms for blocking virus-induced interferon production. J Virol **78:**8411-8420.
206. **Paladino P, Collins SE, Mossman KL.** 2010. Cellular localization of the herpes simplex virus ICP0 protein dictates its ability to block IRF3-mediated innate immune responses. PLoS One **5:**e10428.
207. **Saira K, Zhou Y, Jones C.** 2007. The infected cell protein 0 encoded by bovine herpesvirus 1 (bICP0) induces degradation of interferon response factor 3 and, consequently, inhibits beta interferon promoter activity. J Virol **81:**3077-3086.
208. **Takeda K, Kaisho T, Akira S.** 2003. Toll-like receptors. Annu Rev Immunol **21:**335-376.
209. **van Lint AL, Murawski MR, Goodbody RE, Severa M, Fitzgerald KA, Finberg RW, Knipe DM, Kurt-Jones EA.** 2010. Herpes simplex virus immediate-early ICP0 protein inhibits Toll-like receptor 2-dependent inflammatory responses and NF-kappaB signaling. J Virol **84:**10802-10811.
210. **Zhang J, Wang K, Wang S, Zheng C.** 2013. Herpes simplex virus 1 E3 ubiquitin ligase ICP0 protein inhibits tumor necrosis factor alpha-induced NF-kappaB activation by interacting with p65/RelA and p50/NF-kappaB1. J Virol **87:**12935-12948.
211. **Dell'Oste V, Gatti D, Giorgio AG, Gariglio M, Landolfo S, De Andrea M.** 2015. The interferon-inducible DNA-sensor protein IFI16: a key player in the antiviral response. New Microbiol **38:**5-20.
212. **Veeranki S, Choubey D.** 2012. Interferon-inducible p200-family protein IFI16, an innate immune sensor for cytosolic and nuclear double-stranded DNA: regulation of subcellular localization. Mol Immunol **49:**567-571.
213. **Ansari MA, Dutta S, Veettil MV, Dutta D, Iqbal J, Kumar B, Roy A, Chikoti L, Singh VV, Chandran B.** 2015. Herpesvirus Genome Recognition Induced Acetylation of Nuclear IFI16 Is Essential for Its Cytoplasmic Translocation, Inflammasome and IFN-beta Responses. PLoS Pathog **11:**e1005019.
214. **Unterholzner L, Keating SE, Baran M, Horan KA, Jensen SB, Sharma S, Sirois CM, Jin T, Latz E, Xiao TS, Fitzgerald KA, Paludan SR, Bowie AG.** 2010. IFI16 is an innate immune sensor for intracellular DNA. Nat Immunol **11:**997-1004.
215. **Orzalli MH, Broekema NM, Diner BA, Hancks DC, Elde NC, Cristea IM, Knipe DM.** 2015. cGAS-mediated stabilization of IFI16 promotes innate signaling during herpes simplex virus infection. Proc Natl Acad Sci U S A **112:**E1773-1781.
216. **Cuchet-Lourenco D, Anderson G, Sloan E, Orr A, Everett RD.** 2013. The viral ubiquitin ligase ICP0 is neither sufficient nor necessary for degradation of the cellular DNA sensor IFI16 during herpes simplex virus 1 infection. J Virol **87:**13422-13432.
217. **Bonizzi G, Karin M.** 2004. The two NF-kappaB activation pathways and their role in innate and adaptive immunity. Trends Immunol **25:**280-288.
218. **Kim JC, Lee SY, Kim SY, Kim JK, Kim HJ, Lee HM, Choi MS, Min JS, Kim MJ, Choi HS, Ahn JK.** 2008. HSV-1 ICP27 suppresses NF-kappaB activity by stabilizing IkappaBalpha. FEBS Lett **582:**2371-2376.
219. **Rawlings JS, Rosler KM, Harrison DA.** 2004. The JAK/STAT signaling pathway. J Cell Sci **117:**1281-1283.

220. **Johnson KE, Song B, Knipe DM.** 2008. Role for herpes simplex virus 1 ICP27 in the inhibition of type I interferon signaling. Virology **374:**487-494.
221. **Verpooten D, Ma Y, Hou S, Yan Z, He B.** 2009. Control of TANK-binding kinase 1-mediated signaling by the gamma(1)34.5 protein of herpes simplex virus 1. J Biol Chem **284:**1097-1105.
222. **Ma Y, Jin H, Valyi-Nagy T, Cao Y, Yan Z, He B.** 2012. Inhibition of TANK binding kinase 1 by herpes simplex virus 1 facilitates productive infection. J Virol **86:**2188-2196.
223. **Garcia MA, Gil J, Ventoso I, Guerra S, Domingo E, Rivas C, Esteban M.** 2006. Impact of protein kinase PKR in cell biology: from antiviral to antiproliferative action. Microbiol Mol Biol Rev **70:**1032-1060.
224. **Chou J, Chen JJ, Gross M, Roizman B.** 1995. Association of a M(r) 90,000 phosphoprotein with protein kinase PKR in cells exhibiting enhanced phosphorylation of translation initiation factor eIF-2 alpha and premature shutoff of protein synthesis after infection with gamma 134.5- mutants of herpes simplex virus 1. Proc Natl Acad Sci U S A **92:**10516-10520.
225. **Zhang SY, Jouanguy E, Ugolini S, Smahi A, Elain G, Romero P, Segal D, Sancho-Shimizu V, Lorenzo L, Puel A, Picard C, Chapgier A, Plancoulaine S, Titeux M, Cognet C, von Bernuth H, Ku CL, Casrouge A, Zhang XX, Barreiro L, Leonard J, Hamilton C, Lebon P, Heron B, Vallee L, Quintana-Murci L, Hovnanian A, Rozenberg F, Vivier E, Geissmann F, Tardieu M, Abel L, Casanova JL.** 2007. TLR3 deficiency in patients with herpes simplex encephalitis. Science **317:**1522-1527.
226. **Zhang SY, Jouanguy E, Sancho-Shimizu V, von Bernuth H, Yang K, Abel L, Picard C, Puel A, Casanova JL.** 2007. Human Toll-like receptor-dependent induction of interferons in protective immunity to viruses. Immunol Rev **220:**225-236.
227. **Peri P, Mattila RK, Kantola H, Broberg E, Karttunen HS, Waris M, Vuorinen T, Hukkanen V.** 2008. Herpes simplex virus type 1 Us3 gene deletion influences toll-like receptor responses in cultured monocytic cells. Virol J **5:**140.
228. **Sen J, Liu X, Roller R, Knipe DM.** 2013. Herpes simplex virus US3 tegument protein inhibits Toll-like receptor 2 signaling at or before TRAF6 ubiquitination. Virology **439:**65-73.
229. **Hatada EN, Krappmann D, Scheidereit C.** 2000. NF-kappaB and the innate immune response. Curr Opin Immunol **12:**52-58.
230. **Wang K, Ni L, Wang S, Zheng C.** 2014. Herpes simplex virus 1 protein kinase US3 hyperphosphorylates p65/RelA and dampens NF-kappaB activation. J Virol **88:**7941-7951.
231. **Wang S, Wang K, Lin R, Zheng C.** 2013. Herpes simplex virus 1 serine/threonine kinase US3 hyperphosphorylates IRF3 and inhibits beta interferon production. J Virol **87:**12814-12827.
232. **Fitzgerald KA, McWhirter SM, Faia KL, Rowe DC, Latz E, Golenbock DT, Coyle AJ, Liao SM, Maniatis T.** 2003. IKKepsilon and TBK1 are essential components of the IRF3 signaling pathway. Nat Immunol **4:**491-496.
233. **Seth RB, Sun L, Ea CK, Chen ZJ.** 2005. Identification and characterization of MAVS, a mitochondrial antiviral signaling protein that activates NF-kappaB and IRF 3. Cell **122:**669-682.

234. **Johnson PA, MacLean C, Marsden HS, Dalziel RG, Everett RD.** 1986. The product of gene US11 of herpes simplex virus type 1 is expressed as a true late gene. J Gen Virol **67 (Pt 5):**871-883.
235. **Xing J, Wang S, Lin R, Mossman KL, Zheng C.** 2012. Herpes simplex virus 1 tegument protein US11 downmodulates the RLR signaling pathway via direct interaction with RIG-I and MDA-5. J Virol **86:**3528-3540.
236. **Kok KH, Lui PY, Ng MH, Siu KL, Au SW, Jin DY.** 2011. The double-stranded RNA-binding protein PACT functions as a cellular activator of RIG-I to facilitate innate antiviral response. Cell Host Microbe **9:**299-309.
237. **Kew C, Lui PY, Chan CP, Liu X, Au SW, Mohr I, Jin DY, Kok KH.** 2013. Suppression of PACT-induced type I interferon production by herpes simplex virus 1 Us11 protein. J Virol **87:**13141-13149.
238. **Smiley JR, Elgadi MM, Saffran HA.** 2001. Herpes simplex virus vhs protein. Methods Enzymol **342:**440-451.
239. **Murphy JA, Duerst RJ, Smith TJ, Morrison LA.** 2003. Herpes simplex virus type 2 virion host shutoff protein regulates alpha/beta interferon but not adaptive immune responses during primary infection in vivo. J Virol **77:**9337-9345.
240. **Duerst RJ, Morrison LA.** 2004. Herpes simplex virus 2 virion host shutoff protein interferes with type I interferon production and responsiveness. Virology **322:**158-167.
241. **Suzutani T, Nagamine M, Shibaki T, Ogasawara M, Yoshida I, Daikoku T, Nishiyama Y, Azuma M.** 2000. The role of the UL41 gene of herpes simplex virus type 1 in evasion of non-specific host defence mechanisms during primary infection. J Gen Virol **81:**1763-1771.
242. **Honda K, Yanai H, Negishi H, Asagiri M, Sato M, Mizutani T, Shimada N, Ohba Y, Takaoka A, Yoshida N, Taniguchi T.** 2005. IRF-7 is the master regulator of type-I interferon-dependent immune responses. Nature **434:**772-777.
243. **Hacker H, Redecke V, Blagoev B, Kratchmarova I, Hsu LC, Wang GG, Kamps MP, Raz E, Wagner H, Hacker G, Mann M, Karin M.** 2006. Specificity in Toll-like receptor signalling through distinct effector functions of TRAF3 and TRAF6. Nature **439:**204-207.
244. **Oganesyan G, Saha SK, Guo B, He JQ, Shahangian A, Zarnegar B, Perry A, Cheng G.** 2006. Critical role of TRAF3 in the Toll-like receptor-dependent and -independent antiviral response. Nature **439:**208-211.
245. **Kattenhorn LM, Korbel GA, Kessler BM, Spooner E, Ploegh HL.** 2005. A deubiquitinating enzyme encoded by HSV-1 belongs to a family of cysteine proteases that is conserved across the family Herpesviridae. Mol Cell **19:**547-557.
246. **Wang S, Wang K, Li J, Zheng C.** 2013. Herpes simplex virus 1 ubiquitin-specific protease UL36 inhibits beta interferon production by deubiquitinating TRAF3. J Virol **87:**11851-11860.
247. **Ishii KJ, Coban C, Kato H, Takahashi K, Torii Y, Takeshita F, Ludwig H, Sutter G, Suzuki K, Hemmi H, Sato S, Yamamoto M, Uematsu S, Kawai T, Takeuchi O, Akira S.** 2006. A Toll-like receptor-independent antiviral response induced by double-stranded B-form DNA. Nat Immunol **7:**40-48.

248. **Abe T, Harashima A, Xia T, Konno H, Konno K, Morales A, Ahn J, Gutman D, Barber GN.** 2013. STING recognition of cytoplasmic DNA instigates cellular defense. Mol Cell **50:**5-15.
249. **Parker ZM, Murphy AA, Leib DA.** 2015. Role of the DNA Sensor STING in Protection from Lethal Infection following Corneal and Intracerebral Challenge with Herpes Simplex Virus 1. J Virol **89:**11080-11091.
250. **Kalamvoki M, Roizman B.** 2014. HSV-1 degrades, stabilizes, requires, or is stung by STING depending on ICP0, the US3 protein kinase, and cell derivation. Proc Natl Acad Sci U S A **111:**E611-617.
251. **Hornung V, Hartmann R, Ablasser A, Hopfner KP.** 2014. OAS proteins and cGAS: unifying concepts in sensing and responding to cytosolic nucleic acids. Nat Rev Immunol **14:**521-528.
252. **Sun L, Wu J, Du F, Chen X, Chen ZJ.** 2013. Cyclic GMP-AMP synthase is a cytosolic DNA sensor that activates the type I interferon pathway. Science **339:**786-791.
253. **Su C, Zheng C.** 2017. Herpes Simplex Virus 1 Abrogates the cGAS/STING-Mediated Cytosolic DNA-Sensing Pathway via Its Virion Host Shutoff Protein, UL41. J Virol **91**.
254. **Iqbal J, Ansari MA, Kumar B, Dutta D, Roy A, Chikoti L, Pisano G, Dutta S, Vahedi S, Veettil MV, Chandran B.** 2016. Histone H2B-IFI16 Recognition of Nuclear Herpesviral Genome Induces Cytoplasmic Interferon-beta Responses. PLoS Pathog **12:**e1005967.
255. **Chakarov S PR, Russev GCh, Zhelev N.** 2014. DNA damage and mutation. Types of DNA damage. . Biodiscovery **11: 1**.
256. **Giglia-Mari G, Zotter A, Vermeulen W.** 2011. DNA damage response. Cold Spring Harb Perspect Biol **3:**a000745.
257. **Weitzman MD, Fradet-Turcotte A.** 2018. Virus DNA Replication and the Host DNA Damage Response. Annu Rev Virol **5:**141-164.
258. **Marechal A, Zou L.** 2013. DNA damage sensing by the ATM and ATR kinases. Cold Spring Harb Perspect Biol **5**.
259. **Lilley CE, Schwartz RA, Weitzman MD.** 2007. Using or abusing: viruses and the cellular DNA damage response. Trends Microbiol **15:**119-126.
260. **Lavin MF.** 2008. Ataxia-telangiectasia: from a rare disorder to a paradigm for cell signalling and cancer. Nat Rev Mol Cell Biol **9:**759-769.
261. **MA L.** 2014. Viruses and the DNA Damage Response: Activation and Antagonism. Annu Rev Virol**:**605-625.
262. **Paull TT.** 2015. Mechanisms of ATM Activation. Annu Rev Biochem **84:**711-738.
263. **Bakkenist CJ, Kastan MB.** 2003. DNA damage activates ATM through intermolecular autophosphorylation and dimer dissociation. Nature **421:**499-506.
264. **Lee JH, Paull TT.** 2005. ATM activation by DNA double-strand breaks through the Mre11-Rad50-Nbs1 complex. Science **308:**551-554.
265. **Lee JH, Paull TT.** 2007. Activation and regulation of ATM kinase activity in response to DNA double-strand breaks. Oncogene **26:**7741-7748.
266. **Carney JP, Maser RS, Olivares H, Davis EM, Le Beau M, Yates JR, 3rd, Hays L, Morgan WF, Petrini JH.** 1998. The hMre11/hRad50 protein complex and Nijmegen breakage syndrome: linkage of double-strand break repair to the cellular DNA damage response. Cell **93:**477-486.

267. **Kitagawa R, Kastan MB.** 2005. The ATM-dependent DNA damage signaling pathway. Cold Spring Harb Symp Quant Biol **70:**99-109.
268. **Banin S, Moyal L, Shieh S, Taya Y, Anderson CW, Chessa L, Smorodinsky NI, Prives C, Reiss Y, Shiloh Y, Ziv Y.** 1998. Enhanced phosphorylation of p53 by ATM in response to DNA damage. Science **281:**1674-1677.
269. **Matsuoka S, Rotman G, Ogawa A, Shiloh Y, Tamai K, Elledge SJ.** 2000. Ataxia telangiectasia-mutated phosphorylates Chk2 in vivo and in vitro. Proc Natl Acad Sci U S A **97:**10389-10394.
270. **Powers JT, Hong S, Mayhew CN, Rogers PM, Knudsen ES, Johnson DG.** 2004. E2F1 uses the ATM signaling pathway to induce p53 and Chk2 phosphorylation and apoptosis. Mol Cancer Res **2:**203-214.
271. **Lilley CE, Carson CT, Muotri AR, Gage FH, Weitzman MD.** 2005. DNA repair proteins affect the lifecycle of herpes simplex virus 1. Proc Natl Acad Sci U S A **102:**5844-5849.
272. **Fernandez-Capetillo O, Celeste A, Nussenzweig A.** 2003. Focusing on foci: H2AX and the recruitment of DNA-damage response factors. Cell Cycle **2:**426-427.
273. **Schumacher AJ, Mohni KN, Kan Y, Hendrickson EA, Stark JM, Weller SK.** 2012. The HSV-1 exonuclease, UL12, stimulates recombination by a single strand annealing mechanism. PLoS Pathog **8:**e1002862.
274. **Shirata N, Kudoh A, Daikoku T, Tatsumi Y, Fujita M, Kiyono T, Sugaya Y, Isomura H, Ishizaki K, Tsurumi T.** 2005. Activation of ataxia telangiectasia-mutated DNA damage checkpoint signal transduction elicited by herpes simplex virus infection. J Biol Chem **280:**30336-30341.
275. **Balasubramanian N, Bai P, Buchek G, Korza G, Weller SK.** 2010. Physical interaction between the herpes simplex virus type 1 exonuclease, UL12, and the DNA double-strand break-sensing MRN complex. J Virol **84:**12504-12514.
276. **Lilley CE, Chaurushiya MS, Boutell C, Landry S, Suh J, Panier S, Everett RD, Stewart GS, Durocher D, Weitzman MD.** 2010. A viral E3 ligase targets RNF8 and RNF168 to control histone ubiquitination and DNA damage responses. EMBO J **29:**943-955.
277. **Taylor TJ, Knipe DM.** 2004. Proteomics of herpes simplex virus replication compartments: association of cellular DNA replication, repair, recombination, and chromatin remodeling proteins with ICP8. J Virol **78:**5856-5866.
278. **Jazayeri A, Falck J, Lukas C, Bartek J, Smith GC, Lukas J, Jackson SP.** 2006. ATM- and cell cycle-dependent regulation of ATR in response to DNA double-strand breaks. Nat Cell Biol **8:**37-45.
279. **Smith S, Weller SK.** 2015. HSV-I and the cellular DNA damage response. Future Virol **10:**383-397.
280. **Mohni KN, Livingston CM, Cortez D, Weller SK.** 2010. ATR and ATRIP are recruited to herpes simplex virus type 1 replication compartments even though ATR signaling is disabled. J Virol **84:**12152-12164.
281. **Mohni KN, Smith S, Dee AR, Schumacher AJ, Weller SK.** 2013. Herpes simplex virus type 1 single strand DNA binding protein and helicase/primase complex disable cellular ATR signaling. PLoS Pathog **9:**e1003652.

282. **Mohni KN, Dee AR, Smith S, Schumacher AJ, Weller SK.** 2013. Efficient herpes simplex virus 1 replication requires cellular ATR pathway proteins. J Virol **87:**531-542.
283. **Burma S, Chen BP, Chen DJ.** 2006. Role of non-homologous end joining (NHEJ) in maintaining genomic integrity. DNA Repair (Amst) **5:**1042-1048.
284. **Parkinson J, Lees-Miller SP, Everett RD.** 1999. Herpes simplex virus type 1 immediate-early protein vmw110 induces the proteasome-dependent degradation of the catalytic subunit of DNA-dependent protein kinase. J Virol **73:**650-657.
285. **Epstein A.** 2015. Why and How Epstein-Barr Virus Was Discovered 50 Years Ago. Curr Top Microbiol Immunol **390:**3-15.
286. **Young LS, Yap LF, Murray PG.** 2016. Epstein-Barr virus: more than 50 years old and still providing surprises. Nat Rev Cancer **16:**789-802.
287. **Cho MS, Tran VM.** 1993. A concatenated form of Epstein-Barr viral DNA in lymphoblastoid cell lines induced by transfection with BZLF1. Virology **194:**838-842.
288. **Dutton A, Woodman CB, Chukwuma MB, Last JI, Wei W, Vockerodt M, Baumforth KR, Flavell JR, Rowe M, Taylor AM, Young LS, Murray PG.** 2007. Bmi-1 is induced by the Epstein-Barr virus oncogene LMP1 and regulates the expression of viral target genes in Hodgkin lymphoma cells. Blood **109:**2597-2603.
289. **Bose S, Yap LF, Fung M, Starzcynski J, Saleh A, Morgan S, Dawson C, Chukwuma MB, Maina E, Buettner M, Wei W, Arrand J, Lim PV, Young LS, Teo SH, Stankovic T, Woodman CB, Murray PG.** 2009. The ATM tumour suppressor gene is down-regulated in EBV-associated nasopharyngeal carcinoma. J Pathol **217:**345-352.
290. **Ma X, Yang L, Xiao L, Tang M, Liu L, Li Z, Deng M, Sun L, Cao Y.** 2011. Down-regulation of EBV-LMP1 radio-sensitizes nasal pharyngeal carcinoma cells via NF-kappaB regulated ATM expression. PLoS One **6:**e24647.
291. **Hau PM, Tsao SW.** 2017. Epstein-Barr Virus Hijacks DNA Damage Response Transducers to Orchestrate Its Life Cycle. Viruses **9**.
292. **Dirmeier U, Hoffmann R, Kilger E, Schultheiss U, Briseno C, Gires O, Kieser A, Eick D, Sugden B, Hammerschmidt W.** 2005. Latent membrane protein 1 of Epstein-Barr virus coordinately regulates proliferation with control of apoptosis. Oncogene **24:**1711-1717.
293. **Choudhuri T, Verma SC, Lan K, Murakami M, Robertson ES.** 2007. The ATM/ATR signaling effector Chk2 is targeted by Epstein-Barr virus nuclear antigen 3C to release the G2/M cell cycle block. J Virol **81:**6718-6730.
294. **Nikitin PA YC, Forte E, Bocedi A, Tourigny JP.** 2010. An ATM/Chk2-mediated DNA damage–responsive signaling pathway suppresses Epstein–Barr virus transformation of primary human B cells. . Cell Host Microbe 510–522.
295. **Yang J, Deng W, Hau PM, Liu J, Lau VM, Cheung AL, Huen MS, Tsao SW.** 2015. Epstein-Barr virus BZLF1 protein impairs accumulation of host DNA damage proteins at damage sites in response to DNA damage. Lab Invest **95:**937-950.
296. **Hau PM, Deng W, Jia L, Yang J, Tsurumi T, Chiang AK, Huen MS, Tsao SW.** 2015. Role of ATM in the formation of the replication compartment during lytic replication of Epstein-Barr virus in nasopharyngeal epithelial cells. J Virol **89:**652-668.
297. **Lu J, Tang M, Li H, Xu Z, Weng X, Li J, Yu X, Zhao L, Liu H, Hu Y, Tan Z, Yang L, Zhong M, Zhou J, Fan J, Bode AM, Yi W, Gao J, Sun L, Cao Y.** 2016. EBV-LMP1

suppresses the DNA damage response through DNA-PK/AMPK signaling to promote radioresistance in nasopharyngeal carcinoma. Cancer Lett **380:**191-200.
298. **Wu SG, Tsai TH, Wu SJ.** 2011. Acute cytomegalovirus pneumonitis in patient with lymphomatoid granulomatosis. Emerg Infect Dis **17:**741-742.
299. **Vancikova Z, Dvorak P.** 2001. Cytomegalovirus infection in immunocompetent and immunocompromised individuals--a review. Curr Drug Targets Immune Endocr Metabol Disord **1:**179-187.
300. **Wathen MW, Stinski MF.** 1982. Temporal patterns of human cytomegalovirus transcription: mapping the viral RNAs synthesized at immediate early, early, and late times after infection. J Virol **41:**462-477.
301. **Stamminger T, Fleckenstein B.** 1990. Immediate-early transcription regulation of human cytomegalovirus. Curr Top Microbiol Immunol **154:**3-19.
302. **Xiaofei E, Kowalik TF.** 2014. The DNA damage response induced by infection with human cytomegalovirus and other viruses. Viruses **6:**2155-2185.
303. **Gaspar M, Shenk T.** 2006. Human cytomegalovirus inhibits a DNA damage response by mislocalizing checkpoint proteins. Proc Natl Acad Sci U S A **103:**2821-2826.
304. **Luo MH, Rosenke K, Czornak K, Fortunato EA.** 2007. Human cytomegalovirus disrupts both ataxia telangiectasia mutated protein (ATM)- and ATM-Rad3-related kinase-mediated DNA damage responses during lytic infection. J Virol **81:**1934-1950.
305. **Koganti S, Hui-Yuen J, McAllister S, Gardner B, Grasser F, Palendira U, Tangye SG, Freeman AF, Bhaduri-McIntosh S.** 2014. STAT3 interrupts ATR-Chk1 signaling to allow oncovirus-mediated cell proliferation. Proc Natl Acad Sci U S A **111:**4946-4951.
306. **Ganem D.** 2006. KSHV infection and the pathogenesis of Kaposi's sarcoma. Annu Rev Pathol **1:**273-296.
307. **Mesri EA, Cesarman E, Boshoff C.** 2010. Kaposi's sarcoma and its associated herpesvirus. Nat Rev Cancer **10:**707-719.
308. **Di Domenico EG, Toma L, Bordignon V, Trento E, D'Agosto G, Cordiali-Fei P, Ensoli F.** 2016. Activation of DNA Damage Response Induced by the Kaposi's Sarcoma-Associated Herpes Virus. Int J Mol Sci **17**.
309. **Singh VV, Dutta D, Ansari MA, Dutta S, Chandran B.** 2014. Kaposi's sarcoma-associated herpesvirus induces the ATM and H2AX DNA damage response early during de novo infection of primary endothelial cells, which play roles in latency establishment. J Virol **88:**2821-2834.
310. **Jackson BR, Noerenberg M, Whitehouse A.** 2014. A novel mechanism inducing genome instability in Kaposi's sarcoma-associated herpesvirus infected cells. PLoS Pathog **10:**e1004098.
311. **Shin YC, Nakamura H, Liang X, Feng P, Chang H, Kowalik TF, Jung JU.** 2006. Inhibition of the ATM/p53 signal transduction pathway by Kaposi's sarcoma-associated herpesvirus interferon regulatory factor 1. J Virol **80:**2257-2266.
312. **Seo T, Park J, Lee D, Hwang SG, Choe J.** 2001. Viral interferon regulatory factor 1 of Kaposi's sarcoma-associated herpesvirus binds to p53 and represses p53-dependent transcription and apoptosis. J Virol **75:**6193-6198.
313. **Komatsu T NK, Wodrich H.** 2016. The Role of Nuclear Antiviral Factors against Invading DNA Viruses: The Immediate Fate of Incoming Viral Genomes. Viruses **8**.

314. **Smith S RN, Mohni KN, Schumacher AJ, Weller SK.** 2014. Structure of the Herpes Simplex Virus 1 Genome: Manipulation of Nicks and Gaps Can Abrogate Infectivity and Alter the Cellular DNA Damage Response. J Virol **88:**10146–10156.
315. **Brown JC.** 2017,. Herpes Simplex Virus Latency: The DNA Repair-Centered Pathway. Advances in Virology.
316. **Koopal S FJ, Jarviluoma A, Jaamaa S, Pyakurel P.** 2007. Viral oncogene-induced DNA damage response is activated in Kaposi sarcoma tumorigenesis. PLoS Pathog**:**1348–1360.
317. **Kerr JF, Wyllie AH, Currie AR.** 1972. Apoptosis: a basic biological phenomenon with wide-ranging implications in tissue kinetics. Br J Cancer **26:**239-257.
318. **Thompson CB.** 1995. Apoptosis in the pathogenesis and treatment of disease. Science **267:**1456-1462.
319. **Savitskaya MA, Onishchenko GE.** 2015. Mechanisms of Apoptosis. Biochemistry (Mosc) **80:**1393-1405.
320. **Thomson BJ.** 2001. Viruses and apoptosis. Int J Exp Pathol **82:**65-76.
321. **Papaliagkas V, Anogianaki A, Anogianakis G, Ilonidis G.** 2007. The proteins and the mechanisms of apoptosis: a mini-review of the fundamentals. Hippokratia **11:**108-113.
322. **Elmore S.** 2007. Apoptosis: a review of programmed cell death. Toxicol Pathol **35:**495-516.
323. **Locksley RM, Killeen N, Lenardo MJ.** 2001. The TNF and TNF receptor superfamilies: integrating mammalian biology. Cell **104:**487-501.
324. **Hsu H, Xiong J, Goeddel DV.** 1995. The TNF receptor 1-associated protein TRADD signals cell death and NF-kappa B activation. Cell **81:**495-504.
325. **Wajant H.** 2002. The Fas signaling pathway: more than a paradigm. Science **296:**1635-1636.
326. **Wang L, Du F, Wang X.** 2008. TNF-alpha induces two distinct caspase-8 activation pathways. Cell **133:**693-703.
327. **Schulze-Osthoff K, Ferrari D, Los M, Wesselborg S, Peter ME.** 1998. Apoptosis signaling by death receptors. Eur J Biochem **254:**439-459.
328. **Kataoka T, Schroter M, Hahne M, Schneider P, Irmler M, Thome M, Froelich CJ, Tschopp J.** 1998. FLIP prevents apoptosis induced by death receptors but not by perforin/granzyme B, chemotherapeutic drugs, and gamma irradiation. J Immunol **161:**3936-3942.
329. **Saelens X, Festjens N, Vande Walle L, van Gurp M, van Loo G, Vandenabeele P.** 2004. Toxic proteins released from mitochondria in cell death. Oncogene **23:**2861-2874.
330. **Chinnaiyan AM.** 1999. The apoptosome: heart and soul of the cell death machine. Neoplasia **1:**5-15.
331. **Hill MM, Adrain C, Duriez PJ, Creagh EM, Martin SJ.** 2004. Analysis of the composition, assembly kinetics and activity of native Apaf-1 apoptosomes. EMBO J **23:**2134-2145.
332. **Li P, Nijhawan D, Budihardjo I, Srinivasula SM, Ahmad M, Alnemri ES, Wang X.** 1997. Cytochrome c and dATP-dependent formation of Apaf-1/caspase-9 complex initiates an apoptotic protease cascade. Cell **91:**479-489.

333. **Wang X.** 2001. The expanding role of mitochondria in apoptosis. Genes Dev **15:**2922-2933.
334. **Czabotar PE, Lessene G, Strasser A, Adams JM.** 2014. Control of apoptosis by the BCL-2 protein family: implications for physiology and therapy. Nat Rev Mol Cell Biol **15:**49-63.
335. **Leopardi R, Roizman B.** 1996. The herpes simplex virus major regulatory protein ICP4 blocks apoptosis induced by the virus or by hyperthermia. Proc Natl Acad Sci U S A **93:**9583-9587.
336. **Zhou G, Galvan V, Campadelli-Fiume G, Roizman B.** 2000. Glycoprotein D or J delivered in trans blocks apoptosis in SK-N-SH cells induced by a herpes simplex virus 1 mutant lacking intact genes expressing both glycoproteins. J Virol **74:**11782-11791.
337. **Zhou G, Roizman B.** 2001. The domains of glycoprotein D required to block apoptosis depend on whether glycoprotein D is present in the virions carrying herpes simplex virus 1 genome lacking the gene encoding the glycoprotein. J Virol **75:**6166-6172.
338. **Montgomery RI, Warner MS, Lum BJ, Spear PG.** 1996. Herpes simplex virus-1 entry into cells mediated by a novel member of the TNF/NGF receptor family. Cell **87:**427-436.
339. **Teresa Sciortino M, Medici MA, Marino-Merlo F, Zaccaria D, Giuffre M, Venuti A, Grelli S, Mastino A.** 2007. Signaling pathway used by HSV-1 to induce NF-kappaB activation: possible role of herpes virus entry receptor A. Ann N Y Acad Sci **1096:**89-96.
340. **Medici MA, Sciortino MT, Perri D, Amici C, Avitabile E, Ciotti M, Balestrieri E, De Smaele E, Franzoso G, Mastino A.** 2003. Protection by herpes simplex virus glycoprotein D against Fas-mediated apoptosis: role of nuclear factor kappaB. J Biol Chem **278:**36059-36067.
341. **Munger J, Roizman B.** 2001. The US3 protein kinase of herpes simplex virus 1 mediates the posttranslational modification of BAD and prevents BAD-induced programmed cell death in the absence of other viral proteins. Proc Natl Acad Sci U S A **98:**10410-10415.
342. **Wang X, Patenode C, Roizman B.** 2011. US3 protein kinase of HSV-1 cycles between the cytoplasm and nucleus and interacts with programmed cell death protein 4 (PDCD4) to block apoptosis. Proc Natl Acad Sci U S A **108:**14632-14636.
343. **Yu X, He S.** 2016. The interplay between human herpes simplex virus infection and the apoptosis and necroptosis cell death pathways. Virol J **13:**77.
344. **Perkins D, Yu Y, Bambrick LL, Yarowsky PJ, Aurelian L.** 2002. Expression of herpes simplex virus type 2 protein ICP10 PK rescues neurons from apoptosis due to serum deprivation or genetic defects. Exp Neurol **174:**118-122.
345. **Golembewski EK, Wales SQ, Aurelian L, Yarowsky PJ.** 2007. The HSV-2 protein ICP10PK prevents neuronal apoptosis and loss of function in an in vivo model of neurodegeneration associated with glutamate excitotoxicity. Exp Neurol **203:**381-393.
346. **Jerome KR, Chen Z, Lang R, Torres MR, Hofmeister J, Smith S, Fox R, Froelich CJ, Corey L.** 2001. HSV and glycoprotein J inhibit caspase activation and apoptosis induced by granzyme B or Fas. J Immunol **167:**3928-3935.

347. **Yamauchi Y, Daikoku T, Goshima F, Nishiyama Y.** 2003. Herpes simplex virus UL14 protein blocks apoptosis. Microbiol Immunol **47:**685-689.
348. **Ahmed M, Lock M, Miller CG, Fraser NW.** 2002. Regions of the herpes simplex virus type 1 latency-associated transcript that protect cells from apoptosis in vitro and protect neuronal cells in vivo. J Virol **76:**717-729.
349. **Henderson G, Peng W, Jin L, Perng GC, Nesburn AB, Wechsler SL, Jones C.** 2002. Regulation of caspase 8- and caspase 9-induced apoptosis by the herpes simplex virus type 1 latency-associated transcript. J Neurovirol **8 Suppl 2:**103-111.
350. **Kim JC, Choi SH, Kim JK, Kim Y, Kim HJ, Im JS, Lee SY, Choi JM, Lee HM, Ahn JK.** 2008. [Herpes simplex virus type 1 ICP27 induces apoptotic cell death by increasing intracellular reactive oxygen species]. Mol Biol (Mosk) **42:**470-477.
351. **Gillis PA, Okagaki LH, Rice SA.** 2009. Herpes simplex virus type 1 ICP27 induces p38 mitogen-activated protein kinase signaling and apoptosis in HeLa cells. J Virol **83:**1767-1777.
352. **Aubert M, Blaho JA.** 1999. The herpes simplex virus type 1 regulatory protein ICP27 is required for the prevention of apoptosis in infected human cells. J Virol **73:**2803-2813.
353. **Lovato L, Inman M, Henderson G, Doster A, Jones C.** 2003. Infection of cattle with a bovine herpesvirus 1 strain that contains a mutation in the latency-related gene leads to increased apoptosis in trigeminal ganglia during the transition from acute infection to latency. J Virol **77:**4848-4857.
354. **Hanon E, Vanderplasschen A, Lyaku S, Keil G, Denis M, Pastoret PP.** 1996. Inactivated bovine herpesvirus 1 induces apoptotic cell death of mitogen-stimulated bovine peripheral blood mononuclear cells. J Virol **70:**4116-4120.
355. **Hanon E, Lambot M, Hoornaert S, Lyaku J, Pastoret PP.** 1998. Bovine herpesvirus 1-induced apoptosis: phenotypic characterization of susceptible peripheral blood mononuclear cells. Arch Virol **143:**441-452.
356. **Hanon E, Meyer G, Vanderplasschen A, Dessy-Doize C, Thiry E, Pastoret PP.** 1998. Attachment but not penetration of bovine herpesvirus 1 is necessary to induce apoptosis in target cells. J Virol **72:**7638-7641.
357. **Hanon E, Keil G, van Drunen Littel-van den Hurk S, Griebel P, Vanderplasschen A, Rijsewijk FA, Babiuk L, Pastoret PP.** 1999. Bovine herpesvirus 1-induced apoptotic cell death: role of glycoprotein D. Virology **257:**191-197.
358. **Devireddy LR, Jones CJ.** 1999. Activation of caspases and p53 by bovine herpesvirus 1 infection results in programmed cell death and efficient virus release. J Virol **73:**3778-3788.
359. **Inman M, Zhang Y, Geiser V, Jones C.** 2001. The zinc ring finger in the bICP0 protein encoded by bovine herpesvirus-1 mediates toxicity and activates productive infection. J Gen Virol **82:**483-492.
360. **Henderson G, Zhang Y, Inman M, Jones D, Jones C.** 2004. Infected cell protein 0 encoded by bovine herpesvirus 1 can activate caspase 3 when overexpressed in transfected cells. J Gen Virol **85:**3511-3516.
361. **Qiu Z, Zhu J, Harms JS, Friedrichsen J, Splitter GA.** 2005. Bovine herpesvirus VP22 induces apoptosis in neuroblastoma cells by upregulating the expression ratio of Bax to Bcl-2. Hum Gene Ther **16:**101-108.

362. **Xu X, Zhang K, Huang Y, Ding L, Chen G, Zhang H, Tong D.** 2012. Bovine herpes virus type 1 induces apoptosis through Fas-dependent and mitochondria-controlled manner in Madin-Darby bovine kidney cells. Virol J **9:**202.
363. **Zhu L, Yuan C, Zhang D, Ma Y, Ding X, Zhu G.** 2016. BHV-1 induced oxidative stress contributes to mitochondrial dysfunction in MDBK cells. Vet Res **47:**47.
364. **Nakamichi K, Matsumoto Y, Otsuka H.** 2002. Bovine herpesvirus 1 U(S) ORF8 protein induces apoptosis in infected cells and facilitates virus egress. Virology **304:**24-32.
365. **De Martino L, Marfe G, Consalvo MI, Di Stefano C, Pagnini U, Sinibaldi-Salimei P.** 2007. Antiapoptotic activity of bovine herpesvirus type-1 (BHV-1) UL14 protein. Vet Microbiol **123:**210-216.
366. **Brzozowska A, Lipinska AD, Derewonko N, Lesiak D, Rychlowski M, Rabalski L, Bienkowska-Szewczyk K.** 2018. Inhibition of apoptosis in BHV-1-infected cells depends on Us3 serine/threonine kinase and its enzymatic activity. Virology **513:**136-145.
367. **Takashima Y, Tamura H, Xuan X, Otsuka H.** 1999. Identification of the US3 gene product of BHV-1 as a protein kinase and characterization of BHV-1 mutants of the US3 gene. Virus Res **59:**23-34.
368. **Jones C.** 2013. Bovine Herpes Virus 1 (BHV-1) and Herpes Simplex Virus Type 1 (HSV-1) Promote Survival of Latently Infected Sensory Neurons, in Part by Inhibiting Apoptosis. J Cell Death **6:**1-16.
369. **Nii S, Uno F, Yoshida M, Akatsuka K.** 1998. [Structure and assembly of human beta herpesviruses]. Nihon Rinsho **56:**22-28.
370. **Spear PG.** 2004. Herpes simplex virus: receptors and ligands for cell entry. Cell Microbiol **6:**401-410.
371. **Barry M, Fruh K.** 2006. Viral modulators of cullin RING ubiquitin ligases: culling the host defense. Sci STKE **2006:**pe21.
372. **Kotenko SV.** 2011. IFN-lambdas. Curr Opin Immunol **23:**583-590.
373. **Goodbourn S, Didcock L, Randall RE.** 2000. Interferons: cell signalling, immune modulation, antiviral response and virus countermeasures. J Gen Virol **81:**2341-2364.
374. **Vidy A, Chelbi-Alix M, Blondel D.** 2005. Rabies virus P protein interacts with STAT1 and inhibits interferon signal transduction pathways. J Virol **79:**14411-14420.
375. **Didcock L, Young DF, Goodbourn S, Randall RE.** 1999. The V protein of simian virus 5 inhibits interferon signalling by targeting STAT1 for proteasome-mediated degradation. J Virol **73:**9928-9933.
376. **Ramaswamy M, Shi L, Monick MM, Hunninghake GW, Look DC.** 2004. Specific inhibition of type I interferon signal transduction by respiratory syncytial virus. Am J Respir Cell Mol Biol **30:**893-900.
377. **Andrejeva J, Young DF, Goodbourn S, Randall RE.** 2002. Degradation of STAT1 and STAT2 by the V proteins of simian virus 5 and human parainfluenza virus type 2, respectively: consequences for virus replication in the presence of alpha/beta and gamma interferons. J Virol **76:**2159-2167.

378. **Kubota T, Yokosawa N, Yokota S, Fujii N, Tashiro M, Kato A.** 2005. Mumps virus V protein antagonizes interferon without the complete degradation of STAT1. J Virol **79:**4451-4459.
379. **Saira K, Zhou Y, Jones C.** 2009. The infected cell protein 0 encoded by bovine herpesvirus 1 (bICP0) associates with interferon regulatory factor 7 and consequently inhibits beta interferon promoter activity. J Virol **83:**3977-3981.
380. **da Silva LF, Sinani D, Jones C.** 2012. ICP27 protein encoded by bovine herpesvirus type 1 (bICP27) interferes with promoter activity of the bovine genes encoding beta interferon 1 (IFN-beta1) and IFN-beta3. Virus Res **169:**162-168.
381. **Rost B, Sander C.** 1994. Combining evolutionary information and neural networks to predict protein secondary structure. Proteins **19:**55-72.
382. **Robert X, Gouet P.** 2014. Deciphering key features in protein structures with the new ENDscript server. Nucleic Acids Res **42:**W320-324.
383. **Zhang Y, McKnight JL.** 1993. Herpes simplex virus type 1 UL46 and UL47 deletion mutants lack VP11 and VP12 or VP13 and VP14, respectively, and exhibit altered viral thymidine kinase expression. J Virol **67:**1482-1492.
384. **Stites WE.** 1997. Proteinminus signProtein Interactions: Interface Structure, Binding Thermodynamics, and Mutational Analysis. Chem Rev **97:**1233-1250.
385. **Levy DE, Darnell JE, Jr.** 2002. Stats: transcriptional control and biological impact. Nat Rev Mol Cell Biol **3:**651-662.
386. **Ulane CM, Horvath CM.** 2002. Paramyxoviruses SV5 and HPIV2 assemble STAT protein ubiquitin ligase complexes from cellular components. Virology **304:**160-166.
387. **Komatsu T, Takeuchi K, Yokoo J, Gotoh B.** 2002. Sendai virus C protein impairs both phosphorylation and dephosphorylation processes of Stat1. FEBS Lett **511:**139-144.
388. **Takeuchi K, Kadota SI, Takeda M, Miyajima N, Nagata K.** 2003. Measles virus V protein blocks interferon (IFN)-alpha/beta but not IFN-gamma signaling by inhibiting STAT1 and STAT2 phosphorylation. FEBS Lett **545:**177-182.
389. **Rodriguez JJ, Parisien JP, Horvath CM.** 2002. Nipah virus V protein evades alpha and gamma interferons by preventing STAT1 and STAT2 activation and nuclear accumulation. J Virol **76:**11476-11483.
390. **Rodriguez JJ, Wang LF, Horvath CM.** 2003. Hendra virus V protein inhibits interferon signaling by preventing STAT1 and STAT2 nuclear accumulation. J Virol **77:**11842-11845.
391. **Schindler C, Shuai K, Prezioso VR, Darnell JE, Jr.** 1992. Interferon-dependent tyrosine phosphorylation of a latent cytoplasmic transcription factor. Science **257:**809-813.
392. **McBride KM, Banninger G, McDonald C, Reich NC.** 2002. Regulated nuclear import of the STAT1 transcription factor by direct binding of importin-alpha. EMBO J **21:**1754-1763.
393. **Meyer T, Marg A, Lemke P, Wiesner B, Vinkemeier U.** 2003. DNA binding controls inactivation and nuclear accumulation of the transcription factor Stat1. Genes Dev **17:**1992-2005.
394. **Melen K, Kinnunen L, Julkunen I.** 2001. Arginine/lysine-rich structural element is involved in interferon-induced nuclear import of STATs. J Biol Chem **276:**16447-16455.

395. **Zhou BB, Elledge SJ.** 2000. The DNA damage response: putting checkpoints in perspective. Nature **408:**433-439.
396. **Elledge SJ.** 1996. Cell cycle checkpoints: preventing an identity crisis. Science **274:**1664-1672.
397. **Lim DS, Kim ST, Xu B, Maser RS, Lin J, Petrini JH, Kastan MB.** 2000. ATM phosphorylates p95/nbs1 in an S-phase checkpoint pathway. Nature **404:**613-617.
398. **Yazdi PT, Wang Y, Zhao S, Patel N, Lee EY, Qin J.** 2002. SMC1 is a downstream effector in the ATM/NBS1 branch of the human S-phase checkpoint. Genes Dev **16:**571-582.
399. **Aita K, Irie H, Koyama AH, Fukuda A, Yoshida T, Shiga J.** 2001. Acute adrenal infection by HSV-1: role of apoptosis in viral replication. Arch Virol **146:**2009-2020.
400. **Sheldrick P, Laithier M, Lando D, Ryhiner ML.** 1973. Infectious DNA from herpes simplex virus: infectivity of double-stranded and single-stranded molecules. Proc Natl Acad Sci U S A **70:**3621-3625.
401. **Jongeneel CV, Bachenheimer SL.** 1981. Structure of replicating herpes simplex virus DNA. J Virol **39:**656-660.
402. **De Chiara G, Racaniello M, Mollinari C, Marcocci ME, Aversa G, Cardinale A, Giovanetti A, Garaci E, Palamara AT, Merlo D.** 2016. Herpes Simplex Virus-Type1 (HSV-1) Impairs DNA Repair in Cortical Neurons. Front Aging Neurosci **8:**242.
403. **Tarakanova VL, Leung-Pineda V, Hwang S, Yang CW, Matatall K, Basson M, Sun R, Piwnica-Worms H, Sleckman BP, Virgin HWt.** 2007. Gamma-herpesvirus kinase actively initiates a DNA damage response by inducing phosphorylation of H2AX to foster viral replication. Cell Host Microbe **1:**275-286.
404. **Liang X, Pickering MT, Cho NH, Chang H, Volkert MR, Kowalik TF, Jung JU.** 2006. Deregulation of DNA damage signal transduction by herpesvirus latency-associated M2. J Virol **80:**5862-5874.
405. **Afroz S, Brownlie R, Fodje M, van Drunen Littel-van den Hurk S.** 2016. VP8, the Major Tegument Protein of Bovine Herpesvirus 1, Interacts with Cellular STAT1 and Inhibits Interferon Beta Signaling. J Virol **90:**4889-4904.
406. **Salsman J, Jagannathan M, Paladino P, Chan PK, Dellaire G, Raught B, Frappier L.** 2012. Proteomic profiling of the human cytomegalovirus UL35 gene products reveals a role for UL35 in the DNA repair response. J Virol **86:**806-820.
407. **Schindelin J, Arganda-Carreras I, Frise E, Kaynig V, Longair M, Pietzsch T, Preibisch S, Rueden C, Saalfeld S, Schmid B, Tinevez JY, White DJ, Hartenstein V, Eliceiri K, Tomancak P, Cardona A.** 2012. Fiji: an open-source platform for biological-image analysis. Nat Methods **9:**676-682.
408. **Shiloh Y, Rotman G.** 1996. Ataxia-telangiectasia and the ATM gene: linking neurodegeneration, immunodeficiency, and cancer to cell cycle checkpoints. J Clin Immunol **16:**254-260.
409. **Lai CK, Jeng KS, Machida K, Cheng YS, Lai MM.** 2008. Hepatitis C virus NS3/4A protein interacts with ATM, impairs DNA repair and enhances sensitivity to ionizing radiation. Virology **370:**295-309.
410. **Caldecott K, Banks G, Jeggo P.** 1990. DNA double-strand break repair pathways and cellular tolerance to inhibitors of topoisomerase II. Cancer Res **50:**5778-5783.

411. **Zhu J, Petersen S, Tessarollo L, Nussenzweig A.** 2001. Targeted disruption of the Nijmegen breakage syndrome gene NBS1 leads to early embryonic lethality in mice. Curr Biol **11:**105-109.
412. **Turnell AS, Grand RJ.** 2012. DNA viruses and the cellular DNA-damage response. J Gen Virol **93:**2076-2097.
413. **Lilley CE, Chaurushiya MS, Boutell C, Everett RD, Weitzman MD.** 2011. The intrinsic antiviral defense to incoming HSV-1 genomes includes specific DNA repair proteins and is counteracted by the viral protein ICP0. PLoS Pathog **7:**e1002084.
414. **Branzei D, Foiani M.** 2008. Regulation of DNA repair throughout the cell cycle. Nat Rev Mol Cell Biol **9:**297-308.
415. **Hustedt N, Durocher D.** 2016. The control of DNA repair by the cell cycle. Nat Cell Biol **19:**1-9.
416. **Kitagawa R, Bakkenist CJ, McKinnon PJ, Kastan MB.** 2004. Phosphorylation of SMC1 is a critical downstream event in the ATM-NBS1-BRCA1 pathway. Genes Dev **18:**1423-1438.
417. **Schrofelbauer B, Hakata Y, Landau NR.** 2007. HIV-1 Vpr function is mediated by interaction with the damage-specific DNA-binding protein DDB1. Proc Natl Acad Sci U S A **104:**4130-4135.
418. **Dunkern TR, Fritz G, Kaina B.** 2001. Ultraviolet light-induced DNA damage triggers apoptosis in nucleotide excision repair-deficient cells via Bcl-2 decline and caspase-3/-8 activation. Oncogene **20:**6026-6038.
419. **Lou DI, Kim ET, Meyerson NR, Pancholi NJ, Mohni KN, Enard D, Petrov DA, Weller SK, Weitzman MD, Sawyer SL.** 2016. An Intrinsically Disordered Region of the DNA Repair Protein Nbs1 Is a Species-Specific Barrier to Herpes Simplex Virus 1 in Primates. Cell Host Microbe **20:**178-188.
420. **Stracker TH, Carson CT, Weitzman MD.** 2002. Adenovirus oncoproteins inactivate the Mre11-Rad50-NBS1 DNA repair complex. Nature **418:**348-352.
421. **Dunkern TR, Kaina B.** 2002. Cell proliferation and DNA breaks are involved in ultraviolet light-induced apoptosis in nucleotide excision repair-deficient Chinese hamster cells. Mol Biol Cell **13:**348-361.
422. **Wurzer WJ, Ehrhardt C, Pleschka S, Berberich-Siebelt F, Wolff T, Walczak H, Planz O, Ludwig S.** 2004. NF-kappaB-dependent induction of tumor necrosis factor-related apoptosis-inducing ligand (TRAIL) and Fas/FasL is crucial for efficient influenza virus propagation. J Biol Chem **279:**30931-30937.
423. **Wurzer WJ, Planz O, Ehrhardt C, Giner M, Silberzahn T, Pleschka S, Ludwig S.** 2003. Caspase 3 activation is essential for efficient influenza virus propagation. EMBO J **22:**2717-2728.
424. **Wang X, Ragupathy V, Zhao J, Hewlett I.** 2011. Molecules from apoptotic pathways modulate HIV-1 replication in Jurkat cells. Biochem Biophys Res Commun **414:**20-24.
425. **Sanfilippo CM, Blaho JA.** 2006. ICP0 gene expression is a herpes simplex virus type 1 apoptotic trigger. J Virol **80:**6810-6821.
426. **Kelley LA, Mezulis S, Yates CM, Wass MN, Sternberg MJ.** 2015. The Phyre2 web portal for protein modeling, prediction and analysis. Nat Protoc **10:**845-858.
427. **Roizman B, Carmichael LE, Deinhardt F, de-The G, Nahmias AJ, Plowright W, Rapp F, Sheldrick P, Takahashi M, Wolf K.** 1981. Herpesviridae. Definition,

provisional nomenclature, and taxonomy. The Herpesvirus Study Group, the International Committee on Taxonomy of Viruses. Intervirology **16:**201-217.
428. **Mettenleiter TC, Klupp BG, Granzow H.** 2009. Herpesvirus assembly: an update. Virus Res **143:**222-234.
429. **Latchman DS.** 1988. Effect of herpes simplex virus type 2 infection on mitochondrial gene expression. J Gen Virol **69 (Pt 6):**1405-1410.
430. **Lund K, Ziola B.** 1986. Synthesis of mitochondrial macromolecules in herpes simplex type 1 virus infected Vero cells. Biochem Cell Biol **64:**1303-1309.
431. **Tsurumi T, Lehman IR.** 1990. Release of RNA polymerase from vero cell mitochondria after herpes simplex virus type 1 infection. J Virol **64:**450-452.
432. **Murata T, Goshima F, Daikoku T, Inagaki-Ohara K, Takakuwa H, Kato K, Nishiyama Y.** 2000. Mitochondrial distribution and function in herpes simplex virus-infected cells. J Gen Virol **81:**401-406.
433. **Elliott G, O'Hare P.** 1999. Live-cell analysis of a green fluorescent protein-tagged herpes simplex virus infection. J Virol **73:**4110-4119.
434. **Daikoku T, Ikenoya K, Yamada H, Goshima F, Nishiyama Y.** 1998. Identification and characterization of the herpes simplex virus type 1 UL51 gene product. J Gen Virol **79 (Pt 12):**3027-3031.
435. **Chadha P, Sarfo A, Zhang D, Abraham T, Carmichael J, Han J, Wills JW.** 2017. Domain Interaction Studies of Herpes Simplex Virus 1 Tegument Protein UL16 Reveal Its Interaction with Mitochondria. J Virol **91**.
436. **Castanier C, Arnoult D.** 2011. Mitochondrial localization of viral proteins as a means to subvert host defense. Biochim Biophys Acta **1813:**575-583.
437. **Watkins AM, Wuo MG, Arora PS.** 2015. Protein-Protein Interactions Mediated by Helical Tertiary Structure Motifs. J Am Chem Soc **137:**11622-11630.
438. **Marblestone JG, Edavettal SC, Lim Y, Lim P, Zuo X, Butt TR.** 2006. Comparison of SUMO fusion technology with traditional gene fusion systems: enhanced expression and solubility with SUMO. Protein Sci **15:**182-189.
439. **Lin Z, Rye HS.** 2006. GroEL-mediated protein folding: making the impossible, possible. Crit Rev Biochem Mol Biol **41:**211-239.
440. **Singh B, Patel HV, Ridley RG, Freeman KB, Gupta RS.** 1990. Mitochondrial import of the human chaperonin (HSP60) protein. Biochem Biophys Res Commun **169:**391-396.
441. **Braig K, Otwinowski Z, Hegde R, Boisvert DC, Joachimiak A, Horwich AL, Sigler PB.** 1994. The crystal structure of the bacterial chaperonin GroEL at 2.8 A. Nature **371:**578-586.
442. **Houry WA, Frishman D, Eckerskorn C, Lottspeich F, Hartl FU.** 1999. Identification of in vivo substrates of the chaperonin GroEL. Nature **402:**147-154.
443. **Piccoli C, Scrima R, D'Aprile A, Ripoli M, Lecce L, Boffoli D, Capitanio N.** 2006. Mitochondrial dysfunction in hepatitis C virus infection. Biochim Biophys Acta **1757:**1429-1437.
444. **Azuma A, Matsuo A, Suzuki T, Kurosawa T, Zhang X, Aida Y.** 2006. Human immunodeficiency virus type 1 Vpr induces cell cycle arrest at the G(1) phase and apoptosis via disruption of mitochondrial function in rodent cells. Microbes Infect **8:**670-679.

445. **Tanaka Y, Kanai F, Kawakami T, Tateishi K, Ijichi H, Kawabe T, Arakawa Y, Kawakami T, Nishimura T, Shirakata Y, Koike K, Omata M.** 2004. Interaction of the hepatitis B virus X protein (HBx) with heat shock protein 60 enhances HBx-mediated apoptosis. Biochem Biophys Res Commun **318:**461-469.
446. **Takada S, Shirakata Y, Kaneniwa N, Koike K.** 1999. Association of hepatitis B virus X protein with mitochondria causes mitochondrial aggregation at the nuclear periphery, leading to cell death. Oncogene **18:**6965-6973.
447. **Ghosh JC, Siegelin MD, Dohi T, Altieri DC.** 2010. Heat shock protein 60 regulation of the mitochondrial permeability transition pore in tumor cells. Cancer Res **70:**8988-8993.
448. **Bagkos G, Koufopoulos K, Piperi C.** 2014. A new model for mitochondrial membrane potential production and storage. Med Hypotheses **83:**175-181.
449. **Mott KR, Underhill D, Wechsler SL, Town T, Ghiasi H.** 2009. A role for the JAK-STAT1 pathway in blocking replication of HSV-1 in dendritic cells and macrophages. Virol J **6:**56.
450. **Buckingham EM, Jarosinski KW, Jackson W, Carpenter JE, Grose C.** 2016. Exocytosis of Varicella-Zoster Virus Virions Involves a Convergence of Endosomal and Autophagy Pathways. J Virol **90:**8673-8685.
451. **Saibil H.** 2013. Chaperone machines for protein folding, unfolding and disaggregation. Nat Rev Mol Cell Biol **14:**630-642.
452. **Zhang K.** 2017. Phosphorylation of a major tegument protein VP8 and its regulatory role in infection with bovine herpesvirus type one. PhD Thesis, University of Saskatchewan.
453. **Wang C, Youle RJ.** 2009. The role of mitochondria in apoptosis*. Annu Rev Genet **43:**95-118.
454. **Ma J, Zhang T, Novotny-Diermayr V, Tan AL, Cao X.** 2003. A novel sequence in the coiled-coil domain of Stat3 essential for its nuclear translocation. J Biol Chem **278:**29252-29260.
455. **Srivastava R, Khan AA, Garg S, Syed SA, Furness JN, Vahed H, Pham T, Yu HT, Nesburn AB, BenMohamed L.** 2017. Human Asymptomatic Epitopes Identified from the Herpes Simplex Virus Tegument Protein VP13/14 (UL47) Preferentially Recall Polyfunctional Effector Memory CD44high CD62Llow CD8+ TEM Cells and Protect Humanized HLA-A*02:01 Transgenic Mice against Ocular Herpesvirus Infection. J Virol **91**.